Geology of Carlsbad Cavern and other caves in the Guadalupe Mountains, New Mexico and Texas

by Carol A. Hill

BULLETIN 117 New Mexico Bureau of Mines & Mineral Resources 1987

A DIVISION OF

NEW MEXICO INSTITUTE OF MINING & TECHNOLOGY

Dedicated to
the Joint Venturers
of the Cave Research Foundation

COVER—Cloud linings at the Lake of the Clouds, the lowest point in Carlsbad Cavern. Photo David Jagnow.

Bulletin 117

New Mexico Bureau of Mines & Mineral Resources

A DIVISION OF
NEW MEXICO INSTITUTE OF MINING & TECHNOLOGY

Geology of Carlsbad Cavern and other caves in the Guadalupe Mountains, New Mexico and Texas

by Carol A. Hill
Albuquerque, New Mexico

SOCORRO 1987

NEW MEXICO INSTITUTE OF MINING & TECHNOLOGY
Laurence H. Lattman, *President*

NEW MEXICO BUREAU OF MINES & MINERAL RESOURCES
Charles E. Chapin, *Director and State Geologist*

BOARD OF REGENTS
Ex Officio
Bruce King, *Governor of New Mexico*
Alan Morgan, *Superintendent of Public Instruction*

Appointed
Lt. Gen. Leo Marquez, *President,* 1989-1995, *Albuquerque*
Charles Zimmerly, *Secretary/Treasurer,* 1991-1997, *Socorro*
Diane D. Denish, 1992-1997, *Albuquerque*
J. Michael Kelly, 1992-1997, *Roswell*
Steve Torres, 1991-1997, *Albuquerque*

BUREAU STAFF

ORIN J. ANDERSON, *Geologist*
RUBEN ARCHULETA, *Metallurgical Lab. Tech.*
AUGUSTUS K. ARMSTRONG, *USGS Geologist*
GEORGE S. AUSTIN, *Senior Industrial Minerals Geologist*
AL BACA, *Maintenance Carpenter II*
JAMES M. BARKER, *Senior industrial Minerals Geologist*
PAUL W. BAUER, *Field Economic Geologist*
ROBERT A. BIEBERMAN, *Emeritus Sr. Petroleum Geologist* LYNN A. BRANDVOLD, *Senior Chemist*
RON BROADHEAD, *Senior Petroleum Geologist Head, Petroleum Section*
MONTE M. BROWN, *Photographer*
KATHRYN G. CAMPBELL, *Cartographic Drafter II*
STEVEN M. CATHER, *Field Economic Geologist*
RICHARD CHAMBERLIN, *Field Economic Geologist*
RICHARD R. CHAVEZ, *Assistant Head, Petroleum Section*
RUBEN A. CRESPIN, *Garage Supervisor*
LOIS M. DEVLIN, *Business Services Coordinator*
ROBERT W. EVELETH, *Senior Mining Engineer*
DEBBIE GOERING, *Staff Secretary*
LOIS GOLLMER, *Geotechnical Records Clerk*
IBRAHIM GUNDILER, *Senior Metallurgist*
STEVE HAASE, *Ground-Water Geologist*
WILLIAM C. HANEBERG, *Engineering Geologist*
JOHN W. HAWLEY, *Senior Env. Geologist*
CAROL A. HJELLMING, *Assistant Editor*
GRETCHEN K. HOFFMAN, *Coal Geologist*
GLEN JONES, *Computer Scientist/Geologist*
FRANK E. KOTTLOWSKI, *Emeritus Director/State Geologist*
PHILLIP KYLE, *Geochemist/Petrologist*
ANN LANNING, *Administrative Secretary*
ANNABELLE LOPEZ, *Petroleum Records Clerk*
THERESA L. LOPEZ, *Receptionist/Staff Secretary*
DAVID W. LOVE, *Senior Environmental Geologist*
JANE A. CALVERT LOVE, *Editor*
WILLIAM MCINTOSH, *Volcanologist/Geochronologist*
CHRISTOPHER G. MCKEE, *X-ray Facility Manager*
VIRGINIA MCLEMORE, ***Economic Geologist***
LYNNE McNEIL., *Computer Pub./Graphics Spec.*
NORMA J. MEEKS, *Director of Publications Office*
BARBARA R. POPP, *Chemical Lab. Tech. II*
MARSHALL A. REITER, *Senior Geophysicist*
JACQUES R. RENAULT, *Senior Geologist*
JAMES M. ROBERTSON, *Senior Economic Geologist*
JANETTE THOMAS, *Cartographic Drafter II*
SAMUEL THOMPSON III, *Emeritus Senior Petrol. Geologist*
REBECCA J. TITUS, *Cartographic Supervisor*
JUDY M. VAIZA, *Executive Secretary*
MANUEL J. VASQUEZ, *Mechanic 1*
JEANNE M. VERPLOEGH, *Chemical Lab. Tech. II*
ROBERT H. WEBER, *Emeritus Senior Geologist*
SUSAN J. WELCH, *Assistant Editor*
NEIL H. WHITEHEAD III, *Petroleum Geologist*
MARC L. WILSON, *Mineralogist*
DONALD WOLBERG, *Paleontologist*
MICHAEL W. WOOLDRIDGE, *Scientific Illustrator*
JIRI ZIDEK, *Chief Editor/Geologist*

Research Associates

CHRISTINA L. BALK, *NMT*
WILLIAM L. CHENOWETH, *Grand Junction, CO*
RUSSELL E. CLEMONS, *NMSU*
WILLIAM A. COBBAN, *USGS*
NELIA DUNBAR, *NMT*
CHARLES A. FERGUSON, *Univ. Alberta*
JOHN W. GEISSMAN, *UNM*
LELAND H. GILE, *Las Cruces*
JEFFREY A. GRAMBLING, *UNM*
CAROL A. HILL, *Albuquerque*
ALONZO D. JACKA, ***Texas Tec****h* BOB JULYAN, *Albuquerq**ue***
SHARI A. KELLEY, *SMU*
WILLIAM E. KING, *NMSU* MICHAEL J. KUNK, *USGS* TIMOTHY F. LAWTON, *NMSU* DAVID V. LEMONE, *UTEP*
GREG H. MACK, *NMSU*
NANCY J. MCMILLAN, *NMSU*
HOWARD B. NICKELSON, *Carlsbad* GLENN R. OSBURN, *Washington Univ.*
ALLAN R. SANFORD, *NMT*
JOHN H. SCHILLING, *Reno, NV*
WILLIAM R. SEAGER, *NMSU*
EDWARD W. SMITH, ***Tesuque***
JOHN F. SUTTER, *USGS*
RICHARD H. TEDFORD, *Amer. Mus. Nat. Hist.*
TOMMY B. THOMPSON, *CSU*

Graduate Students

WILLIAM C. BECK
JENNIFER R. BORYTA
TANYA BAKER
ROBERT L. FRIESEN
JOHN GILLENTINE
ROBERT S. KING
DAVID J. SIVILS SHIRLEY
WADE

Plus about 30 undergraduate assistants

Original Printing 1987
Reprinted 1992

Published by Authority of State of New Mexico, NMSA 1953 Sec. 63-1-4
Printed by University of New Mexico Printing Services, June 1992

Available from New Mexico Bureau of Mines & Mineral Resources, Socorro, NM 87801
Published as public domain, therefore reproducible without permission. Source credit requested.

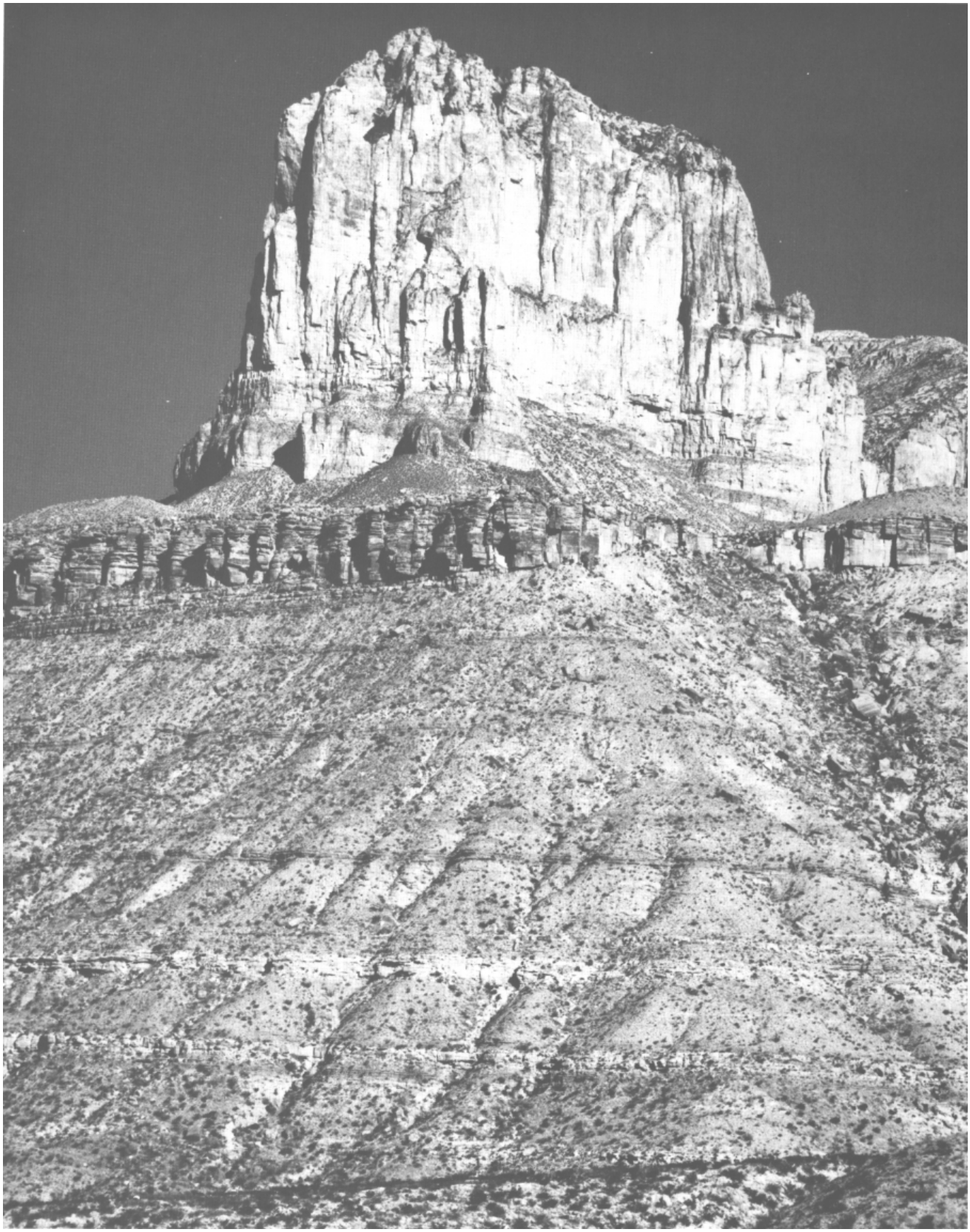

El Capitan, Guadalupe Mountains National Park. Photo National Park Service.

Contents

Figures

Sheets (in pocket)

Plates (in color)

Tables

Preface

This paper is intended for a variety of readers. It is meant for the geologist who wants to understand caves in the Guadalupe Mountains from a regional perspective; for the speleologist who wants to understand how these caves differ from other caves; for the caver who wants to better appreciate what he or she is seeing in Guadalupe caves; and for the visitor to Carlsbad Cavern as an interpretive guide to its geology and mineralogy. Such a multipurpose intent has its problems. Only the experienced speleologist has the background to understand all parts of this paper. Geologists will not necessarily be familiar with the specifics of cave geology or with the speleological terms. Cavers will recognize much of the speleological jargon, but will not necessarily realize the full geological significance of what is being discussed. Cave visitors may be interested in learning only about certain aspects of the caves, e.g. the travertine formations (speleothems) in Carlsbad Cavern.

Because of such problems, the paper has been organized so as to be helpful to all readers. It is divided into two parts, speleogenesis and mineralogy. These parts are interrelated, but are presented in such a way that they can be read and understood separately. In both the speleogenesis and mineralogy sections, pictures have been included of most types of cave deposits and speleothems so that the caver can use the publication as a guide to a number of caves in the Guadalupe Mountains. For the visitor to Carlsbad Cavern, specific reference is made to a number of deposits and speleothems that can be seen along the trail.

Acknowledgments—I wish to thank Ronal Kerbo, William Dunmire, Robert Crisman, Jim Walters, Larry Henderson, Larry Villalva, Phillip Van Cleave, Donna Giannantonio, and John Roth of the National Park Service; Tom Davis, Jerry Trout, Bob Trout, and John Burke of Lincoln National Forest; and Buzz Hummel of the Bureau of Land Management for continued administrative support over the years. Sample collection was permitted by the above agencies.

Roger Anderson, George Bachman, Rane Curl, Donald Davis, Harvey DuChene, Stephen Egemeier, Derek Ford, David Love, George Moore, Robert Osburn, Arthur Palmer, Margaret Palmer, Michael Queen, John Thrailkill, and Sam Thompson III reviewed the manuscript. Other people of professional assistance were Scott Altenbach, Jim Brierley, Douglas Caldwell, Dave DesMarais, Ben Donegan, Paolo Forti, Dave Gillette, John Guilbert, Arthur Harris, David Jagnow, Klaus Keil, Douglas Kirkland, John McLean, Pa-trick Moore, Robert North, Marcel Rider, Steven Sares, Henry Schwarcz, Cyndi Mosch Seanor, Richard Smith, Jim Smith, Ed Speer, Steve Stokowski, Harold Thode, Calvin Welbourn, Steve Wells, and James Wright.

Cyndi Mosch Seanor and Roy Hill were particularly helpful in the field, Bob Buecher, Debbie Buecher, Tom Rohrer, and Bill Wilson in cartography and Alan Hill, Ronal Kerbo, and Cyndi Mosch Seanor in photography. John Burke, Wayne Burks, Kendrick Day, Jeep Hardinge, Dave Jagnow, Pete Lindsley, Tom Meador, Ron Miller, Arthur Palmer, Bob Trout, Jerry Trout, and Jon Vinson also contributed photographs. Derek Ford, Jim Cowart, Rainer Gran, Gerd Hennig, Victor Schmidt, George Brook, Brooks Ellwood, Luis Gonzalez, Kevin Given, Tom Bills, and Russell Harmon were responsible for doing, or helping with, the age or carbon–oxygen determinations. John Husler, Ellen Semarge, and Karl Emmanuel of the University of New Mexico Geology Department, and John Bologna of the Los Alamos Scientific Laboratory, performed the chemical analyses. Jerry Gomez, Ken Kietzke, and Tom Servilla of the University of New Mexico Geology Department did the thin sectioning and feldspar staining. Shell Oil Company and David Jagnow donated thin sections of the chert, and Sandia Laboratory donated the use of a MicroRmeter for gamma-ray measurements. Core Laboratories (Petroleum Reservoir Engineering), Farmington, New Mexico, measured porosity and permeability of bedrock samples and Geochron Laboratories (Krueger Enterprises), Cambridge, Massachusetts, did the sulfur-isotope and fluid-inclusion analyses.

Finally, I wish to thank the Cave Research Foundation for field and cartographic support, and my husband Alan for assistance and moral support over the eighteen years of this study.

Abstract

Sulfur-isotope data, whole-rock analyses, and pH-dependence of the mineral endellite support the hypothesis that the large cave passages in the Guadalupe Mountains were dissolved primarily by sulfuric rather than carbonic acid. Floor gypsum deposits up to 10 m high and native sulfur in the caves are significantly enriched in the light isotope of sulfur; $\delta^{34}S$ values as low as -25.6 indicate that the cave sulfur and gypsum are the end products of biological oxidation and reduction reactions associated with the oil and gas fields of the Delaware Basin. As the Guadalupe Mountains uplifted and tilted to the northeast during the late Pliocene–Pleistocene, oil and gas moved updip in the basin and reacted with anhydrite at the base of the Castile Formation to form H_2S, CO_2, and the "castile" limestone masses. Where halite beds in the Castile Formation remained intact, they acted as impermeable barriers preventing the gas from rising to the surface in the basin. Instead, the hydrogen-sulfide gas rose into the Capitan reef along joints or the Bell Canyon Formation and there reacted with meteoric, oxygenated, ground water to form sulfuric acid. The sulfuric acid attacked the limestone and dissolved out the large caves of the Guadalupe Mountains.

From oldest to youngest, the general sequence of deposits in Guadalupe caves is: breccia, montmorillonite, spar, calcified siltstone–cave rafts, cobble gravel, endellite, silt, chert, gypsum, breakdown, speleothems, sulfur, bat guano, and animal bones. The breccia fills fissures (Solution Stage I caves) truncated by the large cave passages and is believed to be a Late Permian deposit contemporaneous with sandstone-dike fillings in the Guadalupe Mountains. Montmorillonite fills small spongework cavities in the limestone (Solution Stage II caves) and has a speculative age of 188 ± 7 my (Late Jurassic), as determined by the potassium-argon method. It may be Solution Stage II residue which formed in a basic (pH = 8–9), bicarbonate-rich, slow-flowing aquatic environment some time between the Late Permian and the Tertiary.

The large horizontal and vertical passages (Solution Stage III caves) formed in the late Pliocene—Pleistocene when uplift and tilting of the Guadalupe Mountains caused H_2S and CO_2 gas to migrate from the basin into the reef. Uplift of the mountains also initiated a basic pattern of bathyphreatic flow whereby water entering the recharge area took a deep course through the reef bedrock to spring outlets controlled by the position of regional base level. Initial flow was guided by joints, bedding planes, joint intercepts, and facies contacts. Main trunk passages evolved along these routes, and, as discharge springs continually shifted to lower base-level positions, water-table conditions prevailed over bathyphreatic conditions and fast flow was replaced by slow flow.

Just below the descending water table, spar formed in the shallow phreatic zone where slow-flow, barely saturated conditions were responsible for the nucleation and growth of large crystals. Age of spar crystals collected at various levels in Carlsbad Cavern from the entrance down to the Mystery Room (about 200 m elevation difference) all exceed 350,000 yrs (the limit of the U-series dating technique), and spar at the Big Room level has been dated at 879,000 ± 124,000 yrs by the Electron Spin Resonance (ESR) dating technique. While the spar was forming just below the water table, the rafts of the calcified siltstone–cave raft sequence were forming on the surface of the water table. Carbon–oxygen-isotope data and dates on the rafts confirm that these deposits formed early in the Solution Stage III episode and are not the product of a previous exhumation of the reef. The cobble gravel in Carlsbad Cavern may also be an early Solution Stage III deposit. The cobble gravel either underlies, or is interbedded with, paleomagnetically reversed (>730,000 yrs) silt and is believed to be backreef, possibly Ogallala (or Gatuña) material which gravitated into bathyphreatic cave voids near the beginning of the uplift of the Guadalupe Mountains.

Sulfuric acid dissolved out the large Solution Stage III cave passages, and silt residue released during this dissolution settled directly to the floor. During this sulfuric-acid episode, montmorillonite altered to endellite and chert, and massive gypsum precipitated out on top of the silt during water-table conditions of hydrodynamic stagnation. Laminations, microfolding, slickensides, overgrowth crusts, limestone inclusions, insoluble residue, and recrystallization, replacement, and breccia textures in the gypsum attest to its method of precipitation and solidification. Commode holes, drip tubes, and streamlined surfaces in the gypsum represent dissolution features which formed after the gypsum had consolidated.

Breakdown, speleothems, sulfur, bat guano, and animal bones all deposited in the caves after they had become air-filled. Most of the breakdown fell a short time after the subsidence of the water table, one notable exception being Iceberg Rock, which fell between 180,000-513,000 ybp, some time after the water had subsided from the Main Corridor. Speleothems have been dated at approximately 500,000-600,000 ybp in Lower Cave and in the Main Corridor near Iceberg Rock, showing that these cave passages had become air-filled by that time. Speleothems in the upper, Bat Cave level of Carlsbad Cavern can be older than the speleothems in these lower passages, and speleothems in higher-altitude Guadalupe caves, such as Cottonwood and Virgin, can be older still. Many speleothems in Guadalupe caves are severely corroded due to high levels of CO_2 and/or H_2S which degassed at the surface of the water table. Degassing H_2S, which ascended from the basin along with the CO_2, oxidized to native sulfur under air-filled conditions and coated the undersides of bedrock and speleothems. Bat guano and animal bones attest to the fact that bats and animals entered the caves of the Guadalupe Mountains as soon as they had developed entrances. The entrance of Carlsbad Cavern may have been open as long ago as 112,000 ybp, as indicated by dates on sloth *(Nothrotheriops)* bones from the Lower Devil's Den area.

A variety of carbonate and sulfate speleothems formed in Guadalupe caves from dripping, flowing, seeping, pool, and condensation water. Evaporation and carbon-dioxide loss have been prime factors in the deposition of the magnesium-carbonate minerals hydromagnesite, huntite, and dolomite, and in the formation of speleothems such as moonmilk, popcorn, bell canopies, and tower coral. Most travertine material deposited during wet and humid glacial stages of the Pleistocene, about 350,000-600,000 and 140,000-170,000 yrs ago. Then, at about 120,000-130,000 yrs ago and again during the last 10,000 yrs, most travertine ceased growing due to a shift from pluvial to arid climatic conditions. Sulfur-isotope data show that sulfate speleothems, where they do occur in Guadalupe caves, have probably derived from pyrite in the overburden.

PART I: SPELEOGENESIS

Introduction

Purpose

The origin of Carlsbad Cavern and other caves in the Guadalupe Mountains has been one of the great unsolved mysteries of speleogenesis. Geomorphically, Guadalupe caves bear little resemblance to other great cave systems of the world. Rooms are huge, yet passages are not long and terminate abruptly. The caves seem unrelated to surface topography or to ground-water-flow routes. Especially enigmatic are the large deposits of gypsum and the colorful waxy clay in the caves.

For over 30 years the prevailing theory has been that Guadalupe caves formed similarly to other caves; that is, by carbonic-acid dissolution at the water table. Within the past 10 years three new theories of origin have been proposed, all of which differ significantly from one another and from the earlier theory. All of these four theories are based mainly on field observations, despite the pertinence of a number of analytical techniques to speleogenesis problems.

This paper is a summary of a lengthy investigation which has utilized observational, stratigraphic, geochemical, dating, and isotopic techniques. The purpose of Part I is to describe cave deposits and discuss speleogenesis events from Permian time to the present.

Previous work

The first geologist to study any Guadalupe cave was Lee (1924a, 1925a, b). His articles were primarily of a popular nature, and it was not until 1949 that Bretz published his now classic *Carlsbad Caverns and other caves of the Guadalupe Block, New Mexico.* In that paper, Bretz invoked a concept of Davis (1930) to explain cave levels and spongework as phreatic features formed in the zone of saturation. The only exceptions to Bretz's phreatic rule for Guadalupe cave development was a late-stage, gypsum-depositing episode and a brief, silt- and cobble-carrying, vadose-stream episode in Lower Cave of Carlsbad Cavern. Bretz thought that the massive gypsum deposits in Carlsbad Cavern were a consequence of local pooling and that the source of the gypsum was the Castile Formation which lies close to the reef escarpment. The 1.5 m thick gypsum in McKittrick Cave was interpreted by him as a secondary flowstone rather than as correlative in character and origin to the gypsum deposits in Carlsbad Cavern.

Bretz's (1949) interpretation of regional geology hinged strongly on the observations he made in Carlsbad Cavern; together with Horberg (1949b), he postulated three stages of reef modification: (1) a pre-Ogallala exhumation of the reef, during which time the caves in the Guadalupe Mountains formed; (2) filling of the Pecos valley with 400 m of Ogallala alluvium; and (3) a Pleistocene exhumation of the reef, which is still continuing today. Inasmuch as Guadalupe caves are truncated by present-day erosion of the reef and hence are older than the escarpment, and inasmuch as the supposed vadose "stream" in Lower Cave had to exit and descend to a lower base level, Bretz concluded that the caves predated the present erosion cycle. Gale (1957) and Thomas (1971) echoed Bretz's theory of two stages of reef exhumation, and other investigators following Bretz's lead attributed the massive gypsum in the caves to a late-stage back-up of water (Good, 1957; Sanchez, 1964; Bullington, 1968). Black (1954) and Gale (1957) reiterated Bretz's view that the source of the cave gypsum was the Castile Formation in the Delaware Basin.

Nearly 30 years elapsed before the speleogenesis model of Bretz was challenged. Queen (1973) and Queen et al. (1977a, b) introduced an entirely new theory: a speleogenesis model in which gypsum replaced limestone where gypsum-saturated brines in the Delaware Basin mixed with fresh meteoric water in the reef aquifer. When the gypsum was later dissolved by vadose water, cave passages were left void except for a few remnant gypsum deposits on cave floors and walls. Queen et al. (1977a, b) cited replacement textures in the gypsum deposits of Cottonwood Cave as evidence supporting their theory. Queen believed, as had Bretz, that the caves in the Guadalupe Mountains formed in pre-Ogallala time and that there have been at least two exhumations of the reef.

A few years after Queen proposed his startling new theory, Jagnow (1977, 1979) came out with an entirely different one. Jagnow essentially followed Bretz's model of phreatic cave development, but he invoked the notion that sulfuric acid was partly responsible for the dissolution of Guadalupe caves. According to Jagnow, pyrite from the Yates Formation was the source of the sulfuric acid. Acidic solutions moved along bedding planes in the Yates until they reached vertical joints and descended to the Seven Rivers or Capitan Formations where they dissolved out the caves. The reaction between sulfuric acid and limestone produced gypsum as a by-product.

The fourth model of speleogenesis for Guadalupe caves has been advocated by Davis (1979a, b, 1980), whose model is a modification of a theory of speleogenesis first proposed by Egemeier for the caves of the Big Horn Basin, Wyoming. Egemeier (1971, 1973, 1981) termed his theory of speleogenesis "replacement-solution." According to this theory, sulfide-bearing water ascends via thermal springs to base level, where hydrogen sulfide reacts with oxygen in the cave air to form sulfuric acid. The acid attacks the limestone, which is then directly replaced by a thin crust of gypsum. Davis' modification of Egemeier's theory stressed cavern dissolution along upwelling limbs of deeply curving flow paths, and the pits underlying large cave rooms were regarded by him as input points for ascending water. The source of the sulfuric acid necessary for "replacement-solution" was ascribed by Davis to the oil and gas fields of the Delaware Basin and his claim was supported by the finding of Hinds and Cunningham (1970, p. 7) that "hydrogen sulfide is commonly found in formation waters throughout most of Eddy Co."

Geographic setting

Location and physiography

The study area encompasses the Guadalupe Mountains of southeastern New Mexico and western Texas (Fig. 1), a region of sharp limestone ridges and steep-walled escarpments. The Guadalupe Mountains are a wedge-shaped block bounded on the west by a fault-line escarpment and on the east by an exhumed-reef escarpment and the Gypsum Plain (Figs. 2, 3). The area is bounded by the McKittrick Hill anticline on the northeast, Guadalupe Peak on the south-west, the Capitan reef escarpment on the southeast, and the Dark Canyon drainage on the northwest. The highest elevation in the area is Guadalupe Peak at 2,667 m; the lowest point is Wind (Hicks) Cave at 1,115 m. The area forms a narrow band 6.4-9.6 km wide and 80 km long through Eddy County, New Mexico, and Culberson County, Texas.

FIGURE 1—Location of the study area. After Jagnow (1979).

The region is dominated by thick limestone reef deposits and surrounding related rock within which extensive caves have developed. Cave locations are within Carlsbad Caverns and Guadalupe Mountains National Parks, and on lands controlled by Lincoln National Forest and the Bureau of Land Management. The highest cave, Cottonwood, is at an altitude of 2,074 m, and the lowest known cave passage, the Lake of the Clouds, Carlsbad Cavern, is at 1,007 m.

Two notable drainage systems exist in the area: a northeast—southwest drainage system which includes North and South McKittrick Canyons, Cottonwood Canyon, Dark Canyon, West Slaughter Canyon, North and South Rattlesnake Canyons, and Walnut Canyon; and a northwest—southeast drainage system which includes Big Canyon, Black Canyon, Gunsight Canyon, Double Canyon, Lechuguilla Canyon, and Slaughter Canyon (Fig. 5). The drainage systems have downcut the Guadalupe Mountains into a series of northeast- and northwest-trending ridges.

Climate

The climate in the Guadalupe Mountains is semiarid and continental, with characteristically mild winters and warm summers. The average winter temperature is 7°C and the average summer temperature is 27°C. Precipitation aver-ages 35.6 cm annually, with 80% of the rainfall occurring in the May through October period (Houghton, 1967). Vegetation includes cactus, succulents, and desert shrubs in

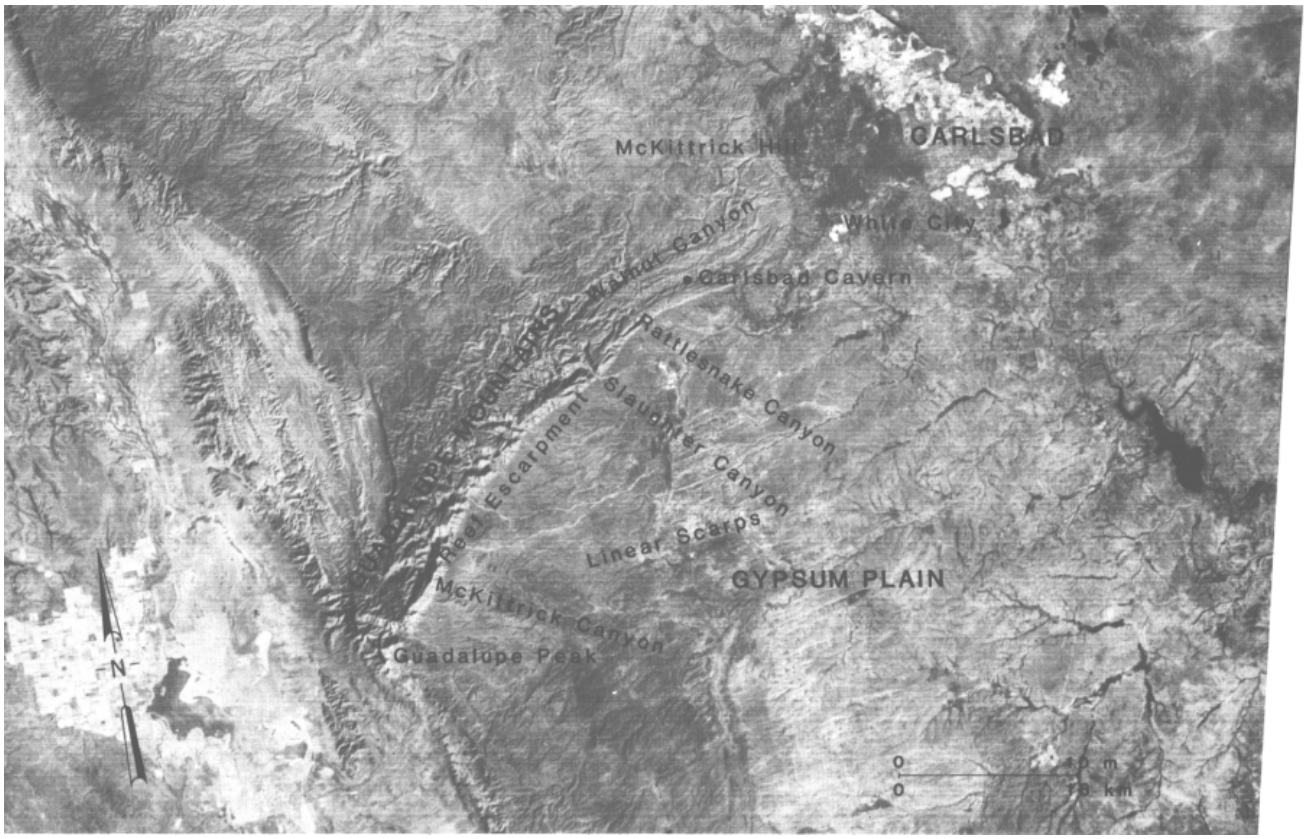

FIGURE 2—Landsat image of the triangular, wedge-shaped Guadalupe Mountains area.

FIGURE 3—The Guadalupe Mountains and Gypsum Plain near Carlsbad, New Mexico. The Capitan reef escarpment rises along the edge of what once was the Delaware Basin. The headquarters of Carlsbad Caverns National Park sits atop the remains of the reef. Guadalupe Peak can be seen at the extreme upper left, Slaughter Canyon is in middle distance, and Walnut Canyon is a snakelike feature on the right. Photo Jeep Hardinge.

the lower Guadalupe Mountains, with transitional to montane coniferous forest on the upper Guadalupe ridges.

Past climate in the Guadalupe Mountains was more moist and cool than it is today. During much of the Pleistocene, coniferous forests reached to lower elevations and animal life included bear, American lion and cheetah, ground sloth, shrew, tapir, bison, bighorn sheep, camel, and llama (Harris, 1985).

Geologic setting

The geology of the Guadalupe Mountain region has been described by Lloyd (1929), King (1942, 1948), Newell et al. (1953), Hayes (1957, 1964), Hayes and Koogle (1958), Kelley (1971, 1972), and many others. In this study, the regional geology is discussed only insofar as it applies to cave-related questions.

Permian rocks in the region can be divided from southeast to northwest into three facies: the Delaware Basin, reef, and Northwest Shelf (Figs. 4, 5). The rock units of interest in the basin are the Bell Canyon Formation of the Guadalupian Series and the Castile, Salado, and Rustler Formations of the Ochoan Series (Table 1). In the basin-margin reef area the formation of interest is the Capitan Limestone, which is subdivided into a massive (reef) member and a breccia (forefeef) member. These two members are transitional with each other both laterally and vertically. The breccia member of the Capitan grades southeastward into the Bell Canyon Formation of the Delaware Basin. In the backreef Northwest Shelf area, the units of interest are the Queen, Seven Rivers, Yates, and Tansill Formations of the Artesia Group. The upper three units are laterally equivalent to the Capitan Limestone.

Tertiary deposits in the area include the Ogallala and Gatuña Formations, alluvial gravels of probable Pliocene and Pleistocene age, respectively (Bachman, 1976).

Summary of geologic history

A lowland that existed in southeastern New Mexico during the Precambrian and Cambrian became inundated by shallow seas in the Late Cambrian through Mississippian. The region first became tectonically active in the Precambrian, and during the Pennsylvanian compressional forces caused movement along a northwest-trending thrust fault. Renewed tectonic activity in the Early Permian resulted in a rapid sinking of the Delaware Basin, an elongate, bowl-shaped depression around which grew an extensive organic reef known as the Capitan Limestone. As this reef grew upward, reef debris slumped basinward, and, as new generations of reef organisms progressively colonized the debris pile, the reef grew over its own debris and outward, toward the basin. In shallow lagoons behind the reef, sandstone, limestone, and dolomite beds of the Artesia Group were deposited contemporaneously with the reef limestone; in the basin itself, thin petroliferous limestone and sand-stone layers of the Bell Canyon Formation and thick evaporite sequences of the Castile Formation accumulated.

At the close of Permian time, roughly 230 my ago, the entire region was tilted and uplifted above sea level, as indicated by an angular unconformity between Late Permian beds and overlying terrestrial beds of the Triassic Dockum Group. The rock record for most of the rest of the Mesozoic is absent, possibly because the Guadalupe Mountain region was above sea level throughout the Jurassic and

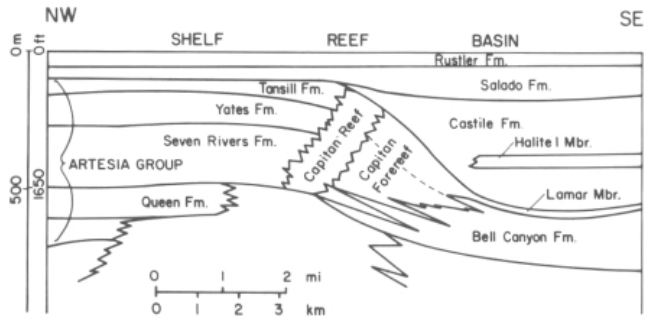

FIGURE 4—Stratigraphic units of the Northwest Shelf, reef, and Delaware Basin during Permian time. After Bachman (1980).

TABLE 1—Major stratigraphic divisions, southeastern New Mexico (after Bachman, 1980).

ERATHEM	SYSTEM	SERIES	GROUP OR FORMATION	AGE ESTIMATE
Cenozoic	Quaternary	Holocene	Windblown sand	10,000 yrs 20,000 yrs
		Pleistocene	Mescalero caliche Gatuña Fm.	500,000 yrs 600,000 yrs
	Tertiary	Pliocene	Ogallala Fm.	1.8 my
		Miocene		5 my
		Oligocene Eocene Paleocene	Absent	22.5 my
Mesozoic	Cretaceous	Lower	Detritus only	65 my
	Jurassic		Absent	141 my
	Triassic	Upper	Dockum Group	195 my
Paleozoic	Permian	STAGES		230 my
		Ochoan	Dewey Lake Red Beds Rustler Fm. Salado Fm. Castile Fm.	
		Guadalupian	Capitan Ls. Bell Canyon Fm. Tansill Fm. Yates Fm. Seven Rivers Fm.	251 my 280 my

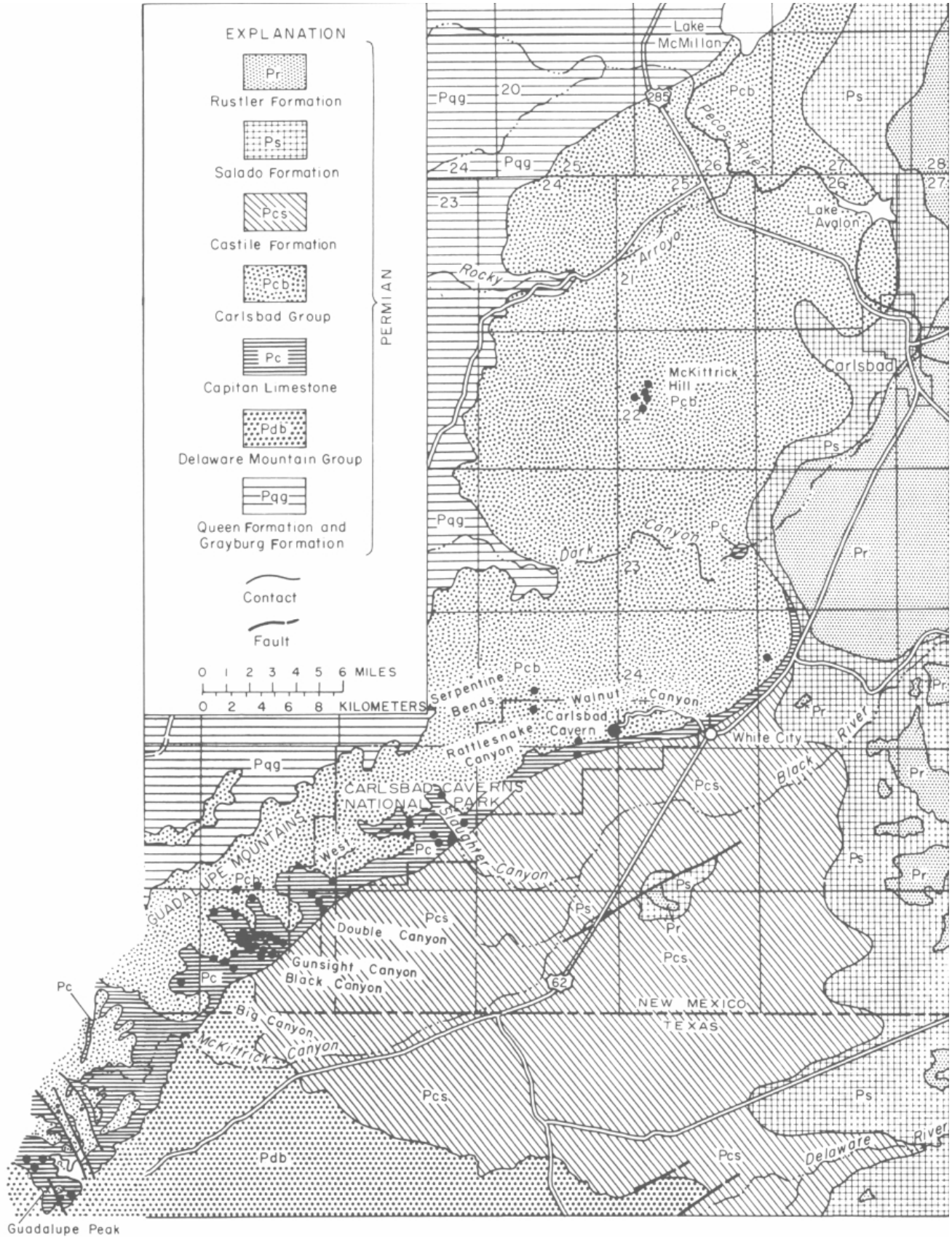

FIGURE 5—Geologic map of the Guadalupe Mountains showing physiographic features, bedrock units, and cave locations. After King (1948) and Moore (1960a).

most of the Cretaceous. The sea again spread over at least part of the area late in the Cretaceous as confirmed by small patches of fossiliferous Cretaceous rock found on the surface and collapsed into the subsurface of the Gypsum Plain. In the Late Cretaceous or early Tertiary, the area was affected by another broad uplift which gently folded bedrock and tilted it slightly to the northeast.

By the middle Tertiary, or roughly 10 my ago, the area was reduced to an erosion surface of low relief. The presence of siliceous gravel, dendritic stream patterns, and entrenched meanders in the Guadalupe uplands are evidence that the area was at or near base level during that time.

The main uplift and tilting of the Guadalupe Mountains occurred in the Pliocene to Pleistocene (1–3 my ago). Concurrent with uplift, oil and gas accumulations in the Bell Canyon Formation of the Delaware Basin migrated updip toward the reef. Hydrologic connection between the Capitan Limestone aquifer and the Pecos River was probably established during this time, and, since then, movement of ground water in the reef aquifer has been controlled by changes in the regional base level of the Pecos River.

Stratigraphy

Permian deposits

Backreef—In Permian time the Capitan reef acted as a discontinuous barrier behind which the light-colored, thin-bedded limestones, sandstones, and dolomites of the back-reef Northwest Shelf facies accumulated. These beds were deposited contemporaneously with the reef itself and dipped toward the reef at angles of a few degrees. The oldest major cave-bearing rocks of the shelf facies are the Queen and Seven Rivers Formations, units composed of dolomite beds which thicken conspicuously as they approach the limestone reef. Overlying the Seven Rivers Formation are the Yates and Tansill Formations which act as caprock protecting the more soluble Seven Rivers from dissolution and truncation.

The Yates Formation is an especially silty and sandy unit containing limonite pseudomorphs after pyrite disseminated in the upper two-thirds of the formation. The Yates Formation is too silty to be cave-bearing except near its contact with the reef or with the Seven Rivers Formation; such caves as Spider Cave and the McKittrick Hill caves are developed at these localities. In Spider Cave, an apparent dip of 2°S has been measured on Yates bedding planes (R. Bridgemon, written comm. 1980). Hill (1972) reported a porosity of 0.5% and a permeability of 0.02 millidarcies parallel to bedding for a silty limestone believed to be part of the Yates Formation in the Main Corridor of Carlsbad Cavern near Devil's Spring.

The Tansill Formation is a thin to medium-bedded, white to tan, microgranular to fine-grained dolomite which Tyrrell (1964) believed to be equivalent in age to the Lamar Member of the Bell Canyon Formation in the Delaware Basin. No younger beds of Permian age overlie the Tansill Formation within the study area, but the Salado Formation overlies it in the subsurface east of the Pecos River. In the vicinity of the entrance to Carlsbad Cavern, the Tansill Formation strikes N77°E and dips about 3–4°SE (Sanchez, 1964). Hill (1972) reported that the Tansill Formation near the cave entrance has a porosity of 2.2% and a permeability of 0.51 millidarcies parallel to bedding and 0.01 millidarcies perpendicular to bedding.

Reef—The Capitan Limestone includes a massive reef-core facies and a breccia (talus) forereef facies. These two facies grade laterally and vertically into each other and together reach thicknesses of 450–600 m. The reef-core facies is poorly bedded to massive and weathers to form steep cliffs in the canyons of the Guadalupe Mountains. The forereef facies is a well-cemented breccia which weathers to ragged slopes; it consists of thick, crudely bedded layers of limestone that have depositional dips of 20–35° (Hayes, 1957; Ward et al., 1986).

The reef-core facies of the Capitan Limestone is a fine-grained, light-gray to cream-colored, vuggy limestone. Fossils are mostly algae and sponges and, in general, are poorly preserved. The Capitan reef limestone is a porous unit which serves as the aquifer for much of the Guadalupe Mountain area. Hill (1972) reported a porosity of 1.5% and a permeability of 14.0 millidarcies for the Capitan Limestone exposed near Iceberg Rock, Carlsbad Cavern. Primary cavities of the reef core are up to several centimeters in diameter, and secondary enlargements can range from pore-size holes to cavern-size chambers (Palmer, 1975). Most of the caves in the Guadalupe Mountains are developed in the reef-core facies.

The forereef facies is a light-buff to pink, dolomitic brecciated limestone. Brachiopods (Fig. 6), bryozoans, crinoids, foraminifers, and sponges are plentiful in the forereef and are commonly well preserved. Breccia fragments in the forereef facies range from sand-sized particles up to boulder-sized clasts. The forereef facies is not nearly as cave-bearing as the reef core; cave passages usually terminate near where forereef beds are encountered.

The Capitan Limestone has been interpreted by most investigators to be a barrier reef (Lloyd, 1929; King, 1942; Adams and Frenzel, 1950; Newell et al., 1953; Hayes, 1964), but others have considered it either a linear organic bank (Achauer, 1969) or a line of organic mounds separated by lagoons connecting the shelf and basin provinces (Motts, 1957; Dunham, 1972; Cronoble, 1974). Achauer divided the Capitan Limestone into three distinct lithologic facies: an organic-skeletal limestone which constitutes the massive reef core, an organic-skeletal dolomite which constitutes the reef talus, and a dolomite breccia, a local facies found at or near the contact of the reef limestone and backreef shelf rocks.

Basin—While an immense reef structure was building upward around the margins of the Delaware Basin, shaly, organic limestones and clean, fine-grained sandstones of the Bell Canyon Formation were contemporaneously being deposited within the basin. Then, as the Delaware Basin became closed off and sea water was restricted from entering it, thick evaporite sequences of the Castile, Salado and Rustler Formations were deposited subsequent to reef growth.

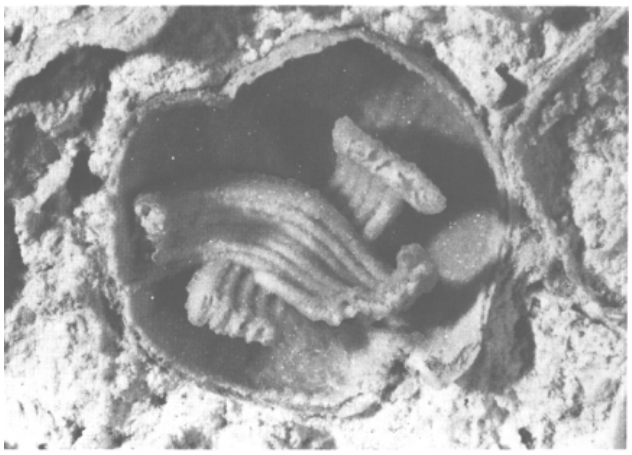

FIGURE 6—Spiriferid brachiopod in a passage near Mabel's Room, Carlsbad Cavern. The delicate spiralia, which provided support for internal organs, are unusually well preserved in this specimen. Photo Arthur Palmer.

The Bell Canyon Formation is composed of five limestone members and five sandstone members. The Lamar Member is the principal oil- and gas-bearing rock in the basin. It is an easily recognizable, black, shaly, petroliferous limestone of low permeability and porosity, widely used by oil geologists as a subsurface marker. The Ramsey sandstone member of the Bell Canyon Formation consists of very clean, well-sorted, fine-grained quartz-sand beds (Grauten, 1965; Watson, 1979); it averages about 26% in porosity and 50 millidarcies in permeability (Table 12). Near the Capitan reef margin the Bell Canyon Formation is characterized by gentle dips (less than 1°), but where it interfingers into the reef, beds dip upward at angles of 10–30° (King, 1942; Adams and Frenzel, 1950).

Overlying the Bell Canyon is the Castile Formation, a thick, deep-water, evaporite sequence composed of several hundred meters of intricately layered anhydrite, gypsum, halite, and subordinate limestone. Layering within the Castile is cyclic, with calcite and anhydrite alternating every few millimeters and with each calcite–anhydrite couplet representing an annual varve or periodic accumulation of material. Based on varve counts, Dean and Anderson (1978) estimated that the rate of gypsum precipitation within the Delaware Basin was approximately 1.9 mm per year. Cycles having periods of 1,000 to 3,000 years are persistent features of the Castile Formation; these cycles have been correlated with great precision over the entire basin for distances up to 113 km (Anderson et al., 1972).

Three halite members occur within the Castile Formation. The lowermost member, Halite I, is the thickest and most extensive. The halite members have become significantly eroded, the top ones having experienced more erosion from meteoric water than the bottom one. All three members extended beyond their present limit into the western part of the basin earlier in the Tertiary, but since then the halite-solution margin has moved progressively eastward and dissolution of the salt has formed blanket-solution breccia zones where the halite used to exist (Anderson et al., 1972).

The eroded surface of the Castile Formation south of Carlsbad, New Mexico, forms what is known as the Gypsum Plain (Fig. 7). It is a karst terrain containing sinkholes, troughs, collapse breccia, sinking streams, and gypsum caves (Lee, 1924b; Weberneck, 1952; Kirkland and Evans, 1976; Gutierrez, 1981; Smith, 1981; Sares, 1984). Unusual features of the Gypsum Plain are the "castiles"—circular, haystack-like, limestone buttes rising a few to 30 m above the level of the plain (Adams, 1944). These steep-sided buttes were created by the replacement of anhydrite and gypsum by calcite, a process which preserved even the most minutely varved and microfolded textures in the evaporite rock (Anderson and Kirkland, 1966). The castile buttes are located at or near the contact of the Castile Formation with the underlying Bell Canyon Formation (Fig. 84) and are the sites of hydrogen-sulfide degassing and sulfur mineralization.

FIGURE 7—The Gypsum Plain as viewed from Big Canyon, Guadalupe Mountains. Note blade-like projections of the unbedded Capitan Limestone and the horizontal bedding planes of the Seven Rivers Formation. Photo Alan Hill.

Tertiary deposits

Tertiary deposits of the Ogallala and Gatuña Formations overlie Permian rocks because Triassic, Jurassic, and Cretaceous sediments were never deposited or have been mostly (Cretaceous) removed by erosion. Gravel of the Ogallala Formation consists primarily of worn cobbles of limestone and pebbles of quartzite, chert, jasper, and basalt (Bretz and Horberg, 1949b). Horberg (1949) reported quartzose gravel on the flat-topped summits of the Guadalupe Mountains and believed they indicated a former peneplain at that level. Horberg thought these gravels were Ogallala in age, but G. Bachman (pers. comm. 1986) favors a Gatuña identity for this gravel. Remnants of this gravel veneer the summit ridge of Carlsbad Cavern 0.4–1.0 km east of the cave entrance (Fig. 8). This gravel consists of: (1) very well-rounded quartzite pebbles of assorted colors (white, tan, gray, pink, black); (2) subrounded pieces of black flint; (3) small subrounded pieces of red jasper; and (4) rare pieces of rounded, scoriaceous lava (Fig. 9). No rounded limestone cobbles coexist with the siliceous gravel on the Carlsbad Cavern Ridge; this is probably due to preferential erosion of the limestone over time with respect to the more resistant siliceous pebbles.

Stratigraphic controls on cavern formation

Four main zones of preferential cave solution are controlled by stratigraphy (Jagnow, 1979; Fig. 10):

(1) *Below the Yates transition into the massive Capitan Formation.* The three largest caves in Carlsbad Caverns National Park—Carlsbad Cavern, Ogle Cave, and New Cave—occupy this stratigraphic position. The relatively impermeable, fine-grained siltstone of the Yates Formation collects oxygenated ground water from the Northwest Shelf area and discharges it directly into the massive member of the Capitan Limestone.

(2) *At the contact between the massive and breccia facies of the Capitan Limestone.* The contact between the massive and breccia facies of the Capitan Limestone is another stratigraphic location for cavern development because it is here that the bedding planes of the breccia facies interrupt the movement of ground water in the vertical joints of the massive facies. Caves which have formed at this contact are Musk Ox, Helen's, Wen, Vanishing River, Pink Fink Owlcove, and Frank's. Carlsbad Cavern, Ogle Cave, and New Cave also occupy this stratigraphic position, in addition to being below the Yates–Capitan transition.

(3) *At the transition of the Capitan Limestone with other members of the Artesia Group.* Oxygenated ground water moves downdip along the Tansill, Seven Rivers, and Queen Formations until it meets with the Capitan Limestone. Caves formed at the junction of these units are Three Fingers, Sentinel, Big Door, Lechuguilla, Pink Dragon, Pink Palette, Pink Panther, Wind (Hicks), Madonna, Goat, Virgin, and Damn.

(4) *Beneath the Yates contact with the Seven Rivers.* Where the Yates caprock is broken by major joints, oxygenated ground water descending from the surface has access to the underlying Seven Rivers Formation. Caves formed at or near this contact are Cottonwood, Queen of the Guadalupes, Hidden, Hell Below, Cave Tree, Decorated, McCollhum's Pit, Black, Dry, Endless, McKittrick, Sand, and Little Sand.

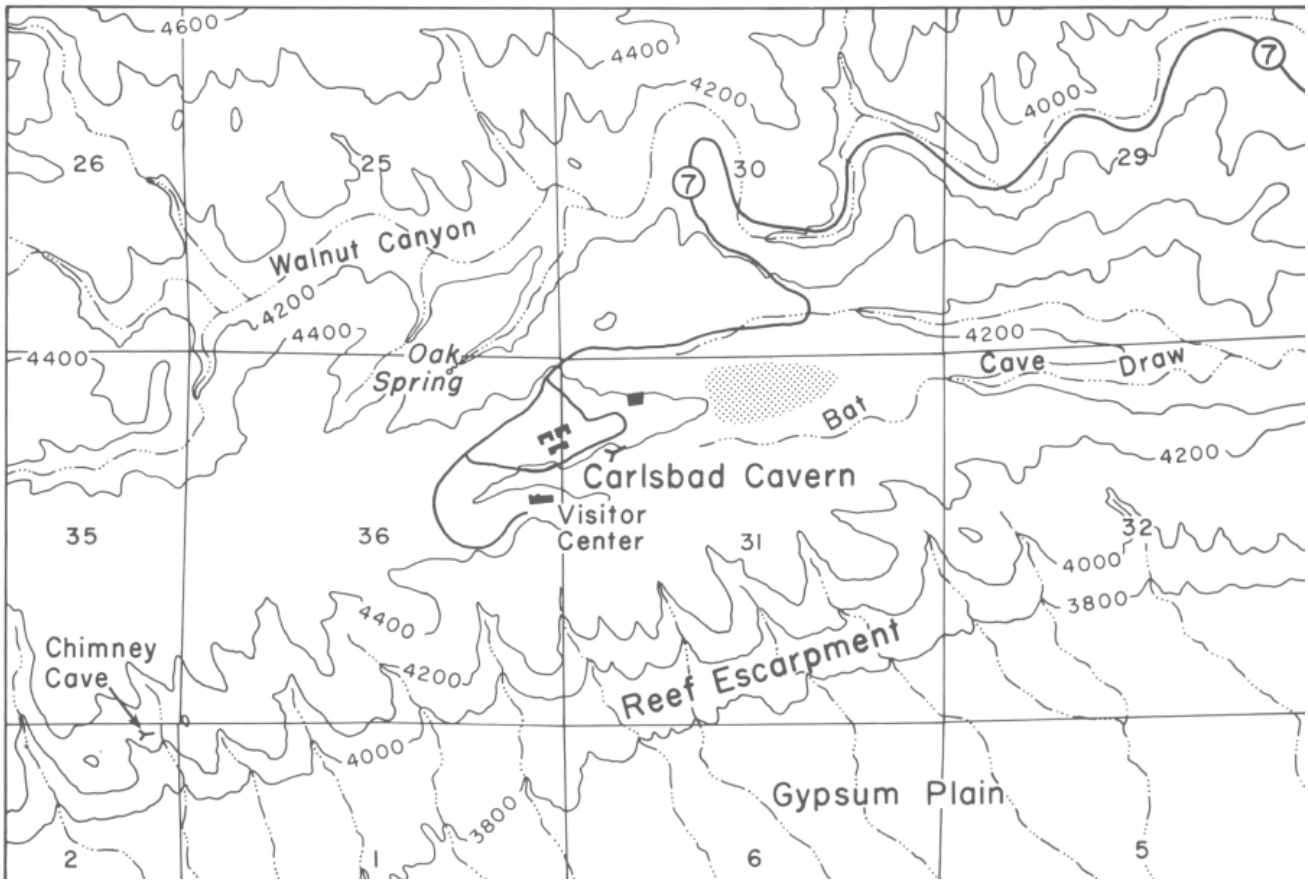

FIGURE 8—Location of Ogallala (or Gatuña) gravel remnants on the surface near Carlsbad Cavern (dotted area).

Structure

Regional structure

Detailed accounts of the structural geology of the Guadalupe Mountains have been given by King (1948), Hayes (1964), Kelley (1971), and DuChene (1971, 1978). The Guadalupe Mountains are structurally simple compared to many other parts of New Mexico. Faults are spaced far apart, fracture frequency is low, and folds are very gentle (a few degrees). The Guadalupe Mountains were uplifted and tectonically folded and faulted in the Tertiary along with the entire western United States, starting about 10 my ago and continuing even today (Reilinger et al., 1979). The eastward to northeastward regional dip of the Guadalupe Mountains from Guadalupe Peak to Carlsbad is about 1°.

Faults—The Guadalupe Mountains are faulted along their western flank where northwest-trending, arcuate, high-angle faults have stratigraphic displacements on the order of

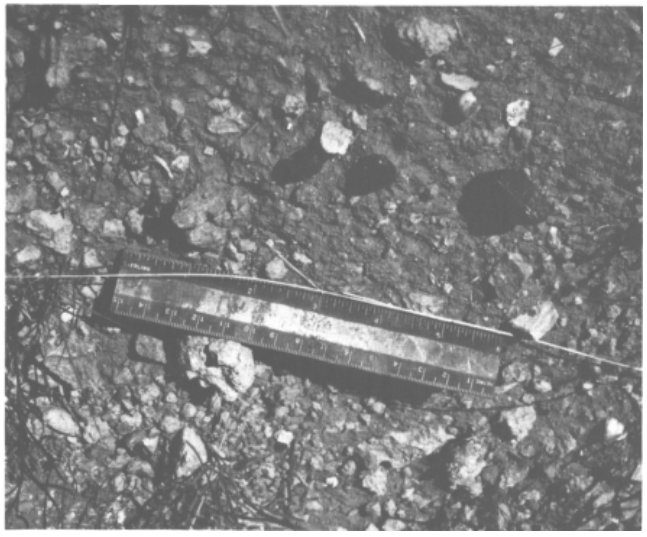

FIGURE 9—Ogallala (or Gatuña) gravel remnants on Carlsbad Cavern Ridge about 0.5 km east of the Natural Entrance. Photo Ronal Kerbo.

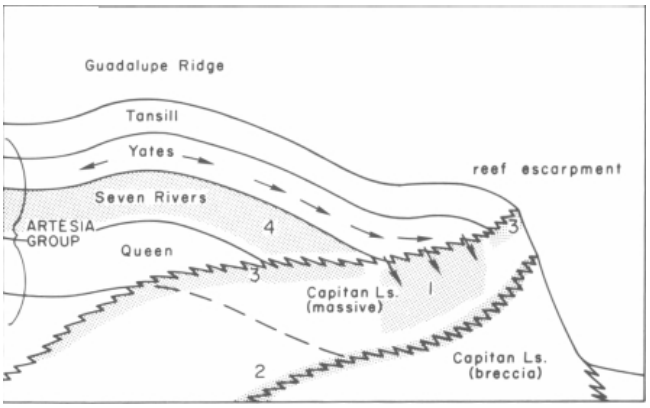

FIGURE 10—Four zones of preferential solution (shaded areas): (1) below the Yates transition into the massive Capitan Limestone, (2) at the contact between the massive and breccia members of the Capitan Limestone, (3) at the transition between the Artesia Group members and the Capitan Limestone, and (4) immediately beneath the Yates Formation in the Seven Rivers. Arrows indicate movement of ground water along impermeable siltstone in the Yates Formation. After Jagnow (1979).

600–1,200 m (Fig. 11). As the Guadalupe Mountains uplifted along their southwest margin, beds were tilted to the northeast. Kelley (1971) proposed that two strike-slip faults parallel the reef escarpment, the Carlsbad fault in the north near Carlsbad, and the Barrera fault which occurs south of the Carlsbad fault but north of Double Canyon. Hayes and Bachman (1979) questioned the presence of both of these faults.

The Castile Formation in the Delaware Basin is marked on its western part by sets of linear fault scarps trending N75°E to N80°E, or approximately parallel to the direction of regional dip (Figs. 2, 11). Olive (1957) called these scarps "solution-subsidence troughs," and described them as being 1-15 km long, up to 1.6 km wide, and less than 6 m deep. The troughs do not extend into the underlying Bell Canyon Formation, but have formed as subsidence blocks from the solution of the Castile evaporites (Davis and Kirkland, 1970). They are restricted to halite-free areas of the Castile Formation (i.e. west of the halite limit; Fig. 85). A second group of faults in the Gypsum Plain have been determined by sulfur test drilling. Smith (1978a) called these faults "graben-boundary faults" and described them as being nearly ver-

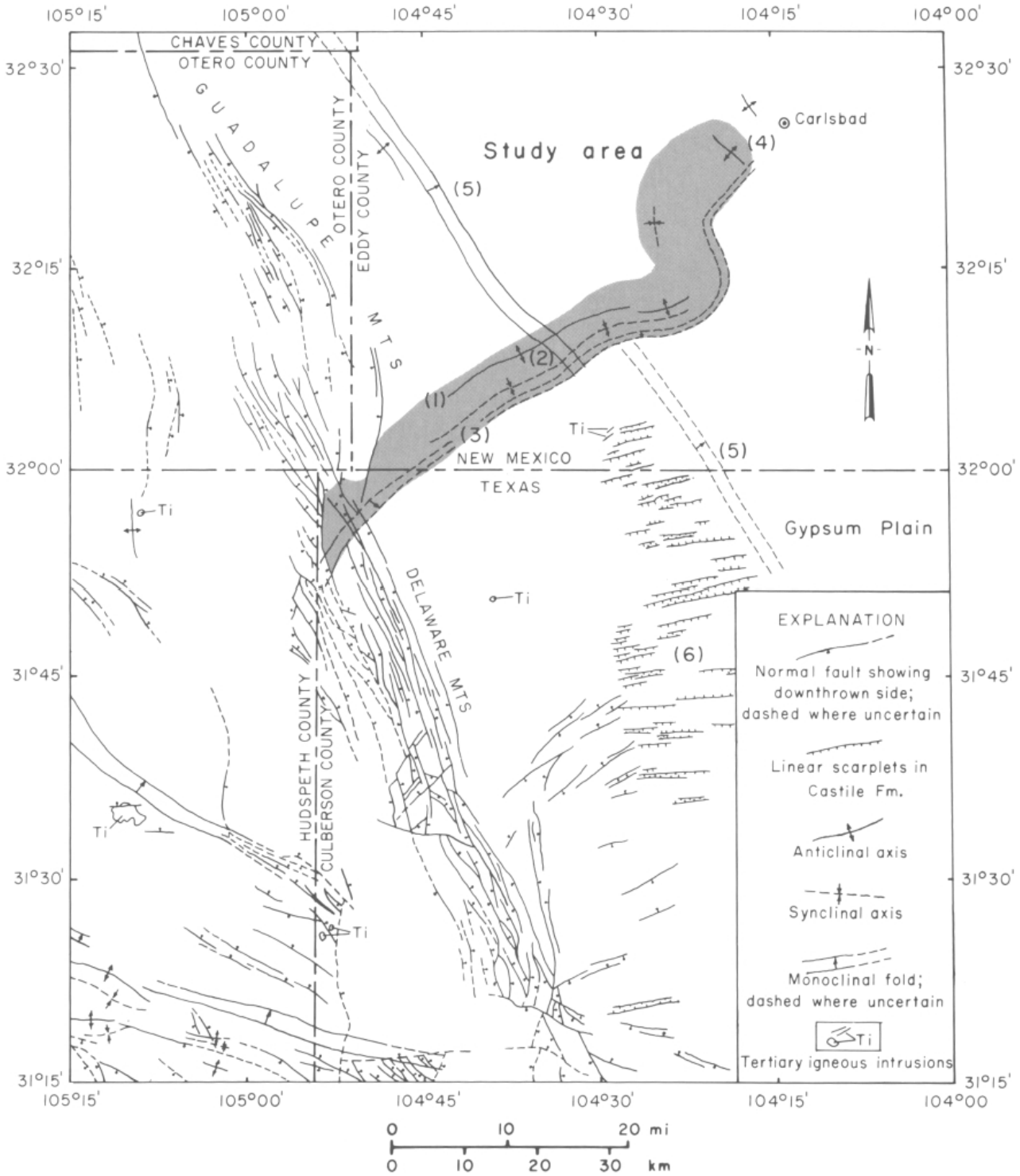

FIGURE 11—Structural map of the Guadalupe Mountains region of southeastern New Mexico and western Texas: (1) Guadalupe Ridge anticline, (2) Walnut syncline, (3) Reef anticline, (4) McKittrick Hill anticline, (5) Huapache monocline, and (6) linear scarps in the Gypsum Plain. After DuChene (1978) and Jagnow (1979).

tical, trending about N65°E, and having displacements on the order of 7-25 m that affect both the upper Bell Canyon Formation and lower Castile Formation (Fig. 84). Sulfur deposits in the castile masses are localized along graben-boundary faults.

Folds—Crossing regional dip and paralleling the reef escarpment is a fold belt approximately 8 km wide, known as the Guadalupe Ridge folds (Fig. 11). Where the reef escarpment turns sharply from northeast to northwest just south of Carlsbad, the Guadalupe Ridge folds also veer in this same direction. A series of folds in the northern part of the belt is called the Carlsbad fold complex; the McKittrick Hill caves are developed along these anticlinal folds. Another main structural feature in the area is the Huapache monocline, a flexure 0.8-4 km wide which dips 3-5° to the northeast. This monocline becomes obscured both at its northwestern and southeastern terminations and also where it intersects the reef escarpment. According to recent sulfur-exploration maps, the monocline in the basin intersects the reef somewhere between Rattlesnake Canyon and Carlsbad Cavern (Fig. 12). The structural relief of the monocline is 90-300 m in the Guadalupe Mountains and on the

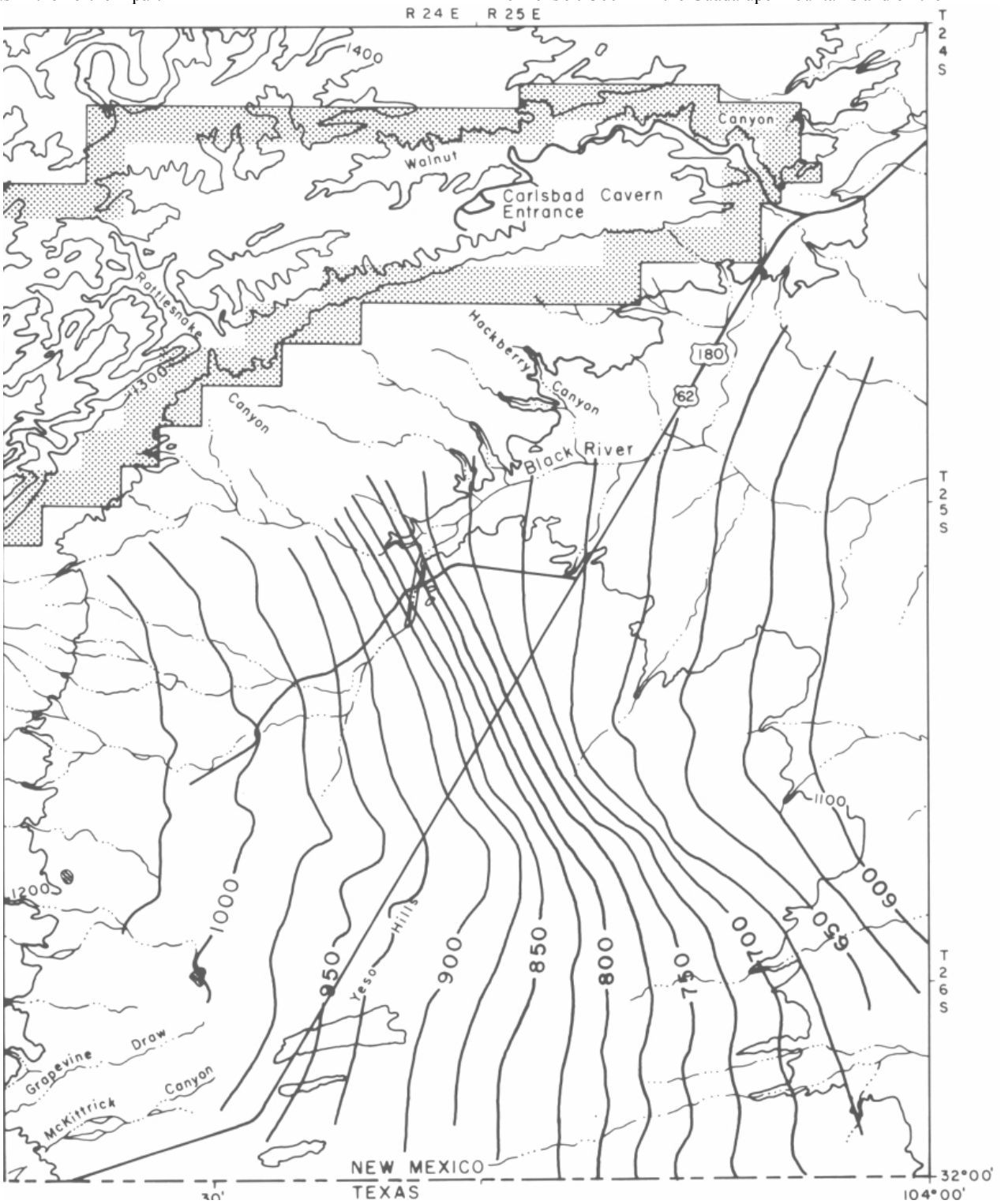

FIGURE 12—Location of the Huapache monocline in the Delaware Basin, contoured (in meters) on top of the Bell Canyon Formation in the subsurface. Courtesy of Leonard Minerals.

order of 90–200 m in the Delaware Basin (Hayes, 1964; Kelley, 1971). The Huapache monocline is a surface representation of the draping of Permian and younger sediments over a thrust fault or series of faults in the pre-Permian basement (Powers et al., 1978).

Small-scale folding has occurred in some backreef shelf beds, especially in the Tansill Formation. These folds, called "tepee structures," have been mildly deformed into chevronlike patterns resembling inverted V's. Tepee structures are up to 9 m high and wide and deformed beds are joined together so as to form steep-crested buckles.

Joints—The Capitan Limestone displays a conspicuous system of nearly vertical joints. Major joints trend either parallel or perpendicular to the reef escarpment; less frequently, joints follow the strike of bedding. Where joints have become case-hardened by mineralizing solutions, prominent blade-like projections stand out in relief along limestone cliffs (Fig. 7). Jagnow (1979) reported a strong correlation between cave locations and mineralized joints, and speculated that solutions mineralizing the rock may have also been responsible for carving out the caves. Within the Delaware Basin, joint sets with northeasterly and north-westerly strike are recognizable (Anderson, 1981).

Sandstone dikes—Sandstone dikes fill joint sets at or near the reef–backreef contact between the Capitan Limestone and the Seven Rivers, Yates, and Tansill Formations (Newell et al., 1953). Hayes (1957, 1964) and Dunham (1972) classified the sandstone dikes in the Guadalupe Mountains into two types based on textural, mineralogical, and size differences: (1) tens of centimeters thick, irregularly branching dikes composed of homogeneous, fine-grained sand cemented in a quartz or quartz–calcite matrix, and (2) several meters wide dikes, sometimes nearly vertical, with a trend generally parallel to the reef escarpment, and composed of coarse sand to gravel cemented with dolomite. Age of the dikes is questionable. Adams and Frenzel (1950) thought that type (1) sand was Yates debris intruded into fractures during reef growth in the Permian. These appear to have filled original connecting voids in the reef limestone (Newell et al., 1953). Horberg (1949) believed type 2 dikes to be of Ogallala age, and King (1948) believed that they might be Early Cretaceous. Jagnow (1979) identified no less than 15 dikes transecting the walls of Ogle Cave and proposed that type (1) dikes were of Permian age and type (2) dikes of Pliocene age.

Structural controls on cavern formation

Five structural controls influence cavern formation; one of them is of regional importance, the others are only of local importance.

(1) *Joint control.* Joints are the primary structural control on cavern development and the major trunk passages of the caves in the Guadalupe Mountains are, almost without exception, aligned along joints which either parallel the reef or are perpendicular to it. Jagnow (1979) found that east of Rattlesnake Canyon the major joints along which caves are developed trend in a northeastern direction parallel to the reef front, whereas west of Rattlesnake Canyon the cave-bearing joints trend in a northwestern direction perpendicular to the reef front, a change which Jagnow ascribed to the structural influence of the Huapache monocline.

(2) *Huapache monocline.* The draped, folded strata of the Huapache monocline act as avenues for solutional enhancement. This control may be one factor responsible for the development of caves in Slaughter Canyon which are located near the monocline in the reef.

(3) *Sandstone dikes.* Sandstone dikes are zones of structural weakness along which water can move. This structural influence seems to be especially pronounced in the case of Ogle Cave.

(4) *Anticlinal folds.* The McKittrick Hill caves—Endless, Dry, Sand, Little Sand, and McKittrick—are all formed along the flanks of the McKittrick Hill anticline. Flexed rocks provide avenues for ground-water movement.

(5) *Tepee structures.* Minor cave development has occurred along tepee structures, local avenues for ground-water movement. Small caves developed along the axial fractures of tepee structures are Tepee Cave and Jurnigans Cave #2.

Hydrology

Regional hydrology

The hydrology of the Carlsbad region has been described by Motts (1957), Bjorklund and Motts (1959), and Hiss (1974, 1975, 1980). The permeable Capitan Limestone acts as the aquifer for the region, and the entire upland surface of the Guadalupe Mountains is the recharge area (about 2,000 km^2). Water percolating through the shelf rocks of the Artesia Group drains downdip into the Capitan Limestone aquifer and then moves slowly through the reef to its point of discharge at Carlsbad Springs. In the vicinity of Carlsbad, the Capitan reef plunges beneath the surface and comes in contact with the alluvial fill of the Pecos River valley. The water of the Capitan Limestone aquifer at Carlsbad is of good quality and has a low dissolved-salt content (Table 2).

Both water-table and artesian conditions exist in the Capitan reef aquifer, but unconfined conditions prevail. Only where the aquifer is confined by overlying alluvial deposits, as in the vicinity of Carlsbad, do continuous artesian conditions persist, and then the hydrologic head is only a few meters at most (Bjorklund and Motts, 1959). Hiss (1975) estimated that the Capitan aquifer has an average gradient

TABLE 2—Water analyses (in ppm) for the Capitan Limestone aquifer: (a) Dark Canyon water supply area, City of Carlsbad; (b) White City; (c) potassium content of water, Dark Canyon water supply area, City of Carlsbad. Data supplied by J. Wright, State Engineer Office, Roswell, and J. Smith, Environmental Improvement Division, Carlsbad.

	(a) Carlsbad, NM						(b) White City, NM	(c)	
Well	23.25.1.4311	23.25.1.331321	23.25.1.44222	23.25.12.214221	23.25.12.312223	23.25.13.1144411	24.25.34.221	Latitude Longitude	K^+ (ppm)
Fe	0.5	0.9	0.4	0.2	0.5	0.6	—	32°19′40″ 104°20′40″	2.15
Ca	74	76	75	83	68	77	90	32°19′40″ 104°21′0″	1.95
Mg	30	36	34	39	36	33	29.9	32°19′40″ 104°21′10″	1.56
Na	25	—	30	—	1	5	11.5	32°19′40″ 104°21′50″	1.56
Ba	0.2	0.21	0.2	0.23	0.23	0.21	—	32°19′45″ 104°22′0″	1.17
HCO_3	256	280	256	274	274	268	228	32°19′10″ 104°20′40″	1.17
SO_4	61	120	105	140	74	96	166	32°19′0″ 104°21′10″	0.78
Cl	64	51	52	85	15	15	11		
NO_3	—	—	—	—	—	—	4.4		
pH	7.18	7.18	7.18	7.16	7.2	—	—		

of about 0.2–0.4 m/km (1–2 ft/mi), but, based on limited well data, it may be as high as 0.85 m/km (4.5 ft/mi) (Sheet 1). Calculations using Darcy's Law and a permeability of 14.0 millidarcies for the Capitan reef limestone (Hill, 1972) show that velocity of flow through primary pores should be approximately 5–20 cm/yr. Secondary conduit flow in the Capitan Limestone aquifer, as determined from the flow rate at Carlsbad Springs, is on the order of 0.4 m^3/sec (13–15 cfs) (Pecos River Joint Investigation, 1942).

The hydrologic system of the Gypsum Plain operates independently of the hydrologic system of the Capitan reef aquifer. The impermeable anhydrite of the Castile Formation forms an effective seal inhibiting water movement between the evaporite basin and the limestone reef. In an important recent study, Sares (1984) showed that the potentiometric (piezometric) level of the alluvial–evaporite aquifer in the Gypsum Plain differs by nearly 107 m from the Capitan aquifer in the reef (Fig. 13). He also showed that upland erosional terraces in the Black Canyon–Chosa Draw area of the Gypsum Plain do not correlate with the major horizontal cave levels in Carlsbad Cavern, a fact that implies that these two aquifers have operated independently in the past as well.

The same hydrologic conditions that exist today in the Carlsbad region have probably operated in a similar manner during the last half-million years or so since the time when the Ancestral Pecos River flowed along the western margin of the Delaware Basin (Bachman, 1984). As the Guadalupe Mountains uplifted and the Gypsum Plain lowered by solution subsidence, the resurgence point for the Capitan aquifer moved from southwest to northeast along the reef until it reached its present location at Carlsbad Springs (Fig. 86).

Hydrologic controls on cavern formation

Caves develop in three hydrologic regimes: the vadose zone, the water-table zone, and the phreatic zone. Vadose caves enlarge predominantly by free-surface streams eroding downward or laterally; water-table caves form along or at shallow depth beneath a potentiometric surface that is of greater extent than the cave; and phreatic caves form under total, permanent water fill where water is under pressure. Deep phreatic caves, where water is under high hydrostatic pressure, are termed "bathyphreatic." A given cave may be wholly vadose, phreatic, or water-table, but more usually it is a combination of two or all of these types.

The caves of the Guadalupe Mountains are a combination of deep phreatic (bathyphreatic) and water table. Water-table conditions have been responsible for the horizontal development of caves along certain levels, and bathyphreatic conditions have been responsible for the strong vertical development of these caves. No vadose cave enlargement has occurred in the Guadalupe Mountains, with the exception of minor modification of cave passages by intermittent, local-invasion, vadose drainage. Typical vadose features such as predominant scalloping, incised meanders, or dome pits are rare or absent in Guadalupe caves.

Bathyphreatic flow in the Guadalupe Mountains was caused by the tectonic uplifting of the mountains and by the low fracture frequency of the reef limestones. If the frequency of fissures penetrable by ground water is low, then recharge water must take a deep course through the bedrock if there is no efficient alternative at lesser depths (Ford and Ewers, 1978; Fig. 14). If substantial uplift occurs in a region, such as it has in the Guadalupe Mountains, then hydraulic gradients can become steep and there is a movement of water from upland recharge areas to springs at lower elevations. Where reservoir capacity is low and the minimum flow path to the spring is long, the potentiometric surface remains high in the rock and is steeply inclined.

The caves of the Guadalupe Mountains show substantial horizontal development where major levels cut across bed-ding and base-level control is traceable between different caves and cave passages (Table 3). After phreatic cave systems have evolved for a substantial length of time, they are

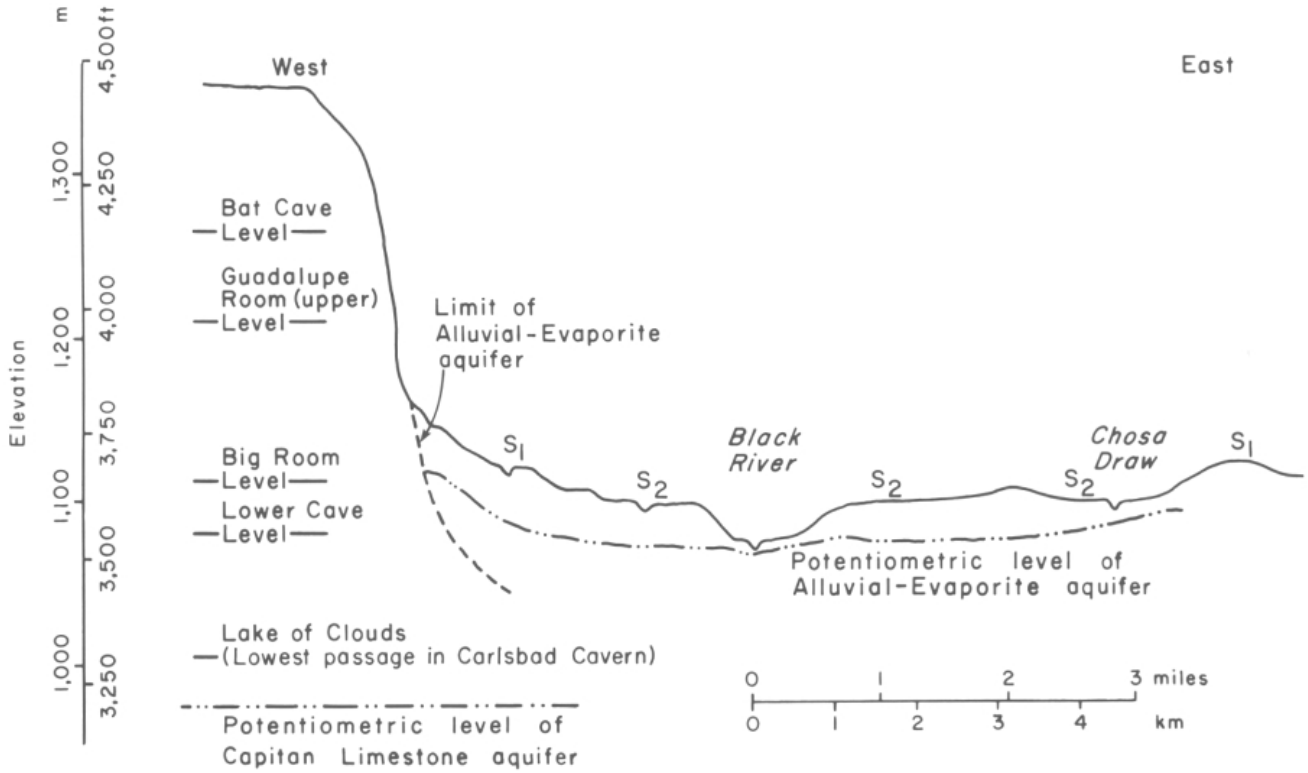

FIGURE 13—Comparison of major cave levels and cave passages in Carlsbad Cavern with terrace levels in the Gypsum Plain. Note that the potentiometric surface in each aquifer is not at the same level. After Sares (1984).

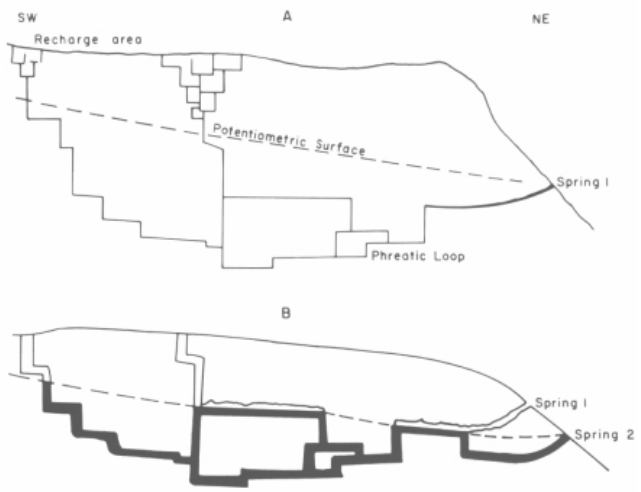

FIGURE 14—**(A)** Model of bathyphreatic flow in the Guadalupe Mountains. Since the massive Capitan reef has a low fissure frequency and a relatively low permeability, water takes a deep course through the limestone. The water ascends under high hydrostatic pressure along joints, bedding planes, and at the contact of the reef with forereef and backreef facies, and eventually exits at a spring down-gradient from the recharge area. Since the reservoir capacity of the limestone is low and the minimum flow path to the spring is long, the potentiometric surface remains high in the rock and is steeply inclined. The future course of integrated passages in the Guadalupe Mountains is highly influenced by the development of these early bathyphreatic flow routes, even though, initially, these routes may be inaccessibly small. **(B)** Caves with a mixture of phreatic and water-table components. As the caves enlarge and water discharges primarily along developing trunk pas-sages, the potentiometric surface "lowers" into sections of these passages which become ideal water-table caves. Spring shafts or joint chimneys constitute phreatic loops between horizontal levels. Spring positions shift down and northeastward as base level lowers. After Ford and Ewers (1978).

subject to modifications which change their character to a system increasingly more concordant with the water table. This is because as fissures enlarge after the onset of karstification and the volume of a cave-trunk system increases, the potentiometric surface slowly "lowers" into the trunk passage (Ford and Ewers, 1978; Fig. 14). The end result are caves, like those in the Guadalupe Mountains, which possess a mixture of phreatic and water-table components.

Description of caves

Topographic and geologic characteristics

Guadalupe caves differ from other cave systems in many ways. The following list categorizes these differences; it is based on the findings of Bretz (1949), Thrailkill (1964), Palmer (1975), Queen et al. (1977a, b), Jagnow (1977, 1979), Davis (1979a, 1980), Queen (1981), Wilson and Ash (1984b), and this study.

(1) Well-developed surface karst landforms such as towers and sinkholes are not prominent features in the Guadalupe Mountains.

(2) Caves lack a clear genetic relationship to surface to-pography. Intersections of caves with the land surface (entrances) are random and have no apparent relationship to recharge or resurgence points, ancient or modern.

(3) Few caves are known in the highest, southwestern part of the Guadalupe Mountains (e.g. the Guadalupe Peak region) and those are very small (e.g. Lower and Upper Sloth Caves, Dust Cave, and Williams Cave). Virgin Cave is the only extensive cave found west of Big Canyon (Fig. 5).

(4) Caves are located within 12 km of the reef escarpment; most are within 4 km (Fig. 5).

(5) Guadalupe cave passages are often large, many exceeding 15 m in height and width. The Big Room of Carlsbad Cavern is 600 m long, 330 m wide, and 87 m high at its tallest point, the Top of the Cross.

(6) Large cave passages end abruptly. The south end of the Big Room, Carlsbad Cavern, and the Entrance Hall, Cottonwood Cave, terminate in unbroken rock, without breakdown collapse or major passage extensions. None of the caves contain extensive linear passageways in the style of Flint–Mammoth Cave, Kentucky.

(7) Walls of large passages are honeycombed with smaller passages called spongework or boneyard—interconnected, nontubular, solution cavities of varied size and irregular geometry arranged in an apparently random, three-dimensional, maze-like pattern (Fig. 15).

(8) Guadalupe caves are deep, but not long. The caves descend via a series of drops of about 30–50 m each. The deepest known single drop in a Guadalupe cave is in the Cave of the Madonna, a total of 64 m. The Four O'clock Staircase, a slot-like series of connected drops in Virgin Cave, is 152 m deep. The deepest cave in the Guadalupe Mountains is Carlsbad Cavern, with a total depth of 312 m (Sheet 1).

(9) Large rooms and horizontal levels are connected or underlain by: (a) enlarged vertical fissures (e.g. Dean's Drop, Cave of the Madonna; Cable Slot, Carlsbad Cavern); (b) vertical tubular pits (e.g. Bottomless Pit, Carlsbad Cavern;

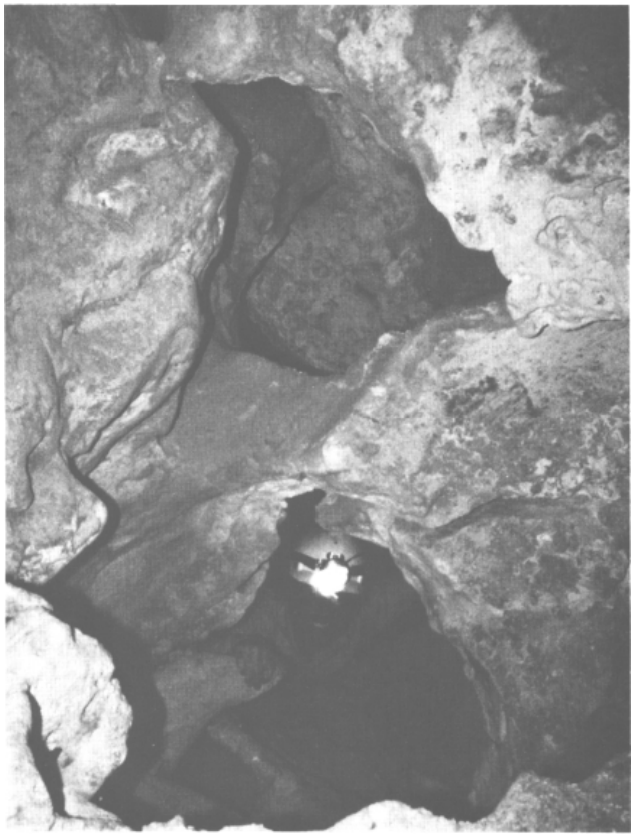

FIGURE 15—Crawling through boneyard, Carlsbad Cavern. Photo Cyndi Mosch Seanor.

FIGURE 16—Rillenkarren on limestone bedrock, Boneyard, Carlsbad Cavern. Photo Ronal Kerbo.

the entrances to Deep and Ogle Caves); and (c) passages which descend at angles of 20—30° (e.g. Main Corridor, Mystery Room, Guadalupe Room, and Lake of the Clouds Passage, Carlsbad Cavern).

(10) Pits, tubes, and vertical fissures lack drains, and avenues for water escape seemingly disappear with depth. Vertical pits and fissures end in breakdown, fill, travertine, pinchouts, or unbroken bedrock (e.g. Nicholson's Pit, Carlsbad Cavern, both pinches out and is filled with breakdown).

(11) Caves reach a certain overall depth and then seem to descend no further even though the water table is below the lowest passage (e.g. the Lake of the Clouds, the lowest passage in Carlsbad Cavern, is about 30 m above the present water table in the Capitan reef aquifer; Sheet 1).

(12) Solutional features point to a non-vadose regime of cavern development. Vertical shafts, domepits, scallops, ripple marks, cutoffs, ceiling channels, flutes, horizontal grooves, and incised meanders are either rare or absent in Guadalupe caves.

(13) Cave sediment is sparse; where it does occur, it is almost always a coarse silt to fine-grained sand.

(14) Thick floor blocks of massive gypsum and thinner wall rinds of gypsum are conspicuous features in many Guadalupe caves.

(15) Native sulfur occurs in Guadalupe caves either associated with massive gypsum or directly overlying bedrock and speleothems.

(16) Colorful, soapy or waxy clay composed of the minerals montmorillonite and endellite fills solution pockets in many Guadalupe caves.

(17) Travertine deposits are profuse. Guadalupe caves have the well-earned reputation of being among the most beautiful in the world.

(18) Cave limestone surfaces are often whitened, rounded, and eaten-away looking (e.g. Boneyard, Carlsbad Cavern). In some places the cave limestone is deeply etched and corroded (Figs. 16, 27).

Caves studied

Caves visited during this investigation include: Big Door, Black, Carlsbad, Christmas Tree, Corkscrew, Cottonwood, Damn, Deep, Dry, Endless, Goat, Helen's, Hell Below, Hidden, Lechuguilla, Little Beauty, Little Sand, Madonna, Mad Russian (Hidden Chimney), McKittrick, Musk Ox, New, Ogle, Pink Dragon, Pink Fink Owlcove, Pink Palette, Pink Panther, Queen of the Guadalupes, Rainbow, Sand, Sentinel, Spider, Three Fingers, Virgin, and Wind (Hicks). Other caves mentioned in the text have been described by cavers or cited in the literature.

The primary focus of this study, Carlsbad Cavern, is depicted in two maps, a horizontal view (Sheet 2) and a profile (Sheet 3). Other maps included in this report are of Cottonwood, Ogle, New, and Dry Caves. Excellent maps and descriptions of many other Guadalupe caves have been given by Jagnow (1977, 1979).

Carlsbad Cavern

The entrance and upper levels of Carlsbad Cavern occupy a limestone ridge 240 m high and 2.4 km wide at the base. This ridge parallels the reef front and is truncated on its western side by Walnut Canyon and on its eastern side by the reef escarpment (Sheet 4, Fig. 17).

Cave passages in Carlsbad Cavern trend in one of three

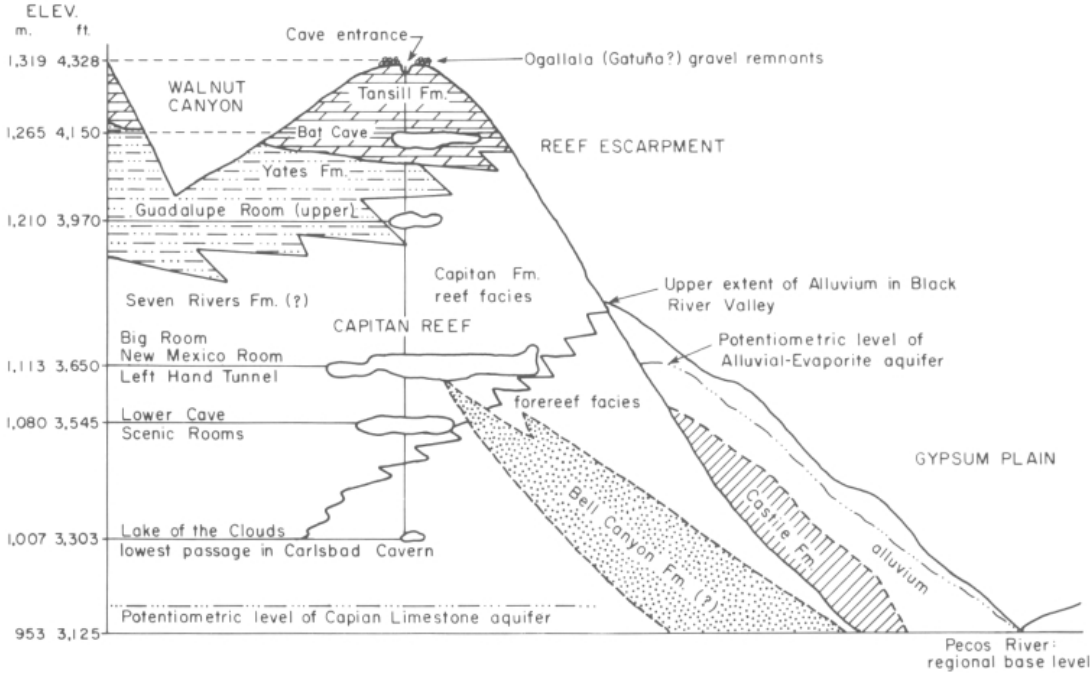

FIGURE 17—Diagrammatic presentation of levels and passages in Carlsbad Cavern with respect to surface topography in the Capitan reef and Gypsum Plain.

directions (Sheet 2). Bat Cave, Left Hand Tunnel, Main Corridor, Guadalupe Room, Scenic Rooms, and Mystery Room all trend approximately N80°E, or parallel to the reef front. Perpendicular to the reef, or trending about N15°W, are Talcum Passage, Mabel's Room, the Cable Slot, Appetite Hill, the west end of Lower Cave, the west and north ends of the Big Room, and the Right and Left Hand Forks of Left Hand Tunnel. Oriented at approximately N40°E are Secondary Stream Passage, the New Mexico Room, parts of Lower Cave, and the middle section of the Big Room from the Salt Flats to the Polar Regions.

Four main levels of horizontal cavern development occur in Carlsbad Cavern: -60 m from the entrance (Bat Cave level); -120 m (New Section level); -230 m (Big Room level); and -260 m (Lower Cave level) (Sheet 3). Passages at different levels are connected by the Main Corridor and the Guadalupe Room—steeply dipping, parallel passages which both descend at an angle of 20-30°. The Bat Cave level corresponds to Spider Cave in altitude, and the Scenic Rooms correspond to the Lower Cave level (Table 3). By far the most dominant level in Carlsbad Cavern is the Big Room horizon which includes not only the Big Room but also the Mystery Room, New Mexico Room, Mabel's Room, Talcum Passage, Left Hand Tunnel, and Bell Cord Room.

Carlsbad Cavern is developed in the reef and forereef facies of the Capitan Limestone; the Tansill, Yates, and possibly the Seven Rivers Formations of the backreef Artesia Group; and possibly also the basinal Bell Canyon Formation (Figs. 17, 18). The Tansill crops out at the cave entrance and Tansill beds delineate the planar ceiling of Bat Cave. The Yates Formation crops out at many levels in the northern part of the cave, from the lower walls of Bat Cave down to a sandstone tongue at the top of the Guadalupe Room, or about 60 m in vertical extent. The Seven Rivers Formation may possibly extend below the Yates Formation in the area of the Lower Guadalupe Room and New Mexico Room (Wilson and Ash, 1984a). The white, clean sands of the Bell Canyon Formation possibly interfinger at the east end of the New Mexico Room and at the south end of the Big Room (Fig. 18).

The reef facies of the Capitan Limestone is the primary unit in which Carlsbad Cavern is developed. Passages terminate near the intersection of the reef limestone with forereef or backreef beds. Crude bedding planes of the forereef facies of the Capitan Limestone slope at an angle of about 30° away from the reef and can be seen intersecting the cave at the southern end of the Big Room and also along the Left Hand Tunnel at intermittent intervals all the way to the Bell Cord Room (Fig. 18). The southeast wall of the middle section of the Big Room and the southeast wall of Lower Cave are located along the contact of the reef-forereef facies, the horizontal offset of the passages at these two levels possibly being due to the progradation of the reef over the forereef, so that in a vertical plane the forereef facies underlies the reef facies at an angle (Figs. 4, 17).

Carlsbad Cavern is the main focus of this study because it is the largest and most extensive cave in the Guadalupe Mountains. It also contains all of the various types of cave deposits: gypsum blocks and rinds, cobble gravel, silt, breccia, calcified siltstone-cave rafts, chert, sulfur, montmorillonite-endellite, and travertine. All of the known events that have occurred in Guadalupe caves are represented by the deposits in Carlsbad Cavern.

Cottonwood Cave

Cottonwood Cave is located between Dark and Black Canyons in a narrow limestone ridge which lies along the crest of the Guadalupe Ridge anticline. The cave is developed primarily in the backreef Seven Rivers Formation which directly underlies the pyritic Yates Formation (Sheet 5). The

TABLE 3—Major cave levels in Guadalupe Mountains.

Elevation		Location	Remarks
1,400-1,426 m level			
1,400 m	4,590-4,594 ft	Slaughter Canyon caves	Floor of Midnight Goat Cave
1,400	4,591	(Jagnow, 1979)	Back part of New Cave
1,398	4,510—4,588		Helen's Cave
1,402	4,600		Main level of Ogle Cave
1,402	4,600		Main level of New Cave
1,402	4,600		Goat Cave
1,402	4,600		Triangle Cave
1,426	4,680		Upper part of New Cave
1,426	4,680		Wen Cave
1,265—1,295 m level			
1,295	4,248	Carlsbad Cavern area;	Ceiling of Bat Cave, Carlsbad Cavern
		McKittrick Hill	Entrance to Endless Cave
			Entrance to Sand Cave
			Entrance to McKittrick Cave
			Entrance to Spider Cave
1,280	4,198		Entrance to Dry Cave
			Entrance to Little Sand Cave
1,265	4,149		Floor of Bat Cave
			Floor of Spider Cave
			Floors of McKittrick Hill Caves
1,115 m level			
1,115	3,657	Carlsbad Cavern	Big Room, Left Hand Tunnel, Bell Cord Room,
		Wind (Hicks) Cave area	New Mexico Room, Mystery Room, Carlsbad Cavern
			Entrance to Wind (Hicks) Cave
			Entrance to Jurnigan Cave #1
1,080 m level			
1,080	3,542	Carlsbad Cavern	Lower Cave, Scenic Rooms, Carlsbad Cavern

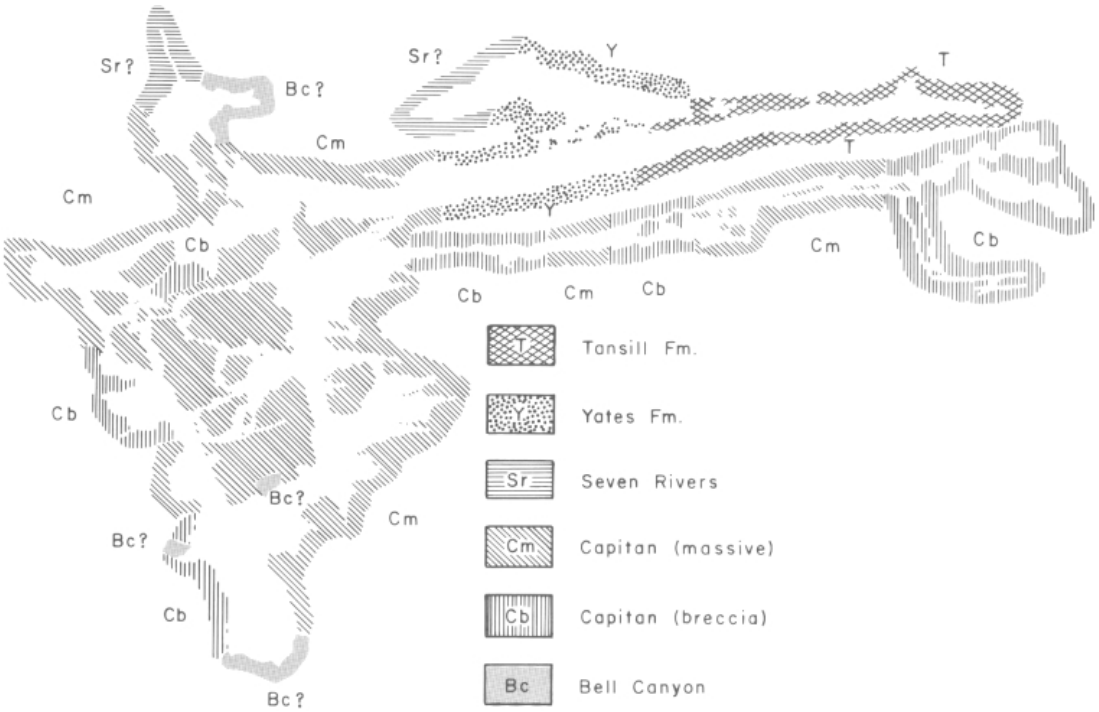

FIGURE 18—Sedimentary-facies map, Carlsbad Cavern. Based on Thrailkill (1965b, 1971), Hart (1969), Queen (1981), Wilson and Ash (1984b), and this study. Cm = Capitan Limestone, massive member; Cb = Capitan Limestone, breccia member; Bc = Bell Canyon Formation; Sr = Seven Rivers Formation; Y = Yates Formation; T = Tansill Formation.

Entrance Hall of Cottonwood Cave is 30–50 m high and 15–20 m wide, and trends N14°W, or approximately perpendicular to the reef escarpment. The sometimes rectangular to square passage cross section of the Entrance Hall represents the intersection of a flat ceiling (caused by collapse along a Seven Rivers bedding plane) with vertical walls (caused by exfoliation of bedrock along a series of parallel, vertical joints). An area of maze passage along the west wall near the very end of the Entrance Hall connects the Hall with the Gypsum Passage, a narrower, parallel, side passage which contains gypsum blocks, native sulfur, and gypsum and epsomite speleothems.

Cottonwood Cave is perhaps the second most important cave in this study, both because of its relatively extensive gypsum and sulfur deposits and also because of the replacement textures exhibited in its gypsum blocks and rinds.

Slaughter Canyon caves

Two major caves, Ogle and New (Sheets 6, 7), plus a number of minor caves (Wen, Midnight Goat, Triangle, Helen's, Goat) are located in ridges intersected by Slaughter Canyon. All of these caves are developed at the contact of the massive and breccia members of the Capitan Limestone, and all are developed along joints perpendicular to the reef escarpment and parallel to the Huapache monocline. As with Carlsbad Cavern, the Slaughter Canyon caves exhibit specific horizontal levels of preferred development (Table 3).

Ogle Cave, the largest Slaughter Canyon cave, has a primarily rectangular cross section averaging 30 m in height and breadth (Sheet 6). DuChene (1966) speculated that a lower bedding plane of the Tansill Formation defines the flat ceiling of the cave, and Jagnow (1978) attributed the vertical walls to exfoliation along vertical joints. The cave has two entrances, the Ogle and the Rainbow. Prominent sandstone dikes of two types and possibly of two ages are exposed at the Ogle Cave entrance and elsewhere in the cave.

McKittrick Hill caves

The caves of McKittrick Hill are developed at the contact of the Yates and Seven Rivers Formations (Smith, 1978b). The five McKittrick Hill caves—Dry (Sheet 8), Endless, McKittrick, Sand, and Little Sand—are all formed along the flanks of the McKittrick Hill anticline, part of the Carlsbad fold complex. The caves are primarily horizontal, having less than a 30 m elevation difference between their upper and lower levels. Lower levels often terminate in flat sandy floors defined by a Yates bedding plane. Most passages in the McKittrick Hill caves are maze-like, with the exception of the Expressway Passages in Dry and Endless Caves which are roughly rectangular in cross section. The majority of passages in Endless Cave are oriented parallel to the escarpment, whereas Dry Cave and Sand Cave have only a few passages trending in this direction. Most of the pas-sages in Sand and McKittrick Caves trend parallel to the strike of bedding.

The McKittrick Hill caves are important to this study be-cause they contain gypsum blocks which often display well-developed dissolution features.

Cave meteorology

Soil temperature, air temperature, relative humidity, air flow, carbon-dioxide levels, radon levels, and gamma-ray dosages have all been monitored in Carlsbad Cavern with sophisticated equipment. Measurements made in other, harder-to-reach, Guadalupe caves consist mainly of temperature and humidity readings recorded with a portable sling psychrometer (Table 4).

McLean (1970, 1971, 1976) studied the climatology of Carlsbad Cavern and carefully recorded both the temperature and relative humidity (Figs. 19–21). Relative humidity varies between 69% and 95% for different parts of the cave; lower humidities prevail from November to April and higher humidities prevail from March to October. The relatively low humidity in Guadalupe caves compared to other cave systems accounts for the relatively high amount of evapo-

TABLE 4—Temperature and humidity of Guadalupe caves other than Carlsbad Cavern. *W. Calvin Welbourn, written comm. 1985.

Cave	Temperature (°C)	Humidity (%)	Month
Cave of the Bell	15.3–15.8	89	February*
Cottonwood Cave	12.1	79	May
Decorated Cave	17.5	97	August*
Deep Cave	11.7	78	May
Dry Cave	16.7	96	May*
	20.0	94	October*
Endless Cave	21.6	94	October*
Helen's Cave	20.0	71	August*
Hidden Cave	11.7	94	April*
Jurnigan Cave #1	19.4	100	February*
Ladder Cave	17.2	86	May*
Lake Cave	17.5	97	August*
Little Beauty Cave	13.3	35	May; Little Beauty is a small cave and low humidity reflects outside humidity.
Lower Sloth Cave	10.5–11.9	34	April*; small cave.
Mad Russian Cave (Hidden Chimney Cave)	11.7	88	May
Musk Ox Cave	18.3–19.4	85–100	November
New Cave	15.3	89	April
	15.5–16.7	89	June*
Ogle Cave	14.4	80	October
Pink Dragon Cave	13.0	97	May
Pink Panther Cave	10.5	70	May
Rainbow Cave	12.5	45	June*
Rock Fall Cave	15.1	90	July*
Spider Cave	17.8	100	April*
	18.3	95	June*
	18.9	90	February
	17.8	95	November; in gypsum area.
		98	November; in dripping area.
Three Fingers Cave	14.5	89	May
Upper Sloth Cave	6.1	42	April*; small cave.

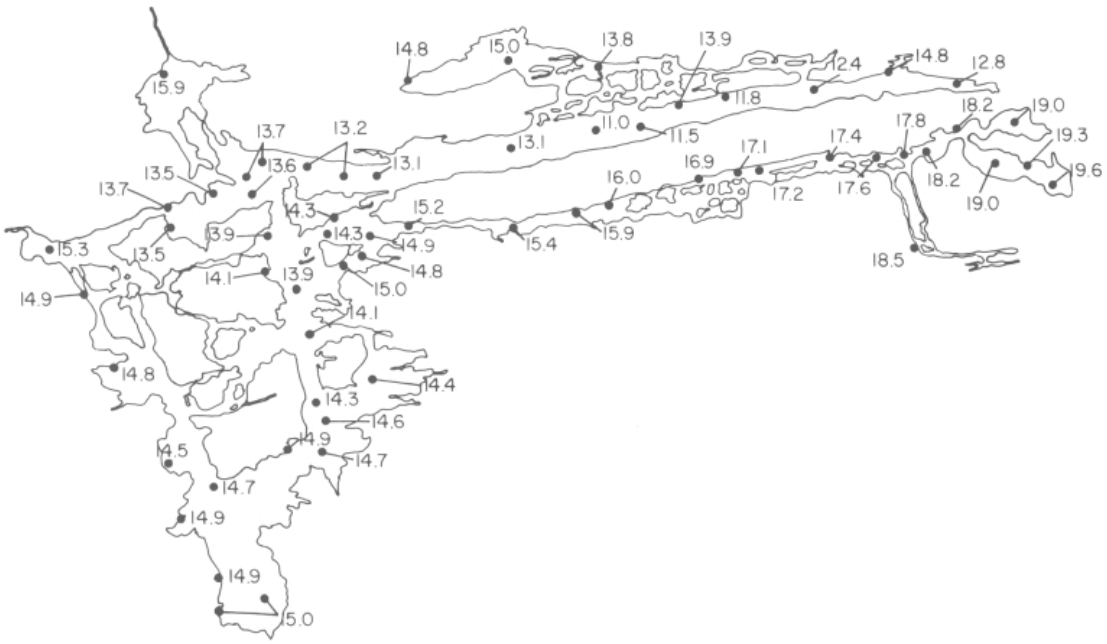

FIGURE 19—Cave-soil temperature, Carlsbad Cavern, in September 1969. After McLean (1971).

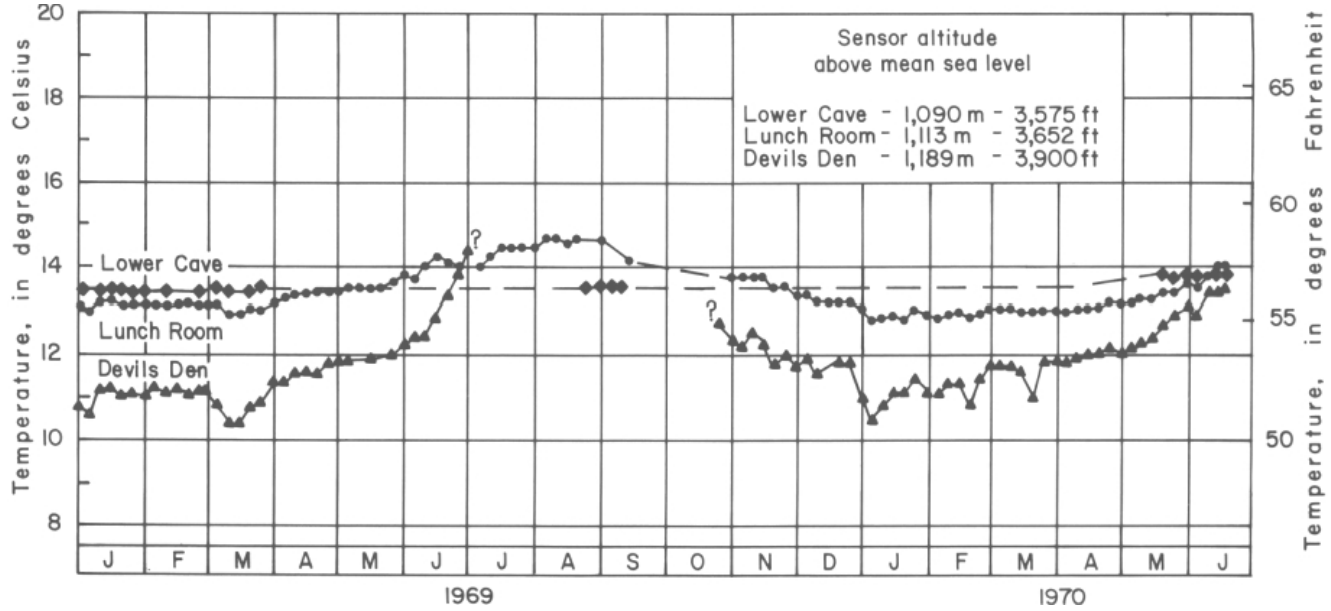

FIGURE 20—Annual variation in air temperature, Lower Cave, Lunch Room, and Upper Devil's Den, Carlsbad Cavern. After McLean (1971).

ration therein. McLean (1971) reported a relative humidity of 88% for the Pump Room–Lunch Room section of Carlsbad Cavern (in October), and a corresponding evaporation loss of 4.18 x 10^{-2} cm/day from a small evaporative pan. Hill (1978b) calculated that 10 times the amount of evaporation should occur in a cave with 88% humidity (e.g. Ogle Cave) than in a cave with 99% humidity (e.g. a cave in the eastern United States).

The temperature in Carlsbad Cavern varies from 12.4 to 19.6°C (Figs. 19, 20) and averages 13.3°C (56°F). The significantly higher temperatures along Left Hand Tunnel and in the Lake of the Clouds Passage may be partly due to a combination of the geothermal-gradient factor and lower air flow in this part of the cave. The geothermal gradient for the Eddy County, Carlsbad, area is reportedly between 0.073 and 0.0103 10^{-3}°C/cm (Clark, 1966), and at the WIPP site in the evaporite rocks of the Gypsum Plain it averages 0.85°F/100 ft (M. Rider, pers. comm. 1986). Using the average of the first numbers, the temperature at the Lake of the Clouds, due to the geothermal-gradient factor alone, should be about 16°C. Using the second number, the calculated temperature should be about 18°C. The actual temperature at the Lake of the Clouds is 19.6°C; this value may reflect a greater geothermal gradient in the reef limestones than in the evaporite rocks of the Gypsum Plain, or it may be a reflection of other, unknown factors.

McLean (1971) measured the carbon-dioxide content in the Lunch Room, Carlsbad Cavern, and found it to vary from 345 to 490 ppm in contrast to an outside carbon-dioxide content of 330 ppm (Fig. 22). In the Left Hand Tunnel and Lake of the Clouds Passage, the carbon-dioxide content of the air is as high as 1,000 ppm (Table 5). McLean attributed the relatively low concentration of atmospheric carbon dioxide in the Lunch Room to a high rate of air circulation. By

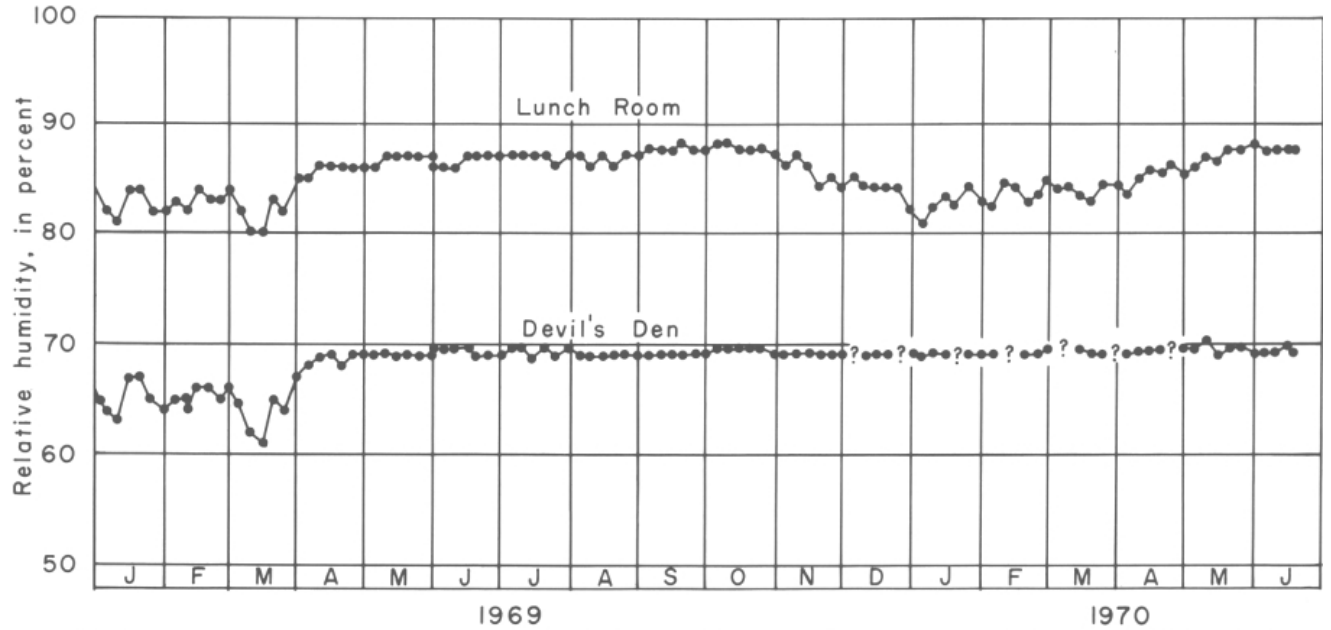

FIGURE 21—Annual variation in relative humidity, Lunch Room and Upper Devil's Den, Carlsbad Cavern. After McLean (1971).

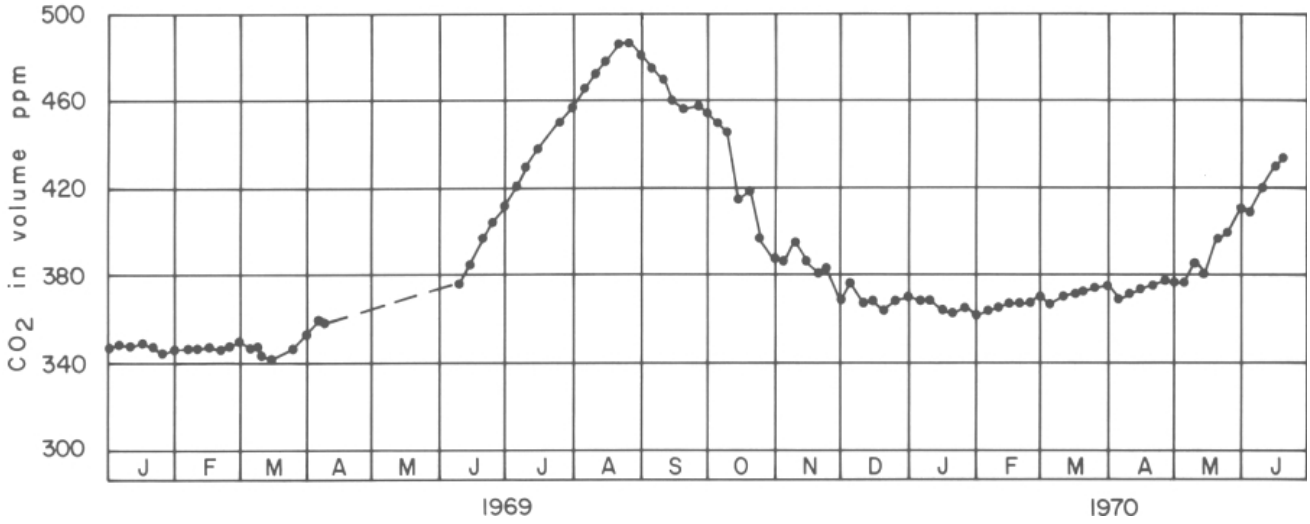

FIGURE 22—Annual variation in carbon-dioxide content of the air, Lunch Room, Carlsbad Cavern. After McLean (1971).

TABLE 5—Temperature, humidity, and carbon-dioxide content of the air, October 1985, Left Hand Tunnel, Lake of the Clouds Passage, and New Section, Carlsbad Cavern. CO_2 measurements made with a Drager Multi-Gas Detector.

Place	Temperature (°C) near floor	Temperature (°C) near ceiling	Humidity (%) near floor	Humidity (%) near ceiling	CO_2 (ppm) near floor	CO_2 (ppm) near ceiling
Surface ~70 m from cave entrance	—	—	—	—	250 ± 50	—
Hall of White Giants, New Section, active speleothem area	—	—	—	—	450 ± 50	—
Sand Passage, New Section, non-speleothem area	—	—	—	—	550 ± 50	—
Lunch Room	15.5	—	88	—	550 ± 50	—
Left Hand Tunnel, first bridge	15.5	16.4	83	93	500 ± 50	850 ± 50
Left Hand Tunnel, The Beach	16.0	16.7	94	94	550 ± 50	650 ± 50
Left Hand Tunnel, 2nd bridge (only ½ way to actual floor & ceiling)	17.2	16.7	89	89	600 ± 50	550 ± 50
Left Hand Tunnel, Survey #69	17.2	18.3	100	100	600 ± 50	650 ± 50
Left Hand Tunnel, turnoff to Lake of the Clouds	18.3	—	100	—	800 ± 50	—
Shelfstone pool, active speleothem area	18.9	—	100	—	750 ± 50	—
Creeping Ear, Top of Lake of the Clouds Passage	19.4	—	96	—	850 ± 50	—
Balcony, Lake of the Clouds Passage	19.4	—	100	—	1,000 ± 50	—
Lake of the Clouds	20.0	—	96	—	1,000± 50	—
By "punk rock" going up into Bell Cord Room	19.4	—	98	—	850 ± 50	—
Bell Cord Room	19.4	—	98	—	1,000 ± 50	—

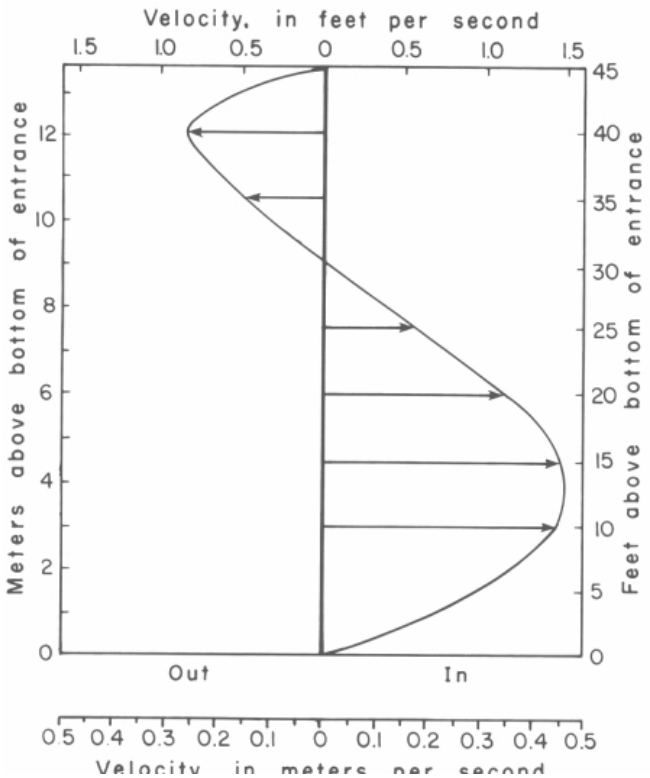

FIGURE 23—Air-flow velocity at the Natural Entrance of Carlsbad Cavern, 11 January 1970, 8:00 p.m. After McLean (1971).

the same reasoning, the much higher values of carbon dioxide in Left Hand Tunnel and Lake of the Clouds are probably due to a poorer air circulation in this part of the cave. It is interesting to note that the carbon-dioxide content near the ceiling along Left Hand Tunnel is higher than that near the floor (Table 5).

Air-flow velocity in Carlsbad Cavern has been deter-mined by actual measurement, and air-flow direction has been inferred from oriented popcorn growth and radon levels. McLean (1971) reported an air-flow velocity of almost 50 cm/sec at the cave entrance (Fig. 23) and an air flow somewhat less than 5 cm/sec in the Lunch Room area. Wilkening and Watkins (1976) reported an air flow of 30–40 cm/ sec for both inflow and outflow of air in the Devil's Spring area of the Main Corridor. Reportedly, the cave "breathes out" during stormy weather (which is associated with a falling barometer), and "inhales" during dry, fair weather (when the outside barometric pressure is high) (Boyer, 1964).

Queen (1981) plotted the distribution of oriented popcorn in Carlsbad Cavern and constructed an air-flow map of the cave from this distribution (Fig. 24). Based on popcorn orientation relative to the two cave entrances in Ogle Cave, Hill (1978b) speculated that a "chimney effect" operates in the cave. In the winter, when temperatures are higher in the cave than on the surface, warm, moist air flows out the upper Rainbow entrance and cold, dry air flows into the lower Ogle entrance.

Atkinson et al. (1983) showed that natural circulation of cave air can be related to radon levels. Radon-222 (^{222}Rn), the daughter product of ^{238}U, is produced from the natural radioactive decay of rocks and soils in the interior of a cave. Actual levels of ^{222}Rn encountered in a cave are dependent upon the net exhalation of radon from the walls of the cave, the volume of the cave, and the degree of mixing of outside air with cave air. Wilkening and Watkins (1976) noted that at Devil's Spring, Carlsbad Cavern, the concentration of radon gas in warm air moving out of the cave averaged about twice that of incoming air. They also noted that the radon concentration in Carlsbad Cavern averages 48 pCi/l in the summer but only 15 pCi/l in the winter. This difference is due to the mixing of cave air with outside air having radon concentrations of only 0.2 pCi/l (Table 6).

Air-flow direction as inferred by radon levels is essentially the same as proposed by Queen (1981) using oriented popcorn growth, with the exception of Lower Cave and Left Hand Tunnel (compare Figs. 24 and 25). The highest radon levels measured in Carlsbad Cavern (99 pCi/l in November; Beckman et al., 1975) were in Lower Cave in the Naturalist Room. High radon levels in the Naturalist Room may relate to the relatively closed-off nature of this room, or possibly to the large amount of montmorillonite clay in Lower Cave. According to R. Kerbo (pers. comm. 1984) the highest radon measurements made in Lower Cave were associated with exposure to the gray-green clay.

The relatively low ^{222}Rn values in Left Hand Tunnel are

FIGURE 24—Air-flow direction (arrows) as inferred from the orientation of popcorn, Carlsbad Cavern. After Queen (1981).

TABLE 6—Radon and gamma-ray measurements, Carlsbad Cavern.

Radon (^{222}Rn) level	Measured in November: Range: 4-99 pCi/l Average (74 readings): 30.7 pCi/l	Beckman et al. (1975)
	Measured in August: Range: 9-92 pCi/I Average (46 readings): 36.5 pCi/l	Beckman & Rapp (1976)
	Summer months, average: 48 pCi/l Winter months, average: 15 pCi/l Difference due to incoming air flow in winter and outgoing air flow in summer.	Wilkening & Watkins (1976)
Gamma radiation	Range: 4-20 uR/hr Average (14 readings): 10.6 uR/hr	Beckman et al. (1975)
	Range: 4-75 uR/hr Average (59 readings): 20.2 uR/hr	Moore (1984)
	Counting rate/hr of spectral components:	Ewing (1982)

Th	U	^{137}Cs	^{40}K
107±10	5,280±30	148±7	155±5
141±18	11,714±30	345±9	89±4

not consistent with radon levels for other parts of the cave. Theoretically, the profile of radon activity in a long, perfectly tubular, cave passage should continually increase from the entrance and down the tube unless there is a tributary current of air entering the cave from the outside, where-upon radon levels suddenly drop. The inconsistent radon levels in Left Hand Tunnel may therefore possibly reflect outside air entering the cave somewhere along the Right Hand Fork or in the "blowing" maze off the passage leading into the Bell Cord Room. Gamma-ray-exposure levels are also lower in the area from the Lunch Room along Left Hand Tunnel to the Lake of the Clouds, the average of 15 readings being 7.5 uR/hr, whereas the average of 59 readings for other parts of the cave being 20.2 uR/hr (Moore, 1984; Table 6). Curiously, bats have been noted to regularly fly in and out along Left Hand Tunnel, another indication that an entrance might exist in this part of the cave.

Cave geomorphology

Cave geomorphology is the description and interpretation of cave patterns and forms in the underground which are due to solution, erosion, corrosion, and breakdown. Geomorphic forms can be classified into two groups: (1) cave-passage forms, which embrace the smallest cavity up to the largest cavern voids and the most elaborately branched cave systems; and (2) cave-karren forms, which originate on the surface of the cave bedrock. The first form defines the shape of the cave passage itself; the second form represents a modification of that cave passage. Both forms attest to the conditions under which caves dissolve and evolve.

There are two main regimes of geomorphic development in caves. The "phreatic" regime is where cave passages or features form beneath the water table by water under pressure, and the "vadose" regime is where cave passages or

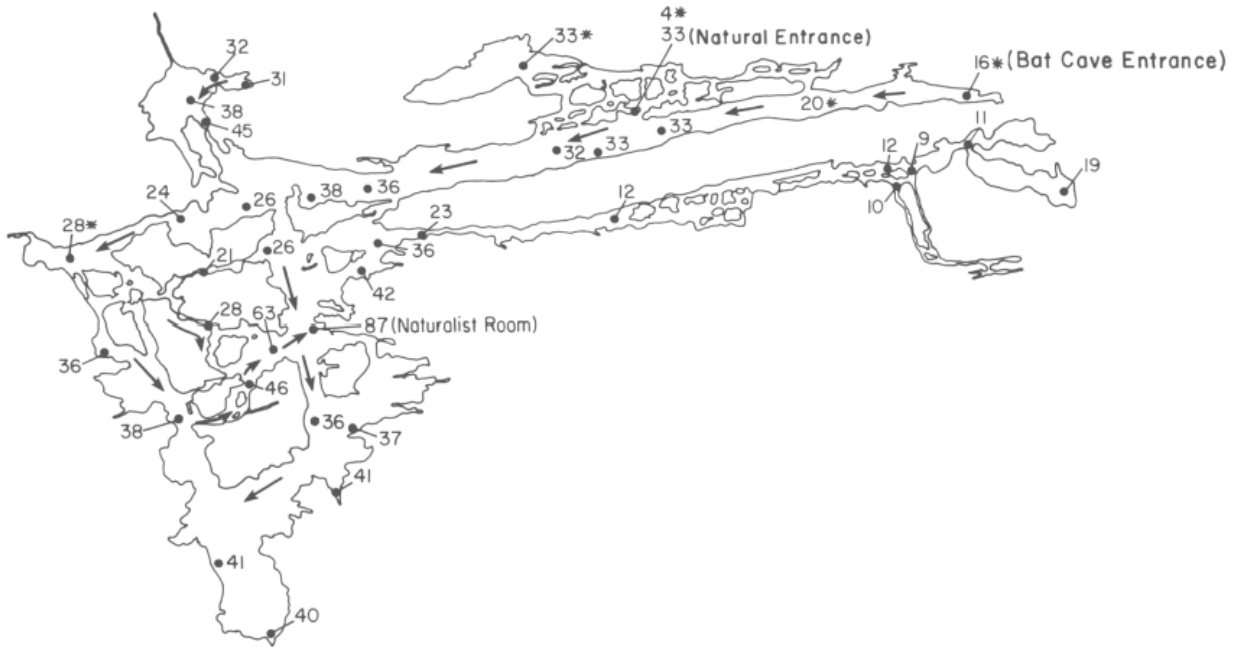

FIGURE 25—Air-flow direction (arrows) as inferred from radon concentration, Carlsbad Cavern. Radon-daughter concentration (pCi/l) was measured by August by Beckman and Rapp (1976), and radon-daughter concentration* was measured in November by Beckman et al. (1975).

features are formed above the water table by free-flowing water. Cave-passage forms in the Guadalupe Mountains are all phreatic, while cave-karren forms may be either phreatic or vadose. In the following discussion of geomorphic forms, the terminology of Sweeting (1973) and/or Bogli (1980) is used, except in cases where new geomorphic forms are being introduced.

Passage forms

Spongework—A three-dimensional, honeycombed, "Swiss cheese" network of cavities a few centimeters or so in diameter and depth. Spongework voids are the result of diffuse circulation of water within pore spaces in bedrock. Every cave in the Guadalupe Mountains is surrounded by bedrock which exhibits a matrix or framework of sponge-work.

Boneyard—A large form of spongework which is separated by stretches of unaffected wall. "Boneyard" is so named because it looks like a jumble of bones (Fig. 15). This integration of space and rock may be a few meters deep and wide, or it may continue for a distance of many meters. A boneyard type of passage form is evidence of non-differential phreatic attack where cave ceilings are subjected to as much solution as cave walls. An example of a boneyard is the Boneyard, Carlsbad Cavern.

Spring shafts—Tubular pits created by upwelling water under pressure. They are distinct from "collapse shafts," which are created by the collapse of underground cavities and are characterized by breakdown on their floors. They are also distinct from vadose, dome pit, "vertical shafts," which are characterized by vertical wall flutes and floor drains. Spring shafts may constitute a "phreatic loop" between two cave levels (Fig. 14) or may lead to the surface. Examples of spring shafts in Guadalupe caves are the tubular entrance to Deep Cave and the Bottomless Pit and Pit Survey Shafts, Carlsbad Cavern.

Joint chimneys—Fissure-shaped canyons rather than tube-shaped shafts. They may connect two cave levels or may lead to the surface. One example of a joint chimney is in the Cave of the Madonna, where Dean's Drop connects the New Year's Eve Room with the Lower Passage.

Solution domes—Semicircular to circular arches in cave ceilings which are a few meters to tens of meters in breadth and depth. In non-bedded rock they display solutional surfaces, but in bedded rock they may exhibit angular surfaces if modified by collapse. Collapse domes are vadose features, but solution domes are created by phreatic water lifting under pressure. Well-developed solution domes (partly modified by collapse) are in Sand Passage, Carlsbad Cavern.

Solution pockets—Spherical cavities in cave walls or ceilings that are tens of centimeters to tens of meters wide and deep. Ceiling solution pockets are approximately equidimensional, or they may be linearly developed along joints. Sometimes ceiling pockets form in a vertical series, where multiple concavities increase in circumference. Wall solution pockets may be approximately equidimensional, or they may be linearly developed along a bedding plane. Some wall solution pockets in Guadalupe caves appear almost scallop-like, but they are not discernibly directional as are scallops, a cave-karren form. Bogli (1980) classified ceiling-and wall-solution pockets as phreatic features, ones which form under low-velocity flow conditions. Equidimensional, linear, and multiple ceiling pockets and equidimensional wall pockets may be seen in the Lunch Room area, Carlsbad Cavern; linear wall pockets can be seen in bedded rock at the top of the Main Corridor.

Karren forms

Scallops—Shell-shaped solutional concavities on cave walls and ceilings which are ridged or crested on their upstream sides and more gently sloping on their downstream sides. Scallops are indicators of past current direction and velocity, the distance between scallop crests being inversely proportional to the flow velocity (Curl, 1974). Scallops are usually small features, not more than a few centimeters long, produced by fast-flowing vadose streams; however, they may also be larger features, indicating the past presence of slower-flowing, sub-water-table streams.

The walls of Guadalupe caves often exhibit scallop-like markings, but these are usually not developed well enough to determine the direction and velocity of past flow. An exception to this rule are the scallop marks in the entrance area of Bat Cave, Carlsbad Cavern. These have scallop lengths of 1.5-5 m and a skewness which indicates that past flow was eastward, along Bat Cave. Using Curl's formulas, this corresponds to a past flow velocity of about 0.5-2 cm/sec, or, for a passage cross section of 30 x 20 m, a flow rate of 3-12 m^3/sec. The size of these scallops suggests that they are of phreatic origin. Two other possible scallop areas are along the south wall of the Main Corridor just before its connection with Appetite Hill, and along the west wall of Appetite Hill. The south-wall scallops appear to point straight up; the west-wall scallops appear to be oriented at about a 30° angle.

Air scallops—Smooth, concave pockets in cave walls and ceilings which resemble water-formed scallops in some respects, but are much larger and exhibit blunt, rather than sharp, crests. Air scallops often truncate travertine material as well as bedrock. They are believed to be condensation-corrosion features where corrosive air flow scallops bedrock and speleothems concordant with each other. It is entirely possible that air scallops are air-corrosion modifications of previously formed phreatic solution pockets. A particularly well-developed air scallop 3 m in diameter can be seen just below the base of two directionally corroded shields about 20 m before reaching the Lake of the Clouds, Carlsbad Cavern (Fig. 93). Other air scallops in Carlsbad Cavern occur at Devil's Spring where they cut across drapery speleothems and bedrock.

Rillenkarren—Grooves with rounded troughs and sharp ridges. They are a common surface geomorphic form in many karst terrains and can also be a cave-karren form. Rillenkarren are created by vadose drippage in areas where water is highly charged with carbon dioxide. In Carlsbad Cavern, rillenkarren are present on bedrock walls and floors in the Left Hand Tunnel, Bell Cord Room, Boneyard (Fig. 16), New Mexico Room, and Cable Slot (Fig. 26). One of the best examples is in the Bell Cord Room, where grooves are up to 30 cm deep, 10 cm wide, and 2 m long. These occur in bedrock and breakdown and also in subaerially formed flowstone (Fig. 27). The rillenkarren on breakdown blocks in the Bell Cord Room originated at semicircular drip points on horizontal slopes and then proceeded to form deep channels on vertical slopes (Fig. 28).

Spitzkarren—A variation on the rillenkarren form is spitzkarren, sharply spiked solutional features in bedrock or breakdown which have been corroded down to sharp-slivered edges or pointed crests (Fig. 29). The only known spitzkarren locality in any Guadalupe cave is at the beginning of the Big Room, Carlsbad Cavern, where the historic trail descends from a high breakdown pile toward the Lunch Room. Here, spitzkarren and rillenkarren occur together, with secondary calcite crusts sometimes covering the surface of the spitzkarren. Where the spitzkarren is not calcite-covered, textural features such as fossils and clay-residue patterns are displayed in relief in the corroded bedrock.

Corrosion channels—Indentations in a cave ceiling or wall which are believed to have been formed by corrosive air. At the very top of the Lake of the Clouds Passage, a curving channel 1.5-3 m wide and 0.6-1 m deep can be followed

FIGURE 26—Distribution of rillenkarren in Carlsbad Cavern (stippled areas). After Queen (1981).

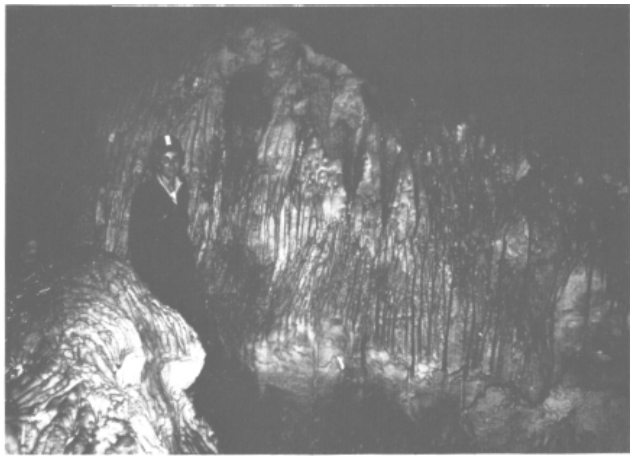

FIGURE 27—Rillenkarren on breakdown (center) and on flowstone (lower left corner), Bell Cord Room, Carlsbad Cavern. Photo Alan Hill.

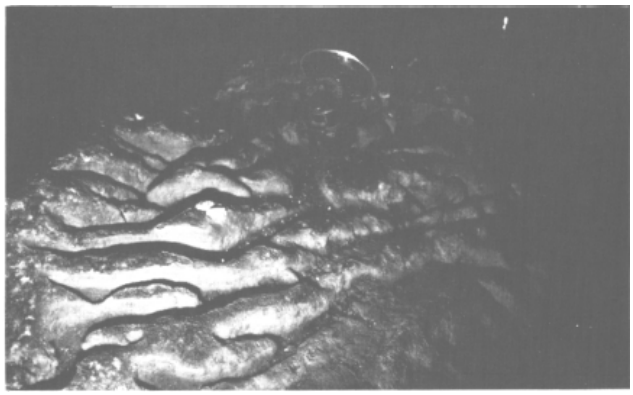

FIGURE 28—Rillenkarren formed on the upper surface of a piece of breakdown, Bell Cord Room, Carlsbad Cavern. Note that the rillenkarren grooves begin at semicircular drip points (lower left of figure). Photo Alan Hill.

along the ceiling to where the passage ascends toward the Bell Cord Room (Fig. 94). Stalactites along this channel are an opaque chalk-white and highly corroded. Corrosion channels also occur at the top of the ascent leading toward the Bell Cord Room where chalk-white calcite "lines" remain of once-present dripstone which has been corrosively at-tacked down into ceiling joints.

Punk rock—Bedrock which has been so highly corroded that it is soft and flaky rather than hard and crystalline. Upon corrosive weathering under air-filled conditions, the residue of the bedrock is exposed, causing the surface of the rock to appear dark brown (Pl. 11A). Where the punk-rock residue has flaked off the wall, it forms debris piles of dark silt on the floor.

Cave hydrology

Water is noticeably absent in the caves of the Guadalupe Mountains. The water table is below all known cave passages (Sheet 1). Flowing vadose streams do not exist in any

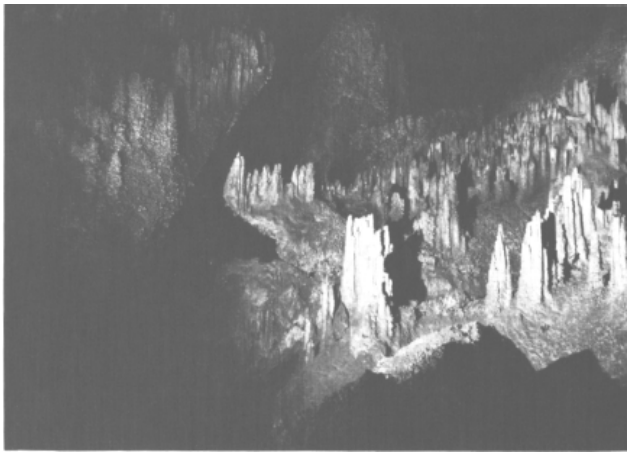

FIGURE 29—Spitzkarren on breakdown near the junction of the Big Room with the Lunch Room, Carlsbad Cavern. The tallest spitzkarren is about 1 m in height. Photo Alan Hill.

of the caves, with the exception of Vanishing River which is located in the bottom of a ravine and captures water during heavy rainfall. The only water in the caves is drip and pool water, vadose meteoric water which slowly seeped down from the surface along joints, bedding planes, and interconnected pores.

After a heavy rainfall, meteoric water is temporarily stored in the subcutaneous zone (upper weathered layer of rock beneath the soil) and then, after some delay, finds its way into the lower vadose zone. McLean (1976), using monthly rainfall and infiltration totals, found no correlation between rainfall and meteoric water entering Carlsbad Cavern. Williams (1983), however, using weekly totals, reported a response lag of 2-14 weeks between rainfall and infiltration. The lack of a clear relationship between lag time and depth in Carlsbad Cavern indicated to Williams that percolation routes through the vadose zone are highly variable, often independent of each other, and subject to "capillary barriers"—capillary-like channels which diminish the pressure pulse effect of storage recharge following rainfall.

Hydrograph measurements of cave-pool levels were made by McLean (1976) for 11 pools in Carlsbad Cavern and these fluctuations were correlated with evaporation rates. In addition, T. Rohrer (pers. comm. 1986) measured the drop in water level in the Lake of the Clouds: from 1966 to 1986 the lake lowered by 31.27 cm.

Description of cave deposits

Cave deposits in Guadalupe caves are discussed using the classification scheme of Pettijohn (1957), whereby clastic deposits are described first, followed by the primary precipitates (gypsum and chert), mineral deposits (endellite-montmorillonite-palygorskite, sulfur, and carbonate speleothems related to speleogenesis problems), and biological deposits (bat guano and animal bones).

Clastic deposits

A clastic deposit is one which is composed of fragments of material. Clastic fragments in caves can be large (e.g. breakdown blocks), small (silt and sand particles), angular (breccia), or rounded (cobbles). The clastic deposits in Guadalupe caves are discussed in order of decreasing clast size, starting with breakdown and ending with mud.

Breakdown

Breakdown is bedrock which has fallen from the ceilings or walls to the floor of a cave. Breakdown pieces originating on cave ceilings often break along bedding planes (e.g. Seven Rivers Formation, Cottonwood Cave), and breakdown pieces originating along cave walls often exfoliate along vertical joints (e.g. the main corridor of Ogle Cave). The most common causes of breakdown collapse are: (1) loss of buoyancy and the drying out of rock directly after water recedes from a cave passage, (2) crystal-wedging of rock by crystalline material such as gypsum which forces bedding planes apart during a subaerial episode, and (3) earthquake tremors. The shape of breakdown pieces depends on whether the rock is bedded or not: breakdown in the bedded Seven Rivers Formation tends to be tabular, whereas in the massive Capitan reef it tends to be equant. Size of breakdown blocks varies from small, fist-size blocks up to blocks tens-of-meters high. The largest known piece of breakdown in any Guadalupe cave is Iceberg Rock in the Main Corridor of Carlsbad Cavern, which was estimated by Bullington (1968, p. 22) to be "170 feet in length and to weigh over 200,000 tons."

Breccia

Breccia is a clastic deposit which consists of angular fragments or clasts sometimes cemented together by matrix material. Breccia occurs in some Guadalupe caves, most notably in Virgin Cave and Carlsbad Cavern (Table 7), and it has also been observed in other caves including Cottonwood, Ogle, and New (M. Queen, pers. comm. 1984). The breccia is exposed in the bedrock walls and ceilings of cave passages, its clasts and matrix material having completely filled early-stage cavities in the rock which have been later truncated by the dissolution of the large cave passages.

Virgin Cave—Breccia deposits are displayed in cave walls and ceilings at the bottom of the first drop, all the way to the Four O'clock Staircase, and beyond to the Cavernacle. The breccia is composed of centimeter to 0.3 m long clasts cemented in a crystalline calcite or mudstone matrix. Many of these clasts appear to have been sheared in place. Virgin Cave is located near the contact of the backreef Seven Rivers and Queen(?) Formations with the Capitan Limestone reef facies. Almost the entire cave seems to be developed along a brecciated zone at or near this contact (Hill, 1984c).

Carlsbad Cavern—Breccia deposits in Carlsbad Cavern are also located primarily at or near the contact of backreef

TABLE 7—Breccia deposits in Guadalupe Caves.

Location	Description	Occurrence
Carlsbad Cavern		
Guadalupe Room	1-33 cm angular clasts in a fine-grained, tan to gray matrix of clastic debris or crystalline calcite.	Breccia exposed in the north wall.
Secondary Stream Passage	1-6 cm clasts in a crystalline calcite matrix.	Breccia exposed in southwest wall near ceiling, Spar Room.
Appetite Hill-Iceberg Rock	1 cm long clasts in dark-orange to tan carbonate and mudstone matrix. Also separate clasts of mudstone in limestone.	Breccia exposed in bottom of Iceberg Rock along trail and along Shortcut Route.
Virgin Cave	1-33 cm clasts cemented in a crystalline calcite and mudstone matrix. Associated with spar crystals and casts of spar crystals.	Exposed in wall and ceiling bedrock from bottom of first drop to top of Four O'Clock Staircase and all the way to the Cavernacle. Whole cave seems developed in a brecciated zone.

FIGURE 30—Distribution of breccia, Carlsbad Cavern (stippled areas). Queen (1981) and this study.

beds with the Capitan Limestone (Fig. 30). Queen (1981) recognized two joint-controlled trends of the breccia in Carlsbad Cavern which he noted as being continuous or parallel to breccia-filled clastic matrix and spar-filled joints in surface-bedrock exposures above the cave.

One of the best breccia exposures in Carlsbad Cavern is in the north wall of the upper Guadalupe Room, near where blocky beds of the Yates Formation interfinger along the wall. In this occurrence breccia clasts, 0.3 m or more in length, are oriented at various angles in a fine-grained, tan to dark-gray mudstone matrix (Pl. 1A). Also in this area, breccia clasts of similar size occur in a matrix of crystalline calcite spar (Fig. 67).

Queen (1981) identified five breccia localities in the Appetite Hill–Iceberg Rock section of the Main Corridor. The breccia consists of abundant dark-gray, fine-grained clasts set in a dark carbonate and mudstone matrix composed of similar material as the clasts themselves. Mudstone clasts along with limestone clasts in a dark-orange matrix are present also along the Shortcut Route near Iceberg Rock. In other breccia occurrences at Iceberg Rock (along the trail climbing up Appetite Hill), individual clasts exist in the limestone not as cavity fillings, but as isolated, angular pieces of mudstone and limestone.

Cobble gravel

One of the most perplexing deposits in Carlsbad Cavern is the cobble gravel, rounded clasts which appear sporadically all the way from Bat Cave, down the Main Corridor, in Upper Devil's Den, down into Secondary Stream Pas-sage, and—most dramatically of all—in Lower Cave, 150 m below the surface (Fig. 31). Only one other Guadalupe cave, Pink Fink Owlcove near Frank's Cave high in the escarpment above Black Canyon, is known to contain rounded clastic deposits. Description of the gravel in these two caves is summarized in Table 8.

Pink Fink Owlcove—This is a small cave about 15 m long, 9 m high, and 6 m wide, developed at the contact of the massive Capitan Limestone with its reef-talus member. Along a small ledge in the lower part of the chamber near the east wall is a lens of cemented gravel about 10 cm thick, both overlain and underlain by yellowish-tan silt. Many of the pebbles in the gravel are characterized by centers which are either hollow or filled with a dry moonmilk-like powder.

Carlsbad Cavern—Along the Main Corridor, near and in the boneyard maze that eventually leads to the Guadalupe Room, is an occurrence of pebble–cobble conglomerate overlain by laminated silt layered roughly parallel to the underlying horizontal bedrock surface. Pebble gravel can be seen packed into a ledge directly along the trail; if one follows the trail to where it turns abruptly, a "nest" of cobbles can be seen along a continuation of the ledge (Fig. 32). The gravel of the Main Corridor can be followed about 12 m into a maze of side passages in the wall, where cobbles and pebbles are overlain by, and mixed with, orange silt.

The next appearance of cobbles is about 30 m down the Main Corridor in Upper Devil's Den, where the first cobbles encountered are located under a pile of huge breakdown to the left of the trail. These cobbles occur below a layer of orangish silt about 15 cm thick. Approximately 7 m further along the trail and directly next to it, cobbles can be seen included in the upper portion of a gypsum deposit.

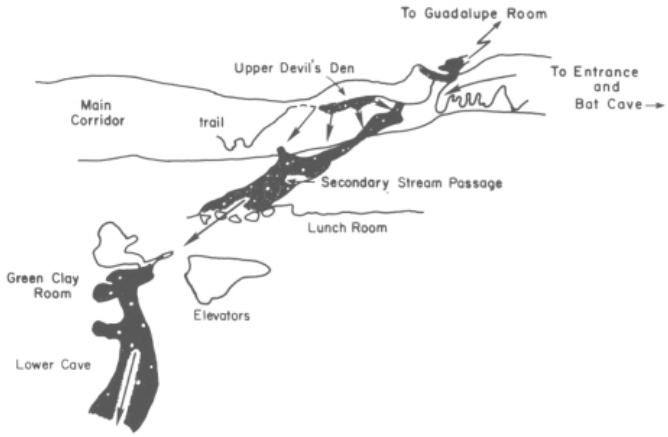

FIGURE 31—Proposed travel route (arrows) of the cobble gravel down the Main Corridor, Secondary Stream Passage, and Lower Cave, Carlsbad Cavern. From Upper Devil's Den to the Green Clay Room the cobbles have almost as much vertical (90 m) as horizontal (120 m) extent.

TABLE 8—Cobble-gravel deposits in Guadalupe Caves.

Location	Description	Occurrence
Carlsbad Cavern		
Main Corridor	Cobble and pebble clasts 10 cm or less in diameter. Black, angular chert pieces.	Gravel packed in wall ledge of Main Corridor. Larger clasts also exposed in maze passages in wall which eventually lead to the Guadalupe Room. Orange silt overlies gravel.
Upper Devil's Den	Cobbles and pebbles 10 cm or less in diameter.	Under breakdown and silt, and included in a gypsum block.
Secondary Stream Passage	Boulder, cobble, and pebble clasts 45 cm or less in diameter. One quartzose pebble found in the cobble gravel (M. Queen, pers. comm. 1983).	Gravel interbedded with orange silt; was once overlain by 1 m thick silt. Space between cobbles filled with fine-grained pebble matrix. Top of cobbles mantled by orange silt.
Lower Cave	Cobbles and pebbles 19.5 cm or less in diameter. 99% limestone clasts, semirounded to rounded, disc-shaped, some with hollow or weathered centers. 1% angular black and white chert pieces; also rounded spar pieces.	Orange silt overlies indurated cobble gravel along a possible unconformity. Gravel appears to have slumped out of solution pockets in the wall. Space between cobbles filled with fine-grained pebble matrix. "Cobblestone" floor exposed in Nooges Realm, location of the trenching site.
Pink Fink Owlcove	Pebbles 4 cm or less in diameter, semirounded, with hollow or weathered centers.	Pebble-gravel conglomerate interbedded with a yellowish-tan silt.

In the Secondary Stream Passage, 60 m vertically below Upper Devil's Den, cobbles again appear abruptly under breakdown, near where the Secondary Stream Passage ascends up into Lower Devil's Den. Rounded limestone clasts in this passage are up to 45 cm in diameter; that is, a few of them are boulder-sized (>256 mm), but most are cobble-and pebble-sized. The cobbles continue intermittently along the Secondary Stream Passage all the way to the Lunch Room, where in places they are partly covered by floor flowstone, while in other places they can be seen filling solution pockets in the cave wall at floor level. The cobbles disappear again, equally as abruptly, where the Secondary Stream Passage joins with the Lunch Room.

The cobble gravel in Secondary Stream Passage is both overlain with silt and interbedded with it. Where the Secondary Stream Passage meets with the Lunch Room, orange silt is interbedded with lenses of lighter-colored, matrixed conglomerate. At this location the cobbles are mantled by laminated orange silt. At the Y-Junction, about 30 m into the Secondary Stream Passage from the Lunch Room, 0.6 m of orange silt is interbedded with 0.5 m of gravel in an orangish matrix. Orange silt once covered the exposed gravel to a depth of 1.5 m at this location, as is evidenced by the presence of orange silt in solution pockets up to 1.5 m above the present level of the cobble gravels, but this thick silt covering has been mostly eroded away. A shallow (0.3 m) trench dug at the Y-Junction revealed that most cobbles at this locality (ca 80%) do not directly touch one another; instead, the interstices between individual cobbles are filled with 3–4 cm of matrix material made up of semi-indurated pebble, sand, and silt. The larger cobbles make molds in the finer material if pried loose from the matrix.

The most extensive cobble-gravel deposits in Carlsbad Cavern occur in Lower Cave (Fig. 33) where they appear intermittently all the way from the Green Clay Room almost to Nicholson's Pit. The most peculiar aspect of the Lower Cave cobbles is their distribution: they do not seem to come from, or go, anywhere. The "upstream" limit of the cobbles is at the Green Clay Room where cobbles occur in a whirlpool-like floor depression about 1 m deep. The Green Clay Room continues on towards the Naturalist Room via a labyrinth of tight crawlways, but there is no evidence (such as cobbles hung-up in the crawlways) that the cobbles entered Lower Cave by this tortuous route. The "downstream" end of Lower Cave is no less an enigma. The cobbled "stream" channel abruptly ends about 30 m before Nicholson's Pit; yet, no cobbles fill the pit, as would be expected if the pit had antedated the cobbles.

FIGURE 32—A "nest" of rounded cobbles exposed along the north wall of the Main Corridor, Carlsbad Cavern. Photo Ronal Kerbo.

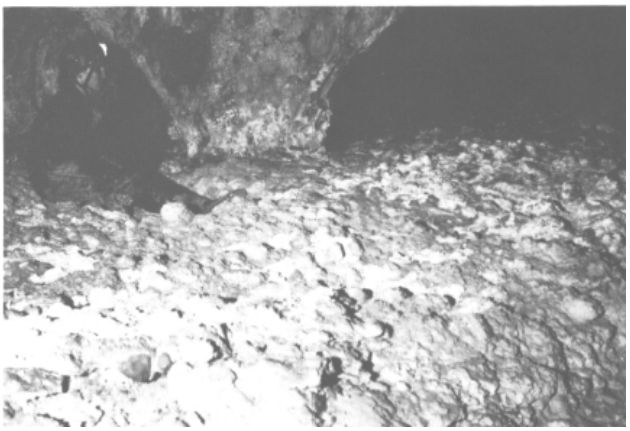

FIGURE 33—Cobble gravel in the Junction Room, Lower Cave, Carlsbad Cavern. The cobbles are coated with a white carbonate crust. Photo Cyndi Mosch Seanor.

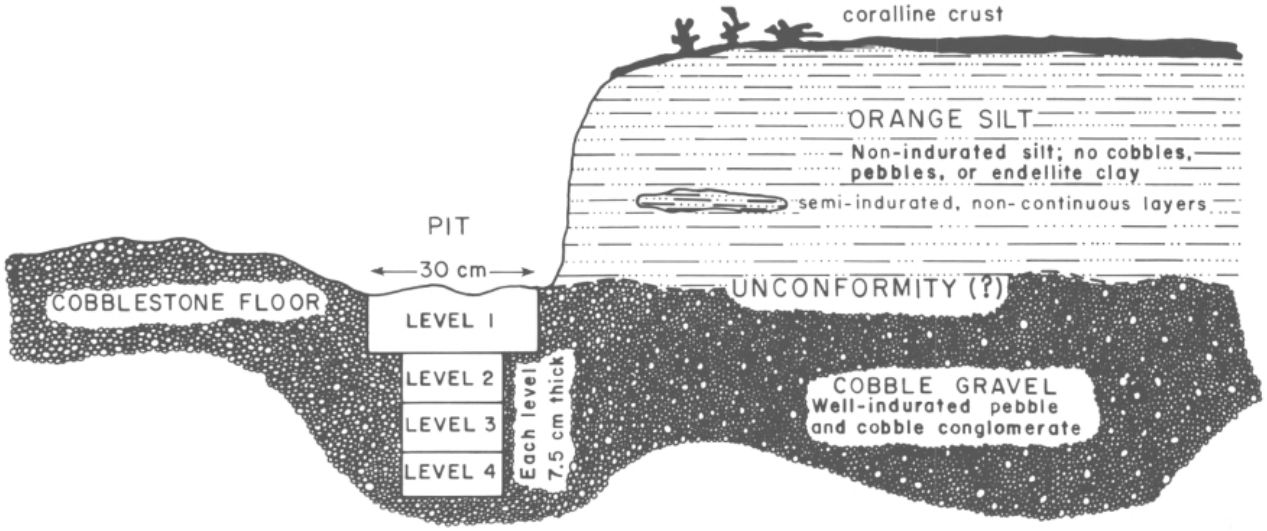

FIGURE 34—Diagrammatic cross section of the trench made in Lower Cave, Carlsbad Cavern, showing a possible unconformity between the cobble gravel and orange silt.

Bretz (1949) claimed to have traced the direction of "stream flow" in Lower Cave by noting the gradient of the passage and by the imbrication of the cobbles. However, most of the cobbles examined during the course of this study do not appear imbricated, the possible exceptions being five cobbles in the "cobblestone" floor at Nooges Realm. The average strike of the five cobbles is 56°, with a range of 37-79°, and the cobbles imbricate 146° "upstream," not "down-stream," in the direction of the 1-1.5° gradient of passage slope in Lower Cave.

The cobble gravel of Lower Cave, unlike that of the Main Corridor and Secondary Stream Passage, is not interbedded with silt, but instead is overlain with orange silt in banks up to 7 m high. These two types of deposits, the gravel and the silt, are completely dissimilar: the cobble gravel contains rounded limestone cobbles up to 19.5 cm in diameter imbedded in a light-tan, well-indurated, and sometimes sparry matrix, whereas the orange silt consists of fine-grained, well-sorted, loosely consolidated material which does not contain a single cobble or pebble-sized clast. Furthermore, the contact between the two deposits is sharp, with the silt resting on top of an undulating cobble-gravel horizon. The contrast in composition between the two deposits and the sharp undulating contact between them suggest that an unconformity exists between the cobble gravel and silt in Lower Cave. The best localities to view this possible unconformity are along a loop-around side passage in the Junction Room (Pl. 1B) and in Nooges Realm; at the latter location, the undulate "cobblestone" can be traced underneath a 1 m high orange silt bank (Fig. 34).

In order to study the possible unconformity, and also to investigate the cobble gravel at depth, a 0.3 m square, 1 m deep pit was dug in the silt and cobble gravel of Nooges Realm, Lower Cave (Fig. 34). Size, sphericity, roundness, and other parameters were ascertained for the cobble gravel excavated. The results for sieved samples of this gravel are shown in Table 9. The size data shows that the cobbles are flattened and disk-shaped according to Zingg's classification of shape (Krumbein and Sloss, 1963), with the average long axis of the cobbles more than twice as long as the short axis. According to the Power's roundness scale (Folk, 1968), the cobbles range from subangular to well rounded. The cobbles in the "cobblestone" floor and in Level 1 of the pit are larger than those in Levels 2, 3, and 4, but below Level 1 there is no statistical difference in cobble size.

The cobble gravel exposed in the pit is heterogeneous, poorly sorted, and lacks internal stratification. Essentially, the gravel contains a chaotic size mixture of debris. The cobbles usually do not touch each other, but instead are matrix-supported. The matrix contains smaller particles of pebble, sand, and silt; it is light-colored and semi-indurated (i.e. the cobbles and pebbles can be dug out from the matrix with a knife but not with the fingers). Many of the cobbles in Lower Cave have fine-grained, moonmilk-like centers similar to those in Pink Fink Owlcove. Cobbles filled with this moonmilk-like substance can lie directly adjacent to

TABLE 9—Data on gravel excavated from a trench in Lower Cave, Carlsbad Cavern.

	Number of clasts >2.5 cm	Largest clast, cm			Average size, cm			Roundness		Weathered or hollow clasts	Angular chert clasts	Spar clasts	Notes
		Long axis	Int. axis	Short axis	Long axis	Int. axis	Short axis	Rge.	Avg.				
Cobblestone floor	123	19.5	—	—	7.3	5.3	3.0	5–6	—	many	—	—	Weathered, moonmilk-centered cobbles may lie directly adjacent to completely crystalline cobbles.
Level 1	163	8.1	7.5	3.8	4.9	3.5	2.3	3–6	4.0	6	1	3	3 rounded spar clasts. 1 piece of black chert.
Level 2	68	8.1	7.5	3.8	3.4	1.7	1.5	3–6	3.8	1	3	0	3 black chert pieces, 1 semirounded mud clot.
Level 3	36	12.5	7.5	6.3	3.7	2.6	1.8	3–6	4.0	0	2	0	1 black chert piece, 1 white chert piece.
Level 4	68	7.5	5.6	4.4	3.2	2.2	1.5	3–6	4.3	1	2	0	2 black chert pieces, 1 semirounded mud clot.

completely crystalline limestone cobbles: both have the same outward appearance, but upon breaking the moonmilk-filled cobbles fall apart like talcum powder.

Almost all (99%) of the debris removed from the Lower Cave pit was composed of limestone with the exception of a few (1%) pieces of chert, iron-oxide fragments, and calcite spar. The chert fragments are angular, white or black, and vary in length from 1.5 mm to 12 mm (Table 9). Semi-rounded, thin pieces of iron oxide were found at all levels in the pit. These look as if they might have once been surface coatings over bedrock which broke off from the rock and then became semirounded. In Level 1 of the pit were found three pieces of spar, which may have once been part of a single rounded crystal.

Sand and silt

Compared with caves like Flint–Mammoth, Kentucky, which have kilometers of sediment-filled passages, the caves of the Guadalupe Mountains are relatively devoid of sediment. Where sand and silt do occur on cave floors, the source of these deposits can almost always be traced to nearby silty or sandy bedrock. Deposits which clearly display this relationship to bedrock units are: (1) Sand Passage, Carlsbad Cavern; (2) New Mexico Room, Carlsbad Cavern; (3) Bottomless Pit area, Carlsbad Cavern; (4) Sand Floor, Sand Cave; (5) Flat Floor Room, McKittrick Cave; (6) Green Lake Room, Endless Cave; and (7) Sand Slope, Cottonwood Cave. For the petrography of some of these deposits see Table 10. Carlsbad Cavern has the best exposures of fine-

TABLE 10—Petrographic description of some sand, silt, and mud deposits in Guadalupe Caves. Roundness according to Powers Scale, size classification after Folk (1968).

Location	Identification, possible source, and description
Carlsbad Cavern	
New Mexico Room	Debris of sandstone bedrock Bell Canyon Formation(?) Very clean, white to light gray, well sorted 90% quartz grains, 5% calcite grains, 5% feldspar 0.1 mm maximum, 0.01–0.05 mm average; coarse silt to fine sand Angular to subrounded quartz grains Some black magnetite(?)
Big Room	
Bottomless Pit	Cream-colored clastic material near wall Bell Canyon Formation(?) 90% quartz grains, 5% feldspar Quartz grains coated with a light-tan clay 0.1 mm maximum, 0.01–0.05 mm average; coarse silt to fine sand Angular to subrounded quartz grains Some calcite, gypsum, chert, and magnetite(?)
Breast of Venus	Material of the quartz-sand half cones Bell Canyon Formation(?) Very clean, white to light gray or tan, well sorted 0.2 mm maximum, 0.01–0.05 mm average; coarse silt to fine sand Angular to subrounded quartz grains A few quartz grains coated with iron oxide Some calcite and magnetite(?)
Lower Cave	Orange silt of the silt banks Forereef facies(?) Clay-coated quartz grains 0.5 mm maximum, 0.04 mm average; coarse-grained silt Angular to subrounded to well-rounded quartz grains Many calcite and gypsum crystals; possible chert pieces and frosted quartz grains
Sand Passage	Orange-brown "sand" along trail Yates Formation Quartz crystals highly masked by iron-oxide 0.1 mm maximum, 0.05 mm average; coarse silt to fine sand Angular to subrounded quartz grains Many needle-like aragonite(?) crystals
Guadalupe Room	Silt of calcified siltstone Yates Formation(?) 80% calcite cement, 20% siltstone 0.2 mm maximum, 0.05 mm average; coarse silt with minor sand Subangular to subrounded quartz in siltstone fraction Dark-brown to orange variegated layers; darker part of the siltstone contains 0.43% iron and 0.06% manganese Mostly calcite crystals
Cottonwood Cave	
Entrance Hall	Sand of Sand Slope at end of Entrance Hall Yates Formation(?) Quartz crystals partially masked by iron oxide 0.2 mm maximum, 0.05 mm average; coarse silt to fine sand Angular to subrounded quartz grains Some calcite crystals; quite a few pieces of magnetite(?)
Mud Passage	Mud of Mud Passage Rounded clots of dark-brown mud No crystals discernible except for a few, highly birefringent calcite crystals

FIGURE 35—Distribution of silt and sand in Carlsbad Cavern (stippled areas).

grained clastics; these are the only deposits that will be elaborated on. Clastic sediment lines the walls of parts of Left Hand Tunnel, covers the floor of a major part of Lower Cave, and occurs sporadically throughout the Big Room (Fig. 35).

Left Hand Tunnel—Orange-silt banks up to 1.5 m high line sections of Left Hand Tunnel (Fig. 36). Many of these banks have been excavated for trail building, an activity which has exposed the slumped and layered nature of the silt. The silt banks are level along the walls on opposite sides of Left Hand Tunnel, but slump toward the middle of the passage wherever a canyon dissects the floor. The orange silt in Left Hand Tunnel appears and disappears in accordance with the appearance and disappearance of the reef-talus and reef-core facies (compare Figs. 18 and 35). Reef-talus sections are characterized by vertical canyons rather than horizontal mazes, by a lack of travertine de-posits, by crude bedding planes which dip approximately 30° to the south, by fossiliferous (brachiopods, crinoids, fusulinid foraminifera) bedrock, and by pods of orange silt in the limestone and orange silt on the floor.

Lower Cave—The most extensive deposits in Carlsbad Cavern are in Lower Cave, where flat-topped silt terraces and banks up to 7 m high line the passage walls (Fig. 37). The sediment directly overlies cobble gravel in many places along Lower Cave (Pl. 1B), and is itself overlain by sub-aerially formed crustal or dripstone deposits (Fig. 69).

Dunham (1972) described the clastic material of Lower Cave as a reddish-tan gypsiferous silt containing particles coated with a hydrated ferric-iron oxide, and crystals of gypsum along with scarce fragments of quartz, dolomite, and calcite. Observations made during this study agree with those of Dunham: silt-sized, clay-coated quartz grains, and calcite and gypsum crystals comprise the bulk of the orange sediment of Lower Cave (Table 10). As elsewhere in the cave, the orange silt of Lower Cave contains no cobbles, pebbles, or montmorillonite–endellite clay.

DuChene (1972) collected samples of silt in Lower Cave (both below the Jumping Off Place and further down the passage near Stegosaurus Rock) and performed a statistical size analysis on them. The mean particle size of the sediment in Lower Cave is 4.65 phi units (0.04 mm), with a standard deviation of 0.158. Thus, the sediments of Lower Cave are a very well-sorted, coarse-grained silt. DuChene

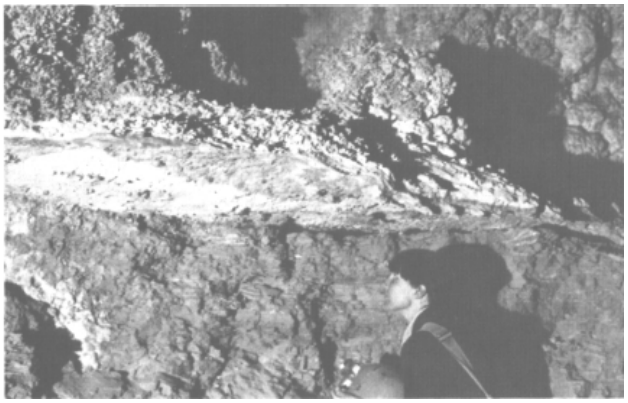

FIGURE 36—A silt bank, Left Hand Tunnel, Carlsbad Cavern. A carbonate crust extends outward over the layered silt where the silt has been excavated for trail construction. Photo Alan Hill.

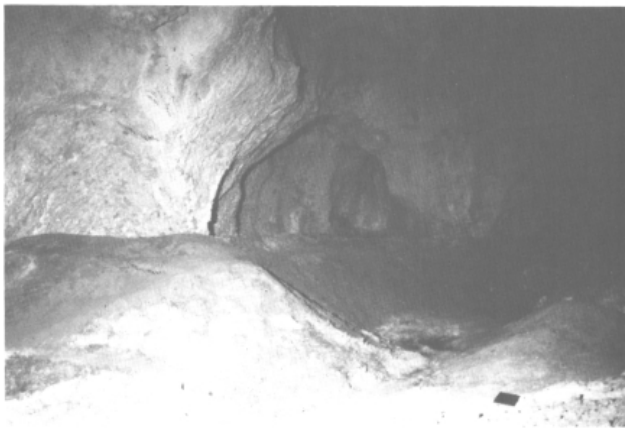

FIGURE 37—Entrenched silt bank, Lower Cave, Carlsbad Cavern. Note the flatness of the bank. Photo Jeep Hardinge.

also determined a water-soluble-salt content of 2.5% for the water-soluble salts of sodium and magnesium, and a carbonate content of between 15% and 40% for the two collection sites, respectively. The 40% carbonate content for the Stegosaurus Rock site is perhaps representative of the carbonate content in the upper parts of the sediment banks where they are covered with carbonate coralline crusts. The sediment near the Jumping Off Place, with a 15% carbonate content, was collected near a site of dripping water and, as such, has probably been leached of part of its carbonate content.

In some places in Lower Cave the silt displays a laminated texture highlighted by bands of lighter carbonate material between laminae. Three sets of bands are most pronounced, the sequence varying from place to place. There is a faint banding at 1 mm between laminae, more conspicuous bands 1-2 cm apart, and the lightest, most conspicuous bands 2-4 cm apart (Pl. 2A). Laminations are usually best preserved in sediment banks located under protected alcoves, but they also can be seen in silt banks within the largest passages in Lower Cave, such as at DuChene's Stegosaurus Rock collection site.

Like the sediment banks in Left Hand Tunnel, the tops of the Lower Cave banks are essentially level, both across the passage and all the way along the entire length of Lower Cave (Table 11). The original upper surface of the flat-topped terraces is difficult to determine because remnant patches of orange silt partially fill solution pockets in the limestone up to 1.5 m above the upper terrace level of the banks. This probably signifies that the silt has compacted since its initial deposition; thus, the sediment bank heights listed in Table 11 should be considered approximate values, varying as much as a meter or so, but not more, from the height of the originally deposited material.

The sediment banks in Lower Cave have been entrenched into erosional V's with slope angles of 30° or more (Fig. 37). A meandering pattern of downcutting is evident along a few segmented portions of Lower Cave, with the meanders confined by the walls of the cave. Downcutting continued throughout the entire silt horizon but stopped once the more competent, underlying cobble-gravel horizon was breached; indurated cobble gravel below the silt has not been downcut more than half a meter or so.

TABLE 11—Sediment bank elevations, Lower Cave, Carlsbad Cavern.

Location	Top of sediment banks	
Upper End of Lower Cave		
Green Clay Room	1,090.9 m	3,575.2
	1,091.3	3,579.5
	1,090.8	3,577.8
	1,090.9	3,578.2
	1,090.8	3,577.8
	1,090.5	3,576.8
Junction Room	1,901.8	3,581.1
	1,090.6	3,577.2
	1,092.7	3,584.1
	1,090.4	3,576.5
	1,090.1	3,575.5
Ladder Room	1,090.7	3,577.5
	1,090.6	3,577.2
	1,090.1	3,575.5
	1,089.8	3,574.5
Rookery	1,092.6	3,583.7
Nooges Realm	1,093.9	3,588.0
	1,092.2	3,582.4
Clay Bank by Stegosaurus Rock	1,093.4	3,586.4
Lower End of Lower Cave		

New Mexico Room—Along the east wall of the New Mexico Room are piles of clean white sand which represent residual sediment from the dissolution of light-colored, steeply dipping sandstone beds which comprise part of the east wall. The identity of these sandstone beds has been the subject of much debate. Black (1954) reported the occurrence of siliciclastic beds in the New Mexico Room which he interpreted as a possible basinward continuation of lower Yates sands. Moran (1955) speculated that the beds represented shelfward tongues of the sandstones of the Delaware Mountain Group (Bell Canyon Formation), possibly deposited on the basinward flank of an early reef. Candelaria (1982) thought that either interpretation was equivocal since neither of these sandstones is continuous enough to be traceable shelfward or basinward. This study favors Moran's contention that the sandstone beds in the New Mexico Room are part of the Bell Canyon Formation. It also favors Moran's definition of the Bell Canyon Formation; that is, that all sandstones on the basinward flank of the Capitan Limestone belong to the Bell Canyon. Evidence supporting a Bell Canyon origin for the New Mexico Room sandstone is:

(1) Strike and dip of beds in the New Mexico Room as measured by Moran (1955), Good (1957), and in this study are N70°E, 20-30°S; N65°E, 33°S; and N62°E, 36°S, respectively; i.e. the beds dip steeply toward the basin. In contrast to these measurements, backreef beds of the Artesia Group dip 3-4° toward the reef.

(2) Newell et al. (1953) and Grauten (1965) described the sandstone of the Bell Canyon Formation as a white, remarkably clean, homogeneous unit containing angular to well-sorted grains in the coarse-silt to fine-sand category. Moran (1955) found the light-tan to white sandstone of the New Mexico Room to be a coarse silt to sand, with over 50% of the particles in the very fine- to fine-sand category, and with negligible hydrocarbon content (0.015 mg/g). This study found the sandstone to be a clean, white, subarkosic (feldspar determined by the Mueller Process), homogeneous, fine-grained unit (Table 10). Where it is pure sand (99% sand, Table 27), it has a porosity and permeability of 28% and 61 millidarcies, respectively; if the carbonate content is greater and the sand content less (35% sand, Table 27), then the porosity and permeability is much lower (4.5% and 0.01 millidarcies, respectively). As is typical of Bell Canyon sands, porosity and permeability varies over short distances (about 5 m for the two collection sites in the New Mexico Room, Table 12).

(3) The New Mexico Room is too low for the sandstone to be part of the silty and sandy Yates Formation. The lowermost Yates beds crop out at the top of the Guadalupe Room, almost 100 m higher than the New Mexico Room level (Fig. 17).

(4) The altitude of the Bell Canyon Formation in the basin 0.5 km south of Carlsbad Cavern is at about 740 m (2,470 ft) (Fig. 12). If Bell Canyon beds dip 10-30° at their inter-section with the reef, as King (1942) stated and as the measured dips in the New Mexico Room indicate might be true, then the Bell Canyon sandstone could intersect the Capitan reef at about the Big Room-New Mexico Room level.

(5) The steeply dipping sandstone in the New Mexico Room is the site of sulfur mineralization. The fact that the sulfur occurs on the undersides of bedrock and gypsum speleothems is important because it indicates that the source of the sulfur (i.e. hydrogen-sulfide gas) may have come from below, or updip from the basin, along the clean, white, porous beds and into the cave. Moran (1955, p. 258) offered a similar opinion, but regarding oil rather than hydrogen-sulfide migration: "such sandstone tongues could serve as possibly conduits for oil from basin to porous reef. Lack of hydrocarbons may indicate that the sandstones have been

TABLE 12—Porosity and permeability of bedrock, Carlsbad Cavern, and Bell Canyon Formation, Delaware Basin.

Formation	Porosity(%)	Permeability (md)
Tansill (parallel to bedding) Natural Entrance Hill (1972)	2.2	0.51
Tansill (perpendicular to bedding) Natural Entrance Hill (1972)	2.1	0.01
Yates (parallel to bedding) Main Corridor Hill (1972)	0.5	0.02
Capitan (unbedded) Iceberg Rock-Appetite Hill Hill (1972)	1.7	14
Bell Canyon(?) (parallel to bedding) New Mexico Room (18 m east of ladder)	28.1	61
Bell Canyon(?) or Seven Rivers(?) (parallel to bedding) New Mexico Room (13 m east of ladder)	4.5	0.01
Ramsey massive "A" sandstone Bell Canyon, Delaware Basin Watson (1979)	10-30	10-150
Ramsey massive "A" sandstone Bell Canyon, Delaware Basin Berg (1979)	26 (avg., 18 samples)	50 (avg., 18 samples)
Ramsey massive "A" sandstone Bell Canyon, Delaware Basin Mercer (1983)	20-28	14-90
Sandstone, Bell Canyon, Delaware Basin Williamson (1979)	20-25	0.1-200

effectively flushed, perhaps during the period of formation of Carlsbad Caverns."

Big Room—Sediment in the Big Room of Carlsbad Cavern differs significantly from sediment in other parts of the cave and also from sediment in other Guadalupe caves. Instead of being a homogeneous orange-tan color, the Big Room sediment varies from cream to brick-red to green, brown, ochre-yellow, and purple. In some places the deposits over-lie montmorillonite-endellite clay and/or are interbedded with chert (Fig. 70).

The sand and silt in the Big Room have been previously described by Good (1957) and Queen (1981). Clay (montmorillonite-endellite) beds are usually overlain by silt and then by sand, but this trend is locally variable. Sand is commonly disseminated throughout the clay and silt, with the sand sometimes in layers of less than 1 cm thick and with each successive layer containing only minor amounts of other size fractions. The upper part of the sand unit is commonly quite pure and consists of very fine-grained, frosted or clear, angular to well-rounded quartz grains, with some of the grains containing black inclusions (Good, 1957).

Other silt deposits of the Big Room show a regular vertical succession of colors, from green and chocolate brown through red and orange to light-orange, yellow, and rarely light-purple (Queen, 1981). Specific colors may be missing at some locations, but the colors never change order. Brick-red silt occurs both on the floor of Bottomless Pit and at the Salt Flats. The Salt Flats silt shows crude to well-developed bedding parallel to the upper surface of the sediment mound except for near the top of the sediment bank where bedding has been highly deformed and folded (Pl. 2B).

A local type of silt deposit in the Big Room is the silt breccia, a 15 cm thick deposit composed of angular fragments of red, yellow, and tan silt and angular pieces of flowstone in a brown silt matrix. The silt breccia is located just to the right of the Texas Trail where it takes off from the main trail. The silt breccia partially underlies flowstone travertine (Fig. 70).

At the Bottomless Pit, along the west wall near the Breast of Venus, and also along the south wall between the Jumping Off Place and the Bottomless Pit, are white- to buff- to cream-colored sands (Fig. 38) that are similar in color, texture, and size distribution to the clean white sands of the New Mexico Room. The sand along the south wall and near the Breast of Venus occurs in semicircular, conical piles called "half cones" by Good (1957), "flowstone-covered alluvial sand cones" by Sanchez (1964), and "sand domes" by Bullington (1968). These white "quartz-sand half cones" of the Big Room are about 3 m high and 6 m in diameter, and abut directly up against the cave walls. The cone at the Breast of Venus is overlain by travertine flowstone, and, where the light-colored sediment has been excavated for trail building, a conical shell of flowstone has been left free-standing. The sand of the cone is iron-stained along its upper part, near its contact with the flowstone.

The "sand" of the half cones is actually not pure sand but a mixture of coarse-grained silt and fine-grained sand, as are the other fine-grained clastic deposits in the cave (Table 10). The silt-sand is clean, well sorted, and according to Queen (1981) some of the clastic particles display beautiful quartz overgrowths.

The presence of the light-colored quartz-sand half cones in Carlsbad Cavern is most curious because this type of deposit is unknown in any other Guadalupe cave. Also, the half cones do not seem to be related to joints, bedding, sandstone dikes, or other such features in the wall lime-stone. In the Breast of Venus occurrence, the apex of the half cone corresponds to a hole in a section of wall directly above it. The sediment appears to have filtered down from above and through the hole, but if one climbs up onto the apex of the cone and looks straight up through the hole, one cannot trace the sand to any pertinent feature in the limestone ceiling. In the four south-wall occurrences, the apices of the cones do not correspond to any particular feature in the wall, not even to a hole along which the sand could have filtered down.

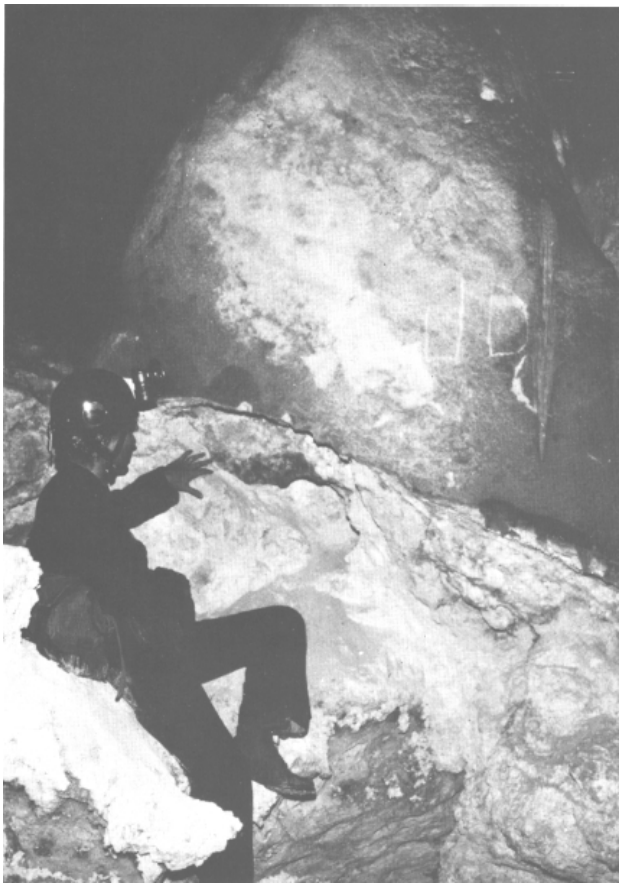

FIGURE 38—Cream-colored silt underlying a gypsum block, Bottomless Pit, Big Room, Carlsbad Cavern. The silt directly overlies floor bedrock. Photo Ronal Kerbo.

Like the clean, white sands in the New Mexico Room, the light-colored silt–sand at the Bottomless Pit and the quartz-sand half cones of the Big Room are thought to be part of the Bell Canyon Formation (Fig. 18).

(1) Strike and dip of the tilted beds at Bottomless Pit range between N60°E–N90°E and 20–50°S (for six readings; J. Roth, pers. comm. 1986).

(2) As with the New Mexico Room sands, the Big Room sands are too low to be part of the Yates Formation. Furthermore, the bedrock at Bottomless Pit differs compositionally from Yates Formation outcrops. The Yates Formation in Sand Cave contains 0.08% silica, while the Bottomless Pit bedrock contains 2.8% silica (Table 26). The interfingering of the Yates Formation at the Auditorium, Carlsbad Cavern, contains 1.7% of insoluble residue, while the bed-rock at Bottomless Pit contains 11.7% of insoluble residue (Table 27).

(3) While there are no bedding planes in the quartz-sand half cones, so that strike and dip cannot be measured, the sand is remarkably white, clean, and well sorted, like the light-colored sand of the Bell Canyon Formation. Good (1957) found the sand of the Big Room half cones to be similar to the sand of the New Mexico Room except for a higher percentage of larger grain sizes. Microscopic examination done during this study showed that the sand of the quartz-sand half cones near the Breast of Venus is nearly identical to that found in the New Mexico Room and at Bottomless Pit (Table 10).

(4) Jagnow (1977) and Queen (1981) were of the opinion that the quartz-sand half cones in the Big Room represent sand-filled fractures in the Capitan Limestone. This interpretation seems doubtful because sandstone fractures are nowhere to be found. The sand of the half cones does not crop out as thin, branching dikes according to either Hayes' (1964) or Dunham's (1972) descriptions. They are conical masses of slumped sand, and as Good (1957) noted, with gradational, not dike-like, contacts. In the two south end exposures of the Big Room, the half cones appear almost like sand balls or sand lenses in the wall which have slumped down into half-cone piles as the cave walls receded by dissolution.

(5) Sulfur occurs at the south end of the Big Room, very near the quartz sand half cones along the wall (see Sheet 2).

Calcified siltstone

Clastic deposits found only in Carlsbad Cavern are the thin-layered, orange-brown, variegated siltstones exposed in wall cavities or in pieces of breakdown on the floor and usually associated with overlying, well-indurated, cave rafts (Fig. 39). Queen (1981) named these deposits "granular flowstones" because they are banded like flowstone and are characterized by grains which reflect light. However, Queen's name is misleading because "flowstone" implies a secondary, subaerially formed, travertine deposit, and "granular" implies that detrital grains such as sand in the deposit reflect the light. Rather than being a flowstone or sandstone, the orange-brown deposit is actually a calcified siltstone with crystalline calcite cement comprising about 80% of the mass and with the remaining 20% composed of silt-sized debris with minor sand (Table 10). The calcite-cement crystal domains are what give the deposit its granular, sparkling texture. The siltstone is banded dark brown and orange, the darker color being caused by a relatively higher percentage of iron and manganese.

The best localities of calcified siltstone are in the Guadalupe Room, Main Corridor, and Lower Devil's Den sec-

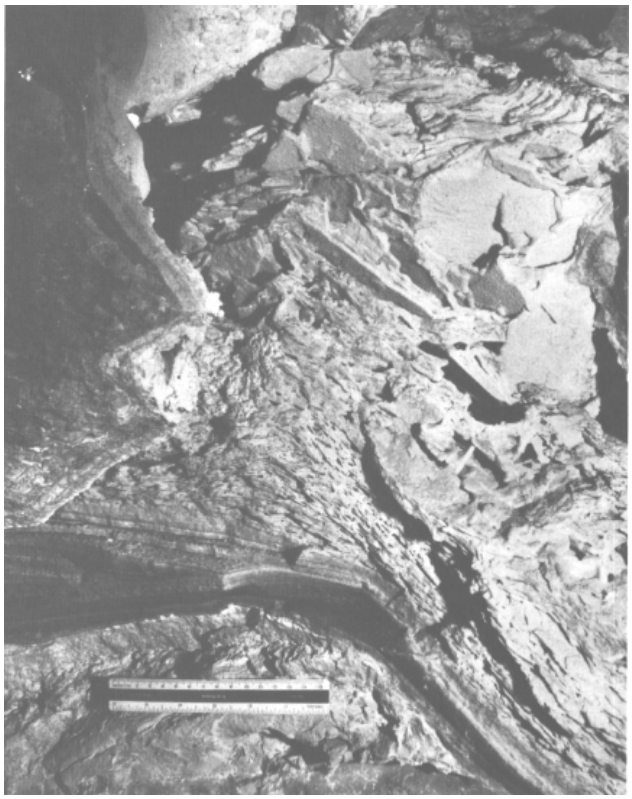

FIGURE 39—Indurated cave rafts directly overlying calcified siltstone, Guadalupe Room, Carlsbad Cavern. The siltstone is present on an up-facing surface, and where the surface starts to drop the siltstone pinches out (lower right). Photo Pete Lindsley.

TABLE 13—Calcified-siltstone–cave-raft deposits, Carlsbad Cavern.

Location	Description	Occurrence
Guadalupe Room	7.5 cm thick, color-variegated siltstone overlain by 20 cm thick sequence of cave rafts.	Exposed in a wall truncated by a large cave passage. Siltstone always lies on upfacing surfaces. Also exposed in breakdown blocks where siltstone-raft sequence overlies spar. Elevation 1,135-1,150 m.
Main Corridor	0.3 m thick siltstone overlain by 0.6 m of rafts.	In a breakdown pile, tilted at about a 20° angle. Along trail before Green Lake. Elevation 1,120 m.
Lower Devil's Den	3 cm thick siltstone overlain by 6 cm thick rafts.	Along wall on left where passage ascends from Secondary Stream Passage up toward Lower Devil's Den. Also about 50 m down passage from Lower Devil's Den in south wall, and in floor breakdown pieces and underlying gypsum blocks. Elevation 1,115-1,130 m.

tions of Carlsbad Cavern (Table 13), and also in lower passages off the New Section. All of these localities are at or near the contact of backreef beds with the Capitan Limestone (Fig. 40). The calcified siltstone always rests on an upfacing surface (Fig. 39) and is usually overlain by cave rafts which have been well indurated and thickened with post-depositional calcite.

In the Guadalupe Room, Lower Devil's Den, and New Section the sequence of calcified siltstone-cave rafts can be observed within small cavities, pockets, or alcoves in the bedrock which have been planed off concordant to the cave walls. In the Guadalupe Room and Lower Devil's Den areas siltstone-rafts are also found in floor breakdown, while in the Main Corridor (just beyond the tunnel before reaching the Green Lake Room) the deposits are in a mass of break-down directly adjacent to the trail.

Mud

Dark-brown mud deposits have been found in many Guadalupe caves—Cottonwood, Endless, Little Sand, McKittrick, Spider, Three Fingers, Virgin, Cave Tree, Jurnigan, Madonna, and Vanishing River. In a side alcove of McKittrick Cave and in the Root Cellar Room of Three Fingers Cave, twig remnants can be picked out of the mud. In the Helictite Room of Spider Cave, leaves and fungus are associated with the mud and there is a light-brown mud line on helictite and flowstone decorations from a back-up of muddy water in the cave. The floor in the Mud Room of Cottonwood Cave is layered with a brown sticky mud of heavy-grease consistency (Boyer, 1964). A microscopic examination of this mud revealed tiny coagulated clumps of dark-brown, uncrystallized material (Table 10). In the Mud Crack Room of Endless Cave, the floor mud is semilaminated, with 1 cm thick lighter layers alternating with darker layers. No leaves or twigs were found in the Endless Cave mud, but fungus was observed growing on top of it. In one place the mud was measured to a depth of 0.3 m; in another place it was found to overlie a gypsum block. Major mud influxes have also occurred in the lower passage in the Cave of the Madonna and in the Mud Room-Grunge Hall and Thanksgiving Room-Deep Throat areas of Virgin Cave (D. Davis, pers. comm. 1984). The Virgin case is interesting because the mud evidently entered at an intermediate level; then a semifluid mudflow poured from the Thanksgiving Room down the Midterm side of the Four O'clock Staircase before reaching the lowest part of the cave. Hill (1984c) tried to correlate the occurrence of mud in Virgin Cave with a valley depression on the surface and speculated that the mud entered the cave via a brecciated zone along which both the depression and cave passages developed.

Gypsum blocks and rinds

Gypsum in Guadalupe caves occurs as (1) blocks and rinds, and (2) speleothems. Blocks and rinds are an alabaster-like, granular type of massive-gypsum deposit, whereas gypsum speleothems are secondary deposits such as stalactites, stalagmites, cave flowers, and selenite needles. Gypsum blocks occur as floor deposits up to 10 m in height

FIGURE 40—Distribution of the calcified siltstone–cave rafts, Carlsbad Cavern (stippled areas). Compare with distribution of breccia in Fig. 30. Queen (1981) and this study.

(Fig. 41); most are segmented into sections and blocks, but some are continuous across sections of the cave floor. Gypsum rinds occur as wall deposits up to 1 m thick, which drape over bedrock or silt (Fig. 42). A description of the massive-gypsum deposits in Guadalupe caves is summarized in Table 14, and their location in Carlsbad Cavern is shown on Sheet 2 (in yellow).

Gypsum blocks and rinds are composed of massive-granular gypsum with individual crystals ca 1 mm long. Crystals larger than this are tabular and cover the outside surfaces of the blocks or rinds. The gypsum making up blocks and rinds can be porous and friable like talcum powder (e.g. the Big Room of Carlsbad Cavern) or it can be dense, hard, and compact (e.g. the McKittrick Hill caves). One attempt to drill a core into the gypsum blocks of the Big Room failed because it was like drilling into loose, uncompacted sugar. The gypsum making up blocks and rinds is white to light yellow except where it has been stained a darker yellow by bat guano or iron oxide. In Lower Devil's Den, Carlsbad Cavern, small segments of a few gypsum blocks are tinted a light mint green from traces of montmorillonite clay (C. M. Seanor and R. North, pers. comm. 1985).

Many gypsum blocks possess a crystalline crust sharply delineated from the main mass of more compacted and less crystalline gypsum. These "overgrowth crusts," as they are called, are up to 30 cm thick and are generally more white and porous than the underlying gypsum. Overgrowth crusts do not possess laminations and other textural features present in the blocks themselves, but occasionally a thin layer of overgrowth crust will highlight lamination ridges in the textured gypsum beneath it. Good examples of overgrowth crusts on gypsum blocks occur in the Big Room, Talcum Passage, and New Mexico Room of Carlsbad Cavern, and in the Balcony Room of Dry Cave. At the Jumping Off Place, Big Room, a 10–20 cm thick, coarse, porous overgrowth

FIGURE 41—A gypsum block with smooth, streamlined sides, Talcum Passage, Carlsbad Cavern. Photo Alan Hill.

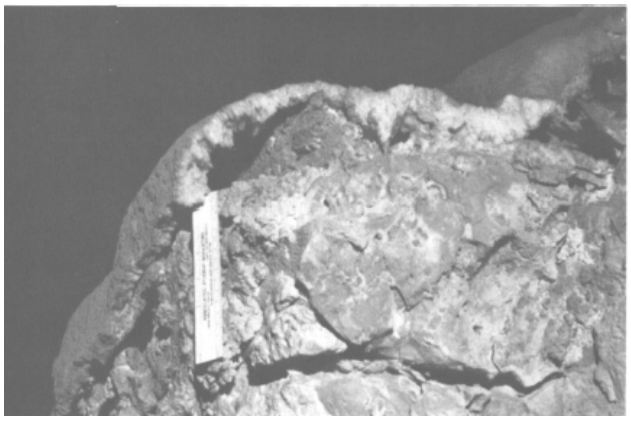

FIGURE 42—A gypsum rind draped over bedrock, Left Hand Tunnel, Carlsbad Cavern. Photo Alan Hill.

crust overlies the regular mass of gypsum (Queen, 1981). In the Talcum Passage and in the Balcony Room of Dry Cave, overgrowth crusts have slumped down along the vertical sides of gypsum blocks (Fig. 43).

Spatial distribution

Gypsum blocks and rinds exist in caves throughout the Guadalupe Mountains. The lowest elevation at which this gypsum has been found is 1,080 m, in Lower Cave, Carlsbad Cavern, and the highest altitude is 2,073 m, in Wonderland, Cottonwood Cave. Gypsum blocks and rinds have been observed in Carlsbad, New, Cottonwood, Lechuguilla, Black, Hell Below, McKittrick, Dry, Sand, Endless, Little Sand, Virgin, Pink Panther, Three Fingers, and Spider Caves (Hill, 1973e). In Black Cave and New Cave only a few gypsum blocks have survived dissolution.

Within each cave, gypsum blocks and rinds display certain distributional trends. Gypsum deposits seem to be more sparsely distributed and/or more highly dissolved in long, linear passages such as Bat Cave, the Main Corridor, and Left Hand Tunnel of Carlsbad Cavern (Sheet 2); the En-trance Hall of Cottonwood Cave (Sheet 5); and the Express-way Passages of Endless and Dry Caves. Gypsum rinds are usually found in boneyard side passages; gypsum blocks usually reside on the floors of large rooms. As a rule, gyp-sum deposits are more abundant in middle cave levels than in upper and lower levels, a trend best demonstrated in the McKittrick Hill caves. The middle level (Middle Maze) of Endless Cave is choked with gypsum blocks 0.6–1.2 m high

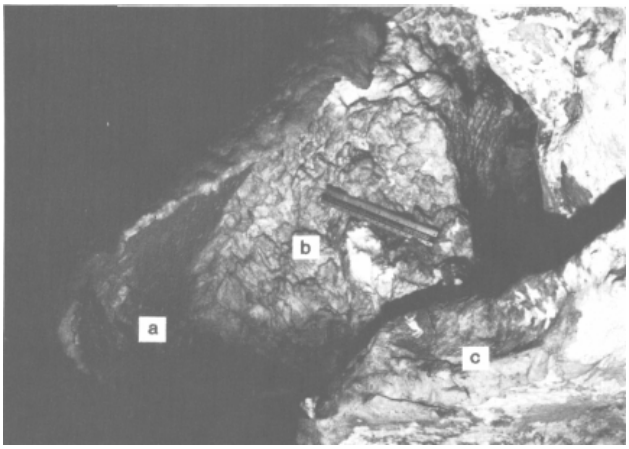

FIGURE 43—An overgrowth crust (a) which slid down over an underlying gypsum block (b), Balcony, Dry Cave. The gypsum block directly overlies bedrock (c). Photo Alan Hill.

TABLE 14—Gypsum blocks and rinds in Guadalupe Caves.

Location	Description	Occurrence
Carlsbad Cavern		
Big Room	Blocks up to 7.5 m high. Massive-granular gypsum, uncompacted. Consistency of sugar. Laminations, microfolding, breccia, inclusions, slickensides, overgrowth crusts, flow features.	Extensive blocks at Jumping Off Place, Bottomless Pit, Salt Flats, and Polar Region.
Lower Cave Upper	Blocks 1 m high. Yellow (iron oxide?) stained.	In Nooges Realm area, blocks directly overlie 3 m high silt banks and are overlain by a <30 cm thick layer of silt.
Devil's Den	Blocks up to 1 m high. Massive-granular, semicompacted. Gypsum contains cobbles. Good laminated texture. Rinds 15 cm thick on wall.	Gypsum located in a protected area of the Main Corridor.
Cottonwood Cave		
Gypsum Passage	Wall rinds up to 0.3 m thick. White-gray banding, replacement textures, and inclusions common. 1 m high blocks. Massive gypsum associated with gypsum and epsomite speleothems and native sulfur.	In upper Gypsum Passage as in-situ blocks and rinds. In lower Gypsum Passage as out-of-place floor blocks.
Endless Cave		
Middle Maze and Lower Maze	Compacted blocks with case-hardened surfaces. 75 cm thick in Middle Maze and 30 cm thick in Lower Maze. Blocks and rinds sometimes intergrade with each other. Commode holes in gypsum, Lower Maze. Streamlined gypsum near the Mud Crack Room.	Extensive blocks in Lower Maze and Middle Maze; sometimes gypsum completely fills passages. Gypsum overlies silt except in Mud Crack Room where mud overlies gypsum.
Dry Cave		
Balcony Room	Blocks 1 m high. Overgrowth crusts, flow features. Blocks compacted and often stained brown by bat guano.	Gypsum directly overlies limestone.
Insane Rain Drain Trench Pit	"Flowing" gypsum cascade about 2 m high.	Gypsum cascades over limestone into trench.
Lechuguilla Cave		
Glacier Bay	Blocks up to 10 m high. Laminations, possible replacement textures, drip tubes, and commodes. One block has laminations on a 1 mm scale, and every 5 cm a darker lamina on a 6 mm scale (D. Davis, pers. comm. 1986).	On the floor as massive blocks overlying limestone and silt.
Rim City and Windy City	Many gypsum rims surrounding holes in gypsum rinds.	Gypsum rinds on walls, ceiling, and floor.

in a 1.2 m high passage, while the upper level (the Expressway) is nearly devoid of gypsum and the lower level (Lower Maze) has gypsum deposits 0.3-0.6 m high in a 2 m high passage. Gypsum once completely choked off the Middle Maze as evidenced by remnant gypsum pillars which reach from the cave floor to the ceiling (Fig. 44), and by gypsum blocks which have surfaces parallel to undulations in the ceiling bedrock (Fig. 45). In Cottonwood Cave, gyp-sum blocks occur at all levels in the Gypsum Passage, but primarily in the middle section intermediate between Wonderland and the lower Gypsum Passage. The lower Gypsum Passage contains many gypsum blocks, but most of these appear to have fallen from above; wherever a bedrock bridge has protected a low section from falling debris, gypsum blocks do not exist on the floor. In Carlsbad Cavern, massive gypsum blocks are rare above the Big Room-Talcum Passage level (Upper Devil's Den and the Music Room Balcony are the exceptions); also, gypsum is much less abundant at the Lower Cave level than at the Big Room level.

Where cave floors slope, such as in the McKittrick Hill caves, gypsum blocks lie at the approximate angle of floor repose. In McKittrick Cave, the slope of the floor gypsum mimics the dip of bedding except where vadose drippage has dissolved the gypsum away (Fig. 46). In Endless Cave, the slope of the floor gypsum approximates the passage dip even in areas where gypsum pillars extend from the floor to the ceiling (Fig. 44). In caves where the floor is roughly horizontal, as in the Big Room of Carlsbad Cavern, gypsum blocks may slope toward the center of a room. The slope, delineated by the top surface of the blocks, can be traced even where the blocks have been separated by erosion (Fig. 47). In Talcum Passage, Carlsbad Cavern, the gypsum blocks slope along the entire length of the passage, from a high of 7 m at the southern end of the passage to where the gypsum completely disappears at the northern end of the passage (R. Lipinski, written comm. 1984).

Another trend seen in some Guadalupe caves is that the height of gypsum blocks is approximately 10-30% the height of the passage in which the blocks reside. In the Big Room of Carlsbad Cavern for example, the blocks are 4.5-6.0 m high in a 45 m high passage. The McKittrick Hill caves have a gypsum/passage height ratio averaging ca 30%. Davis (1980) also noted this correlation between passage height and gypsum-block height.

At many localities, such as the Lower Maze, Endless Cave, and Lower Cave and Upper Devil's Den, Carlsbad Cavern, gypsum floor blocks are continuous with wall rinds, the gypsum thinning upwards along the wall as it grades from a block into a rind (Fig. 48). At other localities, such as Lower Cave and the Polar Regions, Carlsbad Cavern, gyp-

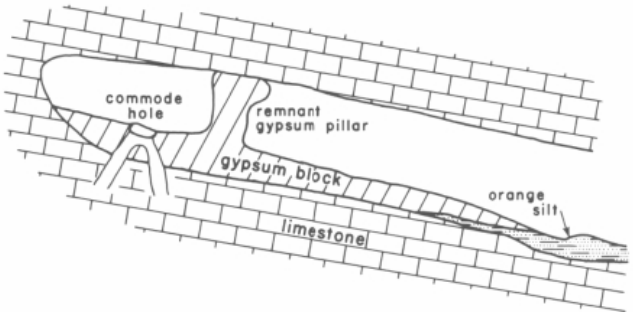

FIGURE 44—A remnant-gypsum pillar, Middle Maze, Endless Cave. Gypsum which once filled the passage has been dissolved away, leaving the pillar intact. Note how the angle of repose of the floor gypsum approximates the dip angle of bedding. A commode hole in the gypsum is an extension of a hole or holes in the floor limestone.

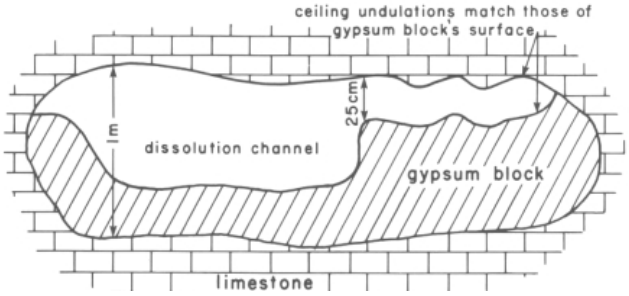

FIGURE 45—A compacted gypsum block, Middle Maze, Endless Cave. Gypsum once extended up to the ceiling, but compacted by a factor of about one-fourth during its solidification. A dissolution channel has been carved in the gypsum at middle left.

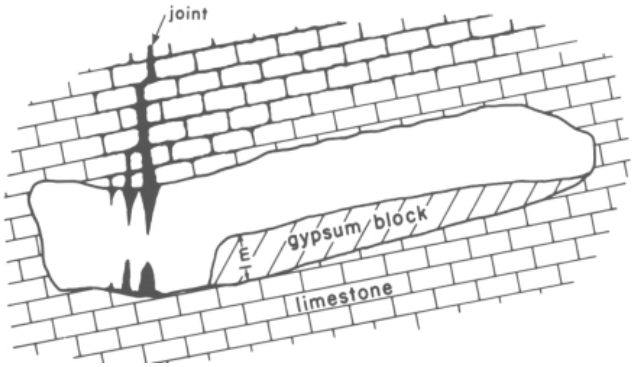

FIGURE 46—A gypsum block in relationship to dipping beds, McKittrick Cave. Water moves downdip along bedding planes until it encounters a vertical joint, whereupon it becomes diverted into the cave so as to form dripstone and to dissolve away the gypsum directly beneath the joint. Note that the angle of repose of the gypsum block approximates the dip angle of bedding.

sum blocks thin into rinds in the downward direction—along bedrock beneath floor blocks. Gyspum is only rarely attached to cave ceilings, one example of this being the archway ceiling of gypsum in the Gyp Joint of Hell Below Cave (Fig. 49) and another being the ceiling crustal rinds in Rim City and Windy City, Lechuguilla Cave (Table 14).

Textural features

Textural features in the gypsum blocks and rinds of Guadalupe caves provide important clues to its origin, and also to its mode of coalescence and solidification. Such textural features are highly variable not only in gypsum deposits of

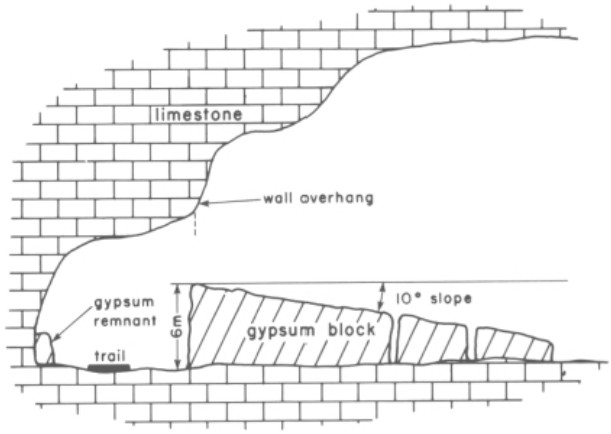

FIGURE 47—Sloping gypsum blocks in the Salt Flats of the Big Room, Carlsbad Cavern. Note that the wall overhang corresponds to the maximum thickness of the block.

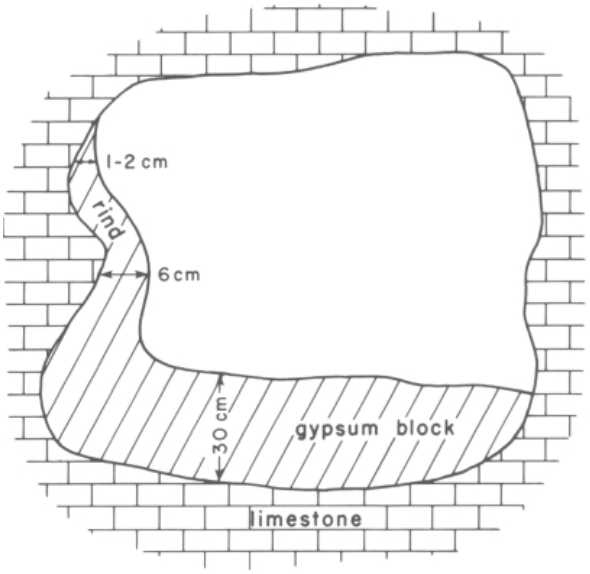

FIGURE 48—A gypsum block thinning upwards into a rind, Lower Maze, Endless Cave.

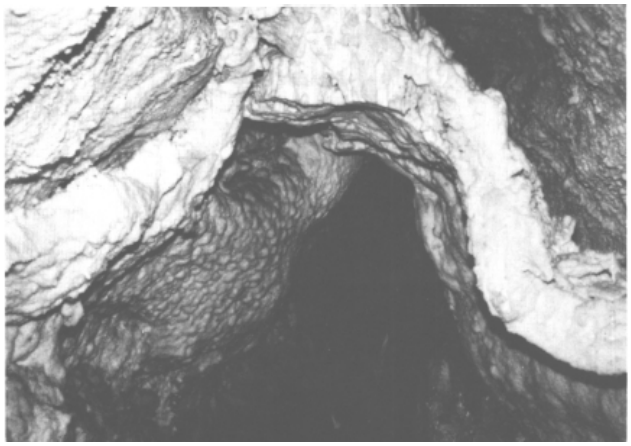

FIGURE 49—Archway of gypsum, Gyp Joint, Hell Below Cave. The passage may have been completely filled with gypsum before a solution channel formed in the gypsum. As the gypsum archway dried and compacted, it partly pulled away from the ceiling and walls. The gypsum is approximately 1.5 m thick. Photo Alan Hill.

different caves, but also within adjacent gypsum blocks in the same cave or even within the same gypsum block or rind over a distance of a few centimeters.

Laminations—Many of the gypsum blocks and rinds in Guadalupe caves display a laminated texture, but these are not obvious to the causal observer because one must look very closely to see them and because overgrowth crusts often hide them. Laminations in the cave gypsum represent a two-component system of colorless selenite alternating with opaque gypsum. Laminae are usually transparent white-translucent white, but in some caves, such as Cottonwood, the layering is a more visible white–gray. Despite their resemblance to the varves in the anhydrite beds of the Castile Formation in the Gypsum Plain, neither the white-gray couplets nor the transparent-translucent couplets contain calcite as do the gypsum-calcite varves of the Castile Formation. An attempt was made to drill into the gypsum blocks of the Big Room, Carlsbad Cavern, in order to correlate lamination sequences similarly to Anderson et al. (1972) in the Castile Formation of the Gypsum Plain. This attempt failed because the cave gypsum at this location has a sugar-like consistency, making the retrieval of a solid core impossible.

Examination of the cave-gypsum laminae in thin section revealed thicker (1 mm) transparent layers alternating with thinner (0.5 mm) opaque layers. One measured section displayed 12–15 laminae/cm. Pods of gypsum, reminiscent of nodular structures in the Castile Formation as described by Dean (1967; pl. 2E), distort some of the laminae, and often the laminae are not continuous but end abruptly. Laminated texture in the gypsum varies from equant in the more trans-parent layers to felty in the more opaque layers. The more felty-looking crystals show preferred alignment perpendicular to layering. In one thin section, a vertical array of large, lath-like gypsum crystals was superimposed upon the smaller, felted crystals, a texture which most likely represents a partial recrystallization of the gypsum.

Laminations in gypsum blocks and rinds are oriented roughly parallel to the surface against which the gypsum rests. Where a limestone wall or ledge is vertical, horizontal, inclined, or curved, the laminations are likewise disposed. In floor blocks, the laminations are usually horizontal or very gently inclined (Pl. 3A). In wall rinds, such as the 0.3–0.6 m thick rinds in the upper Gypsum Passage of Cotton-wood Cave, the laminations are vertical or inclined parallel to the wall. In the area of Mirror Lake, Big Room, Carlsbad Cavern, gently tilted laminated layers of gypsum are overlain by horizontally laminated gypsum, looking like rock layers which have been separated by an angular unconformity. In the first trail arch at the Jumping Off Place, Big Room, tiny faults offset laminations in the gypsum.

Microfolding—Microfolded laminations are a common feature in the anhydrite of the Castile Formation of the Gypsum Plain (Kirkland and Anderson, 1970). The cave gypsum also sometimes displays a microfolded texture, best developed in the gypsum blocks of the Big Room, Carlsbad Cavern. Folding in the cave gypsum is not as tight, regular, or symmetrical as that in the anhydrite of the Castile Formation; it is more gentle and undulant (Pl. 3A). In rare instances, small faults occur at the microfold bends.

Slickensides—Slickensides can be seen in the gypsum blocks at the Jumping Off Place, Carlsbad Cavern, inside of the second of the two trail tunnels (Pl. 3B). They are grooved structures which occur at the contact of an over-growth crust with the underlying gypsum mass. The grooves are not laminations nor do they appear to be mechanical cuts made while tunneling through the gypsum. The striations most closely resemble slickensides created where adjacent rocks have slid past each other. Two small patches of gypsum have slickenside surfaces: one patch is 8 cm long and 5 cm wide, and the other one (below and to the right of the first) is 10 cm long and 7 cm wide. In each case the striations are 1 mm or less apart and are inclined approximately 5–10° from the vertical.

Breccia—Small-scale breccia texture, consisting of jumbled masses of laminated angular fragments, occurs in the gypsum blocks of the Big Room, Carlsbad Cavern (Fig. 50). The breccia closely resembles the brecciated texture in the Castile Formation of the Gypsum Plain (see Dean, 1967, pl. 1G); however, unlike the breccia texture of the Castile Formation, the breccia in the cave gypsum does not seem to be related to microfolding. Breccia texture has been observed only in certain sections of the Big Room such as the Salt Flats, and then usually only in the upper part of the gypsum.

Bedrock inclusions—Pieces of bedrock varying from 1 cm long fragments to large angular blocks are included within the cave gypsum. The bedrock inclusions are in various stages of replacement by gypsum: of five inclusions found in the gypsum blocks of the Big Room, Carlsbad Cavern, three still effervesce in acid (they are still limestone), whereas two do not react (they have altered to gypsum, at least on their surfaces). At one locality in the Big Room, two lime-stone pieces can be seen vertically arrayed in the gypsum as if they had fallen from a single point on the ceiling (Fig. 51).

In Cottonwood Cave, dolomite inclusions derived from the Seven Rivers Formation are in various stages of being replaced by gypsum. Some inclusions have totally altered to gypsum, some only have calcite veins remaining of their original bedrock mass, some are altered only around their edges, and others still remain unaltered dolomite. One inclusion in the gypsum of the upper Gypsum Passage con-

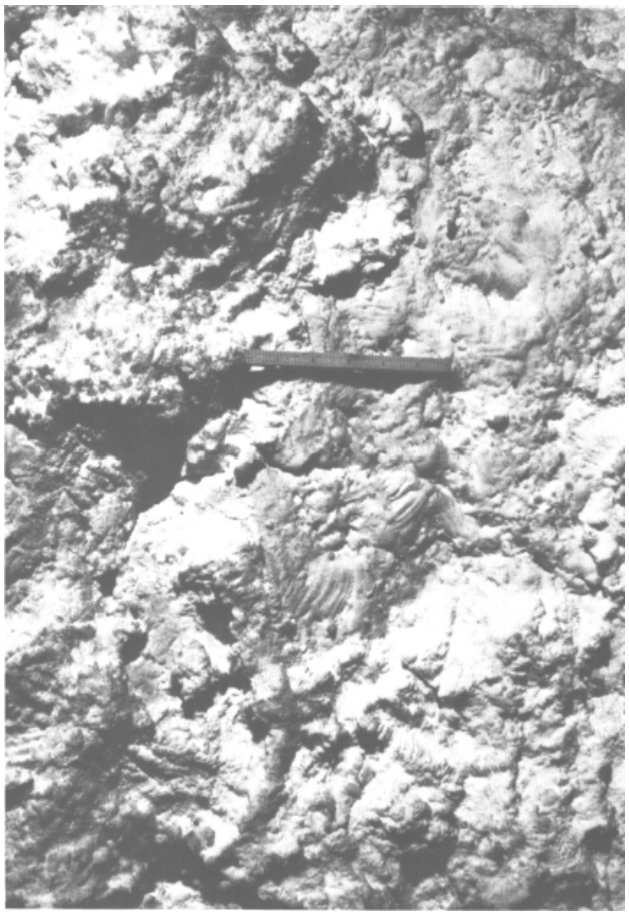

FIGURE 50—Breccia texture in a gypsum block near the Salt Flats, Big Room, Carlsbad Cavern. Note that the laminated breccia pieces are inclined at various angles in the gypsum. Photo Alan Hill.

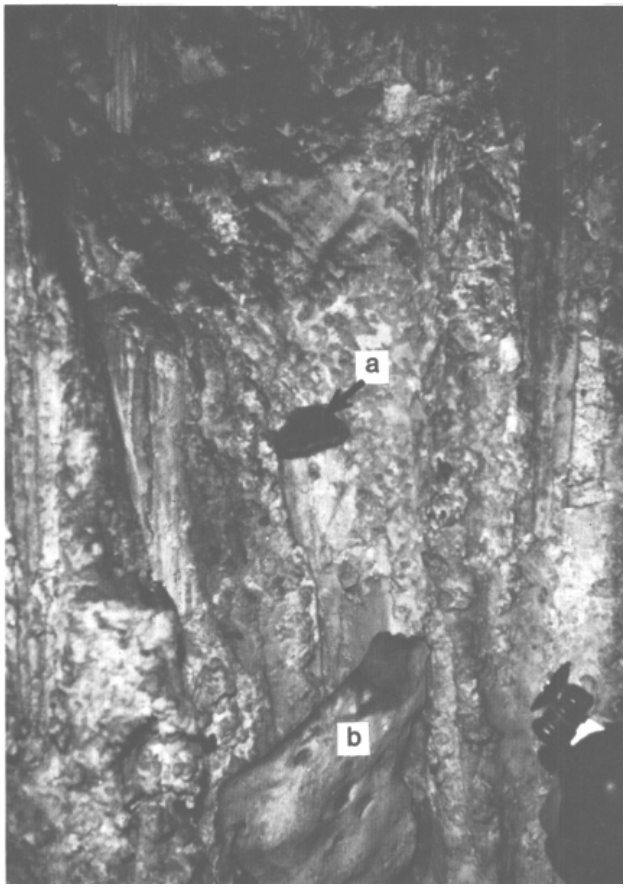

FIGURE 51—Two limestone inclusions (a, b) vertically aligned in a gypsum block, Big Room, Carlsbad Cavern. These particular inclusions have not altered to gypsum, not even on their surfaces. Photo Ronal Kerbo.

sists of a dolomite core 10 cm in diameter, surrounded by a dark, 3–4 cm wide gypsum reaction rim (Fig. 52). A thin section made of one Cottonwood Cave inclusion revealed only gypsum crystals except for a few "ghost" calcite-spar crystals of high, but masked, birefringence.

Inclusions within the gypsum have derived from nearby bedrock either as pieces fallen from the ceiling or pieces exfoliated from the wall. In the upper Gypsum Passage, Cottonwood Cave, inclusions are bedded pieces of dolomite corresponding in thickness to bedding in the Seven Rivers wallrock.

Included bat guano and bat bones—Pockets of orange to red material occur within some of the gypsum blocks of the Big Room and Talcum Passage, Carlsbad Cavern (Pl. 4A). This material is bat guano which has filtered down into the gypsum along cracks, dissolved sections, or drip tubes.

A partial bat skeleton (long bones and skull) has been found in a gypsum block near the trail, Bottomless Pit, Big Room, 4–5 cm down from the top of the gypsum. The bones

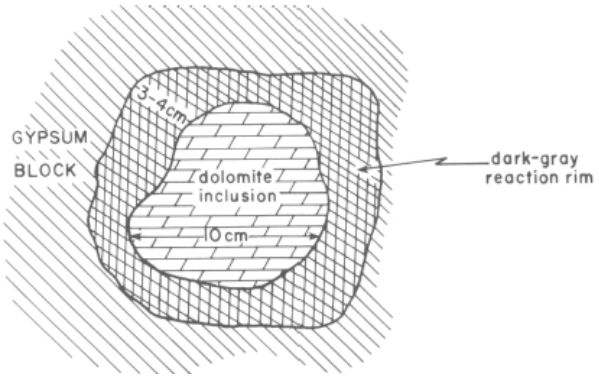

FIGURE 52—Reaction rim of gypsum around a dolomite inclusion, upper Gypsum Passage, Cottonwood Cave. Dolomite has been replaced by gypsum in the reaction rim.

look as if they fell into a drip hole or depression in the gypsum and then were covered over with a powdery mixture of gypsum and limestone.

Insoluble residue—The gypsum deposits of Guadalupe caves are almost devoid of insoluble residue. Two samples of gypsum, one from the Lower Maze of Endless Cave and one from near the Bottomless Pit, Carlsbad Cavern, were collected in order to determine their insoluble-residue con-tent. The gypsum, when dissolved in 50% hydrochloric acid, produced a solution that was not even slightly discolored. However, tiny (0.05–0.1 mm) pieces of angular chert and quartz were identified in the gypsum from both localities; in addition, the Bottomless Pit sample contained black specks (of magnetite?). Insoluble residue in the Bottomless Pit sample was 0.01%, and in the Endless Cave sample it was <0.1% (Table 15). Hydrocarbon content of the gypsum, as determined from a carbon-tetrachloride ex-tract, was only 0.5 ppm. The remarkable purity of the gyp-sum is also supported by the iron content as determined by whole-rock analyses. At four cave localities, the gypsum blocks had less or much less than 0.12% of ferric and 0.03% of ferrous iron (Table 26).

There are a few exceptions to the general rule of residue-free gypsum. In the Pump Room of Carlsbad Cavern and in the Balcony Room of Dry Cave, the top surfaces of the gypsum are banded with orange layers (Pl. 4B). Microscopic examination of the layers revealed that the residue is a fine-grained silt. The silt layers are not necessarily laterally continuous; sometimes the layers disappear suddenly as if their deposition had not been originally continuous. Another occurrence of gypsum that contains silt is an eroded gypsum pillar at the end of the Expressway Passage, Dry Cave. The silt occurs as a 6 cm thick band or "belt" in the gypsum mass together with pieces of limestone (Pl. 5A). The orange silt and limestone pieces are believed to be clastic debris which slumped from a rear passage into the gypsum at the time of its deposition or consolidation.

Flow features—Egemeier (1981) compared the consistency of wet gypsum in the caves of the Big Horn Basin,

TABLE 15—Insoluble residue and hydrocarbon content of gypsum blocks, Guadalupe Caves.

Location	Content	Description
Insoluble-residue content of gypsum block directly adjacent to the Bell Canyon Formation(?), Bottomless Pit, Big Room, Carlsbad Cavern.	0.01%	A few pieces of angular chert and black grains (magnetite?).
Insoluble-residue content of gypsum block, Lower Maze, Endless Cave.	<0.1%	A number of angular chert pieces, a few of which appear zoned.
Hydrocarbon content in a gypsum block, Polar Region, Carlsbad Cavern.	0.5 ppm	Analysis done by J. Husler, Chemistry Laboratory, Geology Department, University of New Mexico.

Wyoming, to that of mud. Flow features in the cave gypsum of the Guadalupe Mountains attest to the fact that it also had a mud-like, semiplastic consistency when still wet. The overgrowth crusts in the Talcum Passage, Carlsbad Cavern, apparently have slid down over underlying gypsum; additionally, in the Talcum Passage, a lower section of a gypsum block looks like it crept down into cracks within the underlying limestone (Fig. 53). The gypsum of the Balcony in Dry Cave appears as if it flowed over the edge of the balcony limestone (Lindsley and Lindsley, 1978); also in Dry Cave, a spectacular cascade of pure-white crystalline gypsum approximately 2 m long plummets like a frozen alabaster waterfall into the Insane Rain Drain Trench Pit.

Replacement features—Queen et al. (1977a) reported numerous replacement textures in the gypsum of the upper Gypsum Passage, Cottonwood Cave. These include pisolites, fossils, travertine, breccia, relict bedding, primary pores, and light/dark laminations. Also, dolomite clasts have been reported in various stages of replacement in the same gypsum (Fig. 52).

Replacement textures in the gypsum deposits of other Guadalupe caves are not nearly so pronounced. Of the numerous gypsum blocks examined in the Big Room, Carlsbad Cavern, only a few possible cases of replacement gypsum were found. The limestone inclusions mentioned previously have been, at least partially, replaced by gypsum on their surfaces. Gypsum laminations cross-cut limestone inclusions in one of the floor blocks of the Big Room, another possible indication of replacement (Fig. 54). A calcified fossil foraminifer was noted in one thin section made from a piece of a gypsum block taken from the Big Room; only a partial test was preserved, the rest apparently having been dissolved away. A thin (<1 cm), patchy crust of possible replacement–solution gypsum has been observed over limestone bedrock near the Bottomless Pit, Carlsbad Cavern. No replacement textures could be seen in this gypsum crust under microscopic examination. Other possible replacement features have been observed in the gypsum blocks of Glacier Bay, Lechuguilla Cave (Hill, 1986).

Recrystallization features—Much of the massive gypsum in Guadalupe caves is recrystallized, sometimes so severely as to completely obscure primary textures. Recrystallization is especially apparent in overgrowth crusts which are typically covered with tabular gypsum crystals 2–3 mm long and 1 mm thick. In Hell Below Cave, recrystallization has produced large crystal faces and perhaps even flower-like forms in the archway of gypsum in the Gyp Joint. Recrystallization may account for the lath-like gypsum laminae which were seen in thin section, and it may also be an alternative explanation for laminations which cross-cut inclusions (Fig. 54).

FIGURE 53—Lower part of a gypsum block in Talcum Passage, Carlsbad Cavern, that flowed down into a crack in the limestone and then solidified. The crack opens up and connects to the ceiling of Lower Cave, the floor of which is 30 m below. Photo Alan Hill.

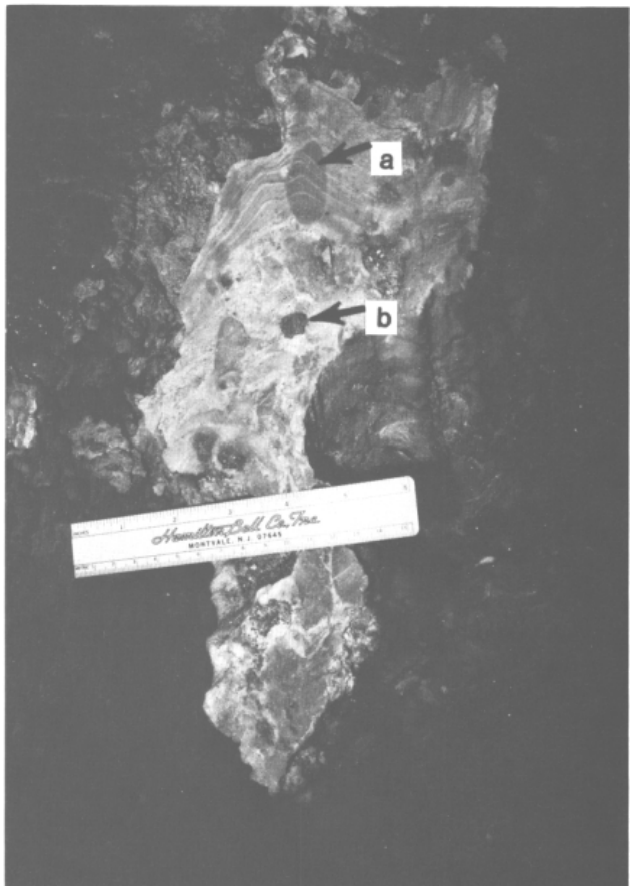

FIGURE 54—Possible replacement or recrystallized gypsum, Big Room, Carlsbad Cavern. Note that the rounded upper inclusion (a) is crosscut by lineations in the gypsum, whereas the lower inclusion (b) is not crosscut. Photo Alan Hill.

Dissolution features

In addition to textural features, gypsum deposits in Guadalupe caves exhibit a variety of dissolution features.

Drip tubes—Gypsum is a soluble material and dripping water readily dissolves vertical holes in blocks. Good (1957) first named such dripping water forms in gypsum "drip tubes," and they have been subsequently referred to as "drip-drill pits" or "drill holes." Drip tubes in gypsum are always vertical (if the gypsum has not been tilted subsequent to drilling). They are found beneath limestone pendants, joints, or stalactites where water drips into the cave, and they are usually vertically fluted due to slight positional changes in the overhanging drip (Figs. 55, 57). In rare instances, drip tubes can become filled with carbonate speleothems such as stalagmites; the dripping water first carves out the tube and then the stalagmite fills it (Fig. 56).

Where a drip tube extends entirely through a gypsum block, water drops splash onto the floor limestone and create a spray. The spray of water then dissolves the bottom of the gypsum block into a dome-shaped form concentric around the drip tube. Such "splash undercuts," can be observed in the gypsum blocks of the Polar Regions, Big Room, Carlsbad Cavern, where they are about 1 m in diameter (Figs. 55, 57).

Commode holes—They resemble drip tubes in that, as viewed from above, they possess round to ellipsoidal holes, but they differ from drip holes in size, spatial configuration, and origin (Fig. 57). Typically, commode holes are of larger

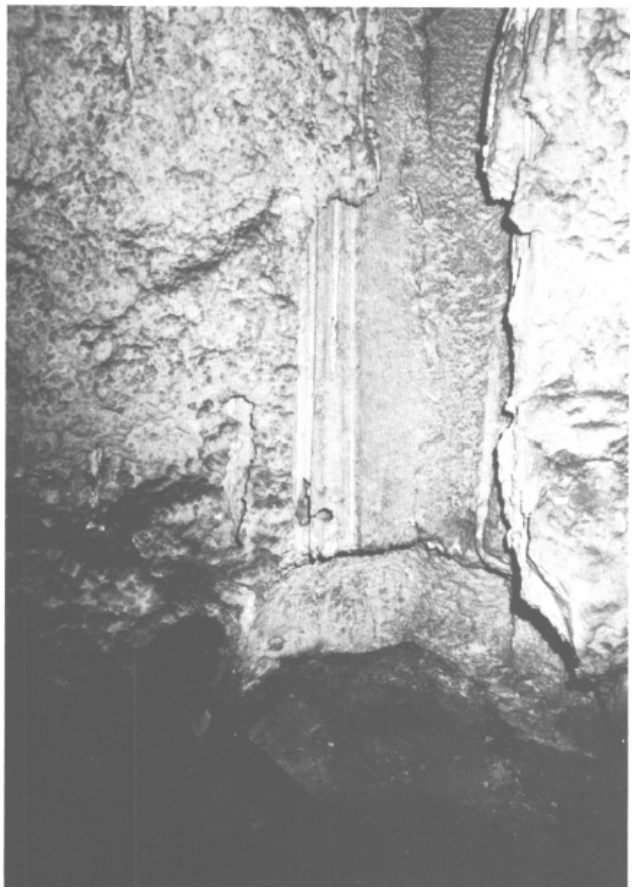

FIGURE 55—A drip tube and splash undercut, Salt Flats, Big Room, Carlsbad Cavern. A drip tube forms where dripping water drills a vertical hole in the gypsum. A splash undercut forms where drip-ping water impacts the bedrock floor and then splashes in a radial pattern so as to create a circular zone of solution in the gypsum directly below the drip tube. The tube is vertically fluted due to slight shifts in the drip point. Photo Alan Hill.

FIGURE 56—Underside of a gypsum block, Big Room, Carlsbad Cavern, showing a stalagmite which has filled a drip tube in gypsum. Photo Alan Hill.

circumference than drip tubes, being about 15–100 cm in diameter; also, they are smooth on their insides and have overhanging upper lips or a rounded crown of gypsum partially rimming the hole. Commode holes also differ from drip tubes in that (1) they do not correspond to overhead limestone pendants, joints, or stalactites; (2) they are not necessarily vertical, but often have sloping insides; (3) they are never vertically fluted, but may be horizontally grooved; and (4) their position is a continuation of holes in the floor limestone (Figs. 44, 57). Commode holes are best developed in gypsum blocks that have been case-hardened on their outer surfaces, but still have granular and uncompacted interiors. The softer, interior gypsum is dissolved away preferentially between the case-hardened upper surface of gypsum and the underlying bedrock limestone.

Commode holes have been identified in Glacier Bay, Lechuguilla Cave, the upper Gypsum Passage, Cottonwood Cave, the Big Room, Carlsbad Cavern, the Gyp Joint, Hell Below Cave, and the entrance area, Spider Cave, but they are best developed in the McKittrick Hill caves, especially in the Lower Maze, Endless Cave (Kunath, 1978). Many of the commode holes in Endless Cave have been modified by gypsum-rim speleothemic material along their tops, and this has caused them to assume bizarre shapes. The Commode of Endless Cave is the classic form of a compound commode hole–rim speleothem feature: the commode hole in this formation extends 1.5 m below floor level where it connects with a maze of small holes in the limestone, and the rim part of this formation projects about 1 m up and around the hole (Fig. 58). Commode holes are usually not vertical; the few vertical ones are called "post holes." Exceptionally large post-hole commodes occur in Glacier Bay, Lechuguilla Cave, and at the Polar Regions of the Big Room, Carlsbad Cavern. The largest of the Carlsbad ones, the "Giant's Commode," is 2 m wide and 2.5 m deep; the largest in Lechuguilla are 3 m wide and 10 m deep. In the upper Gypsum Passage, Cottonwood Cave, a post hole in a gypsum block has exposed an overgrowth crust and a partially replaced dolomite inclusion.

Occasionally, commode holes can be found in other unconsolidated material, such as silt. In the Hall of the White Giant, Carlsbad Cavern, at the bottom of the first pit, is a post hole 0.2 m in diameter and 0.5 m deep in laminated silt. Other commode holes in the silt are not vertical, but wind their way through the silt like worm holes.

Streamlined surfaces—Many gypsum blocks exhibit extremely smooth, rounded surfaces, especially near pits or in areas where one cave level connects with another. Good examples of streamlined gypsum blocks can be seen in the Big Room of Carlsbad Cavern at the Bottomless Pit (Fig. 38), and next to the pits near the Jumping Off Place. In the Talcum Passage, Carlsbad Cavern, gypsum which is highly scoured along its bottom side completely obstructs a fissure (J. McLean, pers. comm. 1979). Also, many of the gypsum blocks in the Talcum Passage show a high degree of rounding (Fig. 41). Other notable examples of streamlined gyp-sum occur in the upper Gypsum Passage, Cottonwood Cave, where, like in the Talcum Passage, the undersides of many of the gypsum blocks are smooth and scoured-looking. In the Mud Crack Room, Endless Cave, gypsum blocks are

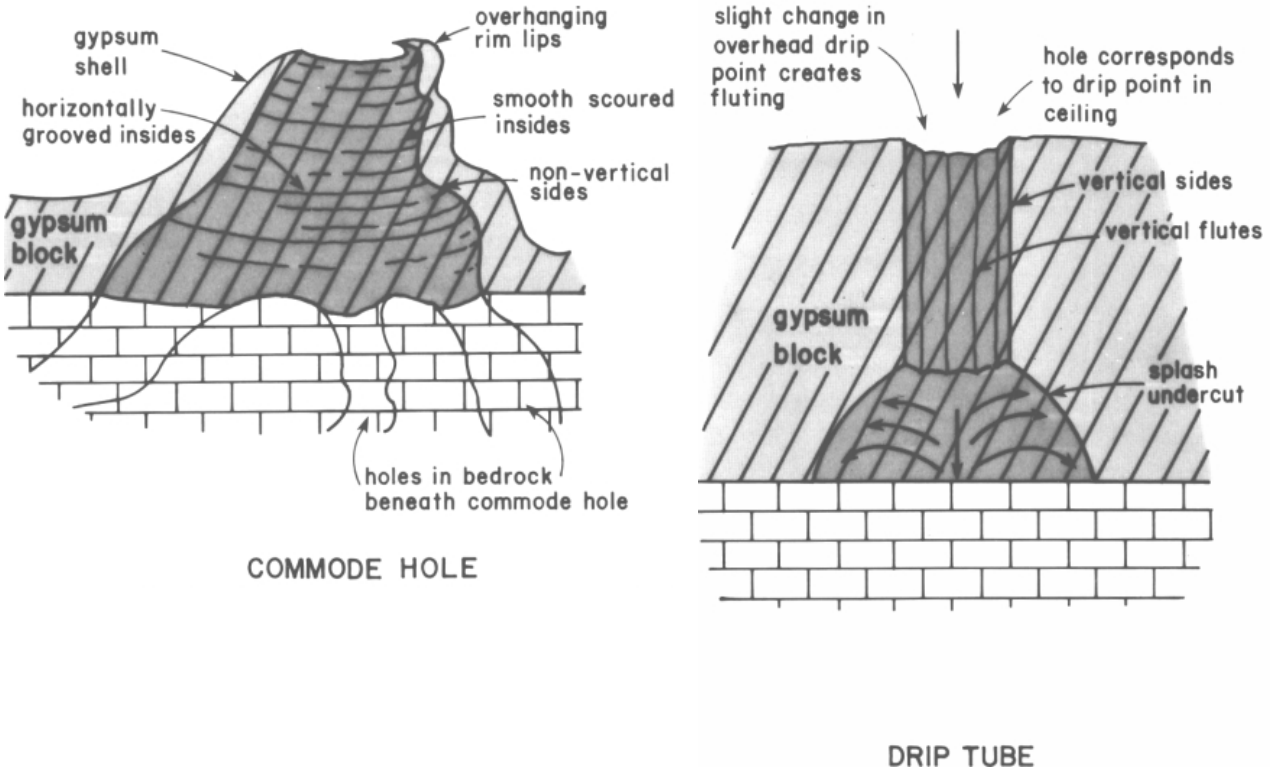

FIGURE 57—A comparison of a commode hole and a drip tube, two dissolution features in gypsum.

truncated flush with the limestone against which they rest, and in the Expressway Passage, Dry Cave, a 1 m high gypsum pillar has been dissolved concordant with the walls and ceiling (Pl. 5A).

Scallops—In the lower Gypsum Passage, Cottonwood Cave, directly next to the floor gate, is a collapse block of gypsum containing scallop marks on its surface (Fig. 59).

Molds and casts—In the Alabaster Balcony, Virgin Cave, dissolution of a gypsum block has left an unusual form: a 0.6 m high tube of calcite 7.5 cm in diameter, which is a cast of a drip tube in gypsum (D. Davis, pers. comm. 1984). The cast formed like a conulite speleothem does in mud: calcite lined a drip tube in gypsum, and when the gypsum was removed by erosion, the more resistant calcite cast was left standing.

A possible mold of a gypsum block exists in the Crystal Springs Dome region of Carlsbad Cavern, where a flow-stone cascade about 2 m^2 surrounds a pentagonal hole. This hole may possibly be a mold of a gypsum block which was dissolved away as the flowstone deposited over it.

FIGURE 58—"The Commode," Lower Maze, Endless Cave. The 1.8 m tall caver is standing in a 1.5 m deep hole in bedrock which is a continuation of the commode hole. A rim of gypsum surrounds the caver's head. Photo Alan Hill.

Chert

Chert is a dense, cryptocrystalline, amorphous variety of quartz which displays conchoidal fracture. The only Guadalupe cave in which chert has been found is Carlsbad Cavern, and there it occurs as an up to 40 cm thick, gray to tan, chalcedonic chert interbedded with colorful silt de-posits in a number of areas in the Big Room (Table 16).

The most impressive exposure of chert is in the area of the Salt Flats, Big Room, where 30–40 cm thick chert is interbedded with brick-red to ocher-yellow silt. The chert is not a continuous deposit in the silt but is lens-like, ex-tending for about a meter or so, and then pinching out. Chert lenses are usually single deposits located near the top of a silt bank, but in one place in the Salt Flats' exposure, two lenses—one directly overlying the other but separated from it by about 5 cm of silt—can be seen between colorful silt layers. The silt bank of the Salt Flats has been excavated

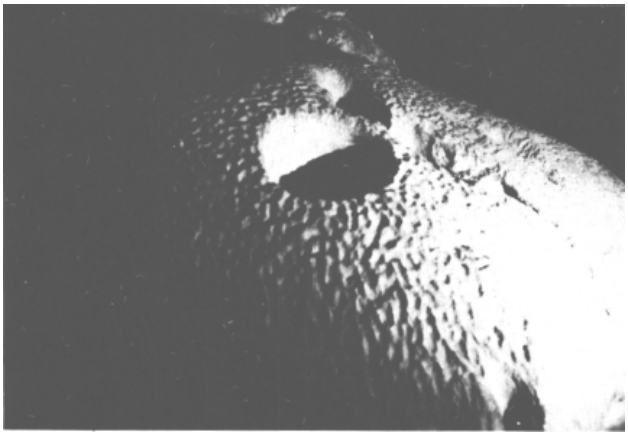

FIGURE 59—Scallops in a gypsum block, lower Gypsum Passage, Cottonwood Cave. Photo Bob Trout.

TABLE 16-Chert deposits. Carlsbad Cavern.

Location	Description	Occurrence
Big Room	1 cm thick, grayish-tan chert overlying tan-layered clay and silt.	By the Lunch Room, near the beginning of the Big Room trail.
	3 cm thick, grayish-tan chert overlying a sequence of colorfully banded silt, but directly underlying a small stalagmite.	Along the Texas Trail, where the silt has been excavated for trail building.
	1 cm thick tan chert which fills in mud cracks in the silt. The chert overlies tan, yellow, and orange silt, and is overlain by white moonmilk.	Texas Trail, ~10 m beyond the trail in a depression made for an electric light.
	40 cm thick, rhythmically banded chert; 5 cm thick micritic chert banded with 7 cm thick porous chert; in lenses. Section made by Shell Research and provided by D. Jagnow.	Salt Flats, in same location as brick-red silt. Chert is out-of-place on floor, in place in sediment banks. Chert and silt underlie gypsum and breakdown.
	1 cm thick chert lenses overlying silt, 3 cm thick white endellite, and gray-green montmorillonite.	To the west of large breakdown blocks by Totem Pole.

for trail building so that lenses of chert now lie on the floor where they were undermined of silt. One large piece of undermined chert, which has slid some distance toward the base of a silt bank and onto a gypsum block, displays a remarkable internal structure: three bands of finely laminated micritic chert, each 4-6 cm thick, are interbedded with three other, more porous, granular bands, each 6-9 cm thick (Pl. 5B). Other chert lenses also display this rhythmic sequence, but do not have as many bands. In all observed cases, a porous-chert band is at the bottom of a sequence, while a micritic layer is at the top. As seen in thin section, the porous layers display angular to well-rounded quartz grains 0.1-1 mm in diameter, contained in a matrix of chert. The micritic layers are composed of pure chert. Some minor calcite fills veins and pods in the porous layers, most usually in the zone between the micritic and porous sections.

Another important exposure of chert is in the Big Room along the Texas Trail next to a light fixture, where chert can be seen filling in polygonal cracks in the silt (Queen, 1981). Good exposures of chert showing stratigraphic relationship to other types of deposits in the Big Room also exist along the Texas Trail (near to the main trail) and under breakdown past the Salt Flats near the stalagmite called the Totem Pole (Fig. 70).

Endellite-montmorillonite-palygorskite

In Carlsbad Cavern and other caves of the Guadalupe Mountains, waxy, colorful (blue, blue-green, pure-white, and lavender) clay, and less waxy, soapy-feeling, colorful (gray-green, pink, brick-red, and brown) clay fills sponge-work pockets in the limestone or underlies clastic sediment. The waxy clay usually occurs as veins, pods, or stringers within the soapy-feeling clay, with a sharp color differentiation displayed by the two clay types.

Three minerals have been found to constitute these clay deposits: montmorillonite, $(Na, Ca)_{0.33}$ $(Al, Mg)_2$ $Si_4O_{10}(OH)_2 \cdot nH_2O$; palygorskite (attapulgite), $(Mg,Al)_2Si_4O_{10}(OH) \cdot 4H_2O$; and endellite, $Al_2Si_2O_5(OH)_4 \cdot 2H_2O$. Davis (1964a, b) reported that the soapy-feeling, gray-green deposits are composed of montmorillonite, with a minor amount of endellite. The pink deposits he found to be a mixture of roughly equal amounts of "attapulgite" and montmorillonite. ("Attapulgite" is an obsolete name for palygorskite; Fleischer, 1983.) At Davies' collection site in Lower Cave, Carlsbad Cavern, the pink "attapulgite"-rich clay directly overlies the gray-green montmorillonite clay, and both partially fill a phreatic solution pocket. The pink clay, which occurs in an exposed position in the pocket, has been hardened by calcite.

The montmorillonite clay is composed primarily of spherical aggregates ca 2.5-3.0 μm in diameter plus a minor amount (<1%) of clay- and silt-size quartz. Trace amounts of feldspar, a fibrous mineral (possibly gypsum), and an extremely fine, black, opaque mineral (magnetite?) are present in the montmorillonite. The surface of one specimen had a brownish-red stain caused by the precipitation of iron minerals (limonite and some hematite) along a fracture.

The waxy clay mineral in Guadalupe caves is endellite. Endellite and its dehydration product, halloysite, are kaolinitic sheet-silicate minerals. Endellite is the stable mineral species under cave conditions of high humidity, but when removed from a cave to a less humid environment, it dehydrates rapidly and irreversibly to halloysite (Bates et al., 1950; Diamond and Bloor, 1970). Collected samples of the waxy mineral have been x-rayed and reported as the mineral halloysite by a number of investigators (Freisen, 1967; Davies and Moore, 1957; Davies, 1964a); however, since endellite is the actual mineral species in the caves, all such clay deposits are hereafter referred to as endellite.

Endellite and montmorillonite have been found primarily in Carlsbad Cavern (Sheet 2, green areas), but these minerals also occur in Cottonwood Cave, Endless Cave, and Dry Cave (Table 17). Bretz (1949) noted that the colorful clay deposits in Carlsbad Cavern have a vertical extent almost as great as the cave itself. The most extensive deposits in Carlsbad are in Lower Cave, where gray-green montmorillonite and, to a lesser extent, blue endellite fill sponge-work voids in the limestone (Pl. 6A). These clay deposits have dried, compacted, and cracked so that they are now sluffing out of the spongework and are piling up as talus debris on the cave floor.

Where endellite and montmorillonite occur together, the endellite forms veins, pods, nodules, and stringers within the surrounding montmorillonite matrix. For example, at the Top of the Cross, Big Room, and in the Mystery Room past the entrance to the Cable Slot, pure-white to light-blue, waxy endellite forms vein-like deposits between the limestone and surrounding brick-red clay matrix (Pl. 6B). Endellite-montmorillonite clay associations display various color combinations with the most usual being sky-blue or blue-green endellite in a matrix of gray-green montmorillonite, or pure-white endellite in an orange-red or brown matrix. Davies and Moore (1957, p. 24) reported: "white clay 6 in. to a foot thick in irregular beds consisting of nodules of the clay mineral endellite . . . in an orange red to brown clay bank in the New Mexico Room. On their outer surface is a layer of black angular quartz grains."

Sulfur

Elemental sulfur has been found in Lechuguilla Cave, Cottonwood Cave, and Carlsbad Cavern. In three of its six occurrences in these three caves, the sulfur is admixed with gypsum, and in three occurrences sulfur crystals directly

TABLE 17-Endellite-montmorrillonite-palygorskite deposits in Guadalupe Caves.

Location	Description	Occurrence
Carlsbad Cavern		
Main Corridor	Light-green to tan clay, banded parallel to surface of underlying limestone.	Along floor, on left side of trail ~60 m before reaching upper Devil's Den. Fills solution pockets.
Lower Devil's Den	Green clay, slightly waxy; probably montmorillonite.	Fills pockets in limestone on way down from upper Devil's Den to lower Devil's Den.
Boneyard	Brown clay, slightly waxy, banded parallel to surface of underlying limestone.	10 m from trail where clay fills solution pockets in the floor.
Guadalupe Room	Stratified brown endellite clay.	In small room at bottom of large collapse pit in lower Guadalupe Room (Friesen, 1967).
Big Room	Waxy, pure-white endellite in brick-red matrix.	In floor pocket along trail near the Top of the Cross.
	Pearly to opalescent blue-green waxy clay.	2 m off trail, Polar Region.
	Blue-green to lavender, waxy endellite clay.	Spongework maze off of Bottomless Pit, 20 m beneath Big Room (Friesen, 1967).
	3 cm thick white endellite overlying gray-green montmorillonite clay, and underlying a 1 m thick silt deposit capped by chert.	By Totem Pole, just west of large breakdown blocks.
Mystery Room	Brick-red clay with white to light-blue endellite pods and stringers. Gray-green clay downslope from brick-red clay.	Massive floor deposits of the brick-red and gray-green clay on far slope past entrance to Cable Slot.
New Mexico Room	15-30 cm thick white endellite in an orange-red to brown clay mass. Nodules of endellite covered with a layer of black, angular quartz grains.	North side of New Mexico Room, in irregular beds (Davies & Moore, 1957).
	Pods of blue waxy clay.	Across from lake, northeast side of New Mexico Room.
Papoose Room	Grayish-green clay; probably montmorillonite.	Fills a solution pocket adjacent to a spar-filled pocket.
Mabel's Room	Grayish-green and brick-red clay, only slightly waxy; probably montmorillonite.	Fills solution pockets along climb from Lower Cave up to Mabel's Room. Clay shards are filtering down into Lower Cave along anastomoses. Green and red clay occurrences only meters apart.
Lower Cave	Grayish-green montmorillonite overlain by pink palygorskite ("attapulgite"). Also blue, waxy endellite with gray-green clay (Davies, 1964b). (U ≡ 320 ppm)	Fills solution pockets and/or occurs as talus piles on the floor in the Green Clay Room, Junction Room, Nooges Realm, and at bottom of Mabel's Room climb.
Cottonwood Cave		
Wonderland	Blue-green, waxy clay.	Fills small solution pockets in the wall. Adjacent to pockets filled with spar.
Endless Cave		
Mud Crack Room	White pods and stringers of waxy clay in a bright, reddish-orange clay matrix.	Fills solution pockets in limestone just past Mud Crack Room.
Lower Maze	Blue-green, waxy clay.	Near The Commode (Kunath, 1978).
Dry Cave		
Balcony Room	Blue-green, waxy clay.	In maze, just past crawlover ledge in Balcony Room (J. Hardy, pers. comm. 1978).

coat bedrock and speleothems. The description of sulfur deposits in Guadalupe caves is summarized in Table 18.

Two occurrences of sulfur exist in the lower Gypsum Passage of Cottonwood Cave, one near a large gypsum stalactite known as the Chandelier, and one about 80 m south of the Chandelier. Respectively, these two occurrences are: (1) a vein-like deposit 45 cm wide and 15 m long, in gypsum exposed along a ceiling joint (Davis, 1973; Pl. 7A); and (2) a crystalline deposit filling 1.2 m long and 0.3 m wide cavities within a gypsum block (Pl. 7B). In the vein-like occurrence near the Chandelier, the massive, dense, light-yellow sulfur sometimes projects out in relief from the gypsum in such a manner as to produce an almost stalactitic form. In the cavity occurrence, the gypsum block which encloses the crystalline, canary-yellow sulfur looks like it either slumped or fell into its present position on the floor. In both of these occurrences, the gypsum looks like it has been eroded away so as to expose the sulfur within it. A sample collected from the vein occurrence of sulfur was examined for the presence of sulfur bacteria. This examination proved negative; the sulfur had neither fossilized or living sulfur bacteria associated with it (D. Caldwell, pers. comm. 1980).

In Carlsbad Cavern, native sulfur is present in the Big Room, New Mexico Room, and in a side passage off of the Christmas Tree Room (Sheet 2, red dots). The Big Room sulfur is located at the Jumping Off Place, just past the second trail tunnel in a block of gypsum and about 2.5 m above the floor. The pale-yellow sulfur covers an area approximately 0.6 m high and 0.3 m wide, where it (1) resides

TABLE 18-Native-sulfur deposits in Guadalupe Caves.

Location	Description	Occurrence
Carlsbad Cavern		
Big Room	Pale-yellow crystals 0.2 mm long, subhedral, straw to honey colored, pleochroic yellow, with refractive index above 1.70.	Admixed with gypsum in a gypsum block. Along trail, Jumping Off Place.
New Mexico Room	Canary-yellow, rhombic crystals 1 mm long.	Crystals coat bedrock, gypsum flowers, and gypsum crust. The sulfur occurs on the underside of dipping Bell Canyon(?) beds.
Christmas Tree Room	Canary-yellow, rhombic crystals 1 mm long.	Crystals coat bedrock, cave rafts, popcorn, and crinkle blisters. The sulfur occurs on the underside of dipping forereef beds.
Cottonwood Cave		
Lower Gypsum Passage, near Chandelier	Massive, pale-yellow, with a waxy luster; breaks with conchoidal fracture.	As a "vein"-like seam in a gypsum block exposed along a ceiling joint.
Lower Gypsum Passage ~80 m south of the Chandelier	Bright canary-yellow, rhombic crystals 3 mm long.	Exposed in cavities within a gypsum block.
Lechuguilla Cave		
The Rift	Lemon-yellow crystals up to 1 mm long.	As a thin layer overlying gypsum crust in an area 3 x 5 cm (J. Roth, pers. comm. 1986).

on an overgrowth crust which lines a drip tube in the gypsum block, (2) occurs as a light covering on dense gypsum where the overgrowth crust has been eroded away, and (3) fills cracks separating the overgrowth crust and the more compacted underlying gypsum. The sulfur occurs on the underside of the cracks and surfaces.

The New Mexico Room sulfur is not admixed with gypsum, but rather directly coats limestone bedrock (PI. 8A) and also subaerially formed gypsum flower and crustal speleothems (Pl. 8B). The sulfur crystals lightly cover the undersides or vertical faces of the bedrock or speleothems, but never the top sides.

The Christmas Tree Room sulfur directly overlies bedrock, crinkle blisters, and popcorn. It also coats, and fills the spaces between, indurated masses of stacked cave rafts. Where the crystals overlie bedrock, they usually occur on the undersides of dipping forereef beds or on projecting fins of limestone. The fins are covered with a thin (<1 mm), yellowish-brown, iron-rich, slaggy crust which directly underlies the sulfur crystals. Elsewhere on the bedrock surface, yellowish-brown "spots" occur with the sulfur crystals and are the same size as the crystals.

Speleothems

A speleothem is a secondary mineral deposit which has formed in a cave. Examples of speleothems are stalactites and stalagmites. Only those speleothem types that are related to speleogenesis problems are discussed in Part I; refer to Part II for a detailed discussion of all speleothem types that occur in Guadalupe caves.

Types related to speleogenesis

Spar—Dogtooth and nailhead spar line bedrock or fill solution cavities in the walls, ceilings, and floors of Guadalupe caves. Dogtooth spar consists of scalenohedrons of calcite and nailhead spar is a more blunted form of calcite consisting of combined flat rhombohedrons and prisms which display uneven-sided triangular patterns. Spar crystals are found in practically every cave in the Guadalupe Mountains, but the finest specimens occur in Carlsbad, Cottonwood, Three Fingers, Geode, Idono Crystal, Crystal, Virgin, Frank's, and Pink Fink Owlcove. The spar in Guadalupe caves can be very large (up to 50 cm in length), and some of it is colored (pale blue) or zoned (transparent centers overlain by an outer zone of milky calcite).

At least two spar episodes are clearly discernible in Guadalupe caves: (1) a spar matrix which fills the spaces between clasts in wall breccia (Fig. 67), and (2) large, well-developed spar crystals which protrude out from cavities or walls (Fig. 60). Large spar crystals are preserved in protected alcoves or spongework cavities. This relationship can best be seen in the Spar Room of the Secondary Stream Passage, Carlsbad Cavern, where large spar crystals occur in protected wall recesses, rounded and highly corroded spar occurs where the recesses open up into the Spar Room (Pl. 9A), and spar molds occur in the center of the room (Fig. 61). In a side passage off of Left Hand Tunnel, rounded and highly etched spar crystals, attached only by thin pieces of corroded limestone or crystalline calcite, project outward in relief from the wall.

In the Mystery Room, Carlsbad Cavern, nailhead spar predominates over dogtooth spar and occurs as columnar crystal linings overlying bedrock. In the Nailhead Spar Lining Room, at the very bottom of the Mystery Room, the crystal linings are 6-10 cm thick and are still in place except where a few sections have fallen to the floor, leaving a

FIGURE 60-Dogtooth-spar crystals, Guadalupe Room, Carlsbad Cavern. Photo Pete Lindsley.

FIGURE 61-Spar molds in limestone bedrock, Secondary Stream Passage, Carlsbad Cavern. Photo Ronal Kerbo.

linoleum-like, triangular pattern imprinted on the bedrock. A large breakdown block in the middle of the Mystery Room (near the Mabel's Room Overlook) also displays the linoleum pattern, but the spar lining that once covered the breakdown has since been almost completely dissolved away.

Cave rafts—Thin planar deposits of calcite and aragonite which precipitate on the surface of a body of water. Cave rafts are a common speleothem type which form on the surfaces of many small cave pools (Pl. 13B). However, in Carlsbad Cavern this speleothem type takes on added significance because well-indurated cave rafts are found exposed in wall cavities where they overlie calcified siltstone (Fig. 39), and because huge conical piles of cave rafts (called cones) litter the floor in places such as the Balcony of the Lake of the Clouds Passage and the East Annex of the New Mexico Room. Three definable episodes of raft formation are displayed in Carlsbad Cavern: (1) Type 1 rafts, well-indurated deposits which are associated with underlying calcified siltstone and are truncated by the large cave passages; (2) Type 2 rafts, semiconsolidated rafts usually in the form of cave cones which occur in areas where the corrosion of speleothems and bedrock is pronounced; and (3) Type 3 rafts which can be seen floating on top of shallow cave pools or which have sunk to the floor of these pools. Type 1 and Type 2 cave rafts are believed related to speleogenesis problems and are discussed in this part of the paper. Type 3 rafts are discussed in Part II.

Type 1 rafts have been significantly widened by post-depositional calcite (an estimated 80% of their mass is post-depositional), and individual rafts have become cemented together with calcite so that they appear stacked like shingled plates (Fig. 39). These consolidated cave rafts usually directly overlie calcified siltstone without any other type of deposit intermediate in the sequence, and they are always the topmost deposit of a sequence, with either air space or subaerially formed travertine above the rafts. In their association with calcified siltstone, Type 1 cave rafts appear to have been packed into wall solution pockets before truncation by the large cave passages.

Type 2 rafts and cones of the Lake of the Clouds and East Annex areas also overlie silt, but both the silt and rafts are not well indurated. In the New Section, Carlsbad Cavern, the consolidation of floor rafts is more complete, but the silt underlying the rafts is not similarly indurated. In the Hall of the White Giant, at the bottom of the first pit, semi-indurated raft ledges 15-20 cm thick extend out from the wall, while laminated, non-indurated silt has compacted about 0.3 m beneath the ledges. Even lower in the New Section, raft bridges reportedly extend across the floor of the passage (D. Davis, pers. comm. 1984).

Popcorn—A type of knobular-shaped coralloid speleothem which decorates many cave passages in the Guadalupe Mountains. Usually this speleothem has no significance to speleogenesis problems, but in Hell Below Cave and Carlsbad Cavern "popcorn lines" cover walls and/or speleothems, lines which may possibly relate to speleogenesis events.

Moore (1960a) was the first to comment on the popcorn line in Carlsbad Cavern, and suggested that there might be a correlation between the level of the line and the tops of the gypsum blocks in the Big Room. Moore's suggestion has not been substantiated by recent leveling surveys (Table 19). The tops of the gypsum blocks at the Jumping Off Place in the Big Room are almost 6 m higher than the nearest popcorn line at the Temple of the Sun. It is probably just a coincidence that the gypsum blocks and popcorn line are nearly at the same elevation in the Big Room, since gypsum blocks exit in many other Guadalupe caves that do not have popcorn lines. Thrailkill (1965b) thought the line was an upper limit of a splash zone, while Jagnow (1977) thought it was a "waterline" corresponding to a past base level. Geologists M. Queen and J. McLean have informally hypothesized that air currents might be the cause of the line: dry-air currents moving into the cave could cause more evaporation and subsequent popcorn development near the floor, while more humid-air currents going out of the cave could be responsible for a lack of popcorn near the ceiling.

The popcorn line in Carlsbad Cavern is characterized by the following features:

(1) The line corresponds to a position of maximum passage width or "notch" in the passage, and it is marked by popcorn growth below the line, but not above it (Pl. 9B). The top of the line is not sharp; it is a zone 0.3-0.6 m thick.

(2) The line is nearly horizontal all the way along Left Hand Tunnel and the Big Room, with an average dip of only 1° that Jagnow (1979) ascribed to regional tilting subsequent to passage development.

(3) The line near the Green Lake Room is at exactly the same elevation as the line in the Big Room-Left Hand Tunnel (Table 19), even though the two localities are in different parts of the cave (Fig. 62).

(4) In many places in the Left Hand Tunnel, Big Room, Secondary Stream Passage, and elsewhere, sprays of flat-bottomed popcorn (trays) occur below the line.

(5) The popcorn line is associated with pronounced cor-

TABLE 19-Comparison of altitudes of the tops of gypsum blocks and the popcorn line, Carlsbad Cavern.

	Elevation	
Top of gypsum blocks		
Polar Region	1,117.5 m	3,665.4 ft
Jumping Off Place	1,121.1	3,677.2
Bottomless Pit	1,116.8	3,663.1
Salt Flats	1,116.6	3,662.5
Talcum Passage	1,123.5	3,685.1
Popcorn line		
Big Room		
Lion's Tail	1,118.6	3,669.0
18 m from elevators	1,117.2	3,664.4
Sword of Damocles	1,118.5	3,668.7
18 m beyond the Lion's Tail	1,118.6	3,669.0
Temple of the Sun	1,115.4	3,658.5
Left Hand Tunnel		
Average elevation from Lunch Room to Left Hand Fork (Jagnow, 1977)	1,117.7	3,666.1
Fissure Passage, between Green Lake and New Mexico Room	1,118.1	3,667.4

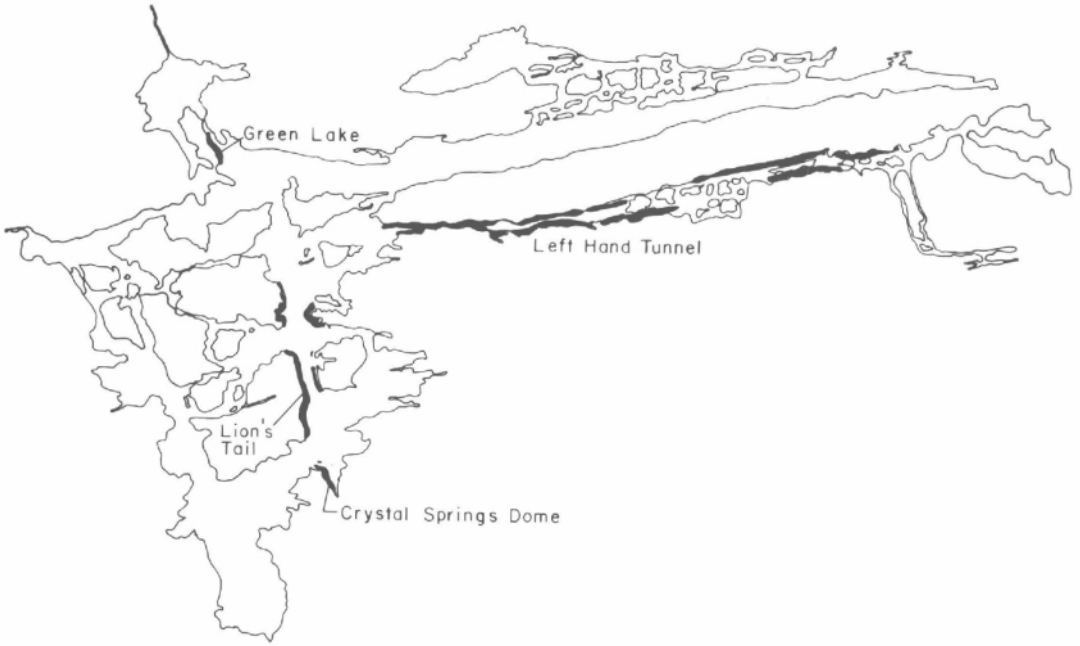

FIGURE 62 Distribution of the popcorn line in Carlsbad Cavern.

rosion: above the line speleothems and bedrock are highly corroded, whereas below the line they are not corroded.

(6) According to Jagnow (1979), the line disappears in the Big Room just south of the Hall of Giants, descending abruptly near the Temple of the Sun. Also, the line seems to "fall" into cross joints, with 30° dips over short distances (M. Queen, pers. comm. 1983).

(7) Except for the Green Lake area, the main popcorn line is not recorded at the Big Room level in other areas such as the New Mexico Room or Appetite Hill. Vague lines do occur in the Mystery Room and Lower Cave below the level of the Big Room.

(8) The popcorn of the popcorn line covers massive speleothems, both in the Lion's Tail area of the Big Room and in the Green Lake Room area of the cave.

(9) The line is not directly associated with pool speleothems such as rimstone, shelfstone, cave rafts, or subaqueous coralloids or coatings.

Rims—A cave rim is a projection of crystalline material on bedrock or speleothems which is smooth and scoured on the inside and rough and coralline on the outside. In Guadalupe caves, rims are composed of either carbonate (usually aragonite) or sulfate (gypsum) material. Sulfate rims line commode holes in gypsum blocks and these can build up around the commode hole so as to create bizarre shapes (Fig. 58). Carbonate rims line holes in bedrock or form as a continuation of a corroded area on speleothems (Fig. 63). They are another speleothem type associated with corrosion and late-stage speleogenesis events.

Corrosion features

Many speleothems are severely corroded in sections of Carlsbad Cavern, Spider Cave, and Wind (Hicks) Cave. Chalk-white and flaky, they assume an almost ghostly appearance (Pl. 10A). In some cases, these speleothems have been corroded down to their very cores along with adjacent corrosion of cave walls and ceilings (Pl. 10B). The speleothems look almost as if they have been wind-eroded because they are planed off concordant with the bedrock (Palmer and Palmer, 1975; Hill, 1976c, 1979). Speleothems in Spider Cave are highly corroded in the Ghost Chambers, a series of rooms named for their "unearthly ... dead, chalk-like stalagmites and curtains" (Nymeyer, 1938, p. 40). Corrosion

FIGURE 63-A carbonate rim on the flank of the Creeping Ear stalagmite, Lake of the Clouds Passage, Carlsbad Cavern. The banded area on the right is the corroded part of the stalagmite; the thin, white, crystalline shell to which the ruler is pointing is the rim. Both the stalagmite layers and the rim are corroded concordant with each other. Photo Cyndi Mosch Seanor.

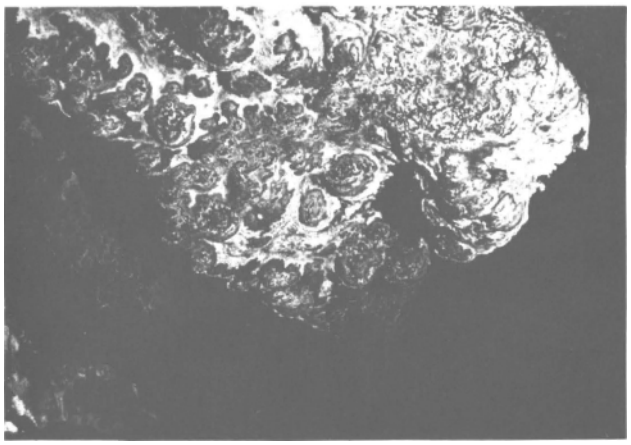

FIGURE 64-Corroded cloud linings with exposed layers of black manganese, Balcony, Lake of the Clouds, Carlsbad Cavern. Photo Pete Lindsley.

features are most dramatically represented in Carlsbad Cavern in the Left Hand Tunnel, Lake of the Clouds-Bell Cord Room-Bifrost Room area, Mystery Room, Taffy Hill, and East Annex and Balcony areas of the New Mexico Room. Corroded speleothems include stalactites, stalagmites, draperies, and "cloud" linings (Fig. 64). In sections of Carlsbad Cavern where speleothem corrosion is pronounced, and also in Spider and Wind (Hicks) Caves, two generations of speleothems are recognizable: (1) chalk-white, corroded speleothems which grew prior to corrosion, and (2) "normal," uncorroded speleothems which grew subsequent to corrosion (Pl. 11A). The first generation of speleothems is often corroded on one side and in a preferred direction (Fig. 63). In the Lake of the Clouds-Bell Cord Room-Bifrost Room area, the direction of corrosion consistently points towards the Lake of the Clouds (Fig. 93). In the upper part of the Mystery Room, the direction of corrosion faces the Cable Slot, not towards the lower chambers of the room (where speleothems are uncorroded).

Corroded stalagmites may be preferentially weathered along one side (Fig. 63), or they may possess hollow centers. A stalagmite and its hollow center form from the same drip point on the ceiling; the stalagmite formed from saturated water, the hollow center from undersaturated and corrosive water. Hollow-centered stalagmites of calcite and aragonite occur in the Big Room (along the trail) and in the Christmas Tree Room near the Lake of the Clouds Passage.

Bat guano

Carlsbad Cavern is world-famous for its bats. Allison (1937, p. 80) estimated that the cavern had a population of over 8.7 million bats, and compared an evening bat flight to "smoke pouring out from a volcano." The bats usually reside in Bat Cave (the upper level of Carlsbad), but isolated bats can also be seen in other parts of the cave and at any level, either live or mummified (Baker, 1963, Fig. 102). Likewise, bat guano is found at all levels in the cavern. The guano is in various stages of decay; it ranges from fresh, pungent droppings to material unrecognizable except by a chemical analysis (Table 20). Other Guadalupe caves that contain extensive bat-guano deposits are Dry Cave, McKittrick Hill; White Mule Cave, Big Canyon; and Ogle and New Caves, Slaughter Canyon, both of which were mined for guano in the 1930's and 1940's.

Decayed bat guano closely resembles cave silt and much care must be taken to distinguish between these two types of deposits. In general, bat guano is more uncompacted and fluffy than clastic silt; one typically sinks down into guano but stands firm on silt. Bat bones are usually present in guano and absent in silt, but this is not a hard and fast rule because bats can fall into cave silt or bat guano can be mixed with large amounts of silt.

The bat guano of New Cave is unusual in that it has a high silica (silt) content (D. DesMarais, pers. comm. 1983). Also, bat bones in the guano-silt have a distribution which suggests that they have been water-washed (S. Altenbach, pers. comm. 1983). Heavier jaw bones and solid finger bones tend to be located deeper in the guano deposits, whereas

TABLE 20-Composition of bat guano in Carlsbad Cavern and New Cave.

Location	NO_3 (ppm)	N_2O_5 (wt %)	P_2O_5 (wt %)	N (%)	K_2O (%)	H_2O (%)
Carlsbad Cavern						
Hill (1981c)						
Bat Cave, under mining shaft	1754	10.90	3.45			
Bat Cave, 1.2 m vertical cut, 5 samples 0.3 m apart:						
Youngest, top, #1	<1	11.30	2.32			
#2	20	12.09	1.89			
#3	63	11.60	1.88			
#4	517	12.10	1.63			
Oldest, bottom, #5	101	11.28	2.58			
Hutchinson (1950)						
Bat Cave (9 samples)						
#1			2.91	1.40	trace	-
#2			3.70	8.68	-	23.88
#3			4.48	5.74	-	16.51
#4			12.02	4.97	-	17.08
#5			-	4.27	-	-
#6			-	9.03	-	-
#7			11.34	5.67	0.48	14.55
#8			8.06	5.04	0.66	-
#9			11.20	0.48	0.48	-
New Cave						
Hill (1981c)						
Orange fraction, near jeep route	160	2.69	6.57			
Black fraction, near jeep route	35	0.07	1.75			
Orange fraction, near path	40	2.05	0.43			
Black fraction, near path	<1	0.52	7.48			

TABLE 21-Paleontology of Guadalupe Caves.

Cave	Type of bones found	Radiocarbon date (yrs) (U-series)	Reference
Burnet Cave (Rocky Arroyo Cave)	Cave bear, extinct bison, camel, horse, shrub ox, a cervid, American mountain deer	11,000-11,500	Howard (1932), Schultz & Howard (1935), Hester Schultz et al. (1970), Kurten (1975), Harris (1985)
Carlsbad Cavern Lower Devil's Den	Ground sloth *Nothrotheriops shastensis*	>29,700 U-series on bone = 111,900 U-series on calcite crystals in bone = 58,000	Hill & Gillette (1985, 1987)
Dark Canyon Cave	Peccary, birds	-	Howard (1971)
Dry Cave Balcony Room Bison Chamber	Sloth, condor, dire wolf Bison, bear, shrew, bighorn sheep, horse Human	29,290-33,590 10,730-15,030 3,135	Harris (1970, 1978, 1980, 1985), Harris & Mundel (1974), Harris & Porter
Hermit's Cave	Dire wolf, mammoth Shrew	11,850-12,900 12,000-13,000	Ferdon (1946), Hester (1960), Findley (1965), Schultz et al. (1970)
Musk Ox Cave	Bush ox, dire wolf, American lion and cheetah, extinct horse	18,140-25,500	Logan (1981)
Pink Panther Cave	Short-faced bear	-	A. Harris (pers. comm. 1985)
Pratt Cave	"Pleistocene deposits"	-	Gehlbach & Holman (1974), Lundelius (1979)
Upper Sloth Cave, Lower Sloth Cave, and Dust Cave	Shrew Sloth *Nothrotheriops* Black vulture, bighorn sheep	11,760 10,750-11,060	Logan (1975, 1977, 1983), Devender et al. (1977), Logan & Black (1979), Spaulding & Martin (1979), Logan (1983)
Williams Cave	Sloth *Nothrotheriops* (dung)	11,140-12,100	Ayer (1936), Van Devender et al. (1977), Spaulding & Martin (1979)

lighter long bones and skull parts tend to be located near the top of the deposit.

Animal bones

Animal bones have been found in Carlsbad Cavern, Musk Ox Cave (Fig. 65), Dry Cave, Hermit's Cave, Burnet (Rocky Arroyo) Cave, Pratt Cave, Dust Cave, Upper Sloth Cave, Lower Sloth Cave, Pink Panther Cave, Dark Canyon Cave, and Williams Cave (Table 21). One of the most important of these paleontological finds is the ground sloth, *Nothrotheriops shastensis,* discovered in Lower Devil's Den, Carlsbad Cavern, in 1947 and then at another site in the cave (which has not been relocated) in 1959 (Hill and Gillette, 1985, 1987). Most of the sloth bone fragments that still r-main in Lower Devil's Den are highly disturbed, but a few in-situ shards of bone on top of undisturbed silt occur in a 4-5 m radius around the site and look as if they might have been gently washed and water-laid. At the second site, the bones were covered by a thin coating of mud.

FIGURE 65-Bush-ox bones in Musk Ox Cave. Photo Ronal Kerbo.

Stratigraphy of cave deposits

Stratigraphic problems

Past investigators have failed to decipher stratigraphic relationships between the different kinds of cave deposits and, consequently, the proper time sequence of speleogenesis events in Guadalupe caves has never been understood. There have been many reasons for this failure. For one, clean contacts between deposits are often difficult to find. For another, some deposits are hard to identify in the field; for example, decayed bat guano closely resembles silt. But perhaps the most fundamental reason is the basic misunderstanding of the mechanisms producing some of the cave deposits, particularly speleothem deposits such as popcorn coralloids. Previous investigators assumed that all popcorn forms under water because they saw nodular speleothems growing in cave pools. It is now known that, while some coralloids are subaqueous in origin, most coralloids form subaerially by a number of mechanisms: water seeping through cave walls, thin films of flowing water, or splash

FIGURE 66-A thin crustal rind of gypsum which has been pushed outward from the wall by seeping-water-type popcorn, Left Hand Tunnel, Carlsbad Cavern. The gypsum is older than the popcorn. Photo Alan Hill.

solutions. Thus, popcorn may underlie another deposit and look like it is older than that deposit, when in reality it may be younger. For example, thin crustal rinds of gypsum in Left Hand Tunnel, Carlsbad Cavern, overlie wall popcorn, and so look younger than the popcorn (Fig. 66); actually, the popcorn grew from water seeping through the wall behind the gypsum and pushed the earlier-formed gypsum out from the wall. In like manner, solutions can seep through bedrock and deposit popcorn and other carbonate material under gypsum blocks and breakdown or under and over silt. In Left Hand Tunnel, seeping water has deposited a moonmilk-like zone of carbonate mineralization at the contact between bedrock and floor silt (Sheet 9, column E); the moonmilk-like material underlies the silt, yet postdates it. Coralloidal crusts which overlie silt deposits in Left Hand Tunnel and Lower Cave are deposited by water seeping through the silt toward the silt-air evaporative surface (Figs. 34, 36).

Another stratigraphic problem in Guadalupe caves concerns bat guano. Since guano falls from the ceiling in loose, uncompacted masses, it can easily gravitate below older features such as breakdown or gypsum blocks. For example, orange-colored bat guano has settled into the drip tubes of some of the gypsum blocks in the Big Room, Carlsbad Cavern (Pl. 4A). In the Talcum Passage, it has filtered completely through and under dissolved parts of the blocks so as to underlie portions of the gypsum. Another problem concerning bat guano is that it looks practically identical to silt when it decays. Both deposits are brownish orange and each may contain bat bones. The "bat guano under silt" described by Good (1957) as occurring in Bat Cave, Carlsbad Cavern, is a prime example of mistaken identity. M. Queen (pers. comm. 1984) analysed the "guano" material "under silt" and verified it to be more silt, a determination which is consistent with other observed stratigraphic relationships in the cave; that is, bat guano overlies silt, or in rare cases is mixed with silt, but it never underlies silt. The brick-red "guano" underlying gypsum blocks near the Salt Flats of the Big Room (Pl. 2B) is also silt, having an analyzed silica content of 57.55%. At least some of the material in New Cave thought to be pure bat guano is silt, as determined by analyses done by D. DesMarais (pers. comm. 1983). The only absolute way of distinguishing between bat guano and silt is to perform a chemical analysis on these deposits.

Stratigraphic sequence of deposits

The stratigraphic sequence of deposits in Guadalupe caves has been worked out mainly in Carlsbad Cavern where cave deposits of all types occur. This sequence was determined by crosscutting relationships and by stratigraphic superposition wherever clean contacts could be observed. Stratigraphic sections of cave deposits were correlated according to continuity and similarity of type; a number of representative sections are shown on Sheet 9. The sequence (ascending) of cave deposits in Carlsbad Cavern is as follows:

(1) **Breccia**—This is the earliest cave deposit. It is truncated by the large cave passages and thus predates all deposits lying within these passages. Breccia clasts are often embedded in a crystalline-spar matrix, and the breccia thus predates the spar event (events). The early age of the breccia relative to other deposits is shown most clearly by exposures in the wallrock and breakdown of the Guadalupe Room (Figs. 67, 68). The breccia predates the spar, the calcified siltstone-cave raft sequence, and all speleothemic material (Sheet 9, column A).

(2) **Montmorillonite-endellite**—These clays are found compacted into spongework cavities within the limestone. Both the cavities and the clay have been crosscut by the large cave passages, and hence predate them. It should be mentioned that while the clay fillings themselves are unquestionably older than the large cave passages, the type of clay mineral making up the filling may have a later origin (i.e. the endellite is believed to have reconstituted from montmorillonite later on).

(3) **Spar**—Spar crystals often fill solution pockets which have been truncated by the large cave passages; these crystals have been pitted, etched, and dissolved according to their proximity to this truncation. The stratigraphic relationship of the spar to the montmorillonite clay is uncertain, but one occurrence of associated clay and spar suggest that the clay fillings may predate the spar fillings. In the Papoose Room, Carlsbad Cavern, next to the trail and right before the tunnel, are two solution pockets 0.3 m apart, one filled with grayish-green clay and the other lined with spar crystals. Assuming the two solution pockets date from the same episode, then, if the spar had preceded the clay, both the pockets should be crystal-lined because saturated solutions depositing the spar could not have varied over so short a distance. However, if the clay episode had preceded the spar episode, then it is conceivable that the clay could have filled only one of the pockets (assuming that one pocket was connected to other, residue-occupied cavities above and that the other pocket was isolated from above-lying cavities).

(4) **Calcified siltstone-cave rafts**—As observed in the Guadalupe Room and Lower Devil's Den, the calcified siltstone-cave rafts occur as cavity fillings in wallrock truncated by the large cave passages (Sheet 9, column B). In the Main Corridor, Guadalupe Room, and Lower Devil's Den the siltstone-rafts are included in pieces of floor breakdown, one of which shows the siltstone-raft sequence directly overlying (and postdating) spar (Fig. 68). In Lower Devil's Den, a siltstone-raft deposit has been found beneath a large gypsum block (Sheet 9, column C), but it is hard to tell whether this deposit is in place beneath the gypsum block or on a piece of breakdown; either way, the siltstone-rafts definitely predate the gypsum. Such stratigraphic exposures place the calcified siltstone-cave rafts after the spar, but before the gypsum and before the dissolution of at least some of the large cave passages.

(5) **Cobbles**—The time of emplacement of the cobble gravel is uncertain both with respect to the dissolution of the major cave passages and to some of the other cave deposits such as the spar and the calcified siltstone-cave rafts. The cobbles may possibly postdate the spar in the upper levels of the cave and predate the spar in the lower levels-a speculation based on the well-indurated, sparry nature of the matrix material in the cobble gravel of Lower Cave versus the less-

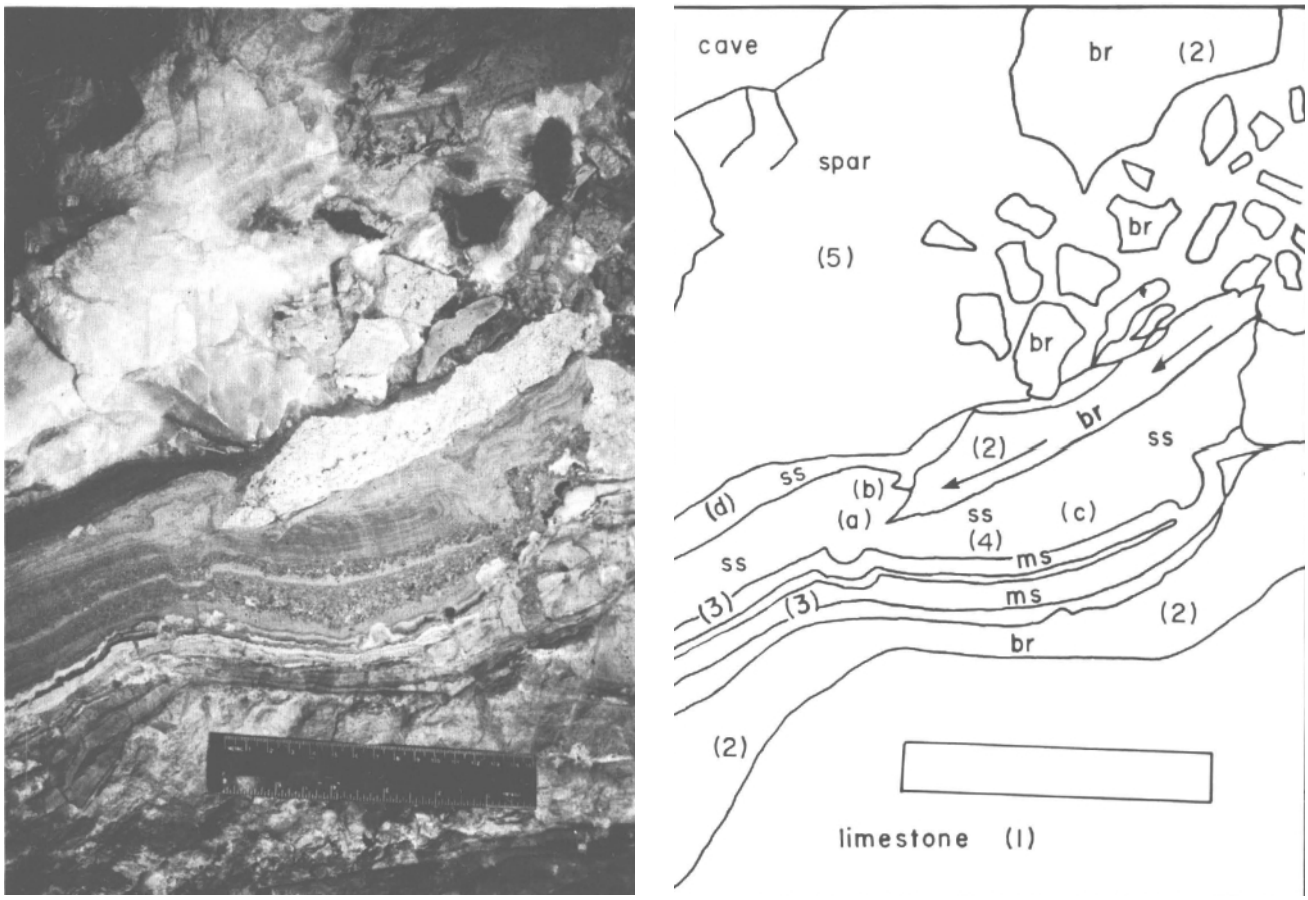

FIGURE 67-Sequence of deposits and events with respect to the breccia and spar, Guadalupe Room, Carlsbad Cavern: (1) formation of voids in the limestone; (2) shearing of breccia in place or emplacement of breccia into voids; (3) deposition of breccia mudstone on top of the breccia; (4) deposition of variegated siltstone on top of mudstone [before the siltstone and mudstone could harden, a large piece of breakdown moved down slightly (arrows) to produce deformation at (a), (b), and (c)], and deposition of siltstone layer (d) after breakdown had moved; (5) filling of remaining spaces between breccia clasts with spar. Photo Cyndi Mosch Seanor.

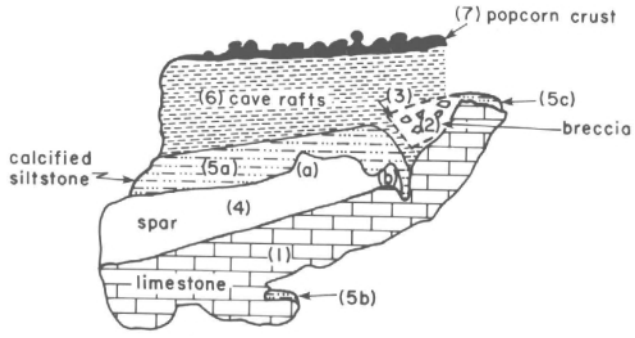

FIGURE 68-Diagrammatic presentation of a breakdown block in the Guadalupe Room, Carlsbad Cavern, showing the spar, breccia, and calicified-siltstone-cave-raft sequence. The entire sequence is about 1.5 m thick. Breakdown is drawn in its originally upright position as determined by the horizontal orientation of 5a, 5b, and 5c. Sequence of events and deposits is: (1) formation of limestone; (2) possible emplacement of the breccia; (3) truncation of breccia; (4) deposition of spar with well-developed crystal faces at (a) and (b); (5) deposition of siltstone on upward-facing surfaces (5a, b, c); (6) deposition of cave rafts; and (7) subaerial crustal growth on top of the cave rafts. The relative time of emplacement of the breccia is speculative, but the breccia and its truncation definitely antedate the siltstone-raft sequence.

indurated matrix material in the Main Corridor and Secondary Stream Passage. The relative age of the siltstone-rafts as compared to the cobble gravel is also unclear, because the two deposits have never been found in direct superposition. However, in the far end of Secondary Stream Passage, where one starts the climb towards Lower Devil's Den, siltstone-rafts are exposed in the wall while cobbles are found nearby on the cave floor. From this setting it seems that the siltstone-rafts may either predate or be contemporaneous with the cobbles, at least in this level of the cave.

The relationship of the cobbles to the silt is more sure. Since the cobble gravel either underlies the silt or is interbedded with it, the gravel must predate or be contemporaneous with the silt. If the undulating contact between the cobble gravel and silt in Lower Cave represents a true unconformity (Fig. 34; Sheet 9, column F), then it cannot indicate a long hiatus, since in the Secondary Stream Passage and Main Corridor the silt and gravel are interbedded or mixed together. In Upper Devil's Den the cobbles are located under a pile of breakdown and hence predate a major breakdown event. At this locality, cobbles can also be seen included in the upper part of a gypsum block, a relationship that might be taken for an indication that the cobbles are contemporaneous with the deposition of the gypsum were it not for many other exposures in which the cobbles always

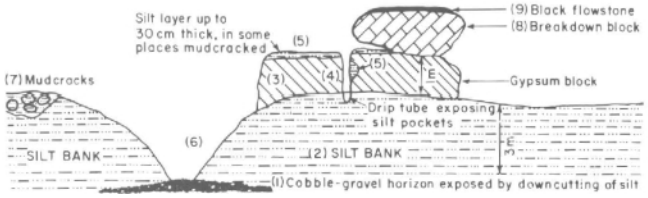

FIGURE 69-Sequence of events and deposits in Nooges Realm, Lower Cave, Carlsbad Cavern: (1) emplacement of cobble gravel; (2) formation of 3 m high silt bank; (3) deposition of 1 m high gypsum blocks; (4) drilling of drip tubes in gypsum by dripping water during first subaerial episode; (5) a back-up of water which stirred up the silt of silt bank and caused a thin (<30 cm) layer of silt to settle out on top of gypsum blocks and into drip tubes; (6) entrenchment of silt and gypsum to cobble-gravel horizon; (7) drying out of silt during second subaerial episode, formation of mud-cracks, and redrilling of drip tubes; (8) fall of breakdown block; (9) deposition of black flowstone on top of breakdown block.

underlie silt which underlies gypsum (Fig. 69). For this reason, it is strongly suspected that the cobbles included in the Upper Devil's Den gypsum reflect a late movement of the cobbles, such as slumping into the gypsum during the time of the gypsum's coalescence.

(6) **Sand and silt**—Fine-grained clastic sediment in Guadalupe caves underlies the massive gypsum and thus pre-dates it. There are numerous examples of this, e.g. at Bottomless Pit (Fig. 38; Sheet 9, column G), Nooges Realm (Fig. 69; Sheet 9, column F), and Left Hand Tunnel, Carlsbad Cavern (Sheet 9, column E); in the entrance area of Spider Cave; in the maze which connects the Entrance Hall with the Gypsum Passage, Cottonwood Cave; and in the Gypsum Room of Endless Cave. The only place where sediment has been observed to overlie gypsum is in Lower Cave, Carlsbad Cavern, where a thin (<30 cm) layer of silt covers a gypsum block which itself overlies a 3 m high silt bank (Fig. 69; Sheet 9, column F).

Silt overlies endellite and montmorillonite clay in the Big Room (Fig. 70; Sheet 9, column I), and it overlies the cobble gravel in Lower Cave. In the latter case, a possible unconformity exists between the silt and the underlying deposit. Silt always underlies flowstone and dripstone speleothems; for example, the stalagmite known as the Texas Toothpick directly overlies silt in Lower Cave. There is but one known exception to this rule: the 15 cm thick silt-breccia deposit of the Big Room overlies a portion of stalagmitic flowstone, which in turn overlies a 2 m high silt bank (Fig. 70).

(7) **Chert**—Chert lenses are interbedded with silt in the Big Room, usually along the top part of the deposit (Fig. 70; Sheet 9, column I). In the Salt Flats' exposure, chert interbedded with brick-red silt underlies gypsum blocks, which in turn underlie bedrock breakdown (Sheet 9, column H). The only place where this sequence is seemingly reversed (i.e. chert overlying gypsum) is where a large, out-of-place chert block (Pl. 5B) slid down on top of an in-place gypsum block, a late-stage movement which crushed part of the block and distorted the orientation of some of the block's drip tubes.

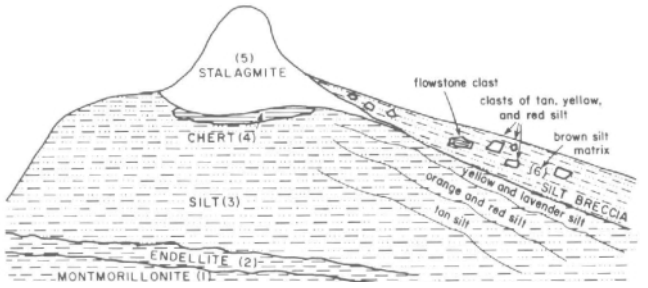

FIGURE 70-Diagrammatic presentation of the deposits in the areas of the Texas Trail and Salt Flats, Big Room: (1) grayish-green montmorillonite; (2) white layer of endellite; (3) silt; (4) chert; (5) stalagmite; (6) silt-breccia. The montmorillonite was transformed to endellite under acidic conditions with the liberation of silica (chert). Silt and travertine were later reworked locally (possibly by pool or drip water) so as to form the silt-breccia which slumped over the travertine. The stalagmitic flowstone (5) has been U-series dated at 107,600 yrs (Table 24, sample 20).

(8) **Gypsum blocks and rinds**—Gypsum blocks and rinds overlie clastic sediment (Fig. 38; Sheet 9, column F), or they may rest directly on bedrock limestone (Fig. 71; Sheet 9, column D). In some places in the Big Room, coralloidal crusts or flowstone can be seen beneath certain gypsum blocks, but these are speleothems formed from water which either seeped or flowed under the blocks. In the Talcum Passage, bat guano seemingly underlies certain sections of gypsum, but this guano has filtered down from above along drip tubes or cracks in the gypsum.

(9) **Breakdown**—Most of the breakdown fell shortly after the gypsum had deposited, but prior to massive speleothem growth. Such a stratigraphic relationship is best exemplified in the Big Room where some of the gypsum blocks with large breakdown pieces overlying them have both tilted drip tubes and vertical drip tubes (Sheet 9, column G). The gypsum blocks were drilled by dripping water before as well as after the impact and tilting by the breakdown pieces. Since no carbonate speleothems occur between tilted gyp-sum blocks and overlying breakdown pieces, the time between gypsum block coalescence and breakdown falling was probably relatively short.

While most breakdown fell approximately at the time of subsidence of the water table, a few pieces are known to predate or postdate this time. Bretz (1949) reported silt deposits in Carlsbad Cavern which postdated collapse break-down; perhaps Bretz was talking about the large breakdown pieces in the Stegosaurus Rock section of Lower Cave which were once completely covered with silt, but were later exhumed by an entrenchment of the silt. Iceberg Rock is a piece of breakdown which fell somewhat later in the cavern's history. The block has tilted dripstone deposits hanging along its bottom side, attesting to the fact that it fell some time after subaerial conditions became established.

(10) **Speleothems**—Speleothems have formed ever since the caves became air-filled. Some speleothems are known to have deposited prior to the native sulfur mineralization (i.e. the New Mexico and Christmas Tree Room sulfur), and some (those on the bottom of Iceberg Rock) grew prior to at least some major breakdown falls.

(11) **Sulfur**—In the Big Room of Carlsbad Cavern, sulfur

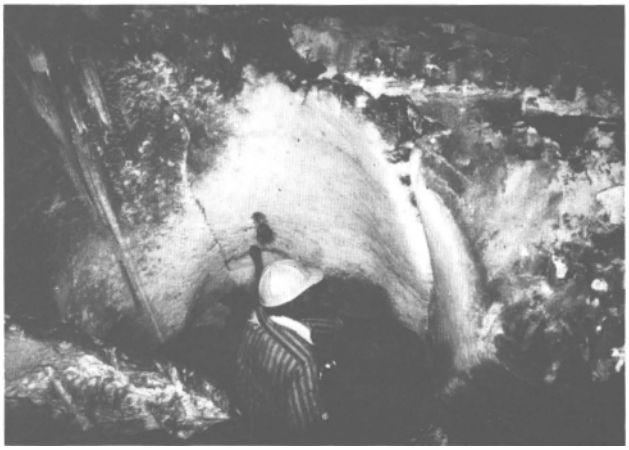

FIGURE 71-A gypsum block directly overlying bedrock limestone, Talcum Passage, Carlsbad Cavern. Photo Alan Hill.

occurs either mixed with gypsum or as a coating over it; thus, the sulfur either postdates, or is contemporaneous with, the gypsum at this site. In the New Mexico Room, sulfur coats speleothems (gypsum flowers and crust) and the undersides of bedrock, but it is not present on breakdown blocks adjacent to the sulfur-coated bedrock. For the sulfur at this locality to have deposited between the gypsum and breakdown events may mean that it formed very shortly after subaerial conditions were established in the cave. In the Christmas Tree Room, sulfur coats bedrock and speleothems (carbonate popcorn, rafts, and crinkle blisters), and, in this instance, it probably formed much later in the cave's history.

(12) **Bat guano—**Bat guano can be underlain, overlain, or interbedded with dripstone and flowstone travertine. Near the sign "decomposed bat guano" by Bottomless Pit in the Big Room, a thin layer of flowstone overlies decomposed bat guano; the guano rests on massive gypsum, which is underlain by silt, sand, and clay (Sanchez, 1964).

(13) **Animal bones—**All animal bones in Guadalupe caves have been found on top of cave sediment (e.g. the sloth bones in Carlsbad Cavern) or in talus piles near a cave's entrance (e.g. the diverse species in the entrance area of Dry Cave; Table 21). A few bones, such as those of the short-faced bear in Pink Panther Cave, or the bush ox in Musk Ox Cave, are covered with travertine and so antedate this late-stage speleothemic material (Fig. 65). The oldest animal bones known in any Guadalupe cave are the sloth bones found in Lower Devil's Den, Carlsbad Cavern; these have been dated at about 111,900 years (Table 24). The other bones found in Guadalupe caves do not exceed 33,590 years (Table 21).

(14) **Mud—**In the Mud Crack Room of Endless Cave, mud overlies a gypsum block and thus postdates the gypsum. Mud also locally covers travertine and animal bones. In all cases the mud is a late-stage material which has been washed into the caves, perhaps recording rare, catastrophic storms in the Guadalupe Mountains. The Mud Crack Room of Endless Cave and the passages of Little Sand Cave are approximately at the same elevation, with a downcutting valley between the two caves. Mud from valley erosion most likely entered both of these caves at the same time when the valley was at a higher level. In Vanishing River Cave, surface flood waters have been observed washing mud and debris into the cave. Mud infiltration into Guadalupe caves is a temporary phenomenon entirely unrelated to, and happening long after, speleogenesis events.

Analytical methods and results

Sulfur-isotope method

Fractionation processes

Sulfur has four stable isotopes with mass numbers 32, 33, 34, and 36. The relative proportions of ^{32}S and ^{34}S in sulfur compounds from various geologic environments vary markedly (Fig. 72), the isotopes being fractionated by long-term geochemical cycling and particularly by metabolic processes of the sulfur bacteria. Bacteria break S-O bonds and so create large isotopic changes, whereas chemical oxidation-reduction reactions affect O-O bonds and so create small isotopic changes. Thus, the sulfur-isotope method is a way of distinguishing sulfur formed by geological processes from that formed by biological processes. When sulfur bacteria interfere in oxidation-reduction reactions, ^{32}S is significantly enriched relative to ^{34}S; such an interference produces isotopic fractionations on the order of 10-20%. On the other hand, geologic leaching of sulfide minerals such as pyrite produces fractionations of less than 1% (Goodwin et al., 1976).

Sulfur isotopes are usually expressed in terms of 8"S values which relate the isotopic ratio $^{34}S/^{32}S$ of a sample to that of a standard:

$$\delta^{34}S = \left[\frac{^{34}S / ^{32}S \text{ sample}}{^{34}S / ^{32}S \text{ standard}}\right] - \left(\frac{^{34}S}{^{32}S}\right)_{std} \times 10^3 \qquad (1)$$

The overall isotopic fractionation effect approaches the sum of several separate steps for the reduction and oxidation of sulfur:

$$SO_4 \xrightarrow{A} SO_3 \xrightarrow{B} H_2S \xrightarrow{C} S \xrightarrow{D} SO_4 \qquad (2)$$

In all four steps the products are enriched in ^{32}S relative to the reactants. In step C, the reaction may proceed with the help of bacteria or, alternatively, may occur spontaneously when the sulfide oxidizes in the presence of oxygen. Variations in kinetics can cause marked changes in the overall isotopic effect of these reactions. Near the range of cave temperatures (12-15°C), the reduction reactions A and B are approximately twice slower than at 25°C (Kaplan and Rittenberg, 1964). As opposed to temperature, isotopic fractionation is relatively independent of pH, because most organisms have internal pH control (Kemp and Thode, 1968).

The sulfur bacteria responsible for the oxidation and reduction of sulfur compounds are *Desulfovibrio desulfuricans,* which reduces sulfate to hydrogen sulfide in the presence of petroleum, and *Thiobacillus thiooxidans,* which can oxidize hydrogen sulfide and sulfur to sulfuric acid and sulfate even

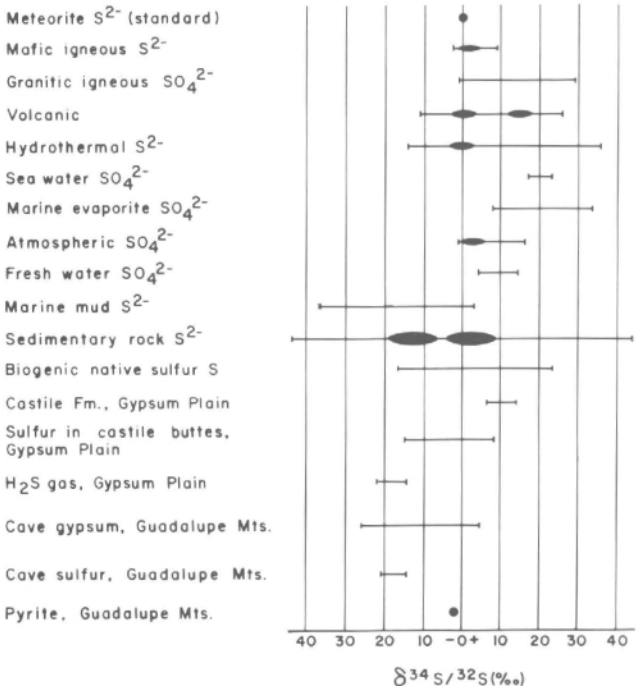

FIGURE 72—$\delta^{34}S$ values for various geologic environments. Gypsum and sulfur in Guadalupe caves are significantly enriched in ^{32}S compared to the gypsum and anhydrite of the Castile Formation in the Gypsum Plain. After Holser and Kaplan (1966).

in a pH regime of 0 (i.e. an environment that is 1N with respect to sulfuric acid; Stanier et al., 1957; Davis and Kirk-land, 1970).

Sulfur-isotope values of cave gypsum and sulfur

The gypsum and sulfur deposits in Guadalupe caves are significantly enriched in the light isotope of sulfur (^{32}S). Hill (1980b, 1981d) reported $\delta^{34}S$ values as low as -21.1 for cave gypsum, and $\delta^{34}S$ values as low as -20.0 for cave sulfur. Kirkland (1982) obtained similar isotopic values for the gyp-sum blocks of the Big Room, Carlsbad Cavern ($\delta^{34}S$ = -15.0 to -22.0). This paper expands on the earlier work of Hill, and includes sulfur-isotope data on sulfate speleothems and pyrite as well as on gypsum blocks and native sulfur (Table 22).

It is interesting to compare $\delta^{34}S$ values obtained for the cave deposits with those reported by Kirkland and Evans (1976) for oil and gas-generated sulfur in the castile buttes of the Gypsum Plain (Fig. 72). The castile sulfur has $\delta^{34}S$ values of +9.2 to -15.1, whereas the cave gypsum and sulfur have $\delta^{34}S$ values of +5.0 to -25.6. Both types of deposits fluctuate widely in their degree of fractionation; such large fluctuations over short distances are diagnostic of biologic systems because bacterial populations are always changing depending on nutrient levels and temperature (Goodwin et al., 1976). The sulfur-isotope values of the cave gypsum and sulfur also compare closely with values obtained for hydrogen-sulfide gas liberated from oil and gas reactions in the Delaware Basin (Fig. 72). According to the U.S. Department of Energy (1983), δ34S values of H_2S associated with brines at the WIPP and ERDA sites averaged -14.4 and -20.5, respectively.

It is also interesting to compare actual $\delta^{34}S$ and fractionation values of the cave gypsum and sulfur with theoretical values expected for reactions A through D in reaction (2), as have been reported by other investigators. If the SO_4^{2-} of reaction A represents the sulfate of the Gypsum Plain anhydrite (with an average $\delta^{34}S$ value of + 10.3) and the SO_4^{2-} of reaction D represents the cave gypsum sulfate, then the average amount of fractionation that has actually occurred in the cave gypsum (-15.1) compares closely with that theoretically expected (-15.6) for biological fractionations in reactions A through D at cave temperatures (Table 23).

Sulfur-isotope values of pyrite

Most of the pyrite in the Yates Formation of the Guadalupe Mountains has weathered to limonite and, therefore, is not suitable for sulfur-isotope analysis. Analyses were attempted on four "pyrite" specimens: one collected from the Hidden Cave Ridge, another from the Guadalupe Room, Carlsbad Cavern, and two from Guadalupe Ridge, 2.5 km east-northeast of the Dark Lookout near McCollum's Pit (collected by D. Jagnow). Only one specimen (one of the Guadalupe Ridge pieces) had enough pyrite (about 1%) for a sulfur-isotope determination ($\delta^{34}S$ = -2.5; Table 22). The same piece of pyrite exhibited concretionary structure in thin section.

Other pyrite in the Delaware Basin has been analyzed for its sulfur isotopic content. Mazzullo (1986) reported a $\delta^{34}S$ value of +1.2 for pyrite associated with Mississippi Valley-type lead-zinc mineralization in the southeastern, Ft. Stockton part, of the Delaware Basin.

Carbon- and oxygen-isotope methods

Fractionation processes

Fractionation involving carbon and oxygen is similar to that involving sulfur: geological and biological processes produce isotopic-exchange reactions which enrich a substance in one isotope relative to another. In the case of oxygen, two isotopes, ^{16}O and ^{18}O, are involved in the exchange, and in the case of carbon three isotopes, ^{12}C, ^{13}C, and ^{14}C, are involved. Plants generally become enriched in

TABLE 22-Sulfur-isotope analysis (by Geochron Labs).

Location	Sample	$\sigma^{34}S$
Carlsbad Cavern		
Big Room	Gypsum block	-13.9
Polar Region, Big Room	Gypsum block, vertical suite	
	(A) Top sample in suite	-17.6
	(B) 30 cm below (A)	-19.9
	(C) 30 cm below (B)	-21.1
Jumping Off Place, Big Room	Native sulfur mixed with gypsum in a gypsum block	
	Native sulfur	-20.0
	Gypsum	-19.0
New Mexico Room	Gypsum block	- 25.6
	Gypsum flower	+ 9.2
	Gypsum crust	+ 8.7
Mabel's Room	Gypsum block	-17.8
	Gypsum stalagmite	+ 7.3
Cottonwood Cave		
Upper Gypsum Passage	Gypsum block	+ 5.0
Lower Gypsum Passage by Chandelier	Native sulfur	-14.6
Lower Gypsum Passage	Gypsum crust	- 0.8
Dry Cave		
Balcony Room	Gypsum block	-12.4
Endless Cave		
Lower Maze	Gypsum block	- 8.6
Guadalupe Ridge		
On surface near Cottonwood Cave	Pyrite in an exposed limonite piece in Yates Fm.; 1% pyrite	- 2.5

TABLE 23-Sulfur-isotope fractionation in oxidation-reduction reactions.

Reaction	Range $\sigma^{34}S$%	Mean $\sigma^{34}S$%	Bacteria	Reference and remarks
Castile Fm. (SO_4^{2-})	—	+10.3	—	Holser & Kaplan (1966)
(A) $SO_4^{2-} \longrightarrow SO_3^{2-}$	−10 to −15	−12.5	*Desulfovibro desulfuricans*	Chambers & Trudinger (1979), Kemp & Thode (1968)
(B) $SO_3^{2-} \longrightarrow H_2S$	−14 to −20	−17.0	*Desulfovibro desulfuricans*	Holser & Kaplan (1966), Kemp & Thode (1968)
(C) $H_2S \longrightarrow S$	−3 to −6	−4.5	*Thiobacillus thiooxidans*	Chambers & Trudinger (1979). May also occur spontaneously without biological interference in the presence of oxygen.
(D) $S \longrightarrow SO_4^{2-}$	−6 to −9	−7.5	*Thiobacillus thiooxidans*	Chambers & Trudinger (1979), Kirkland & Evans (1976)
Total reaction, 25°C	—	−31.2	—	
At 12–15°C, cave temperature, ~1/2 of the fractionation as at 25°C		−15.6		Kaplan & Rittenberg (1964)
Average of cave-gypsum blocks	—	−15.1	—	Average of 10 gypsum blocks from various Guadalupe caves; see Table 22.

^{12}C and depleted in ^{13}C and ^{14}C, whereas calcium carbonate precipitated in isotopic and chemical equilibrium with CO_2 gas is enriched in ^{13}C. In the case of speleothems, the heavier isotopes of carbon and oxygen are enriched relative to rain water which falls above the cave, the degree of enrichment depending solely on the temperature of the depositing solutions provided the system is in isotopic equilibrium. This temperature factor makes the carbon- and oxygen-isotope methods useful in determining paleotemperatures under which speleothems formed, and, when used in combination with absolute-age dating methods, this technique can be an important indicator of past climate.

Stable carbon and oxygen isotopes can also be used in paleoenvironmental studies to determine whether certain material (e.g. spar) deposited under marine or fresh-water conditions. Fresh-water carbonates have characteristic isotope signatures: the oxygen composition of meteoric calcites is invariant with depth, reflecting a narrow range of temperature and oxygen composition in rainwater, and the carbon composition exhibits a marked depletion of ^{13}C (relative to marine carbon signatures) at exposure surfaces and a marked enrichment in ^{13}C with depth (Given and Lohmann, 1986). Such trends represent an initial input of ^{13}C-poor bicarbonate from soil organic processes and progressive addition of ^{13}C-rich bicarbonate from the interaction with carbonate host rock.

Furthermore, carbon-oxygen-isotope data are valuable in understanding speleothem-forming processes. An oxygen-isotope shift (towards an enrichment of ^{18}O) incurs with an increase of temperature and solute concentration, and a carbon-isotope shift (toward an enrichment of ^{13}C) takes place with increasing CO_2 loss. Thus, as incoming ground-water solutions loose carbon dioxide and as evaporation of the solvent takes place, there is a progressive shift from lower $\delta^{18}O$ and $\delta^{13}C$ values to higher $\delta^{18}O$ and $\delta^{13}C$ values.

Carbon-oxygen-isotope values of spar

The carbon-oxygen-isotope method has been instrumental in deciphering three separate spar episodes in the Guadalupe Mountains. Spar I and Spar II events have been defined by Given and Lohmann (1986) for samples collected along a "paleoslope" in reef-forereef limestones, McKittrick Canyon (Fig. 73), and Spar II and Spar III events have been defined for spar samples collected in Carlsbad Cavern during this study and during the studies of M. Queen, A. Palmer, and M. Palmer.

Spar I—Spar I is found in small primary pores and solution cavities occurring in marine-cement intergrowths in the Capitan Limestone. Both the spar and cement are characterized by relatively constant oxygen ($\delta^{18}O$ = -8) and varying carbon ($\delta^{13}C$ = 0 to -7) (Fig. 73), a fact that caused Given and Lohmann (1986) to conclude that both the marine cements and the Spar I crystals represent successive episodes during a single diagenetic event. On the basis of the invariant oxygen composition of Spar I and its restriction to the upper part of the paleoslope (from A to C, but not D; Fig. 73), Given and Lohmann (1986) also concluded that the Spar I diagenetic event represents the establishment of a fresh-water meteoric phreatic system in the reef facies characterized by well-defined downdip gradients in rock-water interaction to level C in the paleoslope, and that this meteoric system was active contemporaneously with the growth of the reef complex (i.e. in Guadalupian time of the Permian; see Table 1). The trend of marked depletion in $\delta^{13}C$ at the top of the paleoslope (stars, Fig. 73) and enrichment in $\delta^{13}C$ with depth (triangles, Fig. 73) represents an

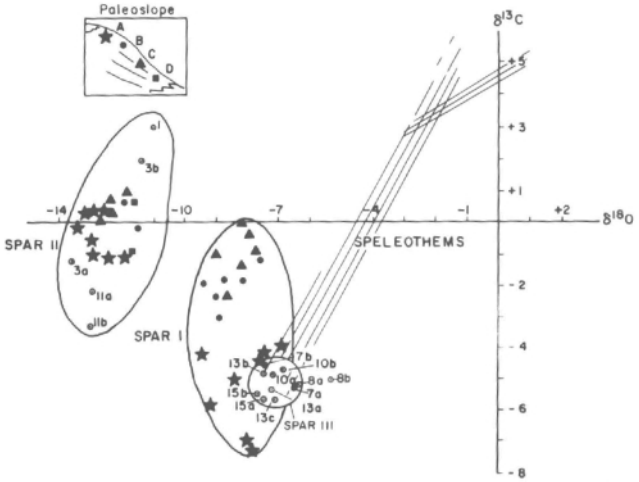

FIGURE 73—Carbon-oxygen composition of spar and speleothems, Guadalupe Mountains and Carlsbad Cavern. The stars, triangles, dots; and squares of Spar I and Spar II represent collection sites on a reef-forereef paleoslope, McKittrick Canyon (Given and Lohmann, 1986). The dotted circles of Spar II and Spar III represent spar and cave rafts collected in Carlsbad Cavern; the a, b, and c's represent the outside to the inside parts of these samples, respectively. The speleothem section is enlarged and elaborated on in Fig. 98.

initial input of ^{13}C -poor bicarbonate from soil organic processes and progressive addition of ^{13}C-rich bicarbonate from interaction with the carbonate host rock.

Spar II—Spar II is found throughout both the reef and forereef facies, where it occurs in fracture systems and at the center of large pores overlying and postdating Spar I material. Depleted oxygen signatures ($\delta^{18}O$ = -11 to -13) characterize Spar II material (Fig. 73), and this, combined with maximum precipitational temperatures implicit in the absense of an exsolved gas phase in primary fluid inclusions, indicates that the Spar II diagenetic event probably did not involve marine-derived fluids and may have been related to an Ochoan (or younger) regional meteoric or shallow-burial phreatic system (Given and Lohmann, 1986). The depleted oxygen composition may possibly be explained by either high temperatures due to burial, or a variation of local meteoric water in $\delta^{18}O$ due to climatic conditions at the time of deposition.

Three samples of spar collected from Carlsbad Cavern have carbon-oxygen-isotope signatures compatible with a Spar II genesis (samples 1, 3, 11, Fig. 73). A. and M. Palmer (written comm. 1985) considered sample 3 to be spar filling pre-cave Permian breccia, Secondary Stream Passage, and sample 11 to be spar from the core of a botryoidal crystalline mass in the Lake of the Clouds area. Sample 1 is a piece of etched dogtooth spar from Left Hand Tunnel.

Spar III—Spar III are large dogtooth crystals which occur in solution cavities or as spar linings (samples 7, 10, 15, Fig. 73). These are not always discernible from Spar II crystals by visible inspection (i.e. Spar II, sample 1), but isotopically they are characterized by relatively constant oxygen ($\delta^{18}O$ = -7) and carbon ($\delta^{13}C$ = -5 to -6). Spar III crystals are those which have uranium-series ages of >350,000 ybp and an Electron Spin Resonance age of 879,000 ± 124,000 ybp at the Big Room level (Table 24); i.e., they are most likely Pleistocene in age. The marked depletion of carbon in Spar III crystals is in the same range as that of Spar I (stars, Fig. 73): that is, Spar III originated from a ^{13}C-poor organic soil and did not experience much interaction with the carbonate host rock. This signifies that Spar III crystals probably formed near the top of the water table rather than at depth.

Carbon-oxygen-isotope values of cave rafts

The cave rafts of the siltstone-raft sequence (Type 1 rafts) have the same carbon-oxygen signature as Spar III crystals (Fig. 73, samples 8, 13). This suggests that both kinds of deposits formed in the same depositional environment, near (the spar) or at (the rafts) the surface of the water table. Type II rafts (the rafts of the cones, Balcony, the Lake of the Clouds Passage) differ from Type I rafts in their carbon composition (Fig. 98) but have similar oxygen compositions, suggesting that these two deposits formed at similar temperatures or from similar meteoric waters, but that the cave may have been experiencing more air flow, evaporation, or carbon-dioxide loss at the time of Type II raft deposition.

Carbon-oxygen-isotope values of speleothem cores

Brook et al. (manuscript) measured the $\delta^{18}O$ and $\delta^{13}C$ composition of stalagmitic cores taken from Lower Cave and the Main Corridor, Carlsbad Cavern. Their results on the Texas Toothpick and Georgia Giant stalagmites of these two areas, respectively, show that $\delta^{18}O$ and $\delta^{13}C$ values were generally much lower during the period from 180,000 to 140,000 ybp, and much higher for the period 140,000 to 60,000 ybp (Figs. 74, 75). They explained the shifts in ^{13}C as due to a change from a more humid, temperate glacial stage dominated by forest types at about 150,000 ybp, to a more semiarid interglacial or interstadial stage dominated by such plants as grasses and sedges at about 125,000 ybp, and the shift in $\delta^{18}O$ as due to different precipitation and atmospheric-circulation patterns during these glacial and interglacial periods.

Carbon-oxygen-isotope values of bedrock

Three bedrock samples were collected in the Lake of the Clouds-Left Hand Tunnel area, Carlsbad Cavern, for carbon-oxygen-isotope analyses. The purpose of these analyses was to try to determine if the cave was dissolved by hydrothermal water. A hydrothermal event in the Guadalupe Mountains may account for anomalous concentrations of metals in the mountains (Light et al., 1985), and in Carlsbad Cavern it might account for the high temperatures in the Lake of the Clouds Passage (Fig. 19) that may not be completely accounted for by the geothermal-gradient factor. A warm-water, lifting model of speleogenesis might also be supported by these data.

The carbon-oxygen data (Fig. 76) do not conclusively prove that cavern dissolution occurred hydrothermally, but do not rule out that possibility either. Note how the carbon-oxygen values of uncorroded limestone [i.e. the insides of samples (1) and (2) and the entire sample (3)] cluster around $\delta^{13}C$ = +4 and $\delta^{18}O$ = -3 to -5, values that are typical of marine limestones. Also note how the carbon-oxygen values become increasingly negative for the outside, corroded surfaces of samples (1) and (2) and how these trends seem to be heading toward the hydrothermal carbon-oxygen regime of calcite.

However, there may be another explanation for these

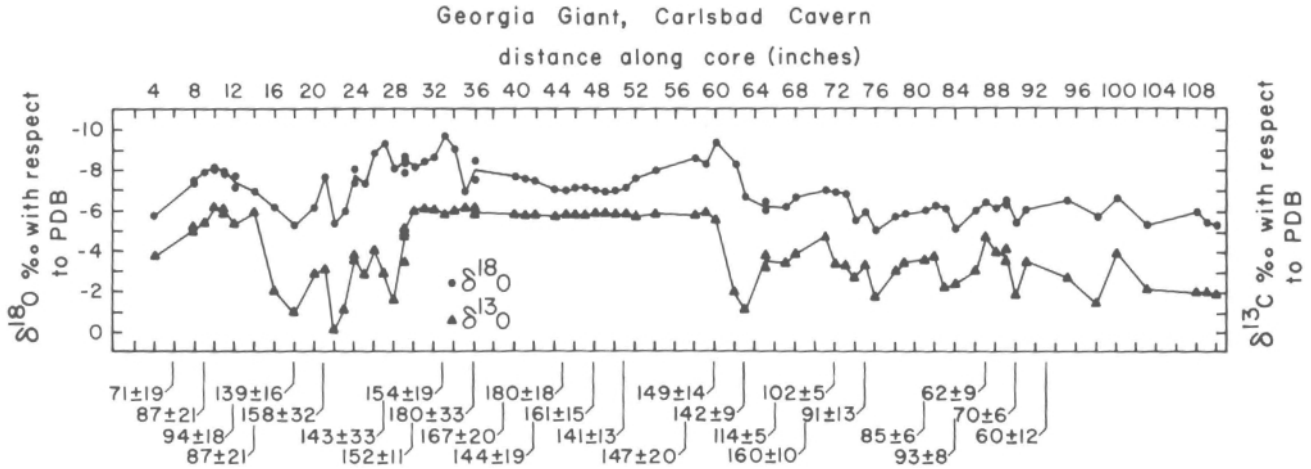

FIGURE 74-Carbon and oxygen stable-isotope data for the Georgia Giant stalagmite, Iceberg Rock, Main Corridor, Carlsbad Cavern U-series ages are given in 10^3 yrs. From Brook et al. (manuscript).

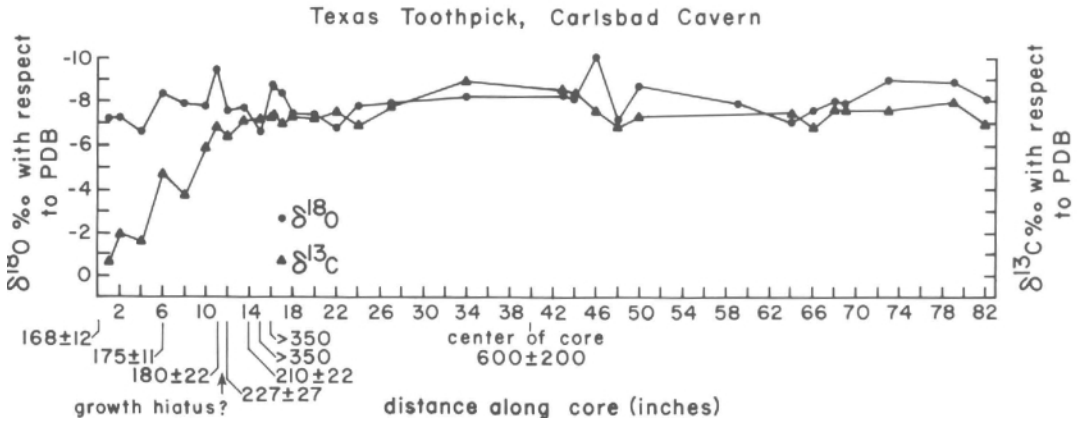

FIGURE 75-Carbon and oxygen stable-isotope data for the Texas Toothpick stalagmite, Lower Cave, Carlsbad Cavern. U-series ages are given in 10^3 yrs. From Brook et al. (manuscript).

trends. Bedrock sample (2) and especially bedrock sample (1) were collected in areas of pronounced condensation-corrosion, a process caused by high CO_2 levels in the cave air. If this CO_2 had derived from the bacterial or inorganic oxidation of methane and thus was characterized by very negative values of $\delta^{13}C$ and $\delta^{18}O$ (i.e. if some of the carbon dioxide came from the basin as is being proposed in this study), then its reaction with the bedrock might have also produced the trends seen in Fig. 76. The fact that Spar III crystals have a carbon-oxygen signature of $\delta^{13}C$ = -5 to -6 and $\delta^{18}O$ = -7 to -8 (Fig. 73), far outside the hydrothermal regime, also supports the contention that condensation-corrosion, rather than temperature, was responsible for the depletion of ^{13}C and ^{18}O in corroded bedrock surfaces. In addition, the work of Light et al. (1985) discourages the idea of a thermal episode in the Guadalupe Mountains. These authors found no evidence of hydrothermal alteration of rock samples collected at approximately 1.6 km (1 mile) intervals along Guadalupe Ridge in the Guadalupe escarpment wilderness study area, even though they often found these rocks associated with heavy-mineral, metal concentrates.

Fluid-inclusion method

In order to further test a hydrothermal model of speleogenesis, a sample of dogtooth spar (believed to be Spar III material) was collected from Left Hand Tunnel and subjected to fluid-inclusion analyses. Single-phase, pure-water inclusions are often trapped in speleothems during the precipitation of calcite and, by ascertaining the isotopic composition of these inclusions, important information on paleotemperatures can be obtained (Schwarcz et al., 1976).

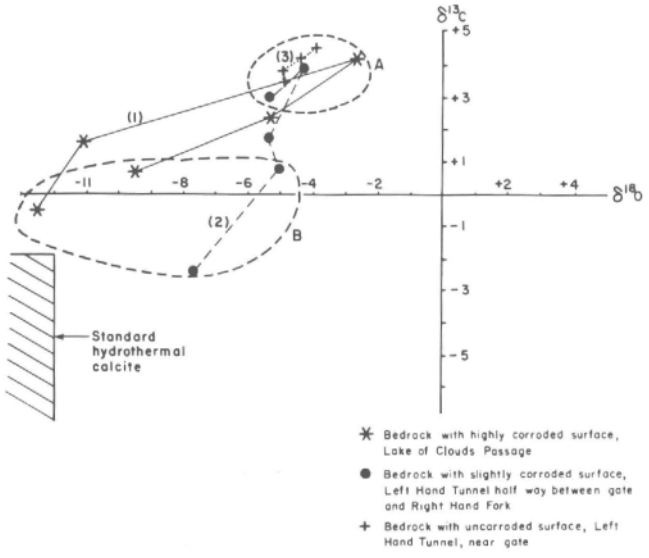

FIGURE 76-Carbon-oxygen isotope data of bedrock, Carlsbad Cavern. Carbon-oxygen isotope values of uncorroded bedrock are typical of marine limestones (A); corroded bedrock is atypical (B).

Fluid inclusions in the spar were analyzed for $\delta^{18}O$, $\delta^{13}C$, and 8D (deuterium/hydrogen). The crystal was an unzoned, dogtooth, Iceland spar, amber-colored and very clear, but highly corroded on its surface. It was acid-cleaned and then physically scraped until clear, uncorroded, crystalline material was reached. The crystal was cleaved (along the c-axis or near to it) to get equal halves for Run A and Run B. The crystalline material was then analyzed for $\delta^{18}O$ and δ13C (from split A only).

The spar sample turned out to be a Spar II crystal ($\delta^{18}O$ = -11, $\delta^{13}C$ = +3, Fig. 73, sample 1). $\delta^{18}O$ values of the fluid inclusions were -46.5 and -41.9, and $\delta^{13}C$ values were -19.6 and -19.9 (Runs A and B, respectively, PDB standard). δD of the fluid inclusions was -86 and -68 (Runs A and B, respectively, SMOW standard).

Since the spar crystal was not Spar III (Pleistocene) material, no information could be derived for or against a warm-water, lifting model of speleogenesis. However, the Spar II crystal did provide information on Late Permian events. The temperature at which the spar crystallized was calculated from the equation:

$$1000 \ln K_{cw} = 2.78 (10^6 T^{-2}) - 2.89 \quad (3)$$

where T is the absolute temperature and K_{cw}, is the temperature-dependent equilibrium constant for the isotopic exchange between calcite and water (Schwarcz et al., 1976). The temperature thus calculated was 55.4°C, a value which corresponds to Kevin and Given's (1986) contention that Spar II precipitated from meteoric water at some temperature between 30 and 65°C. This temperature suggests a depth of burial of less than 1 km.

Dating methods

A number of absolute dating methods have been used in this study: carbon 14, uranium series, electron-spin resonance, potassium-argon, and paleomagnetic. Samples were collected primarily in Carlsbad Cavern and were chosen on the basis of their relevance to speleogenesis problems.

Carbon-14 dating of bone and bat guano

The basic principle behind the carbon-14 dating method is that radioactive ^{14}C decays with a half life of about 5,000 years so that, over time, different ratios of ^{14}C and its daughter product ^{14}N exist. One bone sample-that of *Nothroth-*

eriops, an extinct ground sloth discovered in Lower Devil's Den, Carlsbad Cavern-was carbon-14 dated at >29,700 years by Geochron Laboratories for the amount of bone sample received (Table 21). Bat guano from New Cave and Ogle Cave has been carbon-dated by other investigators, and dates up to >32,500 have been obtained (Table 24).

Uranium-series dating of speleothems and bone

The isotopes of uranium, ^{234}U and ^{238}U, and the isotopes of thorium, ^{232}Th and ^{230}Th, are present in limestone and limestone-derived soils in small amounts. ^{234}U is selectively mobilized in solution and trapped within the calcite lattice at the time of speleothem deposition; thus, by measuring the ratio of ^{238}U to ^{234}U in present-day speleothem-depositing waters and in the speleothem itself (and knowing the half life of the reaction) the time of deposition of the calcite can be determined. Similarly, ^{234}U decays directly to ^{230}Th with a shorter half life, and hence the events of the late Pleistocene can be measured with accuracy. A disadvantage of the uranium-thorium method is that ^{230}Th has a much shorter half life than ^{234}U, so that an isotopic equilibrium is eventually set up in which the decay of parent and daughter proceeds at the same rate. This constraint usually limits the uranium-series (U-series) method to speleothem samples younger than about 350,000 ybp. However, examination of $^{234}U/^{238}U$ ratios may sometimes yield dates as high as 1.25 my, if the ratios indicate that isotopic equilibrium has been established over time (Gascoyne et al., 1983). Also, speleothem growth rates may be very cautiously used to estimate the age of travertine if that travertine is over 350,000 yrs old.

The spar crystals are the oldest speleothems in Carlsbad Cavern, and samples from the cave entrance down to Lower Cave (a vertical extent of almost 240 m) have U-series dates consistently >350,000 ybp. An extrapolation beyond 350,000 yrs based on $^{234}U/^{238}U$ ratios cannot be applied to these dates since it is evident from Table 24 that these ratios have not been constant over time or place but have varied from 0.56-3.4 for all the various types of speleothems dated. Also, the $^{234}U/^{238}U$ ratio has been shown to vary from 1.78-3.13 for recently collected water samples from Carlsbad Cavern (J. Cowart, written comm. 1985).

Cave rafts of the calcified siltstone-cave raft sequence (Type I rafts) appear to be the next oldest deposit, varying

TABLE 24-Age of speleothems and other deposits in Guadalupe Caves. Abbreviations: FSU, Florida State University, Department of Geology, Tallahasse, Florida; UT, University of Texas, Department of Geology, Arlington, Texas; MU, McMaster University, Geography Department, Hamilton, Ontario, Canada; UK, Geologisches Institut der Universitat Köln, West Germany; NLB, Niedersachsisches Landesamt fur Bodenforschung, Hannover, West Germany.

Type of deposit	Sample no.	Location	Dating method	Age (yrs)	$^{234}U/^{238}U$ ratio	Analyses by, notes
Carlsbad Cavern, this study						
Spar	1	Entrance	U-series	>350,000	1.025 ± 0.23	D. Ford, MU; ~4,300 ft elevation.
Spar	2	Lower Guadalupe Room	U-series	>350,000	1.008 ± 0.15	D. Ford, MU; collected by M. Queen; ~3,800 ft elevation.
Spar	3	Secondary Stream Passage	ESR	—	—	G. Hennig, NLB, and R. Grün, UK; saturated; no date obtainable.
Spar	4	Secondary Stream Passage	ESR	879,000 ± 124,000	—	G. Henning, NLB, and R. Grün, UK; collected 10 cm from sample 3; ~3,700 ft elevation.
Spar	5	Bell Cord Room	U-series	>280,000	0.99 ± 0.05	J. Cowart, FSU; ~3,675 ft elevation.
Spar	5	Left Hand Tunnel	U-series	>350,000	0.959 ± 0.148	D. Ford, MU; ~3,650 ft elevation.
	6	Left Hand Tunnel	U-series	>350,000	0.877 ± 0.03	D. Ford, MU; connected to sample 5.
	7	Left Hand Tunnel	ESR	—	—	R. Grün, MU; manganese contamination; no date. Next to sample 5.
Spar	8	Mystery Room	ESR	—	—	G. Hennig, NLB, and R. Grün, UK; saturated; no date.
Spar	9	Lower Cave	U-series	>350,000	0.987 ± 0.025	D. Ford, MU; collected by M. Queen just west and above Nicholson's Pit, 3,570 ft elevation.
	10	Lower Cave	U-series	>350,000	0.982 ± 0.45	Connected to sample 9.
Rounded spar	11	Lower Cave	U-series	—	1.07 ± 0.15	J. Cowart, FSU; found with rounded cobbles in trench; no date due to low thorium concentration.
Cave rafts of siltstone-raft sequence	12	Lower Devil's Den	ESR	257,000 ± 64,000	—	G. Hennig, NLB, and R. Grün, UK; ~3,720 ft elevation.
	13	Lower Devil's Den	U-series	259,600 +40,800 −29,600	1.007 ± 0.018	D. Ford, MU; same collection site as sample 12.
	14	Lower Devil's Den	U-series	213,800 +21,300 −17,800	1.028 ± 0.017	D. Ford, MU; connected to sample 13.
Cave rafts of siltstone-raft sequence	15	Main Corridor	ESR	—	—	G. Hennig, NLB, and R. Grün, UK; saturated; no date obtainable; ~3,675(?) ft elevation.
	16	Main Corridor	U-series	>350,000	1.086 ± 0.234	D. Ford, MU; same as 15; in an out-of-place breakdown block.
	17	Main Corridor	U-series	205,200 ± 52,600	1.06 ± 0.14	J. Cowart, FSU; same as sample 15.
Flowstone	18	Bell Cord Room	U-series	151,700 +8,800 −8,200	1.119 ± 0.14	D. Ford, MU; flowstone corroded by rillenkarren.
	19	Bell Cord Room	U-series	176,000 ± 65,000	1.00 ± 0.07	J. Cowart, FSU; collected 0.5 ft lower than sample 18.
Flowstone	20	Big Room	U-series	107,600 +3,400 −3,300	1.568 ± 0.025	D. Ford, MU; underlies silt-breccia.

TABLE 24, continued.

Type of deposit	Sample no.	Location	Dating method	Age (yrs)	$^{234}U/^{238}U$ ratio	Analyses by, notes
Flowstone	21	Lower Cave	U-series	176,000 ±25,000 at base 148,000 ±10,000 in middle 125,000 ±10,000 at top	2.236 2.169 1.867	D. Ford, MU; overlies cobbles.
	22	Lower Cave	ESR	160,000 ±32,000 at base 125,000 ±25,000 at top	—	R. Grün, MU; same as sample 21.
Popcorn	23	Left Hand Tunnel	ESR	272,000 ±106,000	—	G. Hennig, NLB, and R. Grün, UK; popcorn below the "popcorn line."
	24	Left Hand Tunnel	U-series	>350,000	0.931	D. Ford, MU.
Popcorn	25	Left Hand Tunnel	U-series	33,000 ±800	0.601	D. Ford, MU; collected about 7 m from sample 24; popcorn of "popcorn line."
Popcorn	26	Left Hand Tunnel	U-series	36,300 ±1,800	0.56	D. Ford, MU; popcorn of "popcorn line"; dirty; date may not be reliable.
Popcorn overlying stalagmite	27	Big Room (by Lion's Tail)	U-series	45,000 ±2,000 87,000 ±6,000 102,000 ±4,000	1.971 (outer cm) 2.619 2.005 (inner cm)	D. Ford, MU; drill core in massive stalagmite covered with popcorn of "popcorn line"; core 3 cm deep; outer cm popcorn, intermediate and inner cm stalagmitic travertine.
Stalactite	28	Main Corridor	U-series	>350,000	—	D. Ford, MU; tilted stalactite on bottom of Iceberg Rock.
	29	Main Corridor	ESR	513,000 ±30,000	—	R. Grün, MU; same sample as 28.
Rafts	30	Balcony, Lake of the Clouds	U-series	50,000 ±4,000	—	D. Ford, MU; may represent last speleogenesis event.
Rafts	31	Christmas Tree Room area	U-series	>350,000	—	D. Ford, MU; rafts overlain by sulfur crystals. Date is probably spurious due to high uranium content (U = 238 ppm).
Gypsum block	32	Polar Region, Big Room	ESR	—	—	G. Hennig, NLB, and R. Grün, UK; did not exhibit an ESR-sensitive peak.
Montmorillonite clay	33	Papoose Room	K–Ar	188 ±7my	—	S. Stokowski, Geochron Labs.
Nothrothiops (sloth) bone	34	Lower Devil's Den	C-14	>29,700	—	Geochron Labs.
	35	Lower Devil's Den	U-series	111,900 +13,300 −11,100	0.808	D. Ford, MU; date on bone material.
	36	Lower Devil's Den	U-series	58,000 +5,600 −5,100	0.787 ± 0.13	D. Ford, MU; calcite crystals inside of weathered bone.
Carlsbad Cavern, other studies						
"Texas Toothpick" stalagmite	37	Lower Cave, below Jumping Off Place	U-series	167,000 to >350,000	2.247–2.509	D. Ford, MU; stalagmite overlies paleomagnetically reversed silt; core of stalagmite might approach or exceed 600,000 yrs; core drilled by B. Ellwood, UT. Brooks et al. (manuscript).
"Georgia Giant" stalagmite	38	Main Corridor	U-series	60,000 to 180,000	3.0–3.4	J. Cowart, FSU; stalagmite overlies Iceberg Rock; core drilled by B. Ellwood, UT. Brooks et al. (manuscript).
Soda straw	39	Main Corridor	U-series	20,000 at bottom 50,000 at top	—	J. Cowart, FSU; collected by B. Ellwood, UT, near "Georgia Giant" stalagmite.
Aragonite moonmilk	40	Lower Cave(?)	C-14	18,000 ±580	—	"Mud wholly of aragonite" (Dunham, 1972).
Other Guadalupe caves, other studies						
Stalagmite	41	Ogle Cave	U-series	125,000 to 205,000	—	Harmon & Curl (1978).
Bat guano	42	New Cave	C-14	>17,800	—	Libby (1954).
	43	New Cave	C-14	>28,250 >32,500	— —	20 cm below flowstone caprock. 225 cm below flowstone caprock. Letter from R. H. Brown to Carlsbad Caverns Natl. Park (1981).
Bat guano	44	Ogle Cave	C-14	4,150 to 7,300	—	Upper level of guano, cut by miner's trench (D. DesMaris, pers. comm. 1984).

from about 200,000 to >350,000 yrs (samples 12-17; Table 24). These may all be minimum dates due to the fact that at least 80% of the mass of the cave rafts is post-depositional cement material which was introduced sometime after the rafts themselves had formed.

Dates on the Texas Toothpick stalagmite (Fig. 75) are important to a proper understanding of early speleogenesis events in Carlsbad Cavern, and age dates on the Georgia Giant stalagmite (Fig. 74) are important to the understanding of later speleogenesis events. The Texas Toothpick stalagmite in Lower Cave overlies paleomagnetically reversed (>730,000 yrs old) silt (Table 25) and ages of the travertine in the stalagmite itself exceed the 350,000 limit of the U-series dating technique. Based on its fairly constant $^{234}U/^{238}U$ ratio (between 2.247-2.509) and travertine growth rates (approximately 1 cm/1,000 yrs), a very rough date of 600,000 ± 20,000 yrs can be obtained for the center of the stalagmite core (D. Ford, pers. comm. 1985). When the radiometric ages for the Georgia Giant stalagmite are plotted on a frequency histogram (Fig. 77), they show periods of maximum and minimum growth, and also periods of no growth.

Dates on the popcorn associated with the "popcorn line" range from 33,000 to >350,000 ybp for sites sometimes only meters apart (samples 23-27, Table 24). The relatively low (45,000 yrs) age of the popcorn overlying stalagmitic travertine near the Lion's Tail, Big Room, is consistent with the older ages of the travertine layers directly below it (87,000 ybp for the first centimeter and 102,000 ybp for the next centimeter, sample 27). These dates indicate a steady growth of material from 102,000 to 45,000 ybp and then cessation of growth.

The flowstone (sample 21) overlying the cobbles in Lower Cave, Carlsbad Cavern, shows a steady growth from about 170,000 to 125,000 yrs ago. The date of approximately 150,000-160,000 yrs for the corroded flowstone of the Bell Cord Room, Carlsbad Cavern (samples 18, 19), indicates that pronounced corrosion occurred in this area of the cave some time after 150,000 ybp.

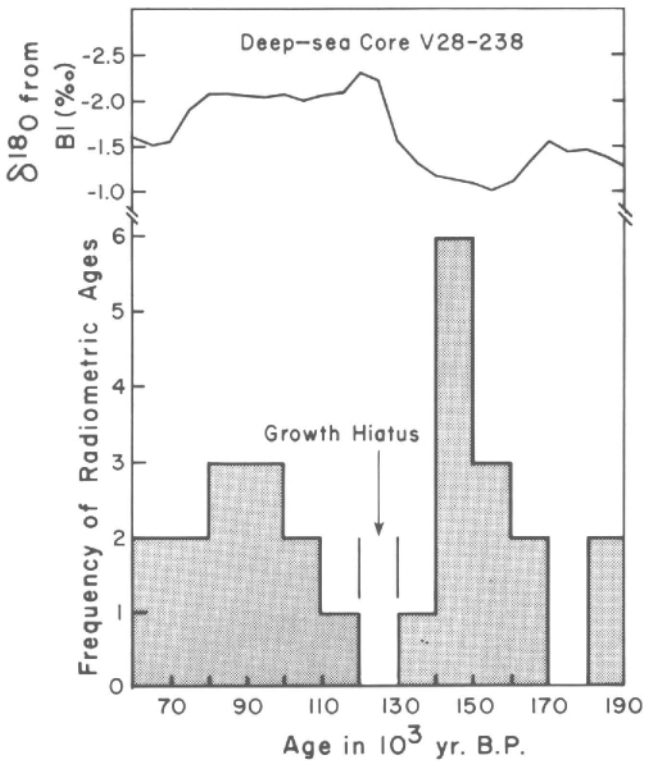

FIGURE 77-Frequency histogram of radiometric ages for the Georgia Giant stalagmite, Carlsbad Cavern, compared to $\delta^{18}O$ variations in a deep-sea core 190,000 to 60,000 yrs old. From Brook et al. (manuscript).

Rafts in the side passage off the Christmas Tree Room were dated in hopes of determining the age of the sulfur crystals overlying the rafts (Table 24, sample 31). Unfortunately, the rafts contained so much uranium (U = 238 ppm) that a reliable date could not be obtained. Rafts making up the outer surface of cones on the Balcony, Lake of the Clouds (Table 24, sample 31) were also U-series dated. The resultant age of 50,000 yrs possibly represents the last fluctuation of base level in the Lake of the Clouds Passage and the last speleogenesis event in the cave.

The U-series date of 111,900 ypb on *Nothrotheriops* bone material (Table 24, sample 35) signifies the time when the sloth died in the cave and was first subjected to the influence of uranium-bearing ground water, and assumes that the uptake of uranium by the bone was relatively rapid and reached some saturation level after a time which is short compared with the age of the bone. The 111,900 ybp date is consistent with the 58,000 ybp date on calcite crystals that grew in marrow already badly weathered (Table 24, sample 36). This U-series date of approximately 112,000 ybp is the oldest absolute date ever obtained for *Nothrotheriops* (Hill and Gillette, 1987).

Electron Spin Resonance dating of speleothems and gypsum

The Electron Spin Resonance (ESR) method is a new dating technique developed over the past few years (Ikeya, 1975, 1978; Hennig and Grun, 1983). The main advantage of the ESR dating method is that it can be used on speleothems which are one million years old or older, and the method thus covers much of the speleogenesis time in Guadalupe caves. Also, this method can sometimes be used on gypsum as well as calcite.

The ESR dating technique is similar to U-series dating, but measures radiation-induced defects in the calcite crystal lattice rather than the amount of daughter isotopes. Radio-active decay produces trapped electrons (CO_3^{3-}) or trapped holes (CO_3^{-}), and the traps are detected by directly measuring microwave adsorption in a strong magnetic field. The number of traps is proportional to the amount of decay and the time involved; hence the age and growth rate of the speleothem can be determined.

ESR age dates are calculated from the archaeological (AD or total) radiation dose and the annual radiation dose. The archaeological-dose rate is evaluated by means of ESR spectrometry and by considering the uranium content of the sample; the annual radiation dose is obtained by measuring gamma-ray exposures at collection sites within the cave. Gamma-radiation exposures, as measured in Carlsbad Cavern, are listed in Table 6; measurements made by Moore (1984) were performed using a Ludlum Micro R Meter.

The results of the ESR dating are listed in Table 24. Of the four spar samples submitted for ESR dating, only sample 4 gave a date; the other three samples (3, 7, 8) were "saturated." The condition of saturation means that all the available traps are occupied, and may indicate either that a sample is very old or that it is contaminated by such impurities as manganese (defect ions which act as traps). In younger (<350,000 yrs), non-spar speleothem samples (12, 22, 23, 29), ESR dates compare nicely with U-series dates for the same samples, a fact that lends credibility to the 879,000 ± 124,000 ESR date on spar sample 4.

The sample of gypsum block, collected from the Big Room, Carlsbad Cavern, did not exhibit an ESR-sensitive peak and so provided no age information.

Potassium-argon dating of montmorillonite clay

Based on stratigraphic relationships, the montmorillonite clay filling solution pockets is believed to be older than at least some of the spar. For this reason, the clay was dated by the potassium-argon method, which is suitable for materials one million years old or older. The potassium-argon method uses the decay of ^{40}K to ^{40}Ar, a gas which can be measured with great accuracy. The method has its difficulties, the most notable being the loss/gain of potassium or the loss of argon from a system, especially in the case of sedimentary deposits which are subject to ground-water leaching. Inheritance of old argon and potassium from the time the limestone was originally deposited can also be a serious problem, one resulting in anomalously old dates. Another problem is that the potassium content of autochthonous cave clay is usually very low and not suitable for dating by this method. Furthermore, dates have never be-fore been achieved on montmorillonite samples (T. Bills, Geochron Labs, pers. comm. 1985); illite is the only clay mineral which has been successfully dated by the K-Ar method.

Montmorillonite clay collected from the Papoose Room, Carlsbad Cavern, has been found high enough in potassium (1.84%) to qualify for potassium-argon dating. The date obtained on the clay was 188 ± 7 my (Early Jurassic). This date is problematical because it is not known how the above factors relate to it. Vadose ground-water contamination has probably been relatively minor, at least in the recent past, since vadose drip water entering the cave is low in potassium (0.39-6.65 ppm; Table 28), and Capitan aquifer water is also very low in potassium (0.78-2.15 ppm; Table 2). Detrital feldspar in the clay contained only 0.13% K, which rules out any significant contamination from this source.

Paleomagnetic dating of silt and speleothems

The magnetic field of the Earth does not remain constant over time, but fluctuates in direction about geographic north and, once every half a million years or so, reverses polarity. Such changes provide a basis for dating rocks and sediments. In this method magnetic material (usually iron-mineral grains) align in the direction of the Earth's magnetic field at the time of rock crystallization, sediment deposition, or calcium-carbonate deposition in a speleothem.

A paleomagnetic determination of calcium carbonate in the Texas Toothpick stalagmite, Lower Cave, was attempted by D. C. Ford (pers. comm. 1985), but not enough iron was found present in this speleothem in order to make a magnetic determination of the travertine. Brook et al. (manuscript) report that some parts of the core of the Georgia Giant stalagmite record a stable remanent magnetism (Fig. 78); Zijderveld vector diagrams for two samples (CB-64, CB-74) demonstrated straight-line decay to the origin with a.f. demagnetization to 50 mT. However, other samples (CB-62, CB-75) were not stably magnetized, and a continuous record of secular variation in the Earth's magnetic field over time thus cannot be constructed with the data so far obtained.

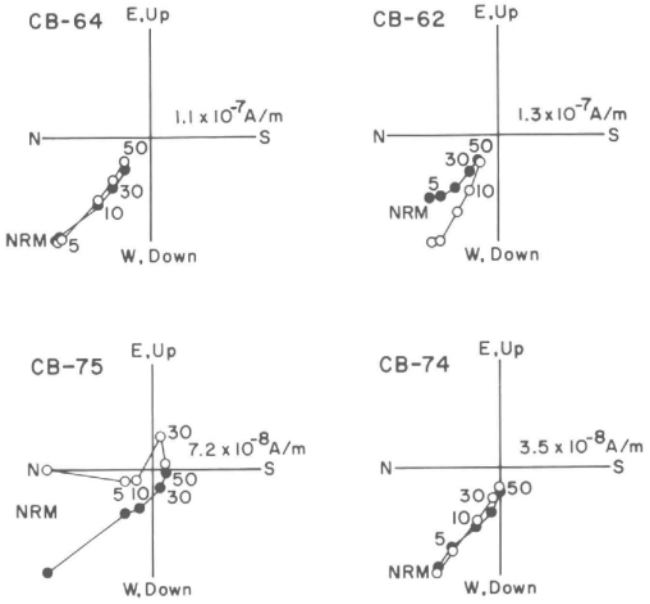

FIGURE 78—Zijderveld vector diagrams showing natural remanent magnetism in the Georgia Giant stalagmite, Iceberg Rock, Main Corridor, Carlsbad Cavern. From Brook et al. (manuscript).

Paleomagnetic age determinations of silt were made during this study on samples collected from Lower Cave, Carlsbad Cavern. Samples of sediment were collected using a 2 cm^2 plastic box while noting proper compass orientations after the manner of Schmidt (1982). Paleomagnetic analyses were performed on the samples by the University of Pittsburg Rock Magnetism Laboratory using a cryogenic magnetometer. The results of this age determination are listed in Table 25.

All of the silt samples collected in Lower Cave had reversed polarity, meaning that the sediments were deposited more than 730,000 yrs ago, before the most recent magnetic-field reversal, the Brunhes/Matsuyama reversal. The data are consistent with the assertion that all the sediment was deposited at the same time, but there is no proof that this was the case. If the sediments were of both normal and reversed polarity in the vertical sequence at Stegosaurus Rock, then the absolute age of the deposit could be better established; but with all the samples showing reversed polarity, only a lower limit of 730,000 yrs can be set for the silt deposits of Lower Cave. While it is possible that the Lower Cave silt was paleomagnetically reversed in a pre-Brunhes/Matsuyama reversal, it is not likely because the extrapolated date (600,000 ± 200,000 yrs) on the Texas Tooth-pick stalagmite, which directly overlies the silt, approaches the lower limit of the Brunhes/Matsuyama reversal (730,000 yrs). Hence the age of the silt in Lower Cave probably has an upper limit of 0.9 my, which defines the lower limit of the next reversal event, the Jaramillo normal episode.

TABLE 25-Paleomagnetism of silt, Lower Cave, Carlsbad Cavern.

Location	Description		Date
Green Clay Room	Laminated silt		>730,000 yrs; magnetically reversed
60 m past Rookery	Nonlaminated silt		>730,000 yrs; magnetically reversed
Nooges Realm	Nonlaminated silt		>730,000 yrs; magnetically reversed
15 m before "Stegosaurus" rock	Nonlaminated silt		
	1.2 m above floor	Vertical sequence	>730,000 yrs; magnetically reversed
	4.5 m above floor		Sample not compact enough, no results
	7.5 m above floor		>730,000 yrs; magnetically reversed

Chemical analyses

Whole-rock analyses

Egemeier (1973, 1981) demonstrated that limestone and overlying gypsum crust on the walls of replacement-solution caves in the Big Horn Basin, Wyoming, are chemically related to each other. Egemeier's chemical correlation was done using paired specimens of gypsum and limestone, with the gypsum crust directly overlying the limestone. The premise of Egemeier's paired-specimen analysis was this: if gypsum formed as a direct replacement of limestone, then it should show chemical similarities to the limestone in the metal ions of calcium, magnesium, sodium, potassium, and iron. Since the sulfate minerals of these metal ions are more soluble than the carbonate minerals, then the gypsum should possess an equal amount or less of these cations than the limestone, depending on the amount of leaching the gypsum has experienced. Egemeier used strontium as a basis for comparison of leaching, because it forms the least-soluble sulfate.

Whole-rock analyses were performed on limestone-gypsum pairs in the hope of defending or rejecting a replacement-solution model of speleogenesis for Guadalupe caves (Table 26). Four separate locations were chosen for sampling on the basis of their being in different limestone facies: (1) the Big Room, Carlsbad Cavern (Capitan Limestone); (2) the Big Room, Carlsbad Cavern (Bell Canyon Formation(?), Bottomless Pit); (3) lower Gypsum Passage, Cottonwood Cave (Seven Rivers Formation); and (4) Sand Cave, Mc-Kittrick Hill (Yates Formation). Inasmuch as gypsum in Guadalupe caves usually forms as floor blocks rather than as thin wall crusts (as is the case in the Big Horn Basin caves), gypsum blocks were sampled as close to the lime-stone bedrock as possible (within one meter).

My analyses for paired gypsum-limestone specimens do not match Egemeier's results. In Egemeier's study, the different cation ratios of Mg/Sr, K/Sr, Ca/Sr, Fe/Sr, and Na/Sr are always equal or higher for limestone than for gypsum in a pair. No such systematic correlation could be found in the gypsum-limestone pairs of Guadalupe caves; for all the cations except magnesium, the cation to strontium ratio was mixed (Fig. 79). In 11 samples, cation ratios for the limestone were higher than the gypsum ratios; in nine samples they were lower.

The whole-rock analyses of Table 26 are also beneficial when comparing the cave gypsum with the gypsum and anhydrite of the Castile and Salado Formations in the Gypsum Plain. The chemical composition of these deposits is very different, especially in strontium, magnesium, sodium, and chloride.

Sulfate content of limestone

A 20 cm deep hole was drilled in the Capitan Limestone (reef facies) near the Salt Flats of the Big Room, Carlsbad Cavern, in order to ascertain whether gypsum had replaced limestone with depth in the wallrock. The core was drilled 1.2 m above the floor and about 1 m away from a gypsum block that abuts against the cave wall. The drilling method was the same as used by Hill (1981c).

The results of the drill-core analyses are shown in Fig. 80. Maximum values of sulfate are about 0.1%; they are highest at the bedrock surface in the first 2.5 cm, decrease for the next 7.5 cm, and then stabilize at about 0.008% sulfate for the remaining 10 cm. This trend compares with that for nitrate in bedrock, Natural Entrance, Carlsbad Cavern (6 ppm for the first 2.5 cm, 1-2 ppm for the next 10 cm, and then stabilizing at about 0.5 ppm; Hill, 1981c). Hand specimens of limestone collected in the Capitan Limestone

TABLE 26-Whole-rock analyses (done by J. Husler, Chemistry Laboratory, Geology Department, University of New Mexico; those denoted by asterisk are by K. Emmanuel, University of New Mexico, and J. Bologna, Los Alamos National Laboratory).

	Laminated anhydrite, Salado Fm. Moore (1960b)	Castile anhydrite, avg. 60 anal. Dean (1967)	Castile anhydrite, R. Anderson's sample	Gypsum block, Big Room, Carlsbad Cavern	Capitan Ls., Big Room, Carlsbad Cavern	Gypsum block, Bottomless Pit, Carlsbad Cavern	Bell Canyon(?) Fm., Bottomless Pit, Carlsbad Cavern	Gypsum block, Gypsum Passage, Cottonwood Cave	Seven Rivers Fm., Gypsum Passage, Cottonwood Cave	Gypsum block, Sand Cave McKittrick Hill	Yates Fm., Sand Cave McKittrick Hill	Avg. of 345 limestones Pettijohn (1957)
Major Elements (wt%)												
SiO_2	0.190	—	—	0.18	0.39	0.10	2.80	0.06	2.07	0.12	0.08	5.19
TiO_2	0.002	—	—	<0.05	<0.02	<0.02	<0.02	<0.02	0.040	0.054	<0.02	0.06
Al_2O_3	0.018	—	—	0.08	<0.01	<0.01	0.16	0.04	0.90	0.12	0.03	0.81
Fe_2O_3	0.012	—	0.9	<0.05	<0.02	<0.02	0.04	<0.002	0.168	0.117	0.03	0.54
FeO	0.011	—		—	<0.01	<0.01	<0.01	<0.01	0.11	0.03	<0.01	
MnO	0.001	—	—	<0.005	0.008	<0.001	0.034	<0.001	0.01	0.001	0.01	0.05
MgO	9.800	1.822	28.7	0.028	0.60	0.038	2.52	0.22	19.2	0.031	15.8	7.90
CaO	31.384	—	0.15	32.31	55.20	32.40	50.40	32.80	32.0	32.1	37.3	42.61
Na_2O	1.766	0.112	—	0.05	0.165	0.10	0.162	0.088	0.09	0.091	0.19	0.05
K_2O	0.090	0.050	—	0.005	0.002	<0.1	0.009	0.007	0.156	0.011	0.011	0.33
P_2O_5	—	—	—	0.021	<0.01	<0.01	0.078	<0.01	0.018	0.041	0.01	0.04
SrO	0.08	2.403	—	0.006	0.014	0.005	0.058	0.011	0.009	0.007	0.010	—
SO_3, S	7	—	—	46.54	<0.01	46.23	<0.1	45.31	<0.1	45.85	<0.1	0.05
H_2O^+, CO_2	2.82	—	—	1.46	43.40	1.92	41.68	3.41	45.10	2.53	45.88	5.14
H_2O^-	0.063			19.30	0.14	19.17	0.73	17.90	0.08	18.65	0.27	0.21
Trace elements (ppm)												
Au	—	—	12	—	—	—	—	—	—	—	—	—
Br^{82*}	<20	—	<0.1	0.6	—	—	—	—	—	—	—	—
Cl	20,500	—	—	—	—	4.6	—	—	—	—	—	—
Co	—	—	4	—	—	—	—	—	—	—	—	—
La^{140*}	—	—	1	0.6	—	—	—	—	—	—	—	—
Np^{239*}	—	—	—	0.3	—	—	—	—	—	—	—	—
Se	—	—	0.37	—	—	—	—	—	—	—	—	—
Sm^{239*}	—	—	0.63	0.1	—	—	—	—	—	—	—	—
U	—	—	0.8	—	—	—	—	—	—	—	—	—
W	—	—	9.3	—	—	—	—	—	—	—	—	—
Total	—	—	—	99.98	99.92	99.86	98.67	99.85	99.95	99.75	99.62	100.9

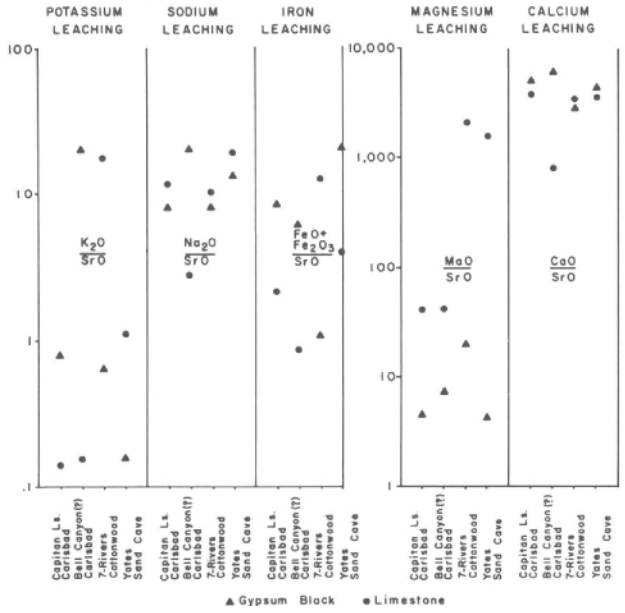

FIGURE 79-Paired specimens of limestone and gypsum collected from the Capitan Limestone and Bell Canyon(?) Formation, Big Room, Carlsbad Cavern; the Seven Rivers Formation, Cottonwood Cave; and the Yates Formation, Sand Cave.

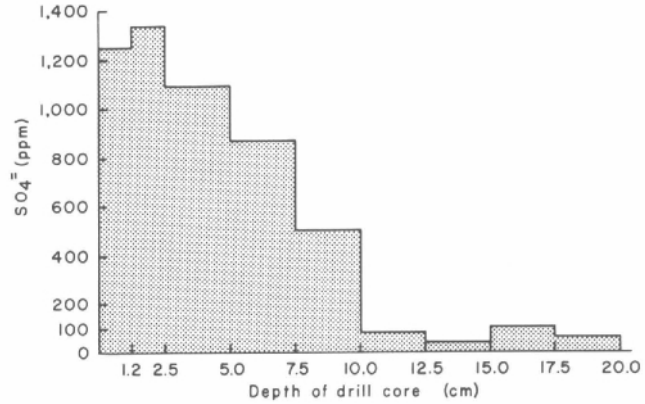

FIGURE 80-Sulfate content in a bedrock core, Big Room, Carlsbad Cavern.

and Bell Canyon Formation(?), Big Room, Carlsbad Cavern, and those collected in the Seven Rivers Formation, Cottonwood Cave, and in the Yates Formation, Sand Cave, also contain less than 0.1% sulfate (Table 26).

Insoluble residue in limestone

Limestone samples from Carlsbad Cavern were analyzed for their insoluble-residue content. The limestone was dissolved in 50% hydrochloric acid and the insoluble residue filtered out, weighed, and described. The samples yielded between 0.1 and 99.3% insoluble residue, with the highest residue content in the limestone of the Bell Canyon(?) Formation in the New Mexico Room (Table 27).

Color, grain size, and the amount of insoluble residue vary within a particular limestone facies, as shown by the samples collected at different locations along Lower Cave.

The insoluble residue in the Bell Canyon(?) facies in the New Mexico Room and at Bottomless Pit, Big Room, was quite different from residue in the reef-forereef limestone collected in Lower Cave. The residue in bedrock at these localities exactly matches (in color, grain size, and included black magnetite?) the white to cream-colored, fine-grained silt on the floor (compare the description of the Bottomless Pit and New Mexico Room silt in Table 10 with that of the insoluble residue in bedrock at the same locations in Table 27). Insoluble residue derived from Lower Cave limestone is orange to tan, which agrees with the description of silt on the floor (again, compare Tables 10 and 27).

Sulfuric-acid experiment on limestone

Two small-scale laboratory experiments were performed in order to show the reaction of sulfuric acid on limestone. First, finely powdered calcium carbonate was combined with 0.05 M sulfuric acid and stirred vigorously; after 24 hours, fluffy white gypsum precipitated to the bottom of the beaker, with a thinner layer of gypsum coating the lower sides of the beaker and also the stirring rod. This simple experiment mimicked one feature seen in Guadalupe caves: the gypsum thinning from the bottom upward along the sides of the beaker is visually analogous to gypsum floor blocks grading into gypsum rinds along cave walls (Fig. 48).

TABLE 27-Insoluble residue in bedrock, Carlsbad Cavern.

Location	Formation	Description of residue	Insoluble residue (%)
Bat Cave (near entrance)	Tansill	Not described (Hill, 1972)	1.6
Auditorium	Yates(?)	Not described (Hill, 1972)	1.7
Main Corridor	Capitan (reef)	Not described (Hill, 1972)	0.9
Big Room, Bottomless Pit	Bell Canyon(?)	Cream-colored, fine-grained; black specks (magnetite?)	11.7
Lower Cave, Green Clay Room	Capitan (reef)	Grayish brown, fine-grained; some quartz grains (~0.05 mm)	1.3
Lower Cave, Junction Room	Capitan (reef)	Medium-brown, fine-grained silt	0.1
Lower Cave, near entrance to Rookery	Capitan (reef? or reef talus?)	Light tan residue; solution of acid was quite orange	4.5
Lower Cave, beneath Talcum Passage	Capitan (reef)	Light tan; solution of acid was quite orange	1.2
Lower Cave, near the entrance to the Cable Slot	Capitan (reef)	Light tan; solution of acid was quite orange; some gypsum from secondary veins or crust	2.0
New Mexico Room, near descent to East Annex	Bell Canyon(?)	Clean, white to light tan, fine-grained	99.3
New Mexico Room, 5 m from descent to East Annex	Bell Canyon(?) or Seven Rivers(?)	Very light orange, fine-grained	36.1

Next, a more elaborate experiment was conducted using a small piece of Tansill limestone (Fig. 81). A 0.01 M sulfuric-acid solution was added to a large beaker containing the limestone piece, and the solution was slowly agitated on a magnetic stirring plate. After one week the reaction stopped due to an inert layer which had developed over the lime-stone surface. Fresh acid was then periodically added to the solution to keep the limestone constantly dissolving. This was continued over a period of a few weeks and then the solution was allowed to come to rest. The insoluble residue released from the acid reaction with limestone immediately settled out of suspension and sank to the bottom of the beaker. A scum on the surface of the solution was collected and found to contain tiny pieces of chert. Precipitation of the gypsum did not occur until several months later when evaporation concentrated the solution and caused the gypsum to precipitate as a white coating over the top parts of the limestone piece and over the top of a small beaker placed inside the large beaker (Fig. 81). The gypsum precipitate was examined and found to contain small (0.2 mm or less) detrital pieces of chert.

Many parallels exist between this experiment and what can be seen in Guadalupe caves. The insoluble residue sank first to the bottom of the beaker and then relatively pure gypsum precipitated out on top of the silt and limestone. This is exactly the relationship seen between the gypsum and silt in Guadalupe caves. The silt always underlies the gypsum and the gypsum is relatively pure, containing al-most no detritus except for tiny pieces of chert (Table 15).

Water analyses

Analyses of pool and drip water in Carlsbad Cavern have been performed by Boyer (1964), L. Gonzales (unpubl. data 1986), and Hill (this study) (Table 28). A Schoeller-Berkaloff diagram was prepared from these data so that the chemical character of different cave waters could be readily compared (Fig. 82). "Normal" pool and drip water, as described in Fig. 82, are actual samples of water which most closely match the average of 40 samples of pool and drip water analyzed by L. Gonzales.

The chemical signature of water in Carlsbad Cavern is essentially the same for drip and pool water, with the exception of pool water which has been contaminated by bat guano [curves (3) and (7), Fig. 82]. Bat guano in Carlsbad

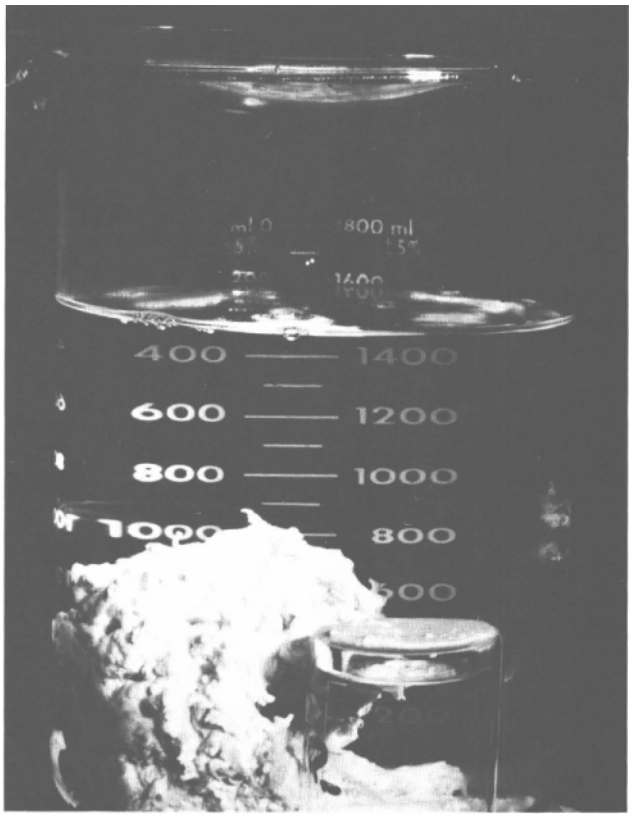

FIGURE 81-Experiment showing a piece of limestone dissolved in sulfuric acid with gypsum formed as a by-product of the reaction. The gypsum precipitated on top of the limestone and also on top of the small glass beaker inside the larger beaker, showing that replacement of limestone by gypsum was not involved in the reaction.

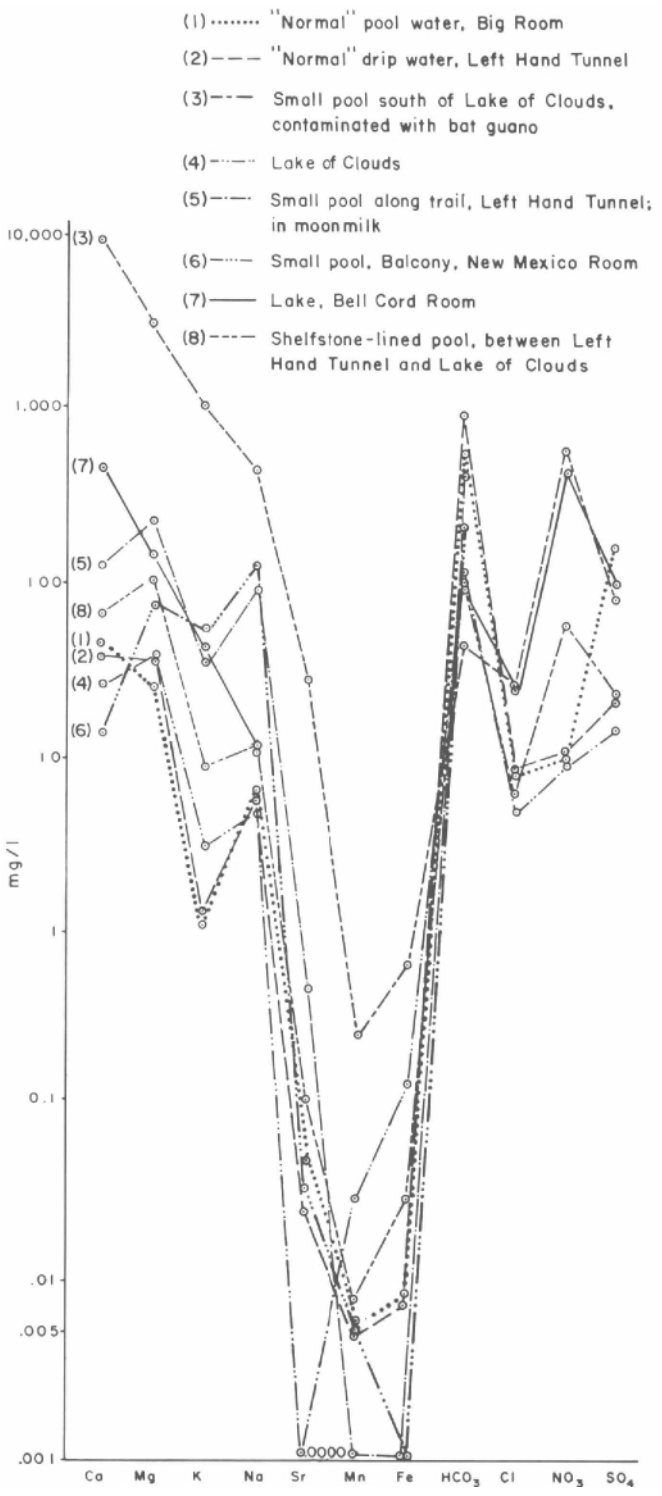

FIGURE 82-Schoeller-Berkaloff diagram of drip and pool water, Carlsbad Cavern.

TABLE 28-Geochemical character of vadose water in Carlsbad Cavern.

		Boyer (1964), mg/l		L. González (unpubl. data 1985), mg/l		This study, mg/l
		Drip water, 37 samples	Pool water, 30 samples	Drip water, 17 samples	Pool water, 22 samples	Pool water, 7 samples
Ca^{++}	range	23.20–66.80	16.40–495.60	17.5705–81.3709	13.6860–9521.6555	—
	mean	39.20	82.80	47.5758	496.4934	—
Mg^{++}	range	11.91–55.16	21.63–211.90	2.2301–64.6130	2.4643–3650.9699	—
	mean	29.89	52.49	31.3651	351.6024	—
K^{+}	range	0.39–6.65	0.78–46.53	0.3922–4.4036	0.4070–1002.9686	—
	mean	1.56	15.64	1.3550	95.5815	—
Na^{+}	range	3.45–9.43	4.83–11.96	1.2495–24.4631	1.3686–1930.3253	—
	mean	5.52	8.05	4.6450	123.4030	—
Sr^{++}	range	—	—	0.0000–0.5669	0.000–29.7908	—
	mean	—	—	0.0612	1.5119	—
Mn^{++}	range	—	—	0.0000–0.0096	0.0000–0.2667	—
	mean	—	—	0.0039	0.0224	—
Fe^{++}	range	—	—	0.000–0.0271	0.0000–0.6972	—
Fe^{+++}	mean	—	—	0.0106	0.0524	—
SO_4^{-}	range	0.00–38.4	00.00–122.88	—	—	10.5–175.0
	mean	14.4	57.84	—	—	63.8
Cl^{-}	range	0.00–194.27	0.71–188.59	—	—	5.05–27.9
	mean	9.57	14.52	—	—	13.6
NO_3^{-}	range	—	—	—	—	9.4–580.0
	mean	—	—	—	—	165.1
HCO_3^{-}	range	204.96–649.04	112.24–912.56	91.10–370.37	46.30–537.59	—
	mean	340.38	315.37	215.93	187.87	—
pH	range	7.30–8.96	7.30–8.57	7.00–8.38	7.31–8.49	—
	mean	7.85	7.87	7.89	8.00	—

Cavern is known to contain nitrate and potassium (Table 20), and bat guano from other caves is known to contain sodium, chloride, magnesium, calcium, and sulfate (Hutchinson, 1950). Thus, bat-guano contamination can account for the relatively high concentrations of these ions in some pool-water samples.

A high Mg/Ca ratio in pool water probably indicates that the pool has undergone a significant amount of evaporation. For example, the pool along Left Hand Tunnel [curve (5)] has probably experienced more evaporation than the pool in the Big Room [curve (1)]. Deep pools such as the Lake of the Clouds [curve (4)] have approximately the same chemical signature as shallow pools, e.g. the ones in Left Hand Tunnel [curve (5)], New Mexico Room [curve (6)], or in the shelfstone-lined pool between Left Hand Tunnel and the Lake of the Clouds [curve (8)], signifying that the water for both came from the same source [dripping water, curve (2)]. However, the absolute amount of cations in solution is much higher in the shallow pools than in the deeper pool due to evaporation.

Discussion of deposits and events

The sequence of events in Guadalupe caves is based on the stratigraphic relationships of cave deposits, on the dating results, and on the carbon-oxygen-isotope paleoenvironmental data. The proposed sequence of deposits and events (numbered 1 through 19) is presented in graphic form in Fig. 83 and in tabular form in Table 29.

Because the development of Guadalupe caves was both multi-level and multi-sequential, each numbered deposit/ event represents the optimum time for the occurrence of that deposit/event. Some events overlap in time (e.g. Solution Stage III cave development and the formation of the endellite) and others occurred continuously over an extended period of time (e.g. speleothems have formed since the caves became air-filled till the present). Or, a deposit could have formed at a lower level (e.g. spar), while at the same time another deposit could have formed at a higher level (e.g. the cave rafts of the siltstone-raft sequence).

Permian deposits and events

Deposition of bedrock

The relatively pure limestone of the reef facies and the less pure dolomites of the backreef and forereef facies were laid down and diagenetically altered in Guadalupian time, a compositional arrangement which would later confine cave development mainly to the residue-free, calcitic reef core. The forereef inclined away from the reef at approximately 20-30°, a depositional slope which may have later defined the slope of some Guadalupe cave passages (e.g. the Main Corridor, Guadalupe Room, Mystery Room, and Lake of the Clouds Passage, Carlsbad Cavern, all of which descend at angles of 20-30°). The backreef facies dipped gently (a few degrees) towards the reef, and this slope was later accentuated by post-Permian uplift and was responsible for directing cave-forming ground water into the limestone-reef core.

In Guadalupian time, the reef was probably emergent during periodic drops in sea level. The fresh-water, carbon-oxygen signature of Spar I occurring with marine-cement intergrowths is thought to represent successive episodes of a single diagenetic event during this time (Given and Lohmann, 1986; Fig. 73).

Solution Stage I

The earliest caves are small, often fissure-like cavities filled with breccia. They are located exclusively at or near the

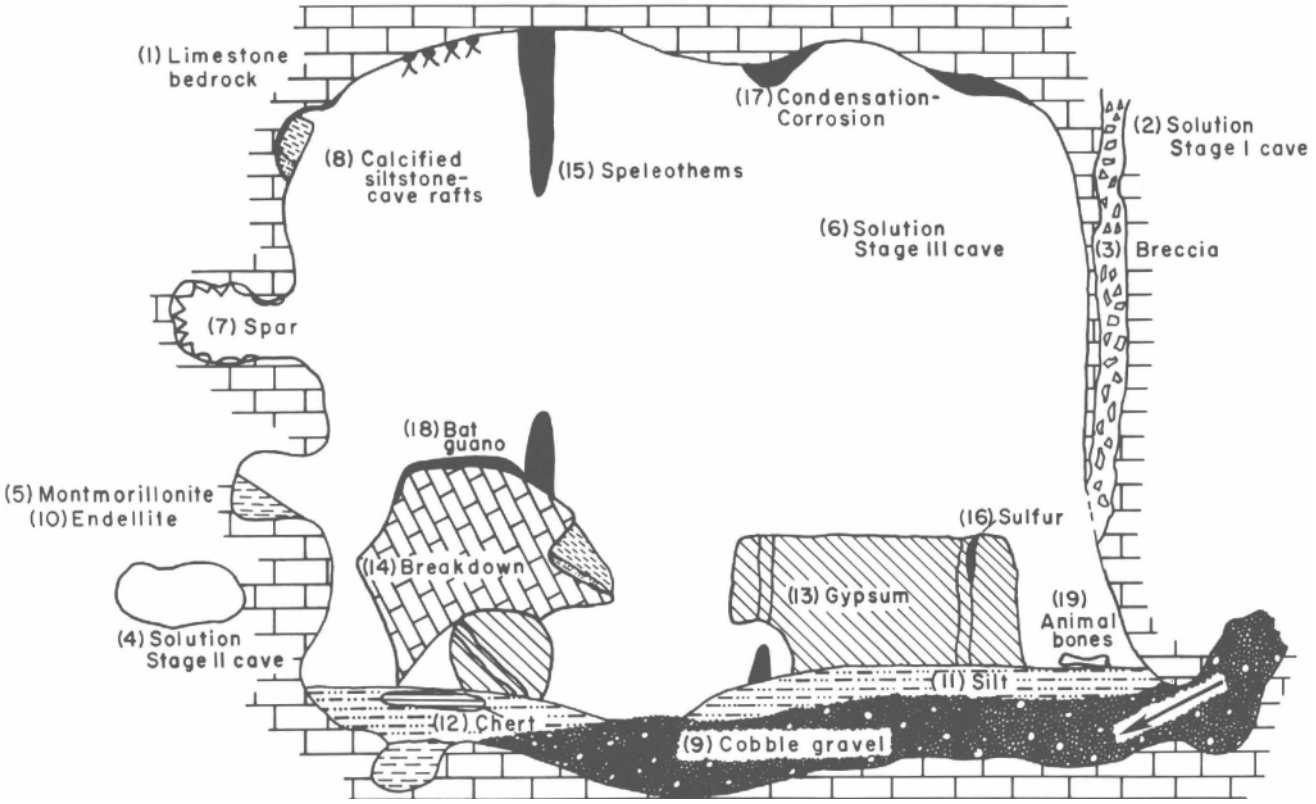

FIGURE 83-Sequence of geologic events in Carlsbad Cavern.

TABLE 29-Sequence of geologic events in Carlsbad Cavern.

Time	Episode or event		Remarks
Permian	Reef limestone	(1)	Barrier reef forms around Delaware Basin; reef, forereef, and backreef units deposit; Spar I intergrowths.
	Solution Stage I fissure caves	(2)	Tectonic and solutional enlargement along reef-backreef contact.
	Breccia	(3)	Breccia fills Solution Stage I caves, with Spar II matrix between breccia clasts; Type 1 sandstone dike fillings.
Permian-Tertiary	Solution Stage II spongework caves	(4)	Episodes of regional uplift; carbonic-acid dissolution along primary pores, joints, and Solution Stage I caves to form spongework.
	Montmorillonite clay	(5)	Residue from Solution Stage II dissolution fills Solution Stage II spongework caves. Montmorillonite reconstitutes from residue under basic, carbonate-rich conditions. Time: 188±7 my.
Pliocene-Pleistocene	Solution Stage III large caves	(6)	Uplift and tilting of Guadalupe Mountains and Delaware Basin; H_2S and CO_2 migration from oil and gas fields in the basin into the reef. Sulfuric-acid dissolution of large cave passages.
	Spar	(7)	Spar III deposits in saturated, shallow phreatic zone just below the water table. Time: 879,000 ± 124,000 ybp at Big Room level.
	Calcified siltstone-cave rafts	(8)	Rafts deposit at surface of water table at beginning of Solution Stage III event. Time: >350,000 ybp.
	Cobble gravel	(9)	Ogallala (or Gatuña?) gravel slumps into Solution Stage III bathyphreatic cave passages. Type 2 dikes.
	Endellite	(10)	Montmorillonite clay partly changes to endellite under sulfuric-acid conditions.
	Silt	(11)	Autochthonous residue from Solution Stage III dissolution of limestone. Time: >730,000 ybp at Lower Cave level.
	Chert	(12)	Colloidal precipitation of chert as a result of montmorillonite-endellite reaction under acidic conditions; color banding of silt.
	Gypsum	(13)	Precipitation of gypsum as a by-product of sulfuric-acid dissolution of Solution Stage III caves, with some replacement of limestone by gypsum.
	Breakdown	(14)	Most breakdown falls just subsequent to lowering of the water table.
	Speleothems	(15)	Speleothems decorate caves as soon as the caves become air-filled. Time: from 600,000 ± 200,000 ybp in Lower Cave and 513,000 ± 10,300 ybp in Main Corridor by Iceberg Rock, to the present.
	Sulfur	(16)	Late-stage degassing of H2S in air-filled cave; hydrogen-sulfide oxidized to sulfur.
	Condensation-corrosion	(17)	Late-stage degassing of CO, causes corrosion of bedrock and speleothems. Time: <150,000 ybp in Bell Cord Room-Lake of the Clouds area.
	Bat guano	(18)	Bats enter caves as soon as entrances are open. Time: >32,000 ybp in New Cave, Carlsbad Caverns National Park.
	Animal bones	(19)	Animals enter caves sometime after entrances are open. Time: ~112,000 ybp in Lower Devil's Den.

contact of reef-backreef sediments (Fig. 30), suggesting formation in response to a lithologic zone of instability between the Capitan reef core and the backreef shelf members of the Artesia Group, perhaps when the shelf facies lithified, compacted, and pulled away from the reef core.

Rarely, individual clasts of mudstone and limestone can be seen exposed in the caves, not as cavity fillings but incorporated into the limestone itself as if they had settled in place before, or contemporaneously with, the solidification of the bedrock. For this reason nearby Solution Stage I cavities filled with similar breccia clasts are believed to date from a very early age-probably from the Late Permian, very soon after the limestone itself had deposited and solidified. Epeirogenic uplift later in the Permian caused the entire region to tilt and rise slightly above sea level; this uplift caused the first flushing of the Capitan Limestone. Fissures which developed along the zone of weakness between reef and backreef sediments thus became the first avenues for water movement and solutional enlargement, and were to influence the position of later cave development from the Permian to the present.

Origin of breccia

Solution Stage I cavities are filled with breccia cemented in a mudstone or calcite-spar matrix. The breccia fragments are angular and many of them appear to have been sheared in place (Fig. 67), suggesting origin at, or close to, the fissures they occupy. The fine-grained mudstone matrix also seems to have been derived locally, as it is composed of the same, although finer-grained, material as the larger breccia clasts (Queen, 1981). The breccia strongly resembles the dolomite breccia fades of Achauer (1969), a local facies found at or near the contact between reef and backreef beds (compare Pl. 1A with Achauer's fig. 10). Achauer, and also Queen (1981), ascribed the fissure-filling breccia clasts to tectonic movement or to solutional collapse just subsequent to the deposition of the limestone. Tectonic activity associated with the uplift and tilting of the reef in the Late Permian may have brecciated the limestone along fissure zones at the shelf-reef margin. As the fissures enlarged by either tectonic or solutional processes, the breccia clasts gravitated downward and filled the voids. The Type 1 sandstone dikes of probable Permian age may have also formed in response to this tectonic, fissure-filling event.

In Virgin Cave, in the Spar Room of the Secondary Stream Passage, Carlsbad Cavern, and in some breccia exposures in the Guadalupe Room, Carlsbad Cavern, a crystalline spar matrix (Spar II) fills the space between breccia clasts. According to Given and Lohmann (1986), Spar II represents a fresh-water deposit related to a presumed Ochoan (or younger) regional meteoric or shallow-phreatic burial system (Fig. 73). This fresh-water, shallow-burial origin fits with Achauer's and Queen's models of tectonic activity and uplift in the Late Permian. It also fits with the temperature of deposition for Spar II (e.g. 55.4°C), as calculated from the fluid-inclusion data.

Permian-Tertiary deposits and events

Solution Stage II

The second episode of cave development involved the enlargement of primary pores and joints in the massive Capitan Limestone into a three-dimensional maze of spongework. Solution Stage II caves are small, randomly orientated, and many of them are partly filled with either large spar crystals or colorful montmorillonite-endellite clay.

In the earliest stages of development of a cave system, there is a complex, three-dimensional array of pores and unsolutioned joints of minimal cross-sectional area in the rock. The pores and joints are not necessarily integrated, so that flow under these "pre-cave" conditions is diffuse, with phreatic water under pressure creating a spongework array of passages. As solution continues over time, this array expands, and there is a progressive integration of cave passages and enlargement of small portions of the array to create a cave system that eventually becomes continuous from input to output (Ford and Ewers, 1978). Solution Stage II caves represent such a development in the Guadalupe Mountains. They dissolved under conditions of complete waterfill and are phreatic passages created by slow-flow, diffuse circulation of aquifer water.

Solution Stage II caves in the Guadalupe Mountains may have had an origin similar to those now forming in the San Andres Limestone aquifer of the Roswell, New Mexico, area. The San Andres Formation, a cavernous limestone full of holes and fissures, was described by Fiedler and Nye (1933) as possessing two types of solutional cavities: (1) solution channels along joints, bedding planes, and fractures, and (2) enlargement of primary pores so as to produce a honeycombed, "worm-eaten" network of interconnected passages. In the Roswell Basin, spongework cavities have been found down to a depth of 297 m below the surface (Lee, 1924b).

Solution Stage II caves were most likely dissolved exclusively by carbonic acid, as is typical of most cave systems, and not by sulfuric acid as has been proposed for the large (Solution Stage III) cave passages in the Guadalupe Mountains. Firstly, Solution Stage II caves are not large, as might be expected from rapid dissolution by sulfuric acid. Secondly, gypsum deposits are rarely associated with spongework except where these cavities have been noticeably enlarged by Solution Stage III acids into boneyard. And thirdly, Solution Stage II spongework is sometimes filled with grayish-green montmorillonite clay, a mineral derived from limestone residue which characteristically forms under a high pH (basic) rather than low pH (acidic) conditions.

The age of Solution Stage II caves is debatable. They predate the Solution Stage III episode because: (1) they and the deposits filling them (montmorillonite and spar) are truncated by the large caves; (2) the spar filling Solution Stage II caves has been etched, pitted, and dissolved with respect to its position relative to the large passages; and (3) the spar at the Big Room level dates from 879,000±124,000 yrs, which means that the Solution Stage II cavities (which the spar fills) must be older. There is evidence to suggest that at least some Solution Stage II cavities may be Late Permian in age. A few dogtooth spar crystals filling Solution Stage II cavities (e.g. sample 1, Fig. 73) display carbon-oxygen-isotope signatures characteristic of Spar II. Since Spar II is believed to be Ochoan (or younger) in age (Given and Lohmann, 1986), the Solution Stage II cavities which the spar fills may be as old as Late Permian.

Solution Stage II spongework cavities may have dissolved in one episode, or, more likely, they dissolved in a number of minor episodes during limestone mesogenesis. Bachman (1980) proposed that pre-Cenozoic times of non-deposition in the basin (mainly in the Jurassic) must have been times of extensive erosion and subsurface dissolution through circulation of meteoric water; the 188 my Jurassic K-Ar date on the montmorillonite clay (which fills a Solution Stage II cavity) supports this idea. According to K. Given (pers. comm. 1986), spar material in the Guadalupe Mountains can display luminescent Spar II centers, but be surrounded by non-luminescent overgrowths of later (Spar III?) material of different isotopic composition. Thus, it appears that Solution Stage II cavities, and the spar filling those cavities, may have a history of continued development extending from the Late Permian to the Tertiary.

Origin of montmorillonite clay

Montmorillonite clay fills spongework (Solution Stage II) cavities. In Carlsbad Cavern this clay is found most abun-

dantly in the lower sections, such as in Lower Cave and the Scenic Rooms. Bjorklund and Motts (1959) reported deep caverns filled with red silt in test wells of the Carlsbad region and speculated that this silt had percolated down from above through open conduits in the limestone. White and White (1968) theorized that horizontal movement of silt through small openings in the limestone is minor because flow velocities are too low to exceed the threshold of transport. Lower paths of water movement are especially prone to low-velocity flow and, therefore, deeper paths tend to fill with silt, a pattern further enhanced by normal gravity settling.

Montmorillonite is a common weathering product of limestone, forming very slowly from limestone residue by the mixing of dilute solutions or colloidal suspensions of aluminosilicates at pH's in the range of 8-9 (Krauskopf, 1967). Four conditions seem to favor the formation of montmorillonite: (1) a basic (high pH) environment, (2) very slow-flow rates, (3) a long period of time for reconstitution, and (4) a relatively high HCO_3^- concentration (>100 ppm) (Berner, 1971). Under slow-flow conditions, a reaction of cations with $Al(OH)_3$ and silica can take place, resulting in the formation of montmorillonite.

The potassium-argon date of 188±7 my for the montmorillonite clay is highly speculative; nevertheless, it still indicates that the clay has a high radiogenic-argon content and suggests that the deposit is very old. Montmorillonite is a mineral which takes a long time to reconstitute from limestone residue. This residue had to have changed to the mineral montmorillonite before the Solution Stage III event, in order for the montmorillonite to change to the mineral endellite during the Solution Stage III event. The montmorillonite could not have formed during the Solution Stage III sulfuric-acid event because of the high pH (basic), carbonate-rich environment required for its formation.

All of these factors suggest that the montmorillonite pre-dates the Solution Stage III episode of cavern dissolution. After the interconnected spongework (Solution Stage II) passages had formed, silt residue released from the dissolution of limestone filtered down through available pathways. The residual silt partially filled interconnected spongework pockets and then remained in a basic bicarbonate environment for a long time, slowly reconstituting into montmorillonite clay.

Pliocene-Pleistocene deposits and events

Solution Stage III

Past theories of speleogenesis have rarely related the caves of the Guadalupe Mountains to regional geology. Davis (1979a) was the first to suggest the possibility of a connection between Guadalupe caves and the oil and gas fields of the Delaware Basin. This study carries the possibility one step further: it attempts to identify the connection and proposes that sulfuric acid derived from oil and gas was responsible for dissolving out the large (Solution Stage III) cave passages.

Sulfur-isotope values of the cave gypsum and sulfur are the primary evidence on which this sulfuric-acid model of speleogenesis is based. Only biologically-produced reduction and oxidation reactions such as have occurred in the basin could have produced the large isotopic fractionations that characterize the cave deposits. Other evidence in the caves for a sulfuric-acid origin is the endellite, a type of clay that is known to form only in an acidic environment.

Relationship of Solution Stage III caves to oil and gas fields in Delaware Basin—The Delaware Basin of south-eastern New Mexico is one of the largest oil and gas producing areas in the world. Characteristic of the natural gas of the region is a high content of hydrogen sulfide and carbon dioxide. Lambert (1978) reported as much as 55% carbon dioxide and 28% hydrogen sulfide from boreholes in the Castile Formation.

When the Guadalupe Mountains uplifted during the Pliocene-Pleistocene, the oil-producing Bell Canyon Formation in the basin was tilted a few degrees to the northeast. A primary consequence of this tilting was the initiation of oil and gas migration updip through interconnecting permeable zones. Graben-boundary faults and joints at or near the base of the Castile Formation allowed hydrocarbons to ascend from the underlying Bell Canyon Formation into overlying Castile anhydrite beds, where they reacted to form hydrogen sulfide, carbon dioxide, and the limestone of the castile buttes (Fig. 84). The following reactions are believed to have produced the hydrogen-sulfide and carbon-dioxide gas in the basin:

$$CaSO_4 + CH_4 = H_2S + CaCO_3 + H_2O \quad (4)$$

$$2H^+ + SO4^{2-} + CH_4 = H_2S + CO_2 + 2H_2O \quad (5)$$

These simple reactions should be regarded only as symbolic of the many biochemically related reactions that could have taken place in the basin with respect to oil and gas. Hydrogen-sulfide gas and sulfur mineralization originating in the castile buttes of the basin are significantly enriched in ^{32}S (Fig. 72); such a pronounced isotopic fractionation of sulfur is known to be caused in nature only by the sulfur bacteria.

Sulfuric acid formed where oxygenated meteoric water mixed with the hydrogen-sulfide gas of the basin (Kirkland and Evans, 1976). The acid immediately reacted with the calcium carbonate of the castiles and dissolved out tubular shafts in the buttes (see the two locations marked "cave" in Fig. 85). Kirkland and Evans (1976), and also Smith (1978a), reported a cylindrical, vertical cavern about 3-4.5 m in di-

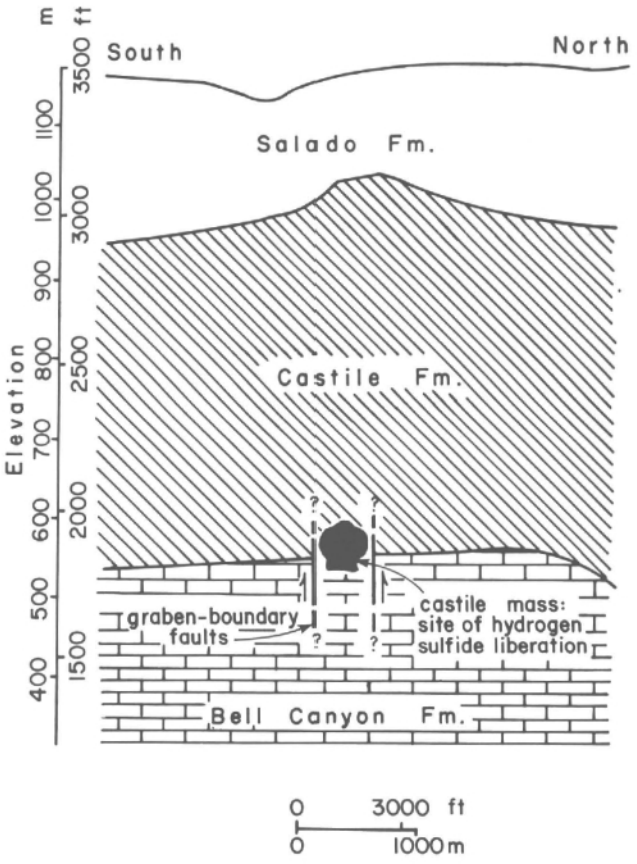

FIGURE 84-Location of the castile buttes underground and in relationship to the Bell Canyon Formation, Gypsum Plain. After Smith (1978a).

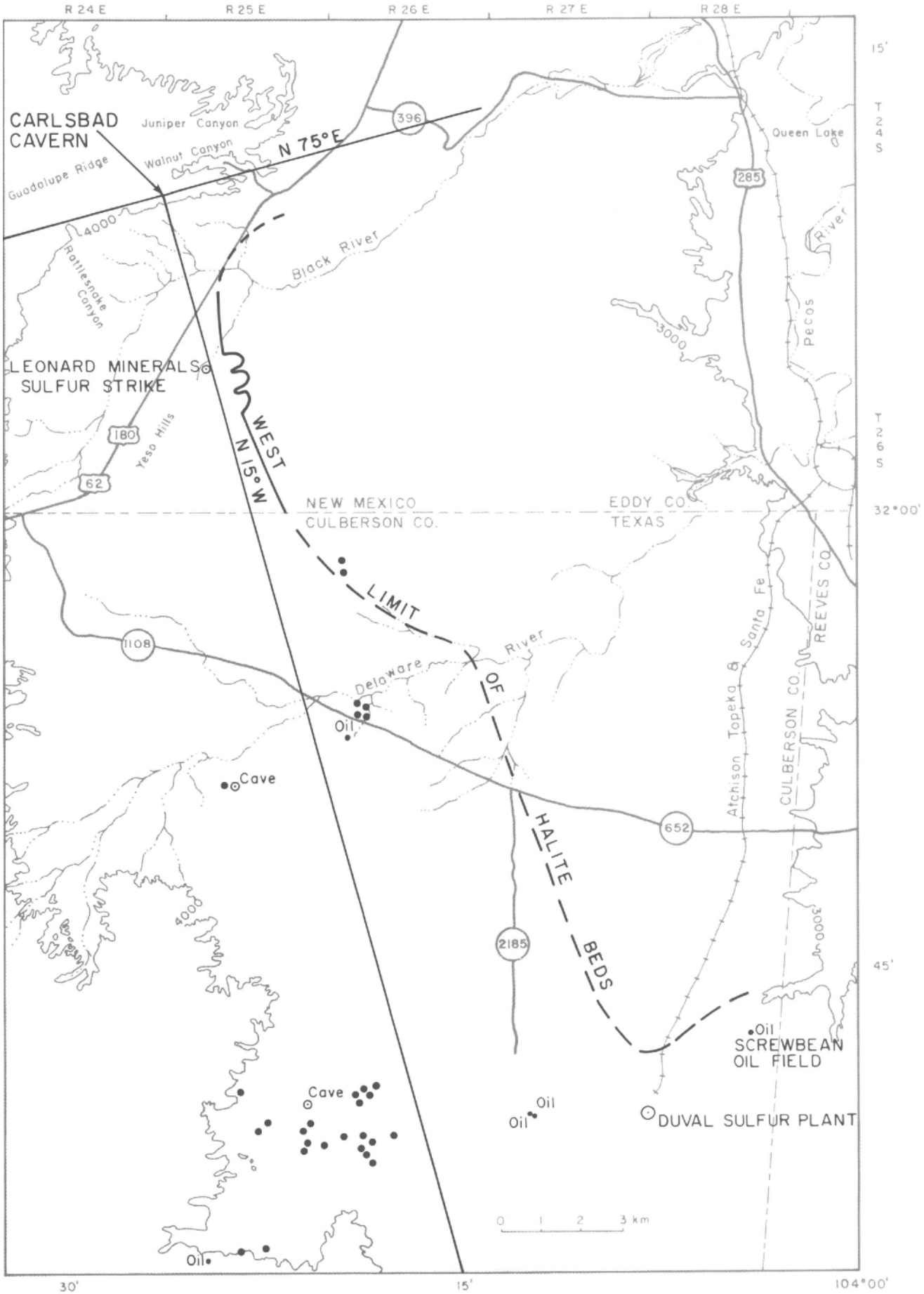

FIGURE 85-Location of Carlsbad Cavern in relation to oil, sulfur, and the castile buttes (circular black dots) of the Gypsum Plain. The straight line is an extension of the trend of the Big Room (N15°W). Dashed and solid line is the west margin of Halite I beds. Caves in the Gypsum Plain are tubular and have degassing H_2S and native sulfur.

ameter and about 30 m deep in one castile butte, which is lined with a 10 cm thick layer of crystalline sulfur and has hydrogen-sulfide gas still issuing from it. The crystalline sulfur formed in cavernous parts of the buttes wherever hydrogen sulfide mixed with oxygen.

Hydrogen-sulfide and carbon-dioxide gas rose to the surface in the basin only where the rock was not capped by impermeable halite or clay beds. Halite is among the least permeable of any rock type, plastic flow of the salt closing up any fractures which might develop in the rock (Swenson, 1974). Sulfur exploration companies find H_2S gas below in-tact halite beds in the basin, but no native sulfur; they find sulfur only along the western erosion edge of Halite I beds where hydrogen sulfide has been oxidized (Fig. 85). Native sulfur is not found far west of the Halite I erosion edge because where ground water has had access to the sub-surface over a long period of time, the sulfur has oxidized to sulfuric acid and sulfate; all that is left of past sulfur zones are blanket-solution breccias with textures that suggest the former presence of sulfur.

It is proposed that the progressive eastward migration of the halite dissolution margin over time could have been a factor controlling the position of cave development in the adjacent reef (Fig. 86). Where H_2S gas moved updip to the western erosion edge of the halite beds, it was oxidized to native sulfur. But where it was trapped below the halite, it sought other avenues of escape out of the system. Northwest-trending joints could have been avenues of gas ascent for such caves as Cottonwood and Hell Below in Black and Gunsight Canyons as demonstrated by the northwest clustering of the caves in these canyons (Fig. 5). Extrapolated into the basin, the N15°W trend of the Big Room, Carlsbad Cavern, passes near a dense concentration of exposed castile buttes (some with sulfuric-acid-derived caves), oil deposits, sulfur deposits, and the western limit of the Halite I beds (Fig. 85). Another avenue along which gas could have travelled from the basin into the reef was along interfingerings of the Bell Canyon Formation (Fig. 87). This scenario may especially apply to the Big Room and New Mexico Room of Carlsbad Cavern, where the Bell Canyon Formation is believed to crop out in the cave. One other possible control for cave development in the case of Carlsbad Cavern is the Huapache monocline. The monocline in the basin is located between Rattlesnake Canyon and Carlsbad Cavern (Fig. 12); the basal part of this fold may have been a structural influence on siphoning gas into the reef in the vicinity of Carlsbad Cavern.

It is not at all clear what factors caused the gas to move from basin to reef. Present-day ground-water flow in the alluvial-evaporite aquifer of the basin is approximately perpendicular to the direction of proposed gas flow into the reef (Hiss, 1980). According to Sares (1984), the potentiometric level of the alluvial-evaporite aquifer is nearly 107 m higher than the potentiometric level of the adjacent Capitan reef aquifer so that very little movement of water, if any, occurs today between basin and reef in the vicinity of the Guadalupe Mountains. The migration of fluids from intracratonic basins into surrounding carbonate rocks is a problem which, in general, is poorly understood. Ore deposits are often found along the margins of basins (as Guadalupe caves are found near the margin of the Delaware Basin; Fig. 5), but the source of the ore, and how the metals together with reduced sulfur (as H_2S) move from basins into surrounding carbonate reef rocks, is still very much a matter of debate (Anderson and Macqueen, 1982). However, it is known that such movement does occur, both during basin formation and long afterwards, in response to gradients established by hydrologic, compaction, thermal, relief, or deformation factors.

Episodes of tectonic movement and faulting may have triggered the release of subsurface gas from solution so that

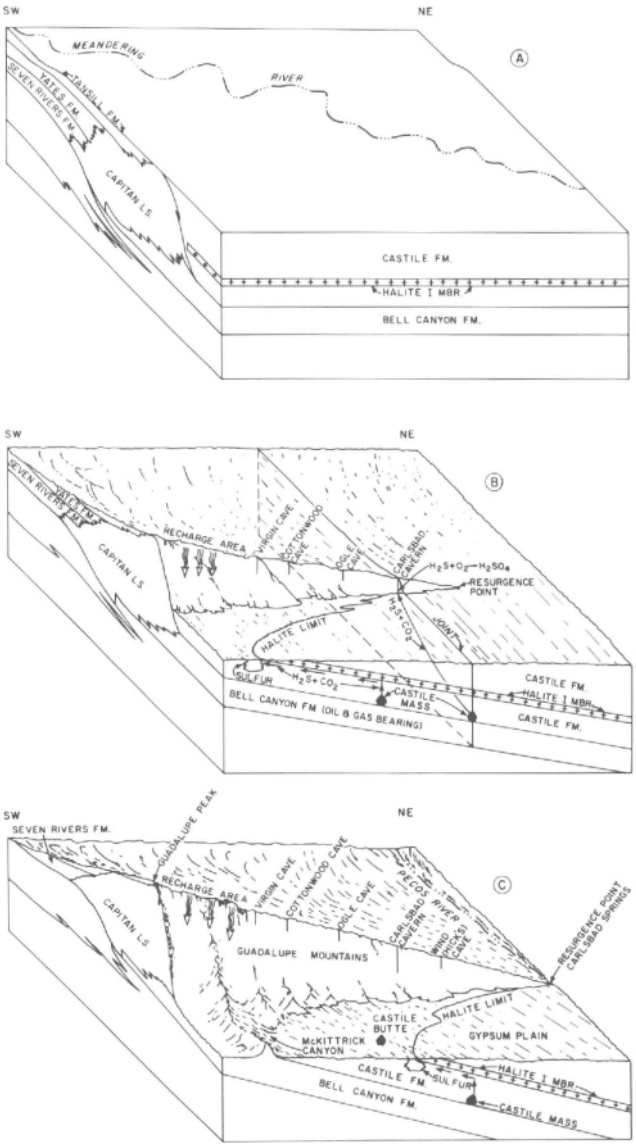

FIGURE 86—Model of Halite I unit in the Castile Formation of the Gypsum Plain in relation to the development of caves in the Guadalupe Mountains. (A) Rivers meandered across a low-lying erosion surface in the Miocene-Pliocene. (B) In the late Pliocene-Pleistocene the Guadalupe Mountains area uplifted and tilted. Oil and gas moved updip in the basin and reacted with the Castile anhydrite to form H_2S, CO_2, and the castile masses underground. Impermeable halite beds trapped the gas in the subsurface so that it either escaped at the western edge of the halite beds or ascended into the reef along joints or interfingerings of the Bell Canyon Formation. As the halite beds in the basin were eroded from west to east, and as spring positions continually shifted from west to east, caves in the Guadalupe Mountains also developed from west to east. As soon as the western limit of the halite beds moved east, past a particular cave location, development of that cave ceased because gas could no longer ascend into the reef at that point. (C) Native sulfur is today found along the western limit of Halite I beds, but never east of this limit below halite beds, or far west of this limit in solution-breccia deposits. H_2S gas is found in the subsurface where halite beds are still intact.

it could begin to migrate from basin to reef. Once released, the gas could have ascended buoyantly into the reef in response to a pressure gradient between the two areas, perhaps by diffusion as microbubbles, as suggested by Ash and Wilson (1985a, b). Local gas migration under a "cap" (the halite beds in the basin) could have been facilitated by avenues which ascended at high angles into the reef (e.g. the Bell Canyon Formation(?), Bottomless Pit, Carlsbad

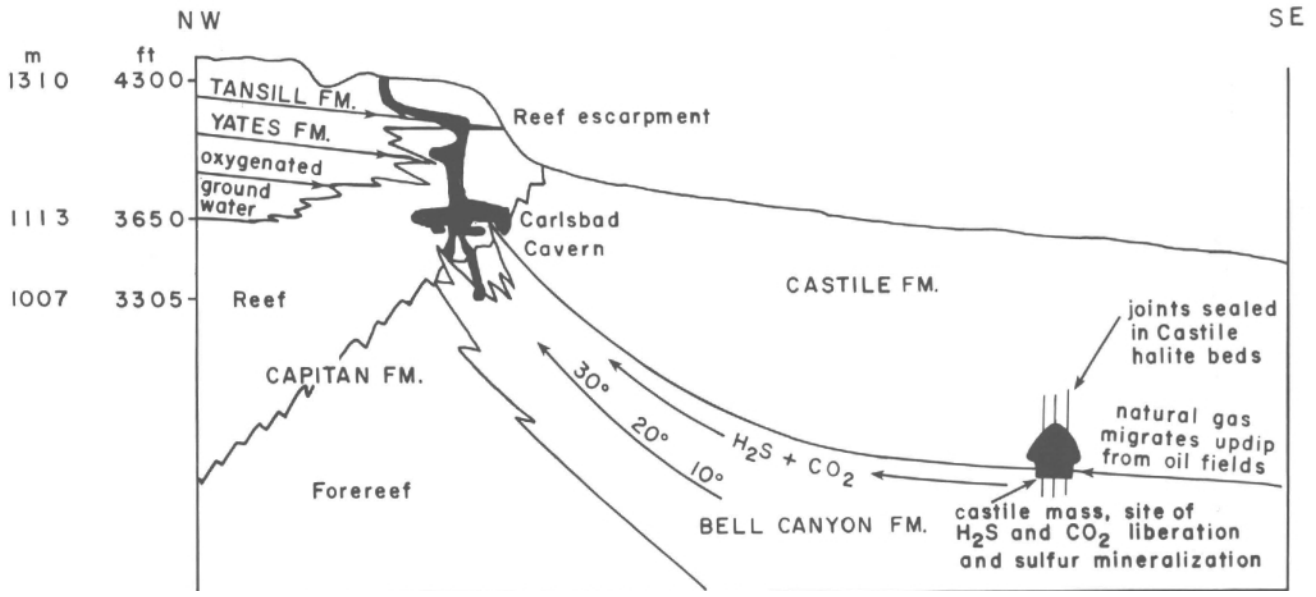

FIGURE 87—Model of gas ascension from the basin into the reef along the Bell Canyon Formation. Natural gas migrated updip from the oil fields to the east and encountered anhydrite at the base of the Castile Formation. Reactions between the gas and the anhydrite produced hydrogen sulfide, carbon dioxide, and the castile limestone masses. The hydrogen sulfide and carbon dioxide continued updip along the Bell Canyon Formation into the Capitan reef, where they mixed with oxygenated ground water moving downdip along backreef beds. The hydrogen sulfide and oxygen combined to form sulfuric acid which dissolved out the large cave passages in the Guadalupe Mountains.

Cavern, dips 20-50º). Water flow may not have been required for the migration of the gas as long as the reservoir rock was water-wet (McAuliffe, 1979).

Sulfuric-acid dissolution of Solution Stage III caves—By whatever avenue and whatever means hydrogen-sulfide gas ascended into the reef, it would have remained in the reduced state until it combined with oxygenated water in the reef. Oxygenated water could have entered the caves as meteoric ground water moving downdip along backreef beds and into the reef (Jagnow, 1979), or it could have entered by diffuse seepage through an overlying land surface deficient in impermeable caprock (Palmer, 1975). Either way, where ascending hydrogen sulfide met with oxygenated water, sulfuric acid was produced.

Two reactions, which may have been aided by bacteria, describe the oxidation of hydrogen sulfide to sulfuric acid:

$$2H_2S_{(aq)} + O_{2(aq)} = 2S_{(s)} + 2H_2O_{(l)} \quad (6)$$

$$2H_2O_{(l)} + 2S_{(s)} + 3O_{2(aq)} = 2HSO_4^-{}_{(aq)} + 2H^+_{(aq)} \quad (7)$$

The sulfuric acid produced by reaction (7) immediately re-acted with the limestone bedrock and carved out the large cave voids:

$$2H^+ + SO_4^{2-} + CaCO_{3(s)} + 2H_2O_{(l)} = CaSO_4 \cdot 2H_2O_{(s)} + H_2O_{(l)} + CO_{2(g)} \quad (8)$$

The carbon dioxide liberated in this reaction, and also carbon dioxide which may have migrated up from the basin along with the hydrogen sulfide, would not have been subject to a chemical reaction which rapidly removed it from the system, and so it would have been more likely to degas at the surface of the water table than the hydrogen sulfide. Any carbonic acid that might have been produced from the CO_2 would have dissolved only a very small amount of limestone compared to that dissolved by the sulfuric acid, since the ionization constant of sulfuric acid is $10^{-1.9}$whereas that of carbonic acid is only $10^{-6.35}$ (Krauskopf, 1967).

From equations (6), (7), and (8) the volume of hydrogen-sulfide gas that produced a cave void the size of the Big Room, Carlsbad Cavern, can be calculated. The volume of the Big Room, as determined by digitizing a map of it on a computer, is roughly 1,343,000 m^3. Assuming that the density of limestone is 2.3 g/cm^3, then 3 x 10^{12} g of limestone must have been removed in order to create the Big Room void, and 6.7 x 10^{11} liters of hydrogen-sulfide gas were needed to dissolve so much limestone. This is about 10 times less gas than the amount of natural gas removed from Eddy County in 1978 (Arnold et al., 1980). Thus, the amount of gas that it took to dissolve the caves of the Guadalupe Mountains is small considering the total amount of gas which has probably been generated in the Delaware Basin over time, and it is not quantitatively unreasonable to assume that the gas came from this source.

Sulfuric-acid dissolution and bathyphreatic cave development—The systematic excavation and integration of cave passages in the Guadalupe Mountains and the evolution of their unique three-dimensional form are the result of bathyphreatic and water-table conditions combined with a sulfuric-acid speleogenesis. Imposed upon the three-dimensional matrix of spongework passages dissolved earlier (i.e. Solution Stage II caves) is a complex of large passageways that descend vertically at steep angles, major horizontal levels containing large rooms, fissures or tubular pits connecting the levels, and boneyard passages underlying and surrounding the large rooms. With the exception of the spongework, all of these types of passages developed during the Solution Stage III episode of sulfuric-acid dissolution. The ideas put forth in the following discussion of bathyphreatic Solution Stage III passages are based on the work of Ford and Ewers (1978), Davis (1979a, 1980), this study, and conversations with D. C. Ford.

The basic pattern of bathyphreatic flow in the Guadalupe Mountains was probably set up before cave development was pronounced (Fig. 14). Flow was guided by joints, bedding planes, joint intercepts, and zones of weakness such as at the reef-backreef and reef-forereef contacts. Cave development was primarily north-south or east-west because water followed major joints that trended either parallel or perpendicular to the reef. High-velocity flow presumably existed when joints were still relatively tight, but with enlargement of the cave passages the velocity decreased. Progressively more water ensued along enlarged paths with

the least resistance to flow, developing trunk passages which carried most or all of the water. Water in these large conduits discharged at major springs, the outlet positions of these springs having been controlled by step-wise lowering of the water table (Fig. 14).

The first spring outlet for Carlsbad Cavern may have been the Natural Entrance (Fig. 88), or what was then the entrance before the Carlsbad Cavern Ridge eroded down to its present position. The Natural Entrance displays a phreatic form to the very top of the entrance lip, a form that was most likely produced by lifting water. As the water table dropped, the Natural Entrance paleospring was abandoned; this shift brought Bat Cave into play as an eastward drain for water and the second natural entrance into play as the next discharge spring. The flow along Bat Cave at that time (as determined by scallop length) was 3-12 m^3/sec (as compared to a 0.4 m^3/sec flow rate for Carlsbad Springs today). Basal water-injection points for both the Natural Entrance spring and the Bat Cave spring probably encompassed practically all of the then-formed cave below the level of Bat Cave, and it is possible that bathyphreatic water could have excavated cave passage all the way from the Bat Cave level down to the Lower Cave level at that time. The Main Corridor was the main line of ascent for lifting water coming up from the Mystery Room, Guadalupe Room, Big Room, and Lower Cave. Water ascending from the Guadalupe Room encountered the impermeable lower units of the Yates Formation and so was forced to diffuse toward the Main Corridor along the level of the New Section. Bottomless Pit in the Big Room was not only a probable water-injection point but also a probable injection point for hydrogen-sulfide gas ascending into the reef along the Bell Canyon Formation(?) (Fig. 87) and/or along a major north-south trending joint (Fig. 85). Hence this area was a region of intense mixing and dissolving that eventually produced an exceptionally large void, the Big Room. Another possible water- and gas-injection point was Lower Cave (along the Cable Slot and Nicholson's Pit); where acidic water ascended at the Jumping Off Place and mixed with water ascending from the Bottomless Pit, it created the large dome in the Big Room ceiling known as the Top of the Cross. The ascending, bathyphreatic water probably never exited via the Top of the Cross (recent balloon exploration of that area shows that the Top of the Cross may not continue upward); rather, the water probably moved northeast along the Big Room, ascended Appetite Hill at an angle toward the Main Corridor, and then lifted vertically up the Main Corridor.

As erosion of the reef and basinal rocks continued, spring positions shifted eastward and downward, as did new basal injection points for lifting water. The next spring outlet for water in Carlsbad Cavern may have been somewhere on the New Section level or, later on, in the Lake of the Clouds-Bell Cord Room section of the cave. The unlikely position and configuration of the Lake of the Clouds Passage, Bell Cord Room, and Bifrost Passage with respect to the rest of the cave at that level (see Sheet 2) suggest that perhaps these passages were the avenues along which water ascended at the time when the water table was lowering to the Big Room level. This spring outlet could have been either in the high dome of the Bell Cord Room or in a passage not yet discovered or one covered by collapse. At that time water no longer proceeded up the Main Corridor, but instead flowed from the Big Room along Left Hand Tunnel and toward the Bell Cord Room spring outlet (Fig. 88).

Sulfuric-acid dissolution and water-table development—The greatest amount of sulfuric-acid dissolution probably took place at the water table, which was a mixing zone for oxygenated vadose water descending from the surface and hydrogen-sulfide gas ascending from the basin. Acidic water dissolved out the major horizontal rooms and passages, transformed the montmorillonite clay into endellite and, as a by-product of the acidic reactions, autochthonous silt released from the limestone settled to the floor and gypsum precipitated on top of the silt (Fig. 89).

As water-table conditions prevailed over bathyphreatic conditions (Fig. 14), the velocity of flow decreased. This change explains the sequence of deposits in Lower Cave, where cobbles (fast-flow environment) are overlain by finely laminated silt (slow-flow environment). The position of gypsum on top of silt is the result of continuous dissolution of limestone (source of silt) but precipitation of the gypsum only when the water reached saturation. Left Hand Tunnel became the lateral connection between the Big Room and the Bell Cord Room spring outlet, and water flowing slowly in that direction could have caused the diffuse pattern of

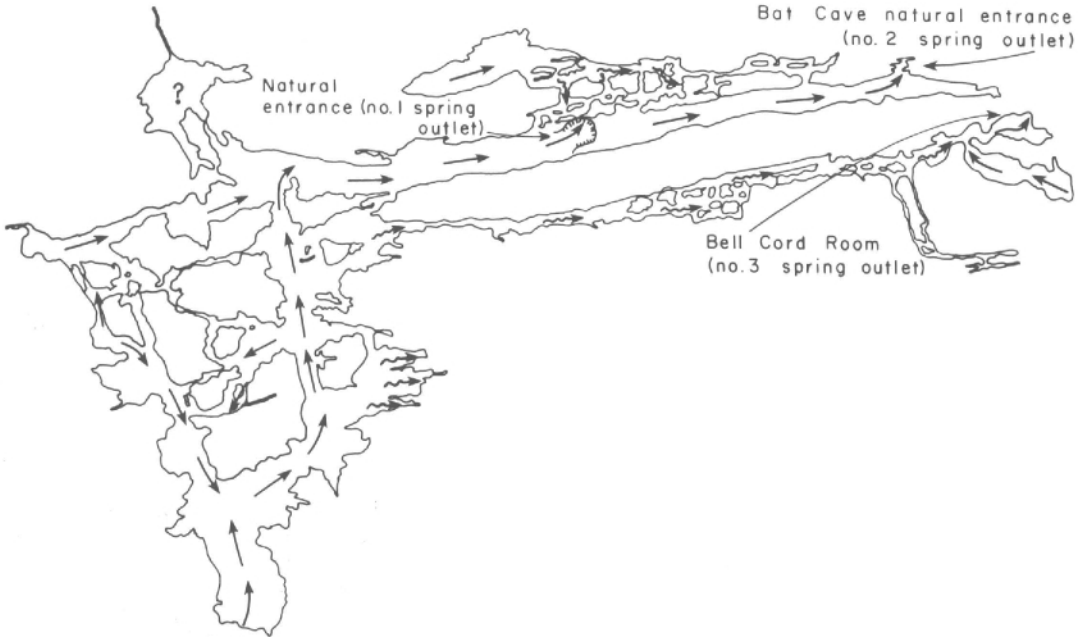

FIGURE 88—Proposed route of bathyphreatic flow and successive spring outlets in Carlsbad Cavern. Straight arrows represent main-flow routes and wavy arrows represent diffuse-flow routes.

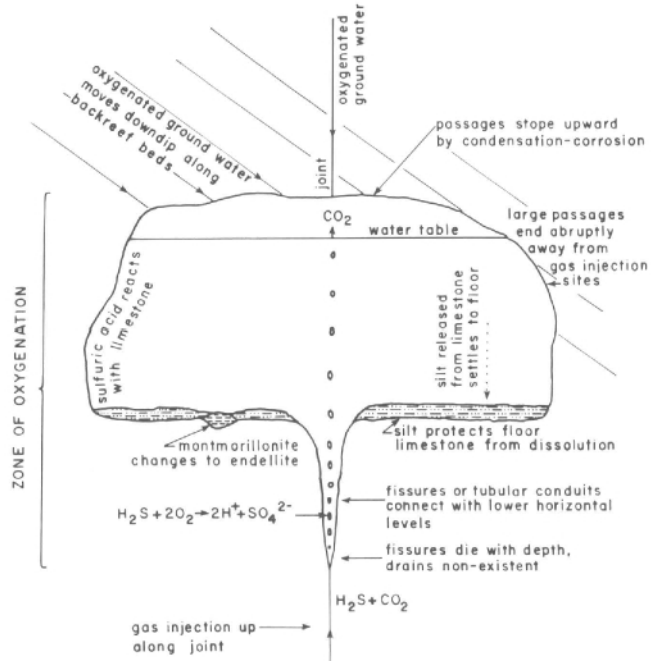

FIGURE 89—Model of hydrogen-sulfide reaction with dissolved oxygen near the water table. Hydrogen sulfide and carbon dioxide from the basin ascended into the reef along injection points and reacted with oxygen in the zone of oxygenation to form sulfuric acid. Sulfuric acid was neutralized by the limestone away from the injection points and, therefore, horizontal rooms end abruptly. The sulfuric-acid reaction did not occur below the zone of oxygenation and hence vertical passages die with depth below large, horizontal rooms. With successive lowering of base level, new horizontal levels became connected with older horizontal levels by spring shafts and joint chimneys.

that passage. Slow-flowing water may have also dissolved the diffuse pattern of passages in the Polar Regions, Big Room, and many boneyard passages (such as those at the base of the New Mexico Room and Appetite Hill; Wilson and Ash, 1984b). Boneyard may represent the contemporary enlargement of Solution II spongework caves in rock surrounding enlarging passages, especially in slack current places.

According to the proposed model of Solution Stage III sulfuric-acid speleogenesis, vertical tubes, fissures, and pits are interpreted as formed along injection points for gas and/or bathyphreatic water, and horizontal levels are interpreted as formed at the water table where dissolved oxygen was most concentrated (Fig. 89). Cave walls of large rooms end abruptly in the horizontal plane because, away from gas-injection points, the acid was neutralized by bedrock. Since the amount of dissolved oxygen decreased with depth below the water table, fissure passages and pits terminate vertically and do not possess bottom drains. Degassing of carbon dioxide at the water table produced atmospheric corrosion of cave ceilings and walls, and the large cave passages grew further by stoping upward.

Origin of spar

U-series and ESR dates, carbon-oxygen-isotope data, and nucleation crystal kinetics suggest that Spar III crystals in Guadalupe caves formed during the present erosion cycle, under saturated conditions, and in the shallow phreatic zone.

The growth of large spar crystals implies that: (1) water flow in the zone of crystallization was extremely slow and crystals thus were free to nucleate and develop; (2) water in the zone of crystallization was barely saturated with calcite; and (3) the right saturation conditions were maintained over a sufficiently long period for the spar to grow large. Under supersaturated conditions the nucleation of crystals is so rapid that most of the excess dissolved mass is precipitated as nuclei, with little material left over for large crystal growth. Cave rafts or cloud linings, such as in the Lake of the Clouds Passage, Carlsbad Cavern, are examples of this type of precipitate which consists of extremely small crystallites of calcite. Under barely saturated conditions nucleation is slow and only a negligible proportion of excess mass is used to form crystal nuclei. In this case, when the nucleation rate is considerably less than the growth rate, surface-reaction-controlled crystallization predominates and crystals can grow large and at the expense of smaller crystals around them (Berner, 1971). Thus, the growth of large spar crystals implies a very delicate balance between depositional and nondepositional equilibrium, at a point where saturation is barely maintained. Zoned spar crystals, such as have been found in the Secondary Stream Passage and Guadalupe Room of Carlsbad Cavern, also demonstrate that equilibrium may have been very delicately balanced between deposition and nondeposition.

Thrailkill (1965b) thought that water movement in a karst aquifer is concentrated in the upper 100 m or so of the phreatic zone, and mainly in the uppermost 10 m, very near the surface of the water table. It is this oxygenated water that is generally undersaturated with calcite and dissolves most of the limestone along a horizontal zone at the surface of the water table. Below this zone the aquifer is much slower-flowing and water can become saturated with calcite. Far below the water table, deep in the phreatic zone, greater pressure causes an increase in the solubility of calcite and, therefore, the water is again undersaturated with calcite. Thus, theoretically at least, there is between the water table and the bathyphreatic zone a middle, shallow-phreatic zone which is barely saturated with calcite and is the ideal location for the growth of large spar crystals.

The concept of a saturated, shallow-phreatic zone as the site of spar formation concurs with the carbon-oxygen data on Spar III crystals (Fig. 73), which were dated at >350,000 yrs by the U-series method and at 879,000 ± 124,000 yrs by the ESR method. The carbon depletion of Spar III crystals indicates origin from ^{13}C-poor organic soil and little inter-action with carbonate host rock. This implies a shallow-phreatic origin for the spar. According to this interpretation the spar formed after fast-flow bathyphreatic cave development, during slow-flow water-table development, but before the large horizontal rooms became highly integrated by sulfuric-acid dissolution at the water table. Thus, spar and spar linings, such as can be seen in the Secondary Stream Passage and Mystery Room, have been dissolved and etched by sulfuric-acid solutions (Pl. 9A, Fig. 90).

Origin of calcified siltstone-cave rafts

Whereas spar precipitated in the saturated, shallow-phreatic zone just below the water table, the Type I cave rafts of the siltstone-raft sequence formed on the surface of the water table where carbon dioxide was degassing and supersaturated conditions were achieved. The almost identical carbon-oxygen composition of Type I rafts and Spar III crystals (Fig. 73) suggests a genetic relationship between the two; that the rafts were forming on the water-table surface during the same time the spar was forming just below the water table (Fig. 90). This model fits the sequence of events as seen in the Guadalupe Room, where the calcified siltstone-cave raft sequence directly overlies spar crystals (Fig. 68); it is also not in discord with the dating results on the spar and siltstone-rafts, assuming that the <350,000 yrs siltstone-raft dates (Table 24, samples 12, 13,

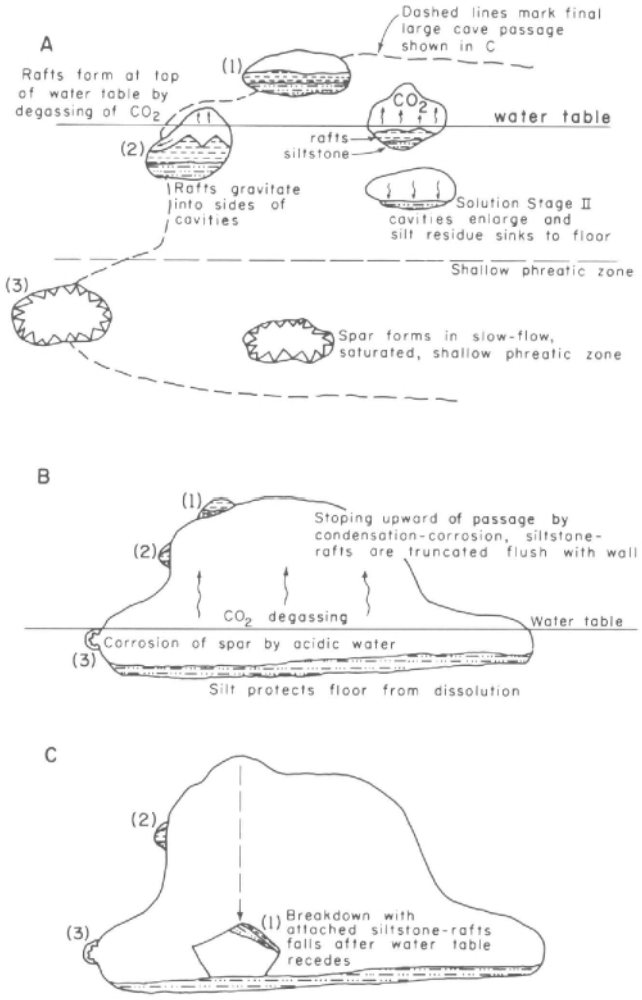

FIGURE 90—Proposed sequence of events producing the calcified-siltstone-cave-raft sequence. (A) At the beginning of Solution Stage III dissolution, acidic water enlarged Solution Stage II cavities and silt residue settled to the floor. Cave rafts formed at the surface of the water table where CO_2 was degassing, and the rafts sank to the floor on top of the silt. (B) Acidic water at and below the water table and corrosive air above the water table dissolved away the bedrock so that, over time, early Solution Stage III caves became large, interconnected voids. Passages stoped upward by corrosion, and the siltstone-rafts became truncated concordant with the wall. (C) The water table lowered from the passage and breakdown blocks (containing exposures of siltstone-rafts) fell to the floor. Sites (1), (2), and (3) correlate in each of the three views, and the dashed lines in (A) correspond to the final cave passage outline in (C).

14) are young ages due to post-depositional calcite cementation of the rafts.

Considering these factors and also the occurrence of the calcified siltstone-cave rafts, these deposits are thought to be the result of early fluctuation phases of water-table development that antedated the final enlargement of Solution Stage III cave passages. The siltstone-rafts occur in the backreef-reef transition zone (Fig. 40) and the siltstone probably represents insoluble residue released from silty backreef beds upon bedrock dissolution. The siltstone-raft deposits always rest on upward-facing surfaces (Fig. 68), signifying that these silts settled out of suspension once they were released from the limestone. The siltstone and rafts almost always occur together, with the rafts directly overlying the siltstone and with both deposits being highly calcified; also, the space above the siltstone-raft sequence is usually air-filled (or covered with subaerially formed travertine). These facts imply that the cave rafts deposited very soon after the siltstone and that the siltstone-rafts date from the present erosion cycle rather than an earlier one, since otherwise the rafts would be covered with silt or spar. This is confirmed by the dates on the rafts.

The fact that the calcified siltstone-cave rafts are truncated by large cave passages may be explained if one assigns the siltstone-rafts to an early episode within the Solution Stage III event (Fig. 90). As with the spar, the siltstone-raft deposits became corroded and truncated as small, isolated passage segments became integrated into large cave passages by sulfuric acid dissolution or by the stoping upward of passages by atmospheric corrosion. Only a small percentage of the siltstone-rafts remains of those originally deposited-those exposed in walls and ceilings and those in pieces of breakdown that fell from the walls and ceilings after the water table had permanently receded from the cave passages (Fig. 90).

Not all Type I rafts are truncated by the large cave passages: some are still located in small solutional rooms. Examples of this are the well-indurated rafts (overlain by sulfur crystals) which occur on the floor and ledges of a small room off the Christmas Tree Room and which have a carbon-oxygen signature characteristic of Type I rafts (Fig. 73, sample 8). It is believed that these rafts may have formed in an area of less acidity, where solutions quickly lost their aggressiveness for dissolving cave wall and thus became saturated with calcite. Solutional cavities with this kind of Type I cave raft represent an early development of Solution Stage III cave which never became fully integrated into large rooms (i.e. the cavities remained in the stage of development shown in A (2) of Fig. 90).

Origin of cobble gravel

Bretz (1949) proposed that the cobbles and silt in Lower Cave and Secondary Stream Passage, Carlsbad Cavern, were the result of a late-stage, short-lived vadose stream which traversed down the Main Corridor, into the Secondary Stream Passage, and then down into Lower Cave, finally exiting somewhere in the Pecos River valley. Gale (1957) further elaborated on Bretz' idea by stating that an earlier period of vadose-stream activity produced the terraced silt banks in Lower Cave, and then a younger vadose stream carved out a channel in the silt and deposited locally derived limestone cobbles along its course. The thesis of a vadose-stream origin for the cobbles was also accepted by Moore (1960a); however, Good (1957) thought the cobbles were reef material rounded in place. Neither theory is supported by the evidence.

(1) The cobbles are backreef material and hence originated outside the cave. This is supported by lithologic studies done by M. Queen (pers. comm. 1984) and by size analyses of the cobbles (Table 9). The cobbles have an average long-axis dimension twice as great as the short-axis dimension, indicating that they are bedded, backreef material rather than nonbedded, reef limestone. The chert pieces found in the Lower Cave trench and in the gravel of the Main Corridor, and the quartzite pebble found by M. Queen in the Secondary Stream Passage (Table 8) may be remnants of the Ogallala (or Gatuña) Formation.

(2) The cobble gravel is a heterogeneous, poorly sorted, non-stratified to crudely stratified deposit. Individual cobbles do not touch each other as is typical of water-laid gravel, but rather are matrix-supported. These facts argue strongly against a stream or flood-water genesis.

(3) The cobbles in Lower Cave were not deposited in a downcut trench after the silt as stated by Bretz (1949) and Gale (1957); they underlie the silt (Pl. 1B, Fig. 34). If the contact between the well-indurated cobbles with tan matrix and the fine-grained, homogeneous, orange silt overlying the cobbles represents a true unconformity, then the cobbles

and silt in Lower Cave were emplaced at different times and may be genetically unrelated to each other.

(4) Cobbles are encased in a gypsum block in Upper Devil's Den. If indeed a vadose stream had deposited the cobbles, then why did it not dissolve away the gypsum?

(5) Cobbles in the lower end of Lower Cave near Nicholson's Pit mysteriously disappear near the pit and do not fill the pit, which suggests that the cobbles may have been emplaced before the pit existed. Cobbles in the upper end of Lower Cave at the Green Clay Room could not have possibly been carried through the crawl-sized passages there by a stream. Flow velocities on the order of 1 m/sec would have been required to carry cobbles so large (up to 19.5 cm in diameter) along a streambed (White and White, 1968). On the other hand, flow velocities of only about 0.3 cm/sec would be required to transport the silt which overlies the cobbles (mean particle size 0.04 mm; see Hjulstrom's diagram, Krumbein and Sloss, 1963).

(6) The cobbles are not deposits of a late-stage stream; they underlie >730,000 yrs old, paleomagnetically reversed silt, which in turn underlies subaerial dripstone dated at 600,000 ± 200,000 yrs. The cobbles underlie silt which in turn underlies travertine; the cobbles never abut up against travertine material. This implies that the cobbles were not emplaced by a free-flowing stream in the vadose zone, but rather were deposited in the phreatic zone; otherwise travertine and cobbles would be adjacent and contemporaneous with each other.

Because of the above objections to a stream-deposited or in-place origin of the cobbles, the theses of Bretz (1949) and Good (1957) are rejected and a new one is proposed. The cobble gravel in Carlsbad Cavern originated similarly to a debris flow—a muddy mixture of water and fine particles that supports and transports abundant coarser material (Friedman and Sanders, 1978). The cobbles originated in backreef beds, were carried and rounded by a surface stream, were dumped into then-forming bathyphreatic cave pas-sages early in the Solution Stage III episode, and then gravitated down into the lower levels of the cave along the Main Corridor. In limestone terrains rocks are honeycombed with voids and surface material may find its way into subterraneous cavities on a large scale (Lee, 1924b).

Much of the evidence points to a subaqueous-debris-flow origin. The cobbles are backreef, possibly Ogallala or Gatuña material. Limestone cobbles, siliceous pieces, and pieces of very old spar (see the $^{234}U/^{238}U$ ratio of sample 11, Table 24) were carried and rounded by a surface stream and then dumped into pre-existing passages. Before entering the cave, the cobbles were weathered, some of them developing moonmilk-like or hollow centers such as described by Bretz and Horberg (1949a) for the leached caliche deposits of the Ogallala Formation in the Pecos River valley. Moonmilk-centered cobbles lie directly adjacent to crystalline cobbles in the "cobblestone" floor of Nooges Realm, Lower Cave, and were also found in the lower levels of the trench (Table 9); both trends would be expected if the cobbles had been weathered prior to entering the cave and then were randomly dumped into place within the cave.

Debris flows are poorly sorted, chaotic mixtures which generally lack internal stratification. Large clasts such as cobbles are easily transported in debris flows because they are supported in part by buoyancy forces due to the high density of the mud in which they are submerged (Blatt et al., 1972). The largest clasts end up on top of the deposit (Gloppen and Steel, 1981) and sometimes display a weak upcurrent imbrication (Allen, 1982). The size data on the cobbles (Table 9) and the "upstream" cobble imbrication measured at Nooges Realm show that both conditions exist for the Lower Cave cobble gravels. Most important, a matrix-supported internal structure, where the cobbles are separated by a finer matrix material, is diagnostic of debris flows.

A debris-flow origin satisfies all the statistical data on the cobbles and explains the distribution of the gravels in the Main Corridor and Secondary Stream Passage (Fig. 31), but it is much less satisfactory in explaining the horizontal distribution of the cobbles along Lower Cave where the pas-sage slope is low (1-1.5°). No really good explanation can be offered for this distribution, but one possibility is suggested. If the cobbles entered the cave early in the Solution Stage III episode when bathyphreatic conditions still prevailed in Lower Cave, then perhaps they were moved along Lower Cave by rapid, sub-water-table flow. Later, when Lower Cave was subject to a slow-flow water-table development, the silt settled out of suspension on top of the cobbles and protected the gravel from further dissolution by Solution Stage III acids.

The relative time of cobble-gravel emplacement is not known with certainty. A debris flow could cut across cave levels and thus antedate events going on at one level, be contemporaneous with events at another level, or postdate events at still another level. The fact that the cobble gravel is interbedded with silt in the Secondary Stream Passage suggests that at this level of the cave the cobbles were slumping into passages contemporaneous with passage enlargement. The cobbles in the gypsum of Upper Devil's Den may have slumped into the gypsum while the gypsum was consolidating, but they had probably entered the Main Corridor long before then.

The proposed scenario for the emplacement of the cobble gravel in Carlsbad Cavern is as follows: The presence of siliceous gravels, dendritic stream patterns, and entrenched meanders on the Guadalupe upland surface indicates that during Ogallala time the Guadalupe Mountains were low and near base level (Motts, 1957). With uplift, sharp meanders such as the Serpentine Bends of Dark Canyon (Fig. 5) were incised into the formerly low-lying plain. Solution Stage II cavities and then-forming bathyphreatic Solution Stage III passages were exposed by incised-valley erosion so that rounded, backreef, stream cobbles were dumped into the voids, progressively working their way down into the lower levels of the cave (Fig. 91). In the higher levels of Carlsbad Cavern such as Bat Cave, the Main Corridor, and Secondary Stream Passage, gravel infilling may have been contemporaneous with Solution Stage III dissolution, and the result was cobbles crudely stratified with silt. According to this model, the cobbles were brought into the cave as a subaqueous debris flow, and the interbedded and overlying orange silt originated as residue from the dis-

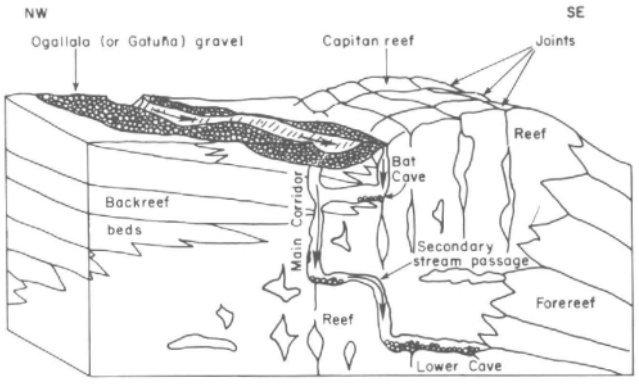

FIGURE 91-Proposed model for emplacement of cobble gravel. As the reef uplifted in the late Pliocene-Pleistocene, rivers that once meandered across a low-lying erosion surface downcut into forming Solution Stage III bathyphreatic caves, and Ogallala (or Gatuña) gravel was dumped into these voids.

solving limestone. However, on the Lower Cave level the cobbles arrived before substantial water-table development began, and so a sharp unconformity exists between the cobbles and silt at that location.

Downcutting streams filled other early caves exposed high along valley walls, such as Pink Fink Owlcove, with gravel. Type 2 dikes of coarse sand to gravel may also date from this episode of cavity filling. The Ogallala (or Gatuña) siliceous gravel remnants still present on the ridge tops of the Guadalupe Mountains, including the ridge east of the Carlsbad Cavern entrance (Fig. 8), may be part of the same cobble gravel that fills the cave. On the Carlsbad Cavern Ridge, most (99%) of the original mass of this gravel (the limestone cobbles) has been eroded away, and the more resistant remnants (1%) of this gravel (the siliceous pebbles) still remain in place.

Origin of endellite

The mineral endellite is another important indicator that the large cave passages of the Guadalupe Mountains had a sulfuric-acid genesis. Endellite is a kaolin mineral and species of this group are highly susceptible to crystallographic change in an acidic environment (DeKimpe et al., 1964).

Cox (1875) and Callaghan (1948) described porcellaneous endellite in Gardner Mine Ridge, Indiana, as bluish, gray, brownish, or snowy-white nodules which occur in a dark mahogany clay; the nodules are dense, waxy, translucent, have prominent conchoidal fracture, and contaminating material (such as iron oxide or manganese), expelled from the structure of the clay, stains the surface of the endellite. The Indiana clay is a residual soil layer derived from limestone; sulfuric acid derived from pyrite in overlying sand-stone beds turned the residue to endellite (Ross and Kerr, 1934; Callaghan, 1948).

Keller et al. (1966) described an occurrence of endellite from Stanford, Kentucky, and postulated the same, sulfuric acid origin. The Stanford endellite is white to light gray, granular to porcellaneous, and forms as lenses and stringers in weathered limestone residue. The lenses are about 10 cm wide and follow pre-existing fractures in the residue. At the zone of endellite formation, pH was 3.0-3.7; pH at the source (pyrite in overlying shale beds) was 1.0.

A third reported location of endellite is at Les Eyzies, France, where kaolin-halloysite (endellite) is trapped in pockets as much as 50 m deep within the pyritic limestone of the Dordogne and Vezere Valleys (Brindley and Comer, 1956). The kaolinitic sediments were stirred and washed and then altered to endellite by sulfuric acid solutions derived from the pyrite.

In Guadalupe caves, endellite occurs with montmorillonite in Solution Stage II spongework cavities that have been cut across by Solution Stage III passages, or it is associated with overlying silt (Fig. 70). Montmorillonite is a clay mineral which can transform to palygorskite (attapulgite) under drying conditions and to endellite under acidic conditions. Berner (1971) stated that montmorillonite weathers to kaolinite (endellite is a type of kaolinite) in an acidic environment, in which case silica (chert) is liberated in the reaction. When Solution Stage III acids corroded limestone honeycombed with Solution Stage II spongework, the montmorillonite clay in the spongework was exposed and some of it transformed to endellite-especially along cracks or seams in the clay or at the contact of the montmorillonite and limestone.

Origin of sand and silt

Clastic sediments in caves are classified as autochthonous if they derive from inside a cave, or as allochthonous if they are brought from outside. The cobble gravel in Carlsbad Cavern is believed to be allochthonous. The fine-grained sediment in Guadalupe caves, however, is believed to be autochthonous, i.e. it is not a stream deposit but a residue released from the limestone at the time of Solution Stage III dissolution. Rare exceptions to this non-stream mode of deposition are: (1) Vanishing River Cave, which is located in the bottom of a canyon wash and so receives flowing water during the time of heavy rain; (2) the entrance of Dry Cave, where flowing water has channeled down several centimeters into the sediment of Fool's Hole (Lindsley and Lindsley, 1978); and (3) the connection between Bat Cave and New Section, Carlsbad Cavern, where a small, abandoned stream bed is entrenched in the floor of the upper part of the connection area (D. Davis, pers. comm. 1984).

Gardner (1935, p. 1269) was the first to propose that the silt in Carlsbad Cavern derived from a stream: "in its lowermost level the channel, now dry, of a stream which was quite active throughout a long period until recent geologic time." Bretz (1949) also thought a stream had traversed through Lower Cave, first depositing the silt and then the cobbles in a downcut trench in the silt. This study contends that the silt is autochthonous residue, based on the following evidence:

(1) Floor sediment is almost always traceable to nearby silty-sandy limestone; the sediment has not been transported more than tens of meters from its source.

(2) Insoluble residue in the bedrock matches nearby floor sediment in color, grain size, and type of impurity. For example, the orange sand on the floor of Sand Passage matches the sand of the Yates Formation which can be seen interfingering along the north wall of the passage. The cream-colored silt on the floor at Bottomless Pit matches the cream-colored insoluble residue in the limestone at that spot (compare Table 10 with Table 27).

(3) Silt underlies floor speleothems such as stalagmites, but it has not covered them or piled up around them as would be expected if the silt was stream-laid.

(4) Sediment terrace banks are level across cave passages. This can be seen in Left Hand Tunnel and also in Lower Cave where the sediment banks are almost level from the upper end to the lower end of the passage (Table 11). The level terraces suggest that the sediment was deposited by flood or aquifer water, not by stream water.

(5) No signs of active streams exist in silt-laden areas; there are no scallops or incised meanders to suggest fast flow under vadose conditions. Laminations in the silt (Pl. 2A) attest to a quiet mode of deposition such as might be produced by flooding or by slowly flowing aquifer water. Also, the fact that excellent paleomagnetic data have been obtained for the silt in Lower Cave suggests that the silt settled out of non-turbulent water where iron mineral grains could align to the Earth's magnetic field.

(6) The silt in Lower Cave was not brought in by a late-stage stream as suggested by past researchers (e.g. Bretz, 1949). The silt is older than 730,000 yrs as determined by paleomagnetic dating.

(7) The laboratory experiment duplicated on a small scale the autochthonous process by which the silt in Guadalupe caves originated. As the limestone was dissolved by acid, the liberated silt residue settled out of suspension and to the cave floor.

Some objections can be raised to an autochthonous origin of the silt.

(1) The up to 7 m high silt banks in Lower Cave cannot be directly traced to a correspondingly high percentage of silt in the limestone (Table 27). So where did the silt in Lower Cave come from?

(2) If the silt deposits in both the Big Room and Lower Cave are a product of Solution Stage III dissolution, then why does the Big Room silt contain color bands, chert, and

is of limited extent, whereas the Lower Cave silt occurs in high banks and is orange colored throughout?

(3) If the silt in Lower Cave and Secondary Stream Passage is autochthonous, then why is it associated with the supposedly allochthonous cobble gravel?

Question (2) partly answers question (1). Consider the amount of residue that had to be liberated by the dissolution of the Big Room. Most of it did not accumulate on the floor of the Big Room, so where did it go? As discussed previously, deeper-flow paths tend to fill with silt because of normal gravity settling; therefore, lower cave passages should fill with silt liberated from the dissolution of upper cave passages so long as the two passages are connected. This is the explanation offered for the Lower Cave silt: It is insoluble residue derived not only from the dissolution of Lower Cave and Talcum Passage, but also, in part, from the dissolution of the connected Big Room. To support this hypothesis, a digitized map of the Big Room, Talcum Passage, and Lower Cave was made, and the volume of residue that should have been liberated from the dissolution of these three rooms was calculated and compared with the actual amount of silt on the floor of Lower Cave. The amount of insoluble residue in the limestone was calculated by averaging the values in Table 27 (excluding the New Mexico Room values), and the height of the silt banks in Lower Cave was calculated using the values in Table 11. The estimated average height of the silt banks in Lower Cave is 1.8 m and, based on the total volume of the three rooms and the average insoluble-residue content in the limestone, the theoretical height that the banks should be is 1.7 m. These calculations do not take into account the amount of silt on the floor of the Big Room, a quantity difficult to estimate since the Big Room is covered with travertine and gypsum in many places. Exposed patches of silt in the Big Room do not nearly match the amount of silt present in Lower Cave, however, and probably would not affect these calculations by more than 10%.

Objection (2) may be countered by invoking a higher overall acidity for the dissolution of the Big Room than for the dissolution of Lower Cave. If the cream-colored sediment at Bottomless Pit and the quartz-sand half-cones of the Big Room really represent interfingerings of the Bell Canyon Formation, as suggested by this study, then these could have been avenues along which hydrogen sulfide entered the Big Room (Fig. 87). In addition, the N15°W joint of the Big Room may have been another avenue along which gas ascended from the basin into the reef (Fig. 85). More hydrogen-sulfide gas entering the system would produce more acid, which in turn would dissolve more limestone, produce more gypsum on the cave floor, liberate more endellite and silica from a montmorillonite transformation, and cause more colloidal migration of silica and iron to form chert and color-banding in the silt. This is exactly what is seen in the Big Room. The Big Room is much larger than Lower Cave and there are more gypsum blocks on the floor. A higher percentage of the Big Room clay is endellite, whereas in Lower Cave it is predominantly montmorillonite. The silt of the Big Room is color-banded due to its iron-oxide content and there is chert interlayered with the silt.

Objection (3) is not difficult to counter in the case of Lower Cave where the possible unconformity suggests the lack of a genetic relationship between the cobbles and silt. Cobbles do not fill Nicholson's Pit because they predate the pit; the cobbles descended into Lower Cave in the bathyphreatic stage of cave development, and, subsequently, Nicholson's Pit and the Cable Slot became injection points for gas. The cobbles were not dissolved by Solution Stage III acids because they were protected by silt released from the dissolution of the Big Room before the water table has descended to the Lower Cave level.

The interbedding of silt and cobbles in the Secondary Stream Passage is not as easy to explain, but the association of silt and cobbles where the passage emerges into the Lunch Room may be a clue. Here the cobbles and pebbles are mantled by layers of laminated orange silt, as if the silt had filtered out of suspension around the upper parts of exposed cobbles. If periodic slumping of the cobbles occurred contemporaneously with the dissolution of this part of the cave, it might account for the interbedding of the two de-posits at this level. As Solution Stage III acids enlarged the cave, the cobble gravel slumped into these voids. These cobbles were immediately covered with silt residue and thus were protected from further acid corrosion. A 1.5m thick layer of silt once covered the cobble gravel in the Secondary Stream Passage. This layer may have been Solution Stage III residue deposited after slumping had stopped; it has since been mostly eroded away.

Silt banks, such as those in Lower Cave (Fig. 37), were probably entrenched by a fluctuating water table in the zone of flooding. V-type entrenchment by flood-zone water is readily apparent in such caves as Flint-Mammoth, Kentucky, where periodic flooding of passages by the back-up of the Green River has cut steep-sided banks in mud, but it is much less apparent in Guadalupe caves where the present-day water table is not intersected by explorable cave passages. In the forereef sections of Left Hand Tunnel, Carlsbad Cavern, where canyons exist in the passage floor, the silt banks slope at an angle concordant with the canyon, as do the slumped layers in the silt. In Lower Cave, Carlsbad Cavern, silt banks were downcut into V's as far as the cobble-gravel horizon, but apparently the entrenching water did not have enough energy to breach this more competent horizon. Entrenchment of the silt in Lower Cave postdated the precipitation of the gypsum, as shown by the sequence of events in the Nooges Realm region where the silt deposited first and the gypsum second, and then both deposits were downcut concordant with each other by the V-shaped channel (Fig. 69).

There is evidence for one or more fluctuations of the water table around base level. At least one back-up of water stirred up the silt sufficiently in Lower Cave in order to produce the <30 cm high layer of silt on top of the gypsum blocks in Nooges Realm. This back-up happened subsequent to a subaerial episode, as evidenced by the silt exposed along the sides of drip tubes in the gypsum blocks (Fig. 69). Corrosion rillenkarren in Lower Cave which are overlain by a layer of silt (M. Queen, pers. comm. 1983), and mudcracks in the area between the Green Clay Room and Naturalist Room which possibly show more than one episode of submergence and wet-dry cracking, also suggest that a back-up of water took place some time after the establishment of subaerial conditions at the Lower Cave level.

Origin of chert

Because of its close association with endellite and montmorillonite (Fig. 70), the chert in the Big Room of Carlsbad Cavern is believed to have been derived from the reaction of acidic solutions on montmorillonite clay with the production of endellite and silica (chert). Silica is a hardened colloidal gel, which may explain the position of chert in the silt deposits of the Big Room, its association with color-banded silt, and its rhythmically banded nature. Colloids carry an electric charge, the colloidal particles migrating to a reversely charged location where they coagulate as their charge is neutralized. Ferric oxide is practically insoluble except when it acts as a colloid, and then it becomes easily transportable. Therefore, the association of chert with color-banded silt may not be a coincidence. Both the ferric oxide and silica may have migrated through the silt as colloids as soon as subaerial conditions prevailed in the cave but before

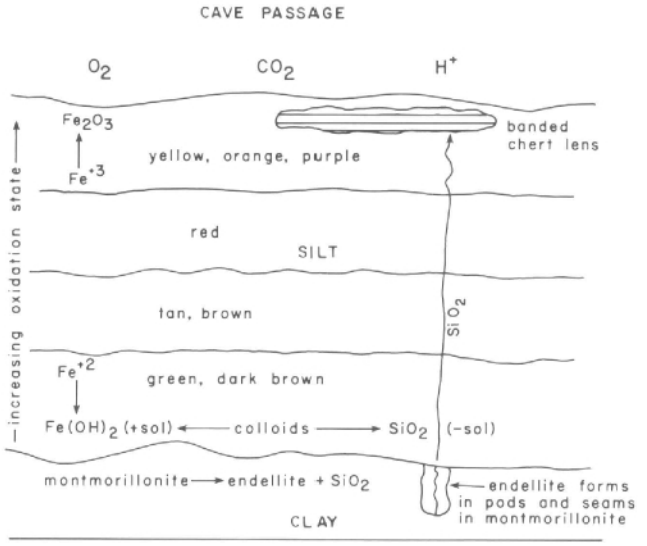

FIGURE 92—Diagrammatic presentation of montmorilloniteendellite clay, color-banded silt, and chert deposits of the Big Room, Carlsbad Cavern. Silica and ferric hydrates acted as colloidal "sols" which moved to positively or negatively charged sites to be neutralized. Colloidal behavior produced the color banding of the silt and the rhythmic banding of the chert.

the silt dried out (Fig. 92). As the silica-rich water was neutralized by excess carbon dioxide near the top of the silt, the solubility of amorphous silica decreased because of the conversion of H_3SiO_4 to H_4SiO_4; supersaturation resulted and silica was precipitated (Berner, 1971). The same type of chemical migration may have been responsible for the color-banding of the silt. As the colloidal iron moved toward the top of the silt bank, it became more highly oxidized and in turn produced colors characteristic of increasingly higher oxidation states (greens to browns to reds and oranges). Cyclic banding in the chert may also relate to colloidal behavior. The rhythmic layers in the chert may have been produced by a liesegang-ring type of phenomena whereby gel-like layers are deposited in alternating porous-compact bands. Richardson (1919) related liesegang-ring gel behavior to the rhythmic or periodic precipitation of silica solutions diffusing through a porous medium, wherein a banded precipitate is separated by constant intervals and is sometimes replaced by a granular zone.

The movement of silica upward to the top of silt may have occurred in response to alternating subaerial and sub-aqueous conditions during the time when water was fluctuating around base level in the Big Room. If water was slightly above the level of silt, silica would have moved toward the top of silt in response to water acidity; if water was slightly below the top of silt, the silt would have dried out, cracked, and then silica could have deposited within polygonal mudcracks in the silt (as it has in the Texas Trail occurrence, Table 16).

Origin of gypsum blocks and rinds

The sulfur-isotope data are essential to a proper interpretation of the gypsum blocks and rinds in Guadalupe caves. The gypsum of the Castile Formation in the Delaware Basin averages $\delta S^{34} = +10.3$, while the gypsum in Guadalupe caves averages $\delta S^{34} = -15.1$ (Table 23). These differences in isotopic fractionation show that the cave gypsum could not have been derived from the Castile Formation according to the local pooling model of Bretz (1949) or the mixing model of Queen et al. (1977a), nor is it likely that it has been derived according to Jagnow's pyrite model of speleogenesis. Instead, the sulfur-isotope data indicate that the cave gypsum is the end result of a series of biological oxidation-reduction reactions related to the oil and gas fields of the Delaware Basin.

There are three theories of how the gypsum has been deposited: (1) by precipitation from a saturated solution; (2) by a replacement-solution mechanism (Egemeier, 1973); and (3) by an in-situ replacement of limestone by gypsum (Queen et al., 1977a). All three mechanisms have probably occurred in Guadalupe caves, but mechanism (1) is believed to have been the predominant one for the following reasons:

(1) Gypsum always overlies silt and sand in Guadalupe caves. If the gypsum formed as a direct replacement of limestone, either according to Queen's mixing model or Egemeier's replacement-solution model, then it should contain the same amount of insoluble residue as the lime-stone. Comparison of Table 15 with Table 27 shows this not to be the case. The bedrock at Bottomless Pit, Big Room, has an insoluble-residue content of 11.7%, whereas a gyp-sum block very near this limestone contains only 0.01% of insoluble residue.

(2) While the sulfuric-acid experiment on limestone was only a model not simulating the geologic parameters of time and space, it nevertheless showed that the cave gypsum could have formed according to a precipitation mechanism. The laboratory-precipitated gypsum mimicked the cave gypsum in that it overlay silt and was residue-free except for tiny pieces of chert. The gypsum precipitated out onto the top of a small glass beaker (Fig. 81), a situation that could not possibly have been produced by a replacement mechanism.

(3) Most of the gypsum in Guadalupe caves does not seem to contain replacement textures as noted by Queen et al. (1977a) in the gypsum of the upper Gypsum Passage, Cottonwood Cave. Rather the laminations and microfolding in the gypsum blocks are reminiscent of the varved and microfolded texture of the Castile Formation in the Gypsum Plain. The gypsum in Guadalupe caves also does not resemble the thin crustal replacement gypsum in Wyoming caves as described by Egemeier (1981). With a few exceptions, in Guadalupe caves the gypsum forms as floor blocks and thick rinds rather than as thin crusts.

(4) Sulfate content of limestone from the drill core in the Big Room bedrock was 0.1% (maximum) at the surface of the wallrock and decreased steadily until it stabilized at about 0.008% (Fig. 80). If, as Queen's model of replacement suggests, the limestone was replaced by gypsum brine, then one would expect sulfate values to be high in the wallrock—at least in some sort of a gradational zone which contains stringers of gypsum or reaction rims such as occur around the partially replaced dolomite inclusion in the upper Gyp-sum Passage of Cottonwood Cave (Fig. 52). Rather, this sulfate trend (like a similar nitrate trend in bedrock at the Natural Entrance) probably reflects the concentration of solutes by seeping ground water at the cave-wall-air evaporation interface.

(5) Paired specimens of gypsum and limestone collected from Guadalupe caves showed no systematic correlation in amount of cations as did Egemeier's replacement-solution gypsum crusts in the Big Horn Basin caves (Fig. 79).

Gypsum precipitation from saturated solution—According to the precipitation model proposed here, the gypsum in Guadalupe caves deposited in much the same manner as did the gypsum of the Castile Formation in the Gypsum Plain. Laminations in the cave gypsum raise the question of whether or not these features are true varves (annual deposits). If the 0.5-4.0 mm translucent-opaque laminations in the gypsum blocks are indeed related to an annual cycle, as are the varves in the anhydrite of the Gypsum Plain, then the 6m high gypsum blocks in the Big Room of Carlsbad Cavern represent roughly 8,000 years of accumulation. Seasonal variations in the volume or rate of water

flow might have triggered the precipitation of the laminated gypsum; or, such triggering might also have been accomplished by seasonal variations in evaporation, temperature, carbon-dioxide loss, or calcium-ion concentration from dripping, speleothemic water.

Assuming a completely closed system, the amount of gypsum that theoretically could have precipitated out of solution according to equation (8) would have exceeded the volume of the limestone excavated. The molar volume of calcite is 36.8 cm^3/gmole and that of gypsum is 74.2 cm^3/gmole; i.e. the solid volume approximately doubles when limestone is converted to gypsum. This explains such areas as the Middle Maze of Endless Cave where the gypsum completely filled the passage before being compacted or partially dissolved (Figs. 44, 45), but it does not explain passages which contain no gypsum, or gypsum which fills 10-30% of the passage height. In the Big Room, the 4-6 m high gypsum blocks represent only about 7% of the gypsum that theoretically could have precipitated. This means that 90-95% of the gypsum must have been lost to flow within the aquifer or other processes such as vadose drippage.

According to the precipitation model proposed here, the gypsum blocks and rinds in Guadalupe caves represent a late-stage, lagoonal-type deposit resulting from hydrodynamic stagnation during the water-table stage of cavern development. Ponding of stagnant water was especially pronounced in the Big Room of Carlsbad Cavern. After water became diverted to the Bell Cord Room spring outlet (Fig. 88), the Big Room became a decoupled and stagnating entity so that gypsum could precipitate out of solution and onto the floor as thick, massive deposits.

The purity of the gypsum blocks suggests that the gypsum was not a direct, immediate product of wallrock dissolution, but precipitated subsequent to passage dissolution. If numerous cycles of bedrock dissolution and gypsum precipitation occurred, then silt should alternate in layers within the gypsum or at least be mixed with it. Evidently, as with the laboratory experiment, the silt fraction settled out to the cave floor first and the gypsum precipitated out later in a single, fairly continuous "snow fall" during a phase of intense brine concentration. The purity of the gypsum also implies that the dissolution of Guadalupe caves may have been very rapid (in the geologic sense) and continuous, otherwise silt should be interbedded with gypsum.

Gypsum replacement of limestone—Replacement textures in the gypsum, especially those in the rinds along the walls of the upper Gypsum Passage, Cottonwood Cave, verify that at least some of the gypsum formed by a re-placement mechanism. But how much of the gypsum had a replacement origin (as opposed to a direct precipitation origin) and how much of it fits Queen's replacement model (versus Egemeier's model) is still a matter of debate.

In the replacement model proposed by Queen et al. (1977a), sulfate ions directly replace carbonate ions in solution. The only way replacement can thermodynamically occur is if the sulfate ion is much more concentrated than the carbonate ion (i.e. SO_4^{2-} $>5.4x10^3$ CO_3^{2-}; A. Palmer, pers. comm. 1986), a situation which may possibly be the case for Capitan aquifer water considering that in Table 2 HCO_3 exceeds SO_4^{2-} by a factor of 2 or 3 and the solubility of HCO_3 is about $8x10^3$>CO_3^{2-}. Thus, under conditions approaching saturation or supersaturation with gypsum, where the SO_4^{2-} ion is much greater than it is in Capitan aquifer water, Queen's mechanism of replacement may be a viable one.

The replacement envisioned by Egemeier takes place in the zone of aeration, where sulfuric acid reacts with limestone and produces a thin crust of gypsum on the wall. This type of replacement is thermodynamically more likely than that proposed by Queen et al. (1977a), but Queen's model is actually more in accord with the type of replacement seen in some Guadalupe caves. The reaction rims around dolomite inclusions (Fig. 52) and the thick replacement rinds in the upper Gypsum Passage of Cottonwood Cave do not suggest a subaerial mechanism of replacement, but rather a replacement of carbonate ions by sulfate ions in a concentrated brine solution. On the other hand, the thin (<1 cm) crusts overlying limestone at Bottomless Pit, Big Room, Carlsbad Cavern, and those in Rim City and Windy City, Lechuguilla Cave, seem to morphologically conform to Egemeier's type of replacement. The low sulfate content in the bedrock core (Fig. 80) also favors either a purely precipitation origin or Egemeier's method of re-placement where limestone alters to gypsum only on the outermost surface of the bedrock.

Solidification of gypsum—Fluctuations of the water table just before its final abandonment of a cave passage alternately caused the gypsum to dissolve, consolidate, dry out, harden, compact, and then partially dissolve again. These processes probably began as soon as the gypsum first started to precipitate, and may extend even to the present day in the case of dissolution by condensation water; however, they occurred primarily while the water table was fluctuating around base level.

Laminations in the gypsum formed during its precipitation, while microfolding, slumping, angular unconformities, brecciation, slickensides, inclusions, overgrowth crusts, recrystallization, and flow features attest to the gypsum's mode of solidification. Egemeier (1981) compared the consistency of wet gypsum in the Big Horn Basin, Wyoming, caves to that of mud. This was also probably true of the wet gypsum in Guadalupe caves; such features as the gypsum cascade in the Insane Rain Drain Trench Pit of Dry Cave or flow features in the Talcum Passage gypsum (Fig. 53) further suggest that the gypsum may have had an almost plastic consistency while still wet.

Possibly the first consequence of drying was the movement of interstitial water to the surface of the gypsum blocks to form overgrowth crusts. In some cases, where the crusts are vertically oriented, as in the Balcony Room of Dry Cave and the Talcum Passage of Carlsbad Cavern, hardened overgrowth crusts slid down over the still plastic interiors of the blocks (Fig. 43). Slickensides were gouged where overgrowth crusts slid down against underlying, more solidified gypsum (Pl. 3B). Precipitation of new gypsum over previously deposited, partly hardened, slumped layers resulted in angular unconformities. And, where hardened upper layers broke and sunk down at various angles into the less consolidated, lower layers of gypsum, a breccia texture was produced (Fig. 50). If pieces of bedrock fell or slumped off into the gypsum while it was still solidifying, the limestone became partially or totally replaced by gypsum depending on the viscous state of the gypsum and the amount of ionic exchange that occurred (Figs. 51, 52). Continued seepage of water to the outside of the gypsum block caused partial recrystallization of its interior mass, resulting in partial or total obliteration of original textures.

As the gypsum blocks completely dried out, they compacted. Undulations in the tops of the gypsum blocks in the Middle Maze of Endless Cave match those in the ceiling limestone (Fig. 45); at such localities the compaction factor seems to be about one-fourth of the original mass. Microfolding of the laminations may have been produced from the compaction, shrinking, and compression of the gypsum while it consolidated.

Dissolution of gypsum—The presence of gypsum blocks and rinds in. some caves and cave passages and their absence in others is one of the most puzzling aspects of the gypsum deposits in Guadalupe caves. As discussed above, most of the gypsum (90-95%) that theoretically could have precipitated according to equation (8) must have been carried out of the caves in solution; otherwise all of the cave passages would be completely filled with gypsum. Four

mechanisms appear to have caused the dissolution of the gypsum:

(1) *Aquifer water*—Most of the solute gypsum that did precipitate from saturated solutions probably redissolved and was removed by fresh aquifer water almost as soon as it formed. In this connection it is interesting to note that Bat Cave and the Main Corridor of Carlsbad Cavern, the Entrance Hall of Cottonwood Cave, the Main Corridor of Hell Below Cave, and the Expressway Passages of Endless and Dry Caves all are nearly devoid of gypsum. This distribution may possibly be explained as due to aquifer water moving more rapidly and less diffusely through these large trunk passages than through constricted passages such as the Gyp Joint of Hell Below Cave, the Gypsum Passage of Cottonwood Cave, the Middle Maze of Endless Cave, or the Polar Regions of Carlsbad Cavern. Also noteworthy is the trend seen in Carlsbad Cavern where very little gypsum exists in passages that trend northeast, parallel to the reef escarpment (e.g. Bat Cave, Main Corridor, and Left Hand Tunnel), whereas in the Big Room (a passage which trends perpendicular to the escarpment) deposits of gypsum are plentiful (Sheet 2). Flow of aquifer water in the northeast direction, toward outlet springs, may have been responsible for preferential gypsum dissolution in the passages which parallel the reef.

(2) *Flood-zone water*—Normal fluctuations of the water table in the zone of flooding may account for some gypsum dissolution, especially for archways of gypsum (Fig. 49), pillars of gypsum (Fig. 44), carved channels in gypsum (Fig. 47), commode holes in gypsum (Fig. 57), and scallops in gypsum (Fig. 59). Also, the entrenchment of gypsum where it over-lies silt was probably caused by a fluctuating water table (Fig. 69).

Flood-zone water would have been only slightly under-saturated with gypsum and, therefore, only gypsum exposed to turbulence-where water rose up through small holes in the limestone or at the intersections of passageways (Pl. 5A)-would have dissolved. This may have been the same aquifer water out of which the gypsum had previously precipitated; only during flooding was the water undersaturated enough to dissolve gypsum.

(3) *Vadose drippage*—This is the most obvious mechanism of gypsum dissolution, but it probably accounts for only a small fraction of the total reduction of the original solute mass. Drip water has severely eroded many gypsum blocks into sharp-spiked crags, crevices, and tubes (Fig. 55). Some of the gypsum has been almost or entirely eroded away by this mechanism, as shown by remnant blocks, molds, and casts. On a small scale, dissolution patterns of vadose drip-ping can be seen in such places as the Gyp Joint, Hell Below Cave, where gypsum remains in alcoves or under archways protected from dripping along joints (Fig. 49). On a large scale, the effects of vadose drippage can be seen in such places as the Big Room, Carlsbad Cavern, where the gypsum abruptly begins and ends at the forereef-reef contact. In the forereef, talus beds tilt at an angle of about 30° away from the reef core so that meteoric vadose water is diverted downdip along these avenues. Hence water does not drip into the cave in most areas of the forereef and the gypsum blocks have been preserved there. In the reef core, however, dripping water readily enters the cave along ceiling joints, forming stalactites and stalagmites and also dissolving away the floor gypsum. Queen (1981) related the trend of gypsum preservation in the Big Room to joint position. At the Jumping Off Place the prominent joint is in the center of the passage and so the gypsum blocks are preserved against the wall; near the Lunchroom, in an area which has no prominent joints marking the Big Room axis, gypsum is found in the center of the room.

(4) *Condensation water*—Condensation water may have been responsible for streamlining the surfaces of gypsum blocks and for scouring the insides of commode holes. Streamlining appears to be most pronounced in areas where air is moving between different cave levels. Examples of this may be observed in the gypsum blocks in the Talcum Passage and at Bottomless Pit, Carlsbad Cavern, where the blocks at the edge of a pit or precipice are streamlined flush with the void (Figs. 38, 41). In the Talcum Passage and in the upper Gypsum Passage, Cottonwood Cave, the undersides of gypsum blocks are partially dissolved where air blows from a lower passage, and in Endless Cave gypsum blocks have dissolved concordant with the limestone walls at a place where air emerges from the Lower Maze into the Mud Crack Room. In the case of commode holes in gypsum, condensation water has smoothed and scoured the inside of the holes and has built up speleothem rims along the sides of the holes (Fig. 58).

Breakdown fall

The greatest amount of breakdown in a cave falls at the time of, or soon after, the lowering of the water table. According to Sweeting (1973), collapse is most likely when water that is forced through passages under considerable hydrostatic pressure loses that pressure and starts flowing freely. Bogli (1980) further stated that the change from a water-filled state to a drying state causes breakdown collapse.

Most of the breakdown in Guadalupe caves seems to coincide with a short interval between water-table lowering and breakdown falling. The breakdown overlies gypsum, but very little or no travertine has deposited between the gypsum and breakdown events. Iceberg Rock in the Main Corridor of Carlsbad Cavern is a notable exception to this rule; it is a piece of breakdown that fell some time after the water table had lowered in the Main Corridor. Tilted drip-stone on the bottom of Iceberg Rock has a U-series date of >350,000 ybp and an ESR date of 513,000 ybp (Table 24, samples 28, 29). The Georgia Giant stalagmite, which grew on top of Iceberg Rock subsequent to its fall, has been U-series dated at 65,000-180,000 ybp (Fig. 74). Hence, it is known that Iceberg Rock fell some time between about 500,000 and 180,000 ybp-probably closer to 500,000 ybp, considering that the dripstone may have been actively growing before the fall.

Speleothem deposition

The various types of speleothems began to decorate the caves of the Guadalupe Mountains as soon as the passages became air-filled. The great mass of speleothemic material dates from humid stages earlier in the Pleistocene when the climate in the Guadalupe Mountains was much wetter than it is today (Fig. 77, Table 24). Notable exceptions to present speleothem inactivity are Crystal Dome, the largest actively forming speleothem in Carlsbad Cavern; the Chocolate Drop, New Mexico Room, Carlsbad Cavern; Temple of the Cave God, Three Fingers Cave (Pl. 16A); and numerous deposits in Virgin Cave, especially in the Cavernacle area. Helictites, soda straws, cave pearls, cave rafts, popcorn, and anthodites are examples of smaller, presently growing speleothems.

Dates on travertine material indicate that the Texas Tooth-pick stalagmite in the Lower Cave level of Carlsbad Cavern began forming about 600,000±200,000 yrs ago (Table 24). Since speleothems in the upper levels of a cave can be older than those in the lower levels, the travertine in passages such as Bat Cave, Carlsbad Cavern, can significantly exceed this age. In other, higher-elevation Guadalupe caves such as Cottonwood and Virgin, the speleothems can be even older than those in Carlsbad Cavern (Fig. 86).

Subaerial speleothem growth has continued uninterrupted to the present day except where it has been subject to a growth hiatus (Fig. 77), condensation-corrosion, or

where possible earthquake tremors have broken speleothems. Davis (1980) speculated that some of the stalactites in the Temple of the Sun, Big Room, were broken by earthquake tremors. In Colonel Boles alcove, Nooges Realm, Lower Cave, two columns are cracked and both are offset about 1 cm in the same direction. This displacement may be explained by earthquake tremors or, more likely, by subsidence and slumping of the silt banks beneath the columns. In the Mystery Room, Carlsbad Cavern, and in Deep and Ogle Caves, massive columns detached along the ceilings and then toppled to the floor, fracturing into naturally cross-sectioned pieces like giant columns in a Roman temple (Fig. 131). Likewise, in the Main Corridor of Carlsbad Cavern, broken pieces of massive stalagmites can be seen along the trail. The fracturing and toppling of these speleothems may have been caused by earthquake shocks or, alternatively, it may simply be the result of speleothem old age.

Origin of sulfur

The native sulfur in Guadalupe caves is believed to have formed as a direct sublimation product of hydrogen-sulfide gas which entered the caves via injection points (i.e. along the Bell Canyon Formation or along joints). Evidence for a subaerial interpretation is:

(1) Sulfur crystals coat the undersides of tilted Bell Canyon(?) bedrock in the New Mexico Room and tilted forereef beds in the Christmas Tree Room, occurrences which suggest that hydrogen-sulfide gas ascended up-dip along bedding planes until it reached the air-filled caves where it reacted with atmospheric oxygen to form native sulfur.

(2) The Big Room sulfur occurs over a drip tube, a sub-aerially formed dissolution feature.

(3) Sulfur crystals fill the crevices between masses of stacked cave rafts in the Christmas Tree Room; this suggests gas infiltration into the crevices.

(4) Sulfur directly overlies gypsum flowers and crusts in the New Mexico Room. If the sulfur had been in aqueous form, it would have dissolved away the gypsum speleothems.

(5) The Cottonwood Cave sulfur is enclosed in massive gypsum, as if H_2S had been pumped up through the drained floor and the decanted gypsum.

The direct oxidation of H_2S cannot occur in the gas phase unless a combustion source is present, but it can form on wet surfaces, especially with the assistance of sulfur bacteria:

$$2H_2S_{(l)} + O_{2(g)} = 2S_{(s)} + 2H_2O$$

The sulfur could have deposited any time after the caves became air-filled, but the sulfur overlying speleothems suggests that it may be a relatively young deposit. In the Christmas Tree Room, the sulfur crystals overlie a yellowish-brown, iron-rich crust on limestone fins; this occurrence may be explained if one postulates more than one episode of H_2S gas infiltration and sulfur deposition. Older sulfur may have oxidized in the moist cave environment to sulfuric acid which dissolved the limestone fins. It may have also reacted with iron in the bedrock to form pyrite which then oxidized to the limonite crusts. If this speculation is correct, it may indicate the episodic release of gas under pressure in the basin and "pulses" of gas injection into the caves of the reef.

Condensation-corrosion

Condensation-corrosion (also called "gas weathering") is the process by which water contained in the air and charged with a high level of carbon dioxide condenses out on bedrock or speleothem surfaces and corrodes them. Three atmospheric conditions are needed in a cave before condensation-corrosion can occur: a high CO_2 level in the air, a high amount of moisture (humidity) in the air, and a temperature gradient between the air in different passages. The temperature gradient drives warm, moisture-laden air to areas of lower temperature and humidity; the dew point of the air is reached, and water condenses on speleothems and bedrock and corrodes them.

The carbon dioxide needed for condensation-corrosion in Guadalupe caves could have derived from meteoric water or, according to the theory of speleogenesis proposed in this study, some carbon dioxide may have migrated up from the basin along with hydrogen-sulfide gas. Carbon dioxide, degassing at the surface of the water table, formed calcite rafts at the water surface and corroded bedrock and speleothems above the water surface (Fig. 89). Both Type I and Type II cave rafts are believed to have originated in this manner. Type I rafts, which are usually associated with calcified siltstone, formed near the beginning of Solution Stage III as depicted in Fig. 90; Type II rafts formed near the end of Solution Stage III probably from static backwater associated with late-stage climatic fluctuations.

Condensation-corrosion as modification of geomorphic and speleothemic forms—Characteristic geomorphic and speleothemic forms are caused by the process of condensation-corrosion. Air scallops develop in areas of pronounced corrosive air flow; they modify phreatic solution pockets and can cut across both bedrock and speleothems. Rillenkarren and spitzkarren are caused by acidic water which condenses on cave ceilings. When the water drips to the floor, it drills corrosion furrows in floor bedrock, breakdown, and flowstone (Figs. 16, 27, 29). Corrosion channels form when CO_2-rich air moves along a cave ceiling. "Punk rock" forms where corrosive air attacks and weathers the bedrock.

Condensation-corrosion can also modify speleothem surfaces or produce distinct speleothem types. Rims are a type of speleothem produced by this process, and the dull-white speleothems in Spider Cave and in the Lake of the Clouds area, Carlsbad Cavern (Pls. 10A, B, Fig. 64), have been highly corroded by this process. Condensation-corrosion may be an ongoing process in some passages, e.g. at Taffy Hill in the Main Corridor, Carlsbad Cavern. Dense fogs sometimes accumulate there, especially in the fall (McLean, 1976), and the condensation water may be responsible for the corrosion of drapery speleothems. Thrailkill (1965b, figs. 28, 31) showed that the water on Taffy Hill flowstone goes from slightly calcite-supersaturated to slightly calcite-undersaturated down-flow, as might be expected if condensation water was diluting flowstone-depositing water. The process of condensation-corrosion may be exemplified by the Lake of the Clouds-Bell Cord Room area, Carlsbad Cavern (Figs. 93, 94):

(1) Carbon dioxide degassed from the water table when the water table was at the level of the Lake of the Clouds Passage. The degassing caused cave rafts to precipitate at the water surface and cave clouds to coat rock projections beneath the water surface (Fig. 94). Water dripping from the ceiling sank the floating rafts and they accumulated at drip points to form the giant cones of the Balcony.

(2) The solubility of carbon dioxide in water increases as the temperature decreases. If the air at the Lake of the Clouds was warmer than the air in upper connected passages (as is the case today, Fig. 19), then this temperature gradient would have forced the air to rise from the Lake toward higher cave passages and to collide with bedrock and speleothems equilibrated at a lower temperature. The carbon-dioxide-charged water thus condensed on speleothems or bedrock and corroded them in a direction facing the Lake of the Clouds. Air flow translocated the condensed water (now saturated with calcium carbonate) around to the edges of the corroded areas, and degassing of excess carbon dioxide caused the deposition of rims along the perimeter of the corroded speleothems or bedrock (Fig. 63).

(3) As the corrosive, moisture-laden air continued to rise

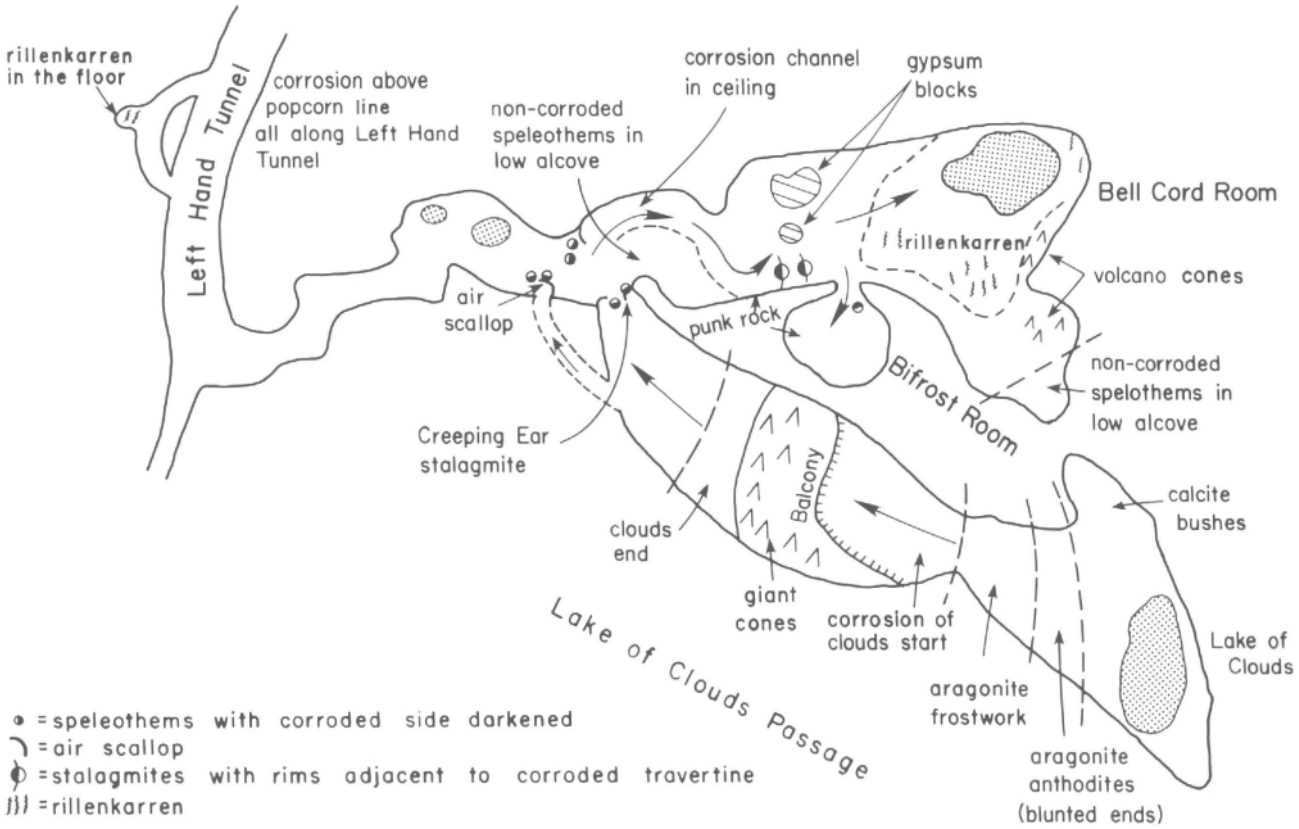

FIGURE 93—Corrosion features in the Lake of the Clouds Passage, Bell Cord Room, and Left Hand Tunnel, Carlsbad Cavern. The corroded sides of speleothems face in the direction of the Lake of the Clouds. Passage width is exaggerated and some side passages are not shown. Arrows indicate direction of air flow causing corrosion. Compare with Fig. 94.

toward the Bell Cord Room, it moved along the ceiling, carving out a corrosion channel and corroding speleothems on the ceiling, but not those on the floor (Fig. 94). Ceiling speleothems became so corroded by the aggressive moisture that, in places, they completely disintegrated down into the joints along which they had formed. Where air flow directly impacted bedrock, the carbonate content of the rock

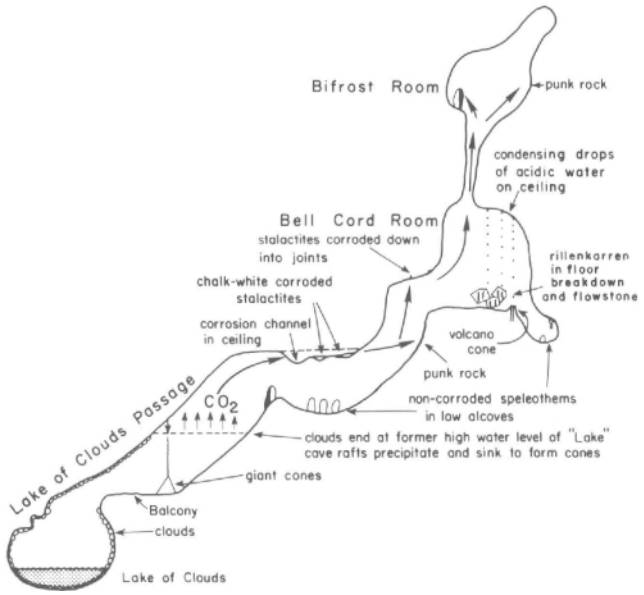

FIGURE 94—Vertical view of Lake of Clouds Passage, Bell Cord Room, and Bifrost Room, Carlsbad Cavern, showing corrosion features. Darkened parts of stalagmites are the corroded sides. Arrows show direction of ascending air flow. Compare with Fig. 93.

was dissolved away, leaving insoluble residue of soft, friable, dark-brown "punk rock." The residue then flaked off onto the floor and formed mounds beneath the corroded punk rock.

(4) In the Bell Cord Room, aggressive water condensed on the ceiling and dripped down onto the floor bedrock and flowstone, corroding out drip points (Fig. 28) and rillenkarren (Fig. 27). This "acid rain" also dripped onto the apices of stalagmites and cave cones, drilling out their hollow centers or volcano-like shapes (Fig. 94).

The process of condensation-corrosion has been documented from caves of other regions as well. In Guisti Cave, Italy, Forti and Utili (1984) found cave clouds, cones, rafts, folia, and corrosion "furrows" (rillenkarren) in an actively forming part of the cave. In Castellana Cave, Italy, P. Forti (pers. comm. 1985) found "corrosion domes" in a dead-end passage of the tourist section of the cave. The air in that passage had 2.5% CO_2, whereas in the non-tourist parts of the cave it had 0.05% CO_2. The corrosion domes in Castellana Cave are believed to have formed within the last 20 years or so, since the cave became commercialized. Sweeting (1973, pgs. 79, 81) described rillenkarren as being "most perfectly developed where water is most highly charged with CO_2… Rillenkarren are formed rapidly, possibly in the space of a few months or years." It is quite conceivable that the corrosion features seen in Carlsbad Cavern and other caves in the Guadalupe Mountains were also produced in a short period of time.

Condensation-corrosion and popcorn line—Condensation-corrosion is believed to have been responsible for the popcorn line of the Big Room-Left Hand Tunnel-Green Lake areas of Carlsbad Cavern. This is supported by the CO_2 measurements and the dating results of this study. U-series and ESR dates on the popcorn of the popcorn line varied from 33,000 ybp to >350,000 ybp (Table 24, samples 23, 24,

25, 26). Thus, the popcorn formed over an extended length of time rather than in one "waterline" episode, as suggested by Jagnow (1979). The dates on the popcorn by the Lion's Tail, Big Room, and on the travertine beneath the popcorn (Table 24, sample 27) show a gradual change from a moist, travertine-depositing environment to a more evaporative, popcorn-depositing environment.

Carbon-dioxide levels along Left Hand Tunnel are consistently higher near the ceiling than they are near the floor (Table 5). (Measurements obtained by the second bridge are an exception to this rule; these were made one-third of the way to the ceiling and one-third of the way to the floor because the actual ceiling and floor were impossible to reach.) Thus, condensation-corrosion should be expected to take place preferentially near the ceiling; this is corroborated by the corrosion on the upper walls and ceilings of the passage, above the popcorn line.

The present-day carbon-dioxide levels (up to 1,000 ppm; Table 5) are probably not nearly as high as in the past, when the water was much higher in the reef and CO_2 was degassing from the surface of the water table. The process of condensation-corrosion has probably been in effect from the beginning of the subaerial stage until the present, but it appears not to be nearly as active today. This is evident from a number of wet and dry "post-corrosion" speleothems in the Lake of the Clouds area that are uncorroded (Pl. 1A). Flowstone in the Bell Cord Room, which displays rillenkarren corrosion (Fig. 27), has been dated at about 150,000 yrs (Table 24, samples 18, 19); the main corrosion event in this area thus took place after that time. One small area of condensation-corrosion in progress can be seen near the second bridge in Left Hand Tunnel, where there is a sudden change from 89% to 100% humidity (Table 5). Here, droplets of water are condensing on the eastward (humid) side of a limestone pendant, and wet, flat-bottomed (tray) popcorn is depositing on the westward (drier) side of the pendant, below the popcorn line.

The popcorn line in Carlsbad Cavern can be related to the process of condensation-corrosion and also to patterns of air flow and density. The Green Lake-Lion's Tail-Crystal Springs Dome areas of popcorn all line up (Fig. 62), as if dry air from the entrance has moved into the cave along this route. Side passages do not experience such direct-line air flow, and so the popcorn line "falls off" into side passages; or, where passages make a turn (such as near the Temple of the Sun), the popcorn line jags abruptly down-ward. Cold, dense air sinks to the floor, whereas warm, less dense, humid, corrosive air rises to the ceiling. Based on the fact that the popcorn line is approximately at the same elevation everywhere in the cave (Table 19), the air that was responsible for it must have been highly stratified, with cold, dry air from the entrance settling to the floor in passages at the Big Room level, and with warm, moist air reaching the ceiling as it flowed out of the cave. The sharpest stratification in temperature, humidity, and CO_2 content appears to have been at the wall "notch," which corresponds to the maximum diameter of the passage.

Bat guano

Bats are known from the fossil record back to Eocene time (Romer, 1966), and so they could have inhabited Guadalupe caves since the passages became open to the surface. Bat guano in Guadalupe caves has been carbon-dated by other studies, but only minimum dates have been achieved for the deposits using this method (Table 24). The bat guano in New Cave has been carbon-dated at >17,800 ybp in one analysis, and from >28,150 (22 cm below a flowstone cap-rock) to >32,500 ybp (2.2 m below the caprock) in another analysis. A guano sample from an upper level in a miner's trench, Ogle Cave, has been dated at 4,150-7,300 ybp (D. DesMarais, pers. comm. 1983).

Animal bones

From the dates on animal bones (Table 21) it appears that Carlsbad Cavern has been open to the surface longer than other Guadalupe caves. This is perhaps due to the fact that the Natural Entrance is at the top of a ridge, whereas en-trances to other Guadalupe caves are deeper in canyons which have been more recently dissected by erosion. The 111,900 ybp date on the sloth bones of Lower Devil's Den, Carlsbad Cavern (Table 24), suggests that the Natural Entrance was open during, and possibly ever since, that time. (Type II rafts on the Balcony of the Lake of the Clouds Passage, dated at 50,000 yrs, have a carbon-oxygen signature which also suggests substantial air flow and evaporation by this time; see Fig. 98, plot of Type II versus Type I rafts.) The dates on animal bones in other Guadalupe caves confirm that erosion of the reef had exposed many cave entrances and pits into which animals wandered or fell by at least 35,000 yrs ago.

Importance of Guadalupe caves to regional geology

Age of Guadalupe caves

The spar at the Big Room level, Carlsbad Cavern, has been ESR-dated at 879,000±124,000 ybp (Table 24). This age probably exceeds (but not by much) the time when the water table was at the level of the Big Room. The approximate 600,000 ± 200,000 ybp date on the Texas Toothpick stalagmite in Lower Cave (Table 24) and the >730,000 ybp (but probably <0.9 my) date on the silt in Lower Cave (Table 25) put the time of water-table development at the Lower Cave level approximately at 750,000-800,000 ybp. The difference in elevation between the Big Room and Lower Cave is 33 m (Fig. 17), so the rate of water-table lowering in Carlsbad Cavern is estimated to have been approximately 0.03-0.07 cm/yr.

Based on these data, the lower levels of Carlsbad Cavern (Lower Cave and the Big Room) are approximately 750,000-850,000 yrs old, and the upper level (Bat Cave) is approximately 1.2 my old (using the 0.05 cm/yr value as the rate of water-table lowering). Caves in the southwestern, higher parts of the Guadalupe Mountains are older than Carlsbad (Fig. 86); if one assumes a constant rate of uplift and water-table lowering over time, then a cave like Cottonwood, with an entrance elevation of 2,074 m (6,819 ft), is roughly 3 my old. Thus, the caves of the Guadalupe Mountains are late Pliocene-Pleistocene in age, a judgment that agrees with King's (1948) contention that the major rise of the Guadalupe Mountains occurred in the late Pliocene to early Pleistocene.

Cave development in present erosion cycle

Based partly on what he thought was evidence of a past "stream" in Lower Cave, Carlsbad Cavern (i.e. the cobble gravel and silt), Bretz (1949) postulated that there had been two exhumations of the reef escarpment: a pre-Ogallala one, at which time the caves developed, and a present-day one, of canyon downcutting. Motts (1957, 1959) and Bach-man (1976) disagreed with Bretz's idea that there had been a post-peneplain Pecos Valley deeper than the present one. Bachman cited drill-core data for thinning of the Ogallala Formation south and southwest of the Llano Estacado, and Motts presented evidence that cave formation is still going on today, even though the potentiometric surface in the

Capitan reef aquifer is over 100 m lower than the potentiometric surface in the Gypsum Plain.

This study supports Motts' and Bachman's thesis of only one exhumation of the reef and contends that: (1) the cobble gravel in Lower Cave may be a debris flow rather than a stream deposit, and (2) the silt overlying the cobbles is autochthonous residue derived from the dissolution of bedrock. Thus, an ancestral Pecos Valley deeper than the present one need not be invoked to explain the cobble and silt deposits in Lower Cave.

The <1,000,000 yr dates on the spar, travertine, silt, and calcified siltstone-cave rafts confirm that the caves date from the present erosion cycle (Table 24). Cave rafts always deposit on a water surface; if the rafts of the siltstone-raft sequence formed at the surface of the water table during an earlier erosion cycle, then this sequence should be covered with other subaqueous deposits rather than having air space or subaerial travertine overlying them.

Rate of canyon downcutting

The bat-guano deposits of New Cave are unusual in that they have been water-washed, mixed with silt, and bat-bone fragments in them have been stratified with respect to different types of bone pieces. The most likely explanation for this distribution is that flood water entered New Cave from the stream bed of Slaughter Canyon when the stream bed was at the level of the New Cave entrance, instead of being 174 m below the entrance as it is today. If this is the correct explanation for these unusual deposits, then the washed guano-silt can be related to the rate of downcutting in Slaughter Canyon. R. H. Brown (in a letter to Carlsbad Cavern National Park, 1981), reported a date of >32,500 ybp for the bat guano in New Cave (Table 24). Using this as a minimum date for the guano, the rate of downcutting in Slaughter Canyon can be calculated at <4.5 cm/yr.

Guadalupe caves and Pleistocene climate

Bachman (1974) assigned the most humid climate and greatest erosion in the Delaware Basin to the middle Pleistocene (approximately 600,000 yrs ago), when the Gatuña Formation was being deposited. This assignment correlates with the carbon-oxygen-isotope data on the Texas Tooth-pick stalagmite in Lower Cave, Carlsbad Cavern, which is approximately 600,000 yrs old in its center (Fig. 75). The carbon-oxygen composition of the Texas Toothpick stalagmite is low for the period >350,000 yrs to the center of the core (600,000 yrs), suggesting that this period may have been dominated by forest types in a wet and humid glacial stage.

Later in the Pleistocene, approximately 140,000-170,000 ybp, there was another wet stage (the penultimate glaciation), during which a large amount of travertine deposited in the Georgia Giant stalagmite, Carlsbad Cavern (Fig. 74). Then, 120,000-130,000 ybp (the last interglacial) there was a cessation of growth which corresponded to a semiarid grass and sedge environment (Fig. 77). Harmon and Curl (1978) found a similar trend of late Pleistocene growth in the travertine of Ogle Cave. Around 200,000 ybp, after the initiation of pluvial glaciation, there was a maximum amount of growth; then, at 125,000 ybp, growth ceased as a change from pluvial to arid climate ensued.

Wet and dry climatic conditions can also be deduced from the amount of travertine deposited during certain intervals. Maximum growth of the Georgia Giant stalagmite on Iceberg Rock, Main Corridor, occurred during a glacial maxi-mum at 140,000-150,000 ybp, and all growth ceased from 120,000-130,000 ybp, during the well-documented warmest phase of the last interglacial (Fig. 77).

Relationship of Guadalupe caves to oil and gas fields of Delaware Basin

According to the findings of this study, the genesis of Guadalupe Mountain caves is related to the oil and gas fields of the Delaware Basin. Where hydrocarbons migrated updip in the basin and mixed with overlying Castile anhydrites, H_2S and CO_2 were produced. These gases moved further up dip along the base of the impermeable halite beds in the Castile Formation until they intersected north-south joints, whereupon the gas moved into the reef to form the caves of the Guadalupe Mountains. Alternatively, the gas generated at the base of the Castile Formation moved up into the reef along the Bell Canyon Formation (Fig. 87). Where halite beds remained intact in the basin, H_2S and CO_2 continued to migrate into the reef to form caves; how-ever, where the margin of halite dissolution moved past a cave location in the reef, development of that cave stopped.

The movement of the halite margin past specific cave locations may be the reason why the caves in the Guadalupe Mountains seemingly "die with depth." The lowest cave passage in the Guadalupe Mountains is the Lake of the Clouds, Carlsbad Cavern; the halite margin in the Gypsum Plain has moved approximately 0.5 km past the north-south extension of this passage (Fig. 85). According to Bachman and Johnson (1973), the horizontal rate of dissolution of halite in the Gypsum Plain has been 10-13 km/1,000,000 yrs (this is a minimum rate according to G. Bachman, pers. comm. 1986). Using this rate and the distance of 0.5 km, it can be calculated that the halite margin moved past Carlsbad Cavern roughly about 50,000 yrs ago. The age of the upper part of the cave-raft cones on the Balcony of the Lake of the Clouds Passage, which probably signifies the last episode of significant CO_2 degassing at the water table in Carlsbad Cavern, is 50,000 ybp (Table 24, sample 30). In the same area of the cave (the Christmas Tree Room), sulfur crystals overlie cave rafts and other speleothems. Thus, the last injection of CO_2 (and presumably H_2S) into Carlsbad Cavern roughly correlates in time with the movement of the halite margin past Carlsbad Cavern.

Implications for evolution of intracratonic basins

Mississippi Valley-type ore deposits

The evolution of intracratonic basins, where carbonate rocks (very often reef masses) host ore deposits along basin margins, has been the topic of much discussion among ore geologists. The results of this study are compatible with the thesis that some sulfuric-acid-formed caves (like those in the Guadalupe Mountains surrounding the Delaware Basin) may be a manifestation of the evolution of intracratonic basins, as are hydrocarbon deposits and Mississippi Valley Type (MVT) sulfide-ore deposits.

Two basic depositional models have been proposed for MVT mineralization: (1) a "non-mixing" model, where metals and reduced sulfur (H_2S) move together in brines from basins into carbonate margins; and (2) a "mixing" model, where metals and reduced sulfur move separately (Anderson and Macqueen, 1982). MVT deposits are known to occur worldwide and are usually karst-related. Considerable variation exists among different MVT deposits, especially in the amount of mineralization and carbonate solution (karst development), and also in the relative timing of gas migration, ore mobilization, sulfide precipitation, and carbonate solution.

Carbonate rocks surrounding the Delaware Basin of southeastern New Mexico contain small deposits of MVT sulfides. Mazzullo (1986) reported Pb-Zn MVT mineralization on the southeastern side of the basin, and barite has been found in the southwestern (Apache Mountains) part of the basin (McAnulty, 1980). Iron (as pyrite, in distinct

large crystals) and other metals are known to occur in the Guadalupe Mountains, on the northwestern side of the basin. The pyrite occurs in shelf rocks (primarily the Yates Formation). One piece of pyrite, collected from Guadalupe Ridge near Dark Canyon Lookout, exhibited concretionary structure in thin section, but no detailed petrographic analyses have been done to determine if the pyrite is of epigenetic or syngenetic origin. Anomalous concentrations of arsenic, barium, cadmium, copper, lead, molybdenum, silver, and zinc have been found at localities near the center of Guadalupe Ridge and on Lonesome Ridge. These metals are concentrated in an iron-stained sandstone unit (the lower Yates?) near the top of the Seven Rivers Formation; this sandstone represents a zone of high permeability that controlled the migration of weakly mineralized epigenetic fluids (Light et al., 1985).

The caves of the Guadalupe Mountains may relate to the problem of MVT sulfides, especially according to the "mixing" model, where metals and hydrogen sulfide move into host carbonate rocks separately, at different times, or from different sources. Using the results of this study and the Delaware Basin as a model, the following interpretation of MVT ore deposits is suggested.

(1) Hydrogen sulfide ascends from the basin in gas-phase transport (as indicated by late-stage, subaerial, sulfur deposits in Guadalupe caves). This mechanism eliminates the problems involved with compaction-driven-flow models such as discussed by Bethke (1985).

(2) Basinal rocks supply the hydrogen sulfide necessary for MVT mineralization, whereas backreef carbonate and evaporite rocks supply the metal. Chloride-rich brines have the ability to leach trace quantities of metals from rocks through which they flow. The metals move downdip along backreef beds by gravity flow until they reach the host reef rocks.

(3) Flow of gas from basin to reef is through shallow carbonate horizons at the basin edge. Hydrogen sulfide, according to the sulfuric-acid mechanism proposed in this study, is responsible for dissolving out cave voids along the reef margin of the basin. These sulfuric-acid reactions prepare the rock for epigenetic sulfide-mineral emplacement in karstic voids along basin margins, and also provide the low pH's necessary for the concentration of metals such as lead and zinc. Stratiform metal sulfides (and cave levels) form within a narrow range of elevations corresponding to water-table base levels where oxidation is the most pronounced.

(4) Ascending hydrogen sulfide mixes with descending metal-bearing solutions; where H_2S and carbonate rock are encountered, metal sulfides precipitate. The metal sulfides thus deposited typically display hopper, colloform, stalactitic, rhythmically banded, and sometimes liesegang-ring type structures where they fill karstic voids.

(5) Cave dissolution (and ore mineralization) do not necessarily occur in a hydrothermal regime (as suggested by carbon-oxygen signatures of bedrock; this study). Homogenization temperatures (50-200°C) of fluid inclusions in MVT ore minerals may possibly be caused by exothermic reactions or other unknown factors.

(6) According to some models of MVT mineralization, low pH and high total dissolved CO_2 are required for ore-forming fluids. According to the model of speleogenesis proposed in this study, both carbon dioxide and hydrogen sulfide ascend from basin to reef and could fulfill these requirements. Sulfuric-acid solutions could be responsible for periods of dissolution and etching of MVT sulfide crystals.

(7) The release of gas in the basin occurs episodically, so that hydrogen sulfide enters the caves in "pulses" or "gasps" (as indicated by possibly more than one episode of sulfur mineralization in the Christmas Tree Room area, Carlsbad Cavern). This episodic infiltration of gas may account for the zoning so commonly seen in MVT sulfide minerals. During each "pulse" the gas diffuses slowly through the wall rock of karstic voids, resulting in well-formed and large sulfide crystals.

(8) Gravity-driven flow may not be essential for hydrogen sulfide entering from basin into reef. According to Sares (1982) there is a hydrologic barrier between basin and reef in the Guadalupe Mountains, and according to Hiss (1980) the hydrologic gradient in the basin is parallel to the reef front, not perpendicular to it; thus, the desired gravity-driven "plumbing system" expected for fluid movement from basin to reef does not seem to exist in the Guadalupe Mountains area. Similar hydrologic conditions have probably been operative during the last half a million years or so (Bach-man, 1984); yet, even possibly as late as 50,000 ybp, gas entered Guadalupe caves along beds dipping up from the basin and into the reef.

(9) If a basin has a limited source of metal but abundant hydrogen-sulfide generation within it (as has apparently been the case of the Delaware Basin), then only small amounts of ore will be deposited along basin margins, but large caves can develop there from H_2S-sulfuric-acid reactions. However, if a basin contains a sufficient source of metal (as has apparently been the case of the Illinois Basin), then the H_2S will react with the metal to form extensive sulfide-ore deposits along basin margins, but karst development will be limited.

(10) One thesis that has been central to MVT ore-mineralization theories is that ore-H_2S-bearing fluids are highly saline, Na-Ca-Cl brines (Anderson and Macqueen, 1982). However, the gypsum deposits in Guadalupe caves-which are the end product of H_2S migration from the Delaware Basin-are notably low in sodium and chloride (Na = 0.05-0.1 wt%, Cl = 4.6 ppm; Table 26). Perhaps, since there seems to be a limited supply of metal associated with the development of the Delaware Basin, very little metal-chloride complexing took place. Or, perhaps, these sodium and chloride ions never became concentrated enough to be precipitated and were instead discharged by the Capitan aquifer system (Na = 1-30 ppm, Cl=11-85 ppm; Table 2).

(11) The pyrite in the Yates Formation may have formed from the reaction of epigenetically introduced hydrogen sulfide (coming up from the basin) with iron (in the silt-stone). Where this hydrogen sulfide reacted with oxygen in cave voids, it formed native sulfur.

(12) Anomalous uranium in the cave rafts of the Christmas Tree Room (U=238 ppm) may also be the result of a MVT-type precipitation mechanism. Uranium is soluble in oxidized form, but where circulating ground water is reduced in an H_2S-rich environment (such as in roll-front deposits), uranium is precipitated. A high concentration of uranium may also be expressed in radon-daughter products and gamma radiation (Table 6); high radon associated with the grayish-green montmorillonite clay in Lower Cave may be especially significant, since uranium is readily taken up or "fixed" by montmorillonite-type clay under low pH conditions (U = 320 ppm; Table 17).

Other cave systems fringing basins

Two other cave systems—Fiumo Vento, Italy, and Akhali Atoni, USSR—fringe basins which are known to generate large quantities of hydrogen sulfide. Fiumo Vento Cave (in the Apennine Mountains that rim the west side of the Adriatic Sea Basin) resembles Guadalupe caves in that it has large rooms, boneyard under large rooms, tubular pits, gypsum blocks and rinds, montmorillonite-endellite clay (with associated opal rather than chert), and condensation-corrosion features (Hill, in press). Hydrogen sulfide is detect-

able near the water table, but the ultimate source of this gas has not been determined (P. Forti, pers. comm. 1986). It is possible that H_2S derives from oil and natural-gas deposits in the Adriatic Sea Basin about 50 km to the east.

Akhali Atoni Cave in the Caucasus Mountains about 2 km from the edge of the Black Sea Basin may be another sulfuric-acid cave like those in the Guadalupe Mountains. Akhali Atoni is developed in thick Mesozoic carbonate rocks which dip southward, toward and underneath the Black Sea. It displays huge chambers and galleries (up to 95 m long, 60 m wide, and 90 m high) and has good phreatic form, as is typical of Guadalupe caves. The current thinking on the speleogenesis of Akhali Atoni is that it was opened by rising warm waters, enlarged by warm-water-meteoric-water mixing effects, and then progressively abandoned by a lateral and downward shift of spring points (D. C. Ford, pers. comm. 1986).

Other models of speleogenesis for Guadalupe caves

The results of the sulfur-isotope study are crucial to understanding the process of speleogenesis which produced the large cave passages in the Guadalupe Mountains. The cave gypsum could not possibly have derived from the Castile anhydrite beds as suggested by the local pooling model of Bretz (1949) or the mixing model of Queen et al. (1977a). The average isotopic composition of the Castile anhydrite is +10.3 (Table 23); if the cave gypsum originated by non-biological precipitation from Castile brines, then the cave gypsum and Castile anhydrite should have almost identical isotopic compositions. The whole-rock analyses, that show the cave gypsum not to be related chemically to the evaporates of the Gypsum Plain (Table 26), provide further evidence against the speleogenesis models of Bretz and Queen.

Egemeier (1971, 1973, 1981) and Maslyn (1979) suggested that the Big Horn Basin, Wyoming, caves dissolved by sulfuric acid. Egemeier, and later Davis (1979a), extended the concept of sulfuric-acid dissolution and replacement-solution to the caves of the Guadalupe Mountains, whereby cave walls are replaced and then enlarged. These authors cited blindly terminating passages of large diameters, native sulfur, and carbonate-free gypsum in Big Horn Basin caves as features mimicking those in Guadalupe caves.

The Big Horn Basin caves do resemble Guadalupe caves superficially, but upon close inspection many important dissimilarities emerge.

(1) Guadalupe caves show little or no evidence of thermal activity such as is associated with the replacement-solution caves of the Big Horn Basin. They do not possess thermal springs or spring slots, features important to Egemeier's replacement-solution model of speleogenesis.

(2) Blind cave-passage terminations do occur in Big Horn Basin caves, but only on their upslope ends, near the input points of thermal springs. Guadalupe caves have no such upslope spacial correlation with respect to pits or fissures.

(3) The gypsum in Guadalupe caves does not form as mounds on the floor corresponding to sluffed-off ceiling crusts; where it has not been dissolved away, the gypsum exists as continuous or segmented floor blocks.

(4) Replacement-solution gypsum crusts in Big Horn Basin caves occur as millimeters or centimeters thick, friable masses overlying cave walls and ceilings. In most Guadalupe caves, thin ceiling or wall crusts are rare or absent.

(5) Gypsum-limestone pairs in Big Horn Basin caves show correspondence in cation ratios, whereas those in Guadalupe caves do not (Fig. 79).

Jagnow (1977, 1979) also suggested that Guadalupe caves dissolved by sulfuric acid, but proposed that pyrite was the source of the acid. According to Jagnow's model, pyrite in the Yates Formation weathered and oxidized to sulfuric acid which moved downdip along backreef bedding planes until it reached the Capitan Limestone, where it dissolved out the large cave passages. A number of objections can be made to Jagnow's pyrite model of speleogenesis.

(1) Not enough pyrite exists in the Yates overburden to explain the immensity of the caves. As pointed out by Davis (1980), large caves like Carlsbad Cavern are not located near pyritic masses in the Yates Formation. Morehouse (1968) found up to 16% pyrite and marcasite in limestone overlying the Dubuque, Iowa, caves, but those caves are of limited extent both vertically and horizontally. Young (1915) described caves associated with pyrite near Battle Mountain, Nevada, but those are also small and are located directly beneath pyrite seams in the rock.

(2) It is highly doubtful that the sulfuric acid derived from pyrite could have remained in an unreactive state while it moved downdip to the cave-forming zone. If bedding surfaces in backreef beds were avenues along which sulfuric acid entered the reef, then why did it not react with the limestone immediately to form caves in the backreef beds (or why did it not dissolve the limestone right at its point of weathering)? Vear and Curtis (1981) reported that for the weathering of pyritic shales in England, more than 99% of the sulfuric acid produced is immediately consumed in carbonate dissolution reactions or in clay-mineral transformations. Keller et al. (1966) measured a pH of 1 in a pyritic shale in Indiana and a pH of 3.5 only 1.2 m below the shale where sulfuric acid reacted with limestone. In the Guadalupe Mountains, immediate reaction of pyrite-derived sulfuric acid with limestone also appears to be the case. On the surface around limonite-after-pyrite crystals one often finds solution cups that are approximately two to three times the diameter of the crystals themselves. This association suggests that, upon weathering and oxidation, an immediate sulfuric-acid reaction etches out a "nest" cup in the limestone around each pyrite-limonite crystal.

(3) When pyrite-produced sulfuric acid reacts with lime-stone, it produces the SO_4^{2-} ion in solution. It is the sulfate ion which moves downdip and into the caves, not the sulfuric acid; the sulfate ion either remains in solution or it precipitates as sulfate speleothems in the air-filled part of the cave. If pyrite was the main supplier of dissolved sulfur to Guadalupe caves, then why are there so few sulfate speleothems in the caves (with the exception of Cottonwood Cave, which lies directly below the pyritic Yates sandstone)? As discussed in Part II of this report, sulfate speleothems have sulfur-isotope signatures that suggest they may have derived from pyrite.

(4) The δ34S value of -2.5 for pyrite in the Yates Formation (Table 22) suggests that the cave gypsum (average $\delta^{34}S$ = -15.1) may not be genetically related to the pyrite.

(5) Native sulfur in Carlsbad Cavern is found on the undersides of bedrock and speleothems, which suggests a source of sulfur from below, not from above as proposed by Jagnow.

(6) As Davis (1980) pointed out, Guadalupe caves do not possess vertical shafts beneath points of sulfuric acid input. Enlarged fissures and shafts are located below, not above, large rooms. The only cave in the Guadalupe Mountains which perhaps conforms to Jagnow's sulfuric-acid model is

the Queen of the Guadalupes, a 60 m deep vertical-shaft complex which underlies limestone containing a gossan mass of hydrated iron oxide.

(7) Jagnow's interpretation of the role of pyrite in speleogenesis may be backward. As discussed in the section on Mississippi Valley-type ore deposits, the pyrite may be the result of cave-forming processes rather than the cause of them.

Recently, DuChene (1986) proposed another source for the hydrogen sulfide that dissolved Guadalupe caves. DuChene agreed with a sulfuric-acid model related to oil and gas as proposed in this study, but he thought that the most likely source area for the H_2S was east of the Guadalupe Mountains and the most likely migration path was updip through the Capitan aquifer. DuChene speculated that the Guadalupe Mountains are hinged near the present location of the Pecos River and that west of this hinge line oil and gas are absent in the reef because they moved updip and out of the system, the H_2S having dissolved out Guadalupe caves during its migration.

DuChene (1986) raised some important objections to the model proposed in this study, in particular hydrologic problems of moving gas from basin to reef, and stratigraphic problems concerned with the non-continuous, lenticular sandstone bodies within the Bell Canyon Formation and with the fact that these sandstones may not intertongue significantly with the Capitan Limestone. It is DuChene's belief that these factors could limit, but not necessarily to-tally prevent, the migration of gas from the Delaware Basin into the Capitan Limestone. DuChene's model, however, also has its problems.

(1) If hydrocarbons once existed in the reef rock of the Guadalupe Mountains before uplift, as they do today in areas of the uplifted shelf rock (Ward et al., 1986, fig. 14), then why is there a negligible hydrocarbon content in Guadalupe caves and cave deposits (0.015 mg/g, Moran, 1955; 0.5 ppm, Table 15)?

(2) Why does there appear to be a correlation in age between the movement of the halite margin in the basin past Carlsbad Cavern and the time of the last speleogenesis events in the cave?

(3) DuChene's model implies that hydrocarbon migration and cave development occurred early in the uplift of the Guadalupe Mountains, and that all the formational oil and gas once contained in these reef rocks has since escaped out of the system. If this is true, then why do sulfur crystals overlie late-stage speleothems in the Christmas Tree and New Mexico Rooms?

(4) In Carlsbad Cavern sulfur is associated with the Bell Canyon(?) Formation and forereef facies, beds that dip directly toward the basin.

Future research needs

This study attempts to tie together all of the depositional events recorded in Guadalupe caves from Permian time to the present. However, it does so in an overview form rather than in detail, and many problems still remain to be re-solved.

Facies—Where exactly are the reef, forereef, backreef, and basinal facies exposed in the caves? What criteria distinguish these facies? Are the Seven Rivers and/or Bell Canyon Formations present in Carlsbad Cavern? Do the sands in the Big Room and New Mexico Room represent intertonguing facies of the Bell Canyon Formation? How has the composition of the limestone and/or dolomite affected the dissolution of the cave passages?

Stability of endellite—How does limestone residue turn to montmorillonite clay and at what acidity does the montmorillonite change to endellite? What processes are involved in the mineral transformation of montmorillonite to endellite and how does the structure exclude contaminant material? What factors cause the different colors of endellite?

Cobble-silt transition—A deeper trench needs to be dug in Lower Cave to see if the cobble-silt interface is a true unconformity. Textural differences of both types of deposits need to be further studied. Floor silt needs to be more thoroughly correlated with amount and kind of silt residue in the surrounding limestone bedrock.

Gypsum textures—How much of the gypsum precipitated from solution and how much of it had a replacement origin? Was replacement via the Queen model, the Egemeier model, or both? Detailed microscopic work needs to be done on the textural features of the gypsum blocks, followed by comparisons with textures in the Castile Formation of the Gypsum Plain.

Chert precipitation—What exactly are the colloidal mechanisms behind the formation of the chert and the color-banded silt in the Big Room? Were the rhythmic bands in the chert formed by a liesegang-ring type mechanism?

Dating of speleothems and silt—More speleothems in key positions need to be dated in order to test the conclusions of this study and to fine-tune geologic events on an absolute time scale. The ESR-dating method needs to be performed on speleothems >350,000 yrs old. More paleomagnetic dating of silts should be done on different levels in Carlsbad Cavern and also in other Guadalupe caves. Since Guadalupe cave passages are believed to range from <600,000 yrs to 3 my in age, a number of paleomagnetic reversals should be distinguishable in the silt deposits. More samples of montmorillonite clay need to be dated by the potassium-argon technique, and problems related to this method need to be resolved.

Sulfur isotopes—More work needs to be done, especially on vertical sequences of gypsum. Why are the sulfur-isotope values of the upper, younger levels of the gypsum blocks in the vertical suite at the Polar Region less depleted in ^{32}S than the older sections of the block (Table 22)? Also, a sampled gypsum block in the upper Gypsum Passage, Cottonwood Cave, is much less depleted than is sampled sulfur in a block, lower Gypsum Passage. Are these real trends and, if so, what factors caused them?

Chemistry—The sulfur chemistry responsible for the sulfuric-acid dissolution of the caves should be analyzed in detail. The chemical reactions may be multi-step processes involving sulfur bacteria.

Hydrology of cave development-A more elaborate model of the three-dimensional pattern of cave excavation needs to be developed for Carlsbad Cavern and other Guadalupe caves. The geomorphic form of Guadalupe cave passages should be more closely studied in order to gain insight into the hydrologic mechanisms which formed them.

Other Guadalupe caves—The main focus of this study is Carlsbad Cavern. Other caves in the Guadalupe Mountains need to be researched in more detail with respect to the sulfuric-acid model presented herein.

Summary

The most important conclusions of the speleogenesis part of this study are:

(1) Three solution episodes occurred in the Guadalupe Mountains. Solution Stage I caves are an early-stage paleokarst development of probable tectonic and/or solutional origin; these are small fissure caves formed at the contact of the reef-backreef facies, probably during the Late Permian. Solution Stage II caves are enlargements of primary pores and joints in the reef; these are spongework caves phreatically formed in one or more episodes between the Late Permian and the Tertiary. Solution Stage III caves are large passages that represent the final episode of cave development in the Guadalupe Mountains; they formed in the late Pliocene-Pleistocene during uplift and tilting of the Guadalupe Mountains.

(2) Solution Stage III caves dissolved primarily by sulfuric acid. The sulfuric acid was derived from hydrogen-sulfide gas that originated in the oil and gas fields of the Delaware Basin and entered the reef via joints or possibly along the Bell Canyon Formation. Massive gypsum and native sulfur in the caves have $\delta^{34}S$ values as low as -25.6 and -20, respectively. These values correspond to $\delta^{34}S$ values of H_2S gas and sulfur in the Gypsum Plain, which are known to have been generated by hydrocarbon-related re-actions.

(3) The progressive eastward migration of the halite dissolution margin in the Gypsum Plain may have been a factor controlling Solution Stage III cave development in the Guadalupe Mountains. Where halite beds remained intact in the basin, they acted as impermeable barriers preventing hydrogen sulfide from rising to the surface in the basin; instead, the gas rose into the Capitan reef to dissolve out the caves there.

(4) The systematic excavation and integration of Solution Stage III cave passages in the Guadalupe Mountains and the evolution of their unique three-dimensional form are the result of deep phreatic (bathyphreatic) and water-table conditions combined with a sulfuric-acid speleogenesis. Bathyphreatic conditions were responsible for the strong vertical development of Guadalupe caves; water-table conditions were responsible for the horizontal development of caves along certain levels.

(5) The general sequence of deposits in Guadalupe caves as seen in Carlsbad Cavern is: breccia, montmorillonite, spar, calcified siltstone-cave rafts, cobble gravel, endellite, silt and sand, chert, gypsum, breakdown, speleothems, sulfur, bat guano, and animal bones.

(6) The breccia fills Solution Stage I cavities and is encased in a mudstone or spar matrix which, based on carbon-and oxygen-isotope data, is believed to be Late Permian in age. As Solution Stage I caves enlarged along the reef-backreef margin due to tectonic and/or solutional processes, breccia clasts were either sheared in place or gravitated down into Solution Stage I voids.

(7) Montmorillonite clay fills Solution Stage II spongework caves and is probably an autochthonous residue de-rived from that solution episode. The montmorillonite reconstituted from limestone residue in a basic (high pH), high-bicarbonate, slow-flow environment. A potassium-argon date of 188 ± 7 my (Early Jurassic) was obtained for the clay; while highly speculative, this date probably indicates that the montmorillonite clay predates the Solution Stage III episode.

(8) U-series dates of >350,000 ybp, an ESR date of 879,000 ± 124,000 ybp, and carbon-oxygen data on the spar suggest that the large Spar III crystals in Guadalupe caves formed in the shallow phreatic zone during the Solution Stage III episode.

(9) The calcified siltstone-cave rafts are interpreted to be the result of early fluctuation phases of water-table development that antedated the final solutional enlargement of Solution Stage III passages. U-series dates, ESR dates, and carbon-oxygen compositions suggest that the rafts of the siltstone-raft sequence formed on top of the water table at the same time as Spar III crystals were being formed below the water table; this occurred during the present erosion cycle, early in the Solution Stage III episode of cave development.

(10) The cobble gravel exposed in Carlsbad Cavern is an allochthonous deposit composed of backreef clasts and is possibly Ogallala (or Gatuña) material. It is a heterogeneous, poorly sorted, crudely stratified, matrix-supported deposit that is interpreted as a debris flow.

(11) The endellite and chert were derived from the reaction of sulfuric acid on montmorillonite during the Solution Stage III episode.

(12) The fine-grained sediment is an autochthonous residue derived from dissolution of the large, Solution Stage III cave passages. In Lower Cave, Carlsbad Cavern, the silt is >730,000 yrs old as determined by paleomagnetic dating.

(13) The massive gypsum blocks and rinds are late-stage, lagoonal-type deposits resulting from hydrodynamic stag-nation during the water-table stage of cavern development. Textures and distribution of the gypsum attest to its precipitation, replacement, recrystallization, solidification, and compaction.

(14) The greatest amount of breakdown fell soon after the lowering of the water table. An exception to this rule is Iceberg Rock, Carlsbad Cavern, which fell later, between about 180,000 and 500,000 ybp.

(15) Speleothem deposition has occurred in Guadalupe caves since the caves became air-filled. The great mass of travertine material dates from more humid, pluvial stages of the Pleistocene. Many of the speleothems have become highly corroded due to high levels of CO_2 in the caves.

(16) Native sulfur in the caves is the result of oxidation of H_2S gas in a subaerial environment.

(17) Bat guano and animal bones in the caves attest to the fact that bats and other animals entered the caves of the Guadalupe Mountains as soon as the passages became connected to the surface. The entrance of Carlsbad Cavern may have been open as long ago as 112,000 ybp, as indicated by dates on *Nothrotheriops* bones in Lower Devil's Den.

(18) The caves of the Guadalupe Mountains are late Pliocene-Pleistocene in age. Dating results suggest that the Big Room level of Carlsbad Cavern is about 800,000 yrs old and the Bat Cave level is about 1.2 my old. Other caves higher in the Guadalupe Mountains may be as old as 3 my.

(19) The caves of the Guadalupe Mountains may be a manifestation of the evolution of intracratonic basins, as are hydrocarbons and Mississippi Valley-type ore deposits.

PLATE 1

A—Breccia exposed in the north wall of the Guadalupe Room, Carlsbad Cavern. A mudstone matrix fills the spaces between breccia clasts. White material overlying parts of the breccia is a thin carbonate crust. Photo Cyndi Mosch Seanor.

B—Possible unconformity between the underlying light-tan cobble gravel and the overlying orange silt, Junction Room, Lower Cave, Carlsbad Cavern. A light-colored carbonate crust overlies the orange silt. Photo Cyndi Mosch Seanor.

PLATE 2

A—Laminated silt, Lower Cave, Carlsbad Cavern. Photo Cyndi Mosch Seanor.

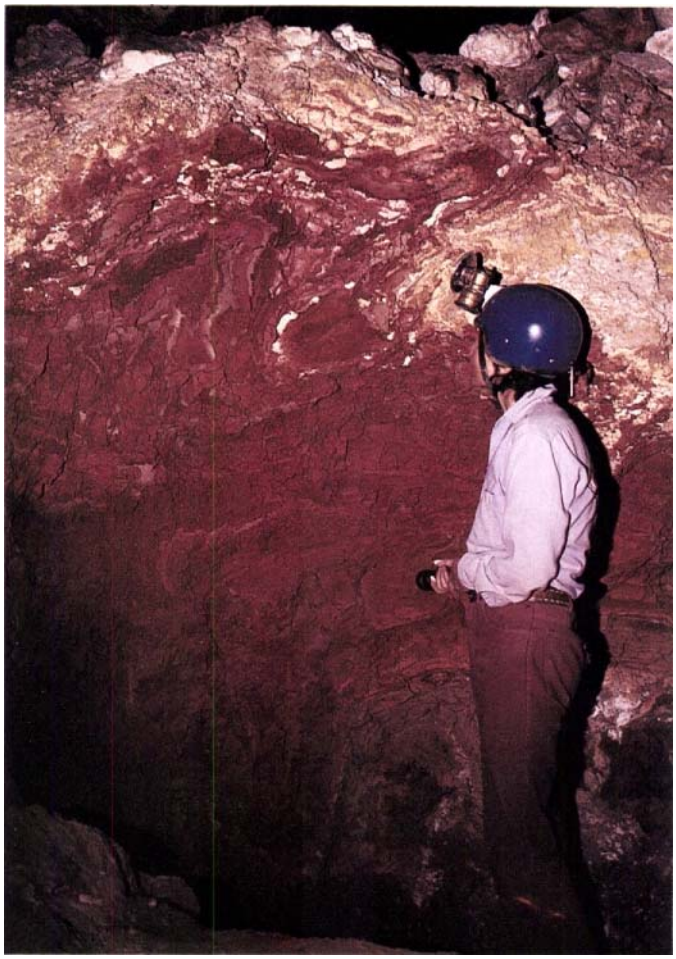

B—Brick-red silt, Big Room, Carlsbad Cavern. White layers are gypsum derived from overlying leached gypsum blocks. Deformation took place while the silt was still wet, and was possibly caused by a piece of breakdown which fell from the roof of the cave. Photo Ronal Kerbo.

PLATE 3

A—Microfolded laminations in a gypsum block near the Jumping Off Place, Big Room, Carlsbad Cavern. Photo Alan Hill.

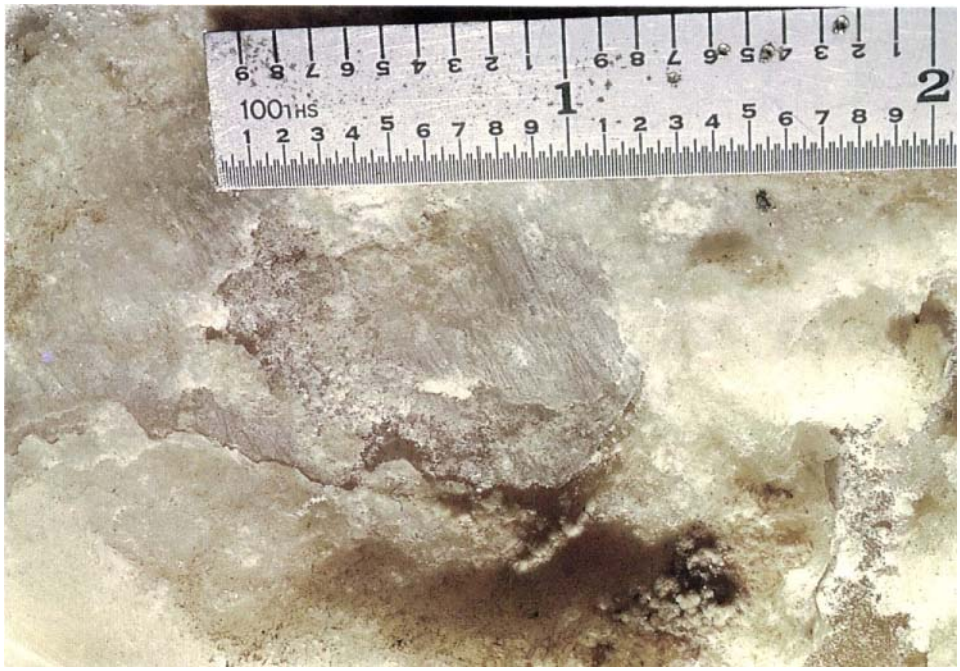

B—Slickensides on a gypsum block, second trail tunnel, Jumping Off Place, Big Room, Carlsbad Cavern. The light-colored gypsum to the right of the slickensides is part of an overgrowth crust. Photo Alan Hill.

PLATE 4

A—Bat guano in a gypsum block, Big Room, Carlsbad Cavern. The guano filtered down into a dissolved hole in the gypsum, and then both the gypsum and guano were drilled and exposed by a drip tube. Photo Ronal Kerbo.

B—Silt banding in a gypsum rind, Pump Room, Carlsbad Cavern. Photo Ronal Kerbo.

PLATE 5

A—Remnant pillar of gypsum, Expressway Passage, Dry Cave. Orange silt and limestone pieces form the darker "belt" of the pillar. Photo Alan Hill.

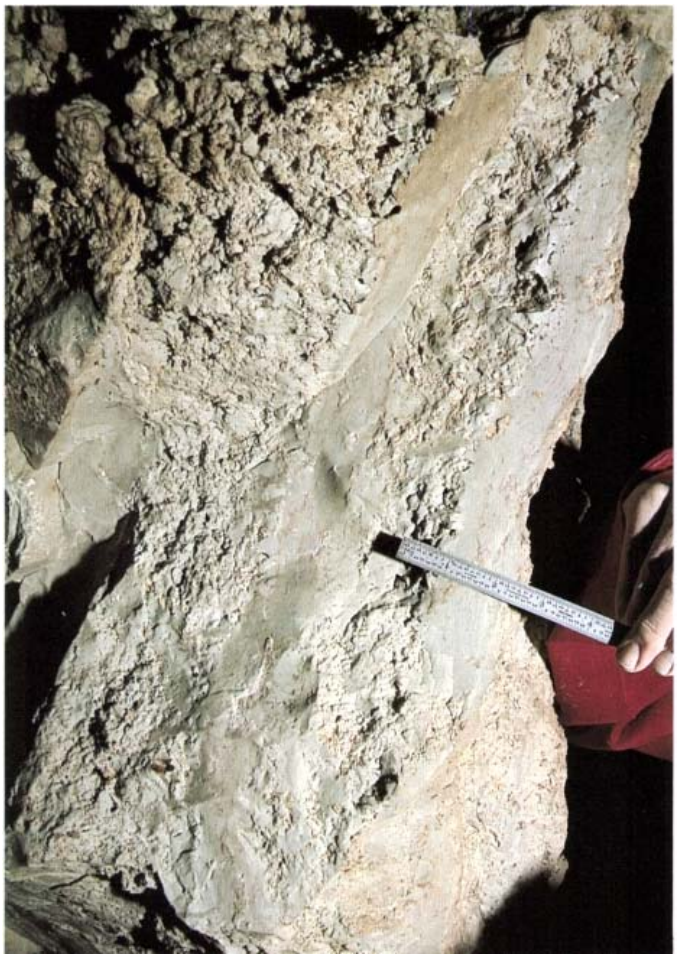

B—Porous and micritic layers in a displaced chert lens, Salt Flats, Big Room, Carlsbad Cavern. The porous layers contain grains of quartz sand in a chert matrix, whereas the micritic layers are free of sand. Note the very fine laminations in the micritic layer where the ruler is resting. Photo Alan Hill.

PLATE 6

A—Grayish-green montmorillonite clay partly filling a solution pocket, Green Clay Room, Lower Cave, Carlsbad Cavern. The clay has dried, cracked, and is sluffing out of the pocket and onto the floor. Photo Alan Hill.

B—Waxy, pure-white endellite in a red-clay matrix, Top of the Cross, Big Room, Carlsbad Cavern. The endellite has formed as a layer between the limestone and the red clay, and also as pods and stringers in the red clay. Photo Ronal Kerbo.

PLATE 7

A—A "vein" of sulfur exposed in a gypsum block filling a joint in the ceiling, Cottonwood Cave. Maximum width of the "vein" is about 1 m. Photo Tom Meador.

B—Canary-yellow crystalline sulfur in a gypsum block, lower Gypsum Passage, Cottonwood Cave. Photo Jerry Trout.

PLATE 8

A—Sulfur crystals on the underside of a projection of bedrock, East Annex of the New Mexico Room, Carlsbad Cavern. Photo Alan Hill.

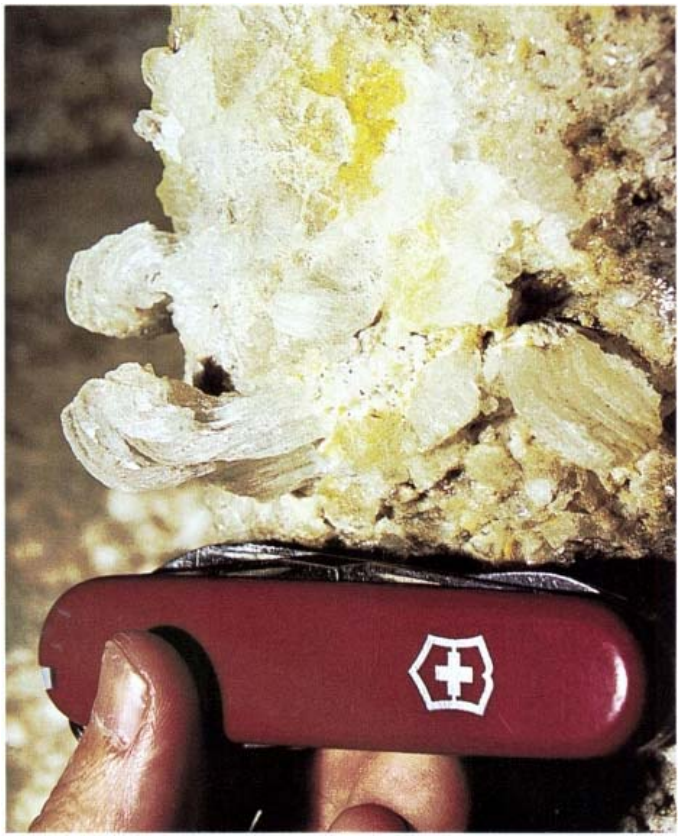

B—Sulfur crystals overlying gypsum flowers and crust, East Annex of the New Mexico Room, Carlsbad Cavern. Photo Cyndi Mosch Seanor.

PLATE 9

A—An etched spar crystal protruding from the wall of the Spar Room, Secondary Stream Passage, Carlsbad Cavern. Photo Cyndi Mosch Seanor.

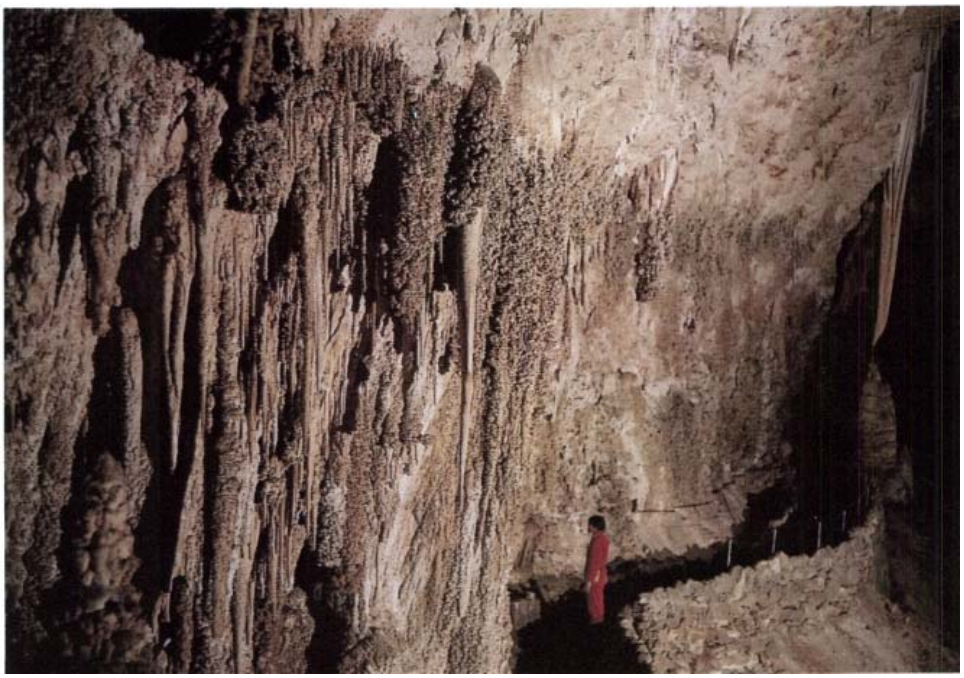

B—Popcorn line along trail near the Lion's Tail stalactite, Big Room, Carlsbad Cavern. Note that the popcorn covers the wall and speleothems below the line, but not above it. Photo Alan Hill.

PLATE 10

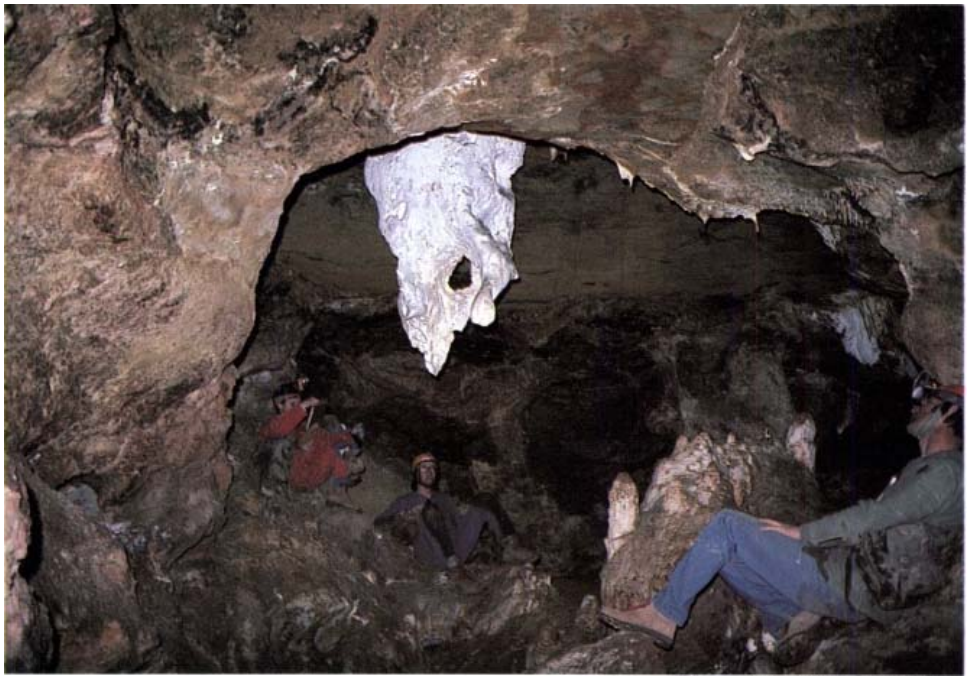

A—A corroded, chalk-white stalactite, Ghost Chambers, Spider Cave. Note the smooth, corroded nature of the bedrock and that the stalactite has been corroded completely through its core in one place. Photo Alan Hill.

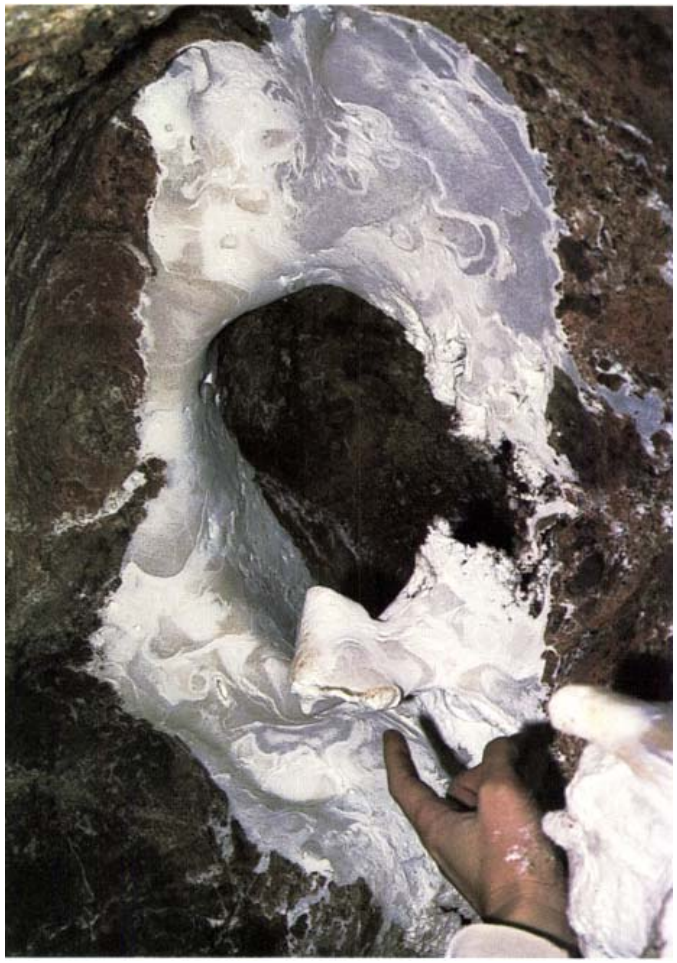

B—Corrosion of ceiling travertine concordant with the ceiling limestone, Spider Cave. Photo Alan Hill.

PLATE 11

A—Lemon-yellow stalactites which have grown subsequent to pronounced corrosion in the Lake of the Clouds–Bell Cord Room area, Carlsbad Cavern. The dark-brown "punk rock" limestone on which the ruer is resting has been corroded in the direction of the Lake of the Clouds, whereas the white-crusted limestone facing in the opposite direction has not been corroded. Photo Alan Hill.

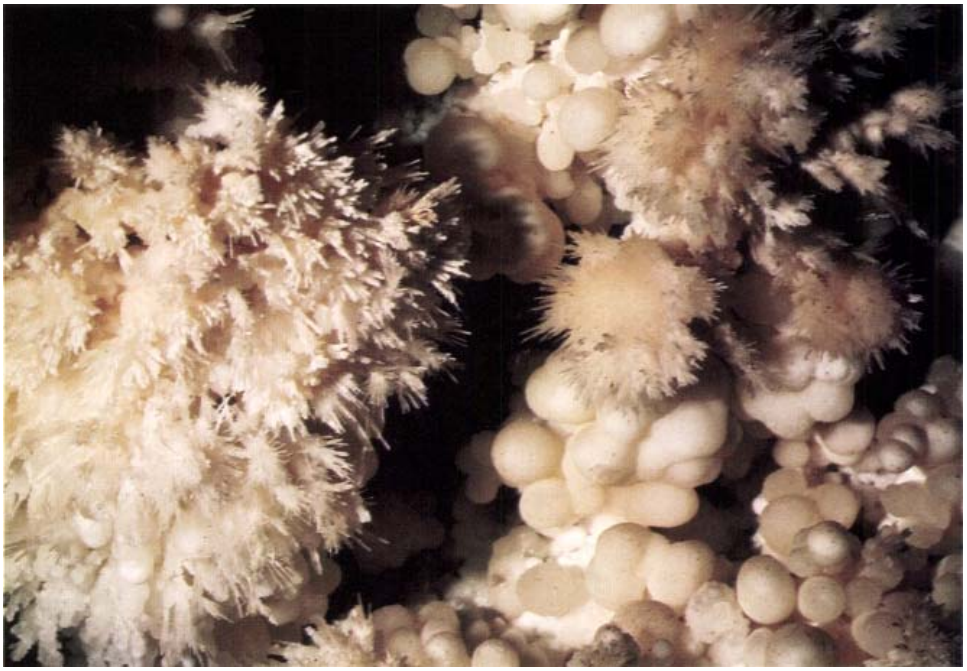

B—Frostwork anthodites of aragonite growing on popcorn nodules, Carlsbad Cavern. Photo Cyndi Mosch Seanor.

PLATE 12

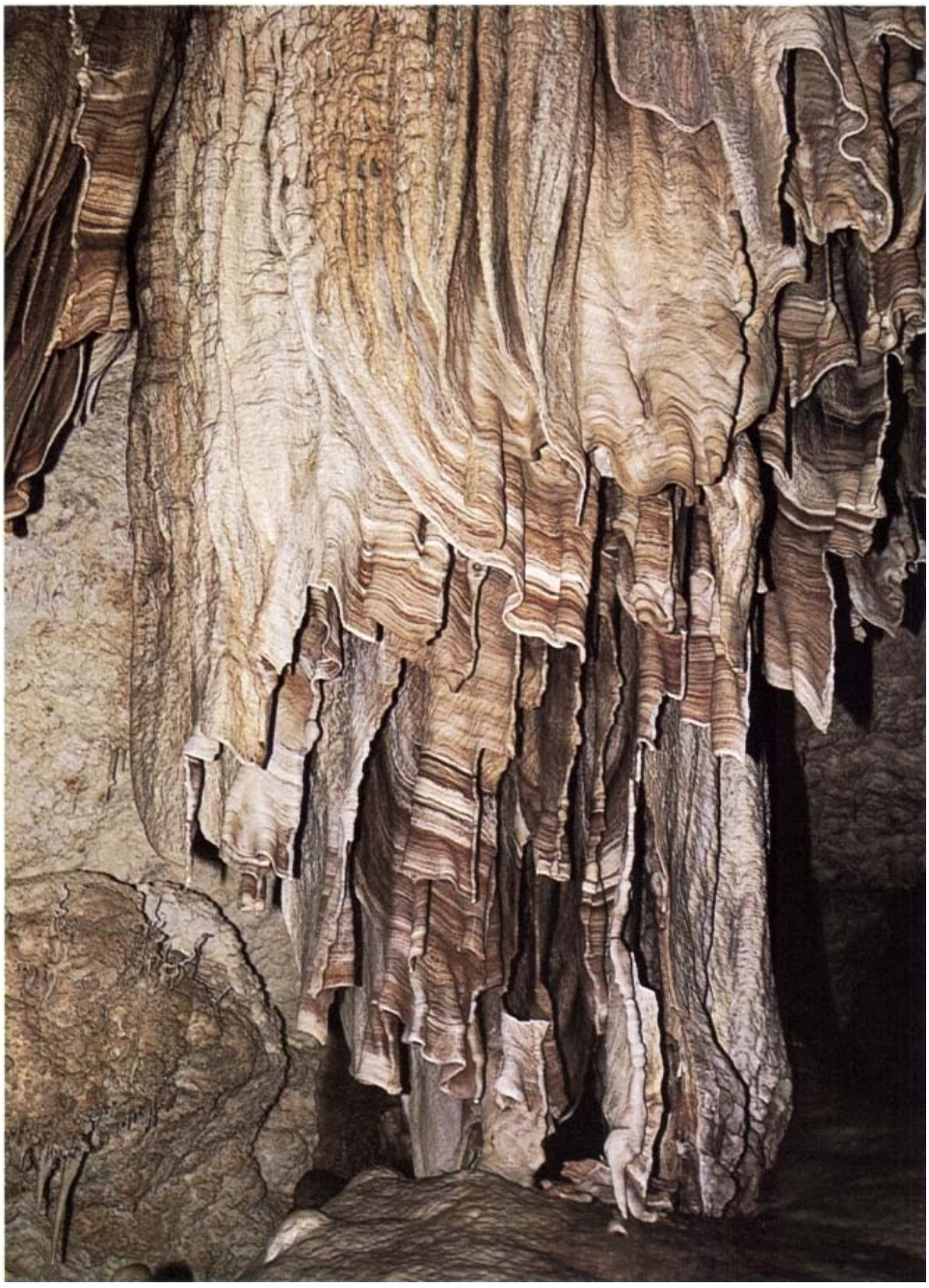

"The Peppermint Tree," a composite drapery—column, Virgin Cave. Photo Alan Hill.

PLATE 13

A—Worm-like helictites, Hell Below Cave. Photo Alan Hill.

B—Cave rafts forming on the surface of a small pool in Virgin Cave. Thin, scum-like rafts formed in the middle of the pool and became thicker where they attached to the edge of the pool. Eventually the rafts could thicken enough to become shelfstone. Subaqueous coralloids can be seen in the upper left of the plate. Photo Alan Hill.

PLATE 14

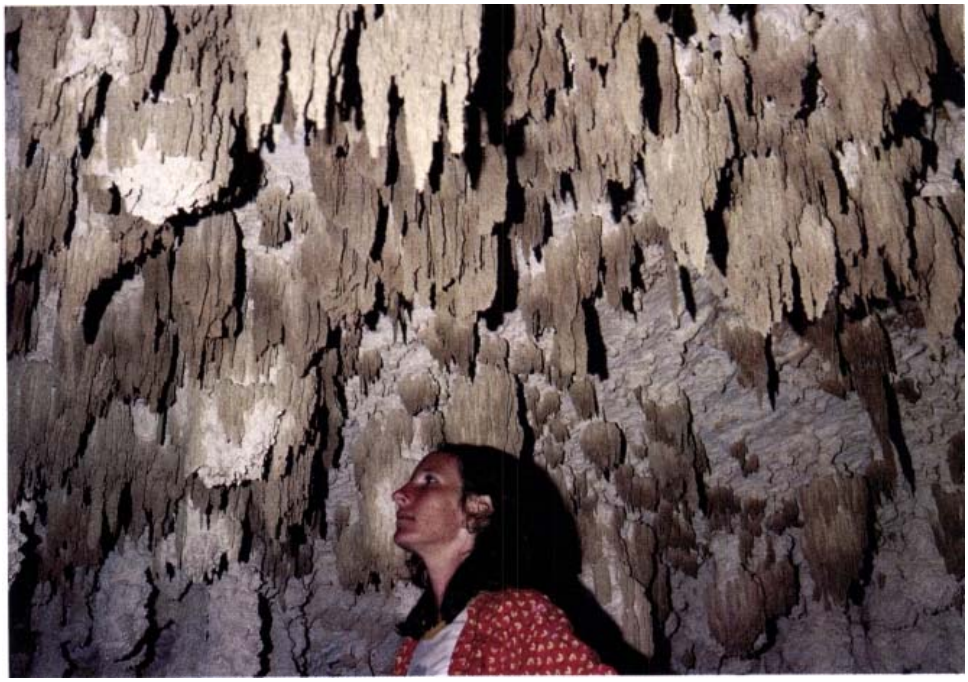

A—"Spanish Moss" stalactites, lower Gypsum Passage, Cottonwood Cave. The "moss" formed when the stalactites became submerged. Photo Alan Hill.

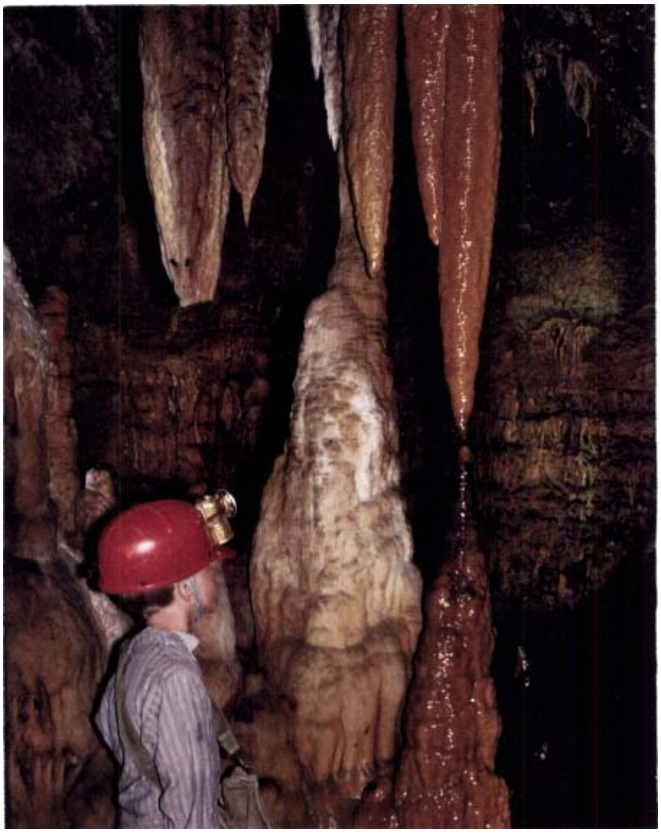

B—A stalactite about to join with its counterpart stalagmite to form a column, Black Cave. Photo Alan Hill.

PLATE 15

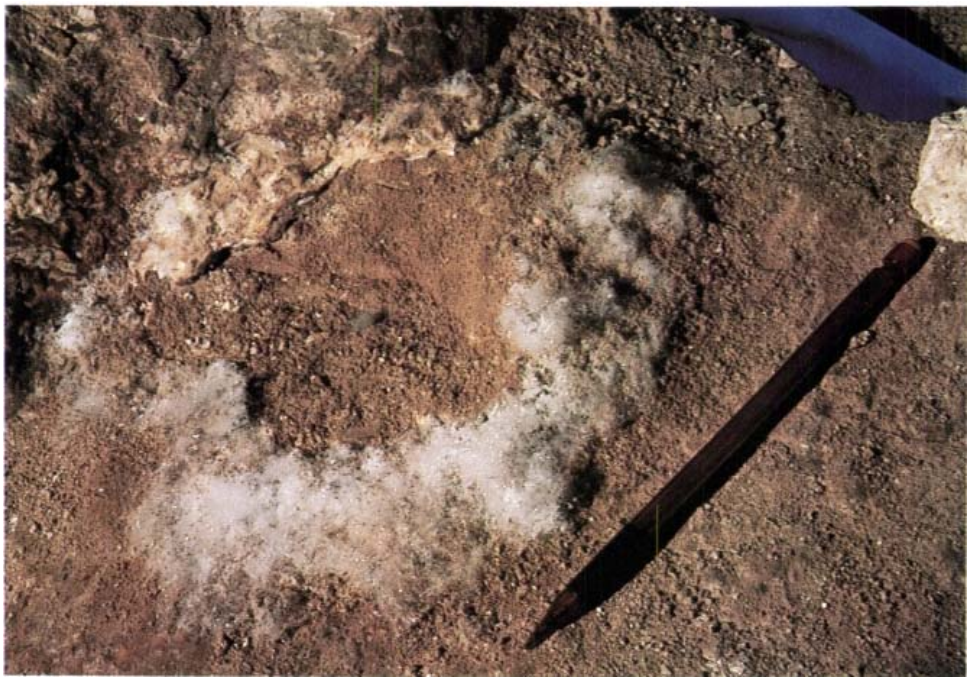

A—Epsomite cotton, Lower Cave, Carlsbad Cavern. Photo Cyndi Mosch Seanor.

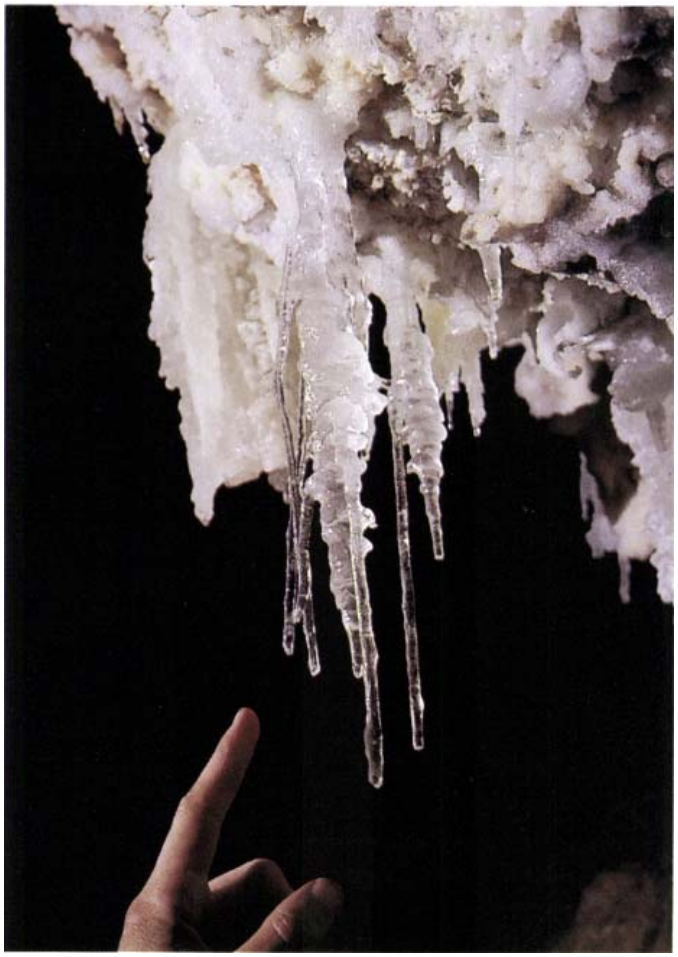

B—Epsomite soda straws and stalactites, lower Gypsum Passage, Cottonwood Cave. Photo Alan Hill.

PLATE 16

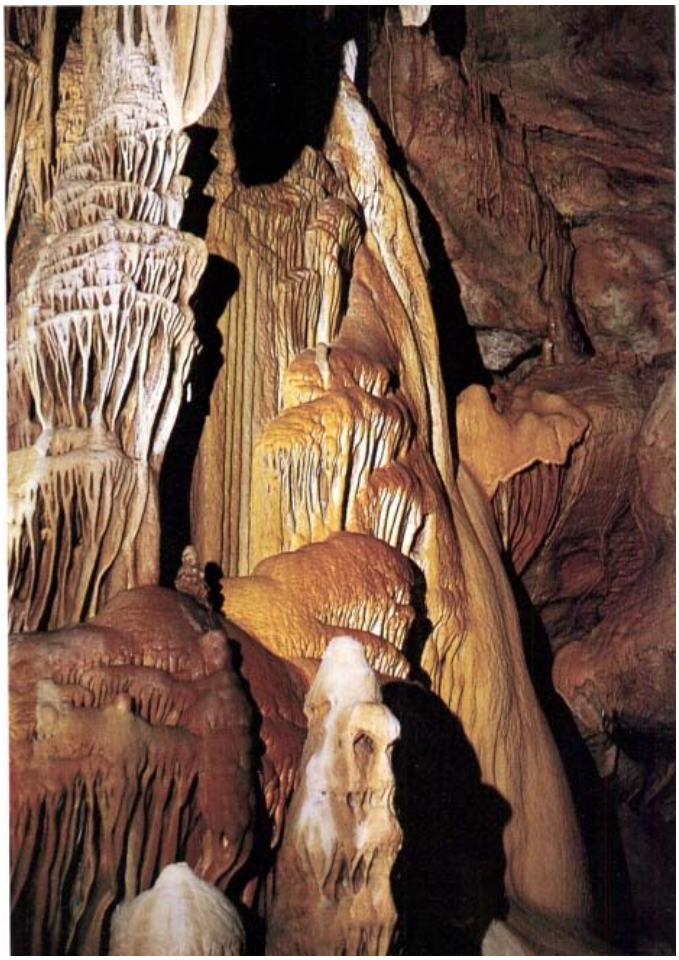

A—The Temple of the Fire God, a colorful flowstone cascade, Three Fingers Cave. Photo Alan Hill.

B—Black onyx flowstone, Sand Passage, Carlsbad Cavern. The joint along which water entered the passage to form the flowstone is the same joint that forms the north wall of Bat Cave. The flowstone has many bat bones embedded in it, and the black coloration is believed to be due to leaching of guano in overlying Bat Cave. Photo Wayne Burks.

PART II: MINERALOGY

Introduction

Purpose

Carlsbad Cavern is well known for the beauty and immensity of its "speleothems," a term used to denote secondary mineral deposits in caves. Stalactites and stalagmites are two of the most common speleothem types, examples of which are the huge Rock of Ages and Crystal Dome stalagmites of the Big Room, the tall, thin, totem-pole stalagmites of the Main Corridor, and the war-club-shaped stalactites of the War Club Room. Other, less common speleothem varieties are those shaped like draperies, grapes, popcorn, clouds, pearls, shields, balloons, lily pads, coke tables, cotton, flowers, needles, and rope. Two bizarre and interesting speleothems are helictites, which twist in any direction like contorted inchworms, and moonmilk, a cream-cheese-like pasty substance composed of a variety of carbonate minerals. All of these and other speleothem types are found in various parts of Carlsbad Cavern (Fig. 95), and also in other caves of the Guadalupe Mountains.

The purpose of Part II of this study is to describe the speleothems of Guadalupe caves and to relate their origin to geologic factors influencing their deposition. Basic questions that the mineralogy discussion will attempt to answer are: Why are Guadalupe speleothems so large? Why are they so profuse? Why are there so many types of speleothems in Guadalupe caves? Why is there so much popcorn-like decoration in the caves? Why is there an abundance of carbonate speleothems but relatively few sulfate speleothems? Why are most of the speleothems dry and inactive?

Previous work

The mineralogical wonders of Carlsbad Cavern were first introduced to the world by Willis T. Lee in two articles in the *National Geographic Magazine* (Lee, 1924a, 1925b). Lee's popularized description of Carlsbad Cavern brought world-wide recognition to the cave, propelling it quickly to National Monument and then National Park status. The first mineralogical article to appear in a strictly scientific journal was by Hess (1929) on the cave pearls of Carlsbad Cavern. Two more popular articles appeared in 1938, one by Burnet on New Cave, and one by Nymeyer, who briefly described the mineralogy of Hidden Cave, Hell Below Cave, Cottonwood Cave, and 19 other caves in the Guadalupe Mountains. Nothing further was written on the mineralogy of Guadalupe caves until the early 1950's, when Donald M. Black, a Park employee, published a number of articles on the cave pearls, rafts, and rimstone dams of Carlsbad Cavern (Black, 1951a, b, 1952, 1953), and one on the "Chinese Wall" rimstone dams of New Cave (Black, 1956). In addition, Thrailkill (1953) published a brief note on the popcorn in Manhole Cave.

The 1960's and early 1970's marked a period of short descriptions of Guadalupe speleothems in grotto newsletters or other publications of the National Speleological Society. It was during this time that cavers began to actively explore the caves of the Guadalupe Mountains and these publications were the news outlets for the cavers' findings. Crisman (1960) gave a brief mention of Guadalupe Moun-

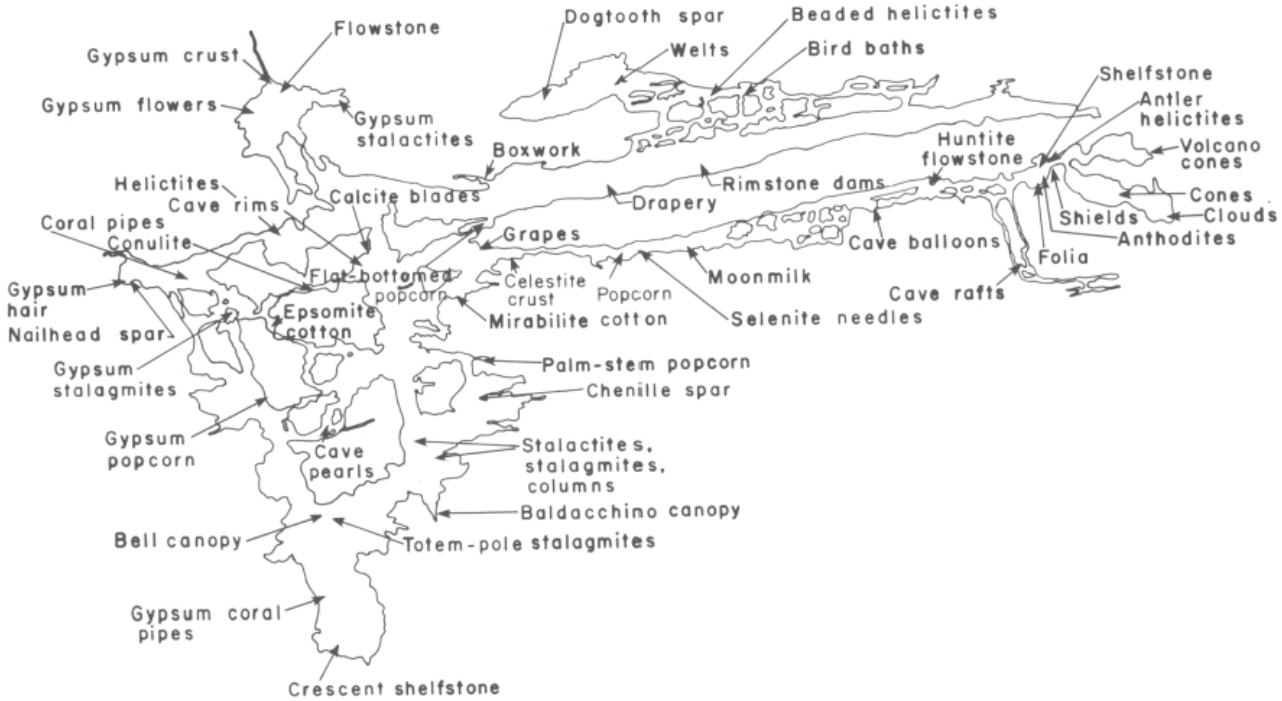

FIGURE 95—Location of best examples of various kinds of speleothems, Carlsbad Cavern.

tain speleothems in a guidebook published by the National Speleological Society. White (1960), Russell (1961), and Frost (1971) wrote on the sulfate mineralization in Cottonwood Cave, DuChene (1967) described the large spar crystals in Idono Crystal Cave, and Davis (1970) reported to Carlsbad Caverns National Park on his discovery of folia in the Lake of the Clouds area, Carlsbad Cavern. It was also during this time that John Thrailkill did his doctoral dissertation on the carbonate mineralogy of Carlsbad Cavern. Thrailkill went beyond the mainly descriptive efforts of past workers. He identified a number of carbonate minerals by x-ray diffraction, discussed the stability of carbonate minerals in a cave environment where the effect of the magnesium ion is pronounced, and described in specific terms the mode of popcorn deposition (Thrailkill, 1963, 1965a, b, 1968, 1971). Thrailkill's dissertation remains the definitive work on the carbonate mineralogy of Carlsbad Cavern.

In the early 1970's, the Cave Research Foundation's long-term commitment to cave survey and research on federal lands brought about the systematic description and study of speleothems in the caves of the Guadalupe Mountains. In 1972-1973, geologists Carol Hill, Harvey DuChene, Dave Jagnow, and Dwight Deal submitted six reports to Carlsbad Caverns National Park in which they discussed various geological topics and also a number of new speleothem types in Carlsbad Cavern, such as hydromagnesite balloons, mirabilite and epsomite cotton, huntite flowstone, cave rims, and various types of coralloids (DuChene, 1972; Hill, 1972; Hill et al., 1972a, b; Hill et al., 1972; Hill, 1973b). Also during this period, Hill published some of these and other mineralogical findings in technical journals (Hill, 1973a, c, d). Since that time, Hill has described the mineralogy of many Guadalupe caves in numerous short articles in the Annual Reports of the Cave Research Foundation (see References).

Significant advancement in the understanding of how travertine layers grow was made in the middle to late 1970's by two sets of investigators. Folk and Asserto (1976) described the crystal fabric of flowstone collected in Carlsbad Cavern and suggested that variations in fabric are controlled by the chemistry of the depositing solution. Kendall and Broughton (1977) questioned some of Folk and Asserto's findings in a reply that favored the importance of the substrate on carbonate mineral fabrics.

Carbonates

Most speleothems are composed of calcite or aragonite, $CaCO_3$. Together, these two minerals probably comprise over 95% of all speleothemic material in caves. In Guadalupe caves the carbonate mineralogy is more complex than that in most other caves due to the effect of the magnesium ion in solution. Besides calcite and aragonite, the magnesium minerals hydromagnesite, $Mg_5(CO_3)_4(OH)_2 \cdot 4H_20$, huntite, $CaMg_3(CO_3)_4$, and dolomite, $CaMg(CO_3)_2$, are present. Thrailkill (1971) tabulated the distribution of these five minerals for various types of speleothems in Carlsbad Cavern (Table 30) and found that, for the samples analyzed, flowstone-type speleothems are composed exclusively of calcite and aragonite, whereas moonmilk is composed exclusively of aragonite and the magnesium carbonate minerals. Other speleothems such as popcorn or wall coatings may be composed of one or a combination of these minerals. Tankersley et al. (1983) did a spectrochemical analysis of major and trace elements in a piece of aragonite flowstone from Carlsbad Cavern (Table 31).

The depositional fabric of minerals making up carbonate speleothems takes a variety of forms. Huntite, dolomite, and hydromagnesite always form as extremely fine-grained precipitates of cream-cheese consistency, whereas aragonite usually forms acicular crystals or feathery arrays of crystals. In flowstone and dripstone travertine, the layers are usually composed exclusively of aragonite and calcite (Table 30), the calcite forming either as clear, columnar, "palisade" crystals with small "crystallite" terminations, or as felted bundles resembling coconut meat. In one 3 cm thick flow-stone sample collected from Carlsbad Cavern, Folk and Asserto (1976) found that the felted "coconut-meat" crystals occurred at the base of the specimen and appeared to be the first type of material deposited after halts in crystallization, possibly during times when the surface of the speleothem had dried out. The distinctive fabric of palisade calcite crystals is believed to be caused by precipitation from thin water films that flow over the growth surface of the speleothem (Kendall and Broughton, 1977, 1978).

Deposition

The five carbonate minerals found in Guadalupe caves derive from vadose seepage along joints, bedding planes, and connected pores in overlying bedrock units of limestone and dolomite. Incoming solutions are charged with carbonic acid derived from carbon dioxide in the air and in the soil zone above the cave. Carbonic acid dissolves the limestone and dolomite rock below the soil zone and water entering the caves is enriched in the ions of calcium, magnesium, and bicarbonate (Table 28). Upon entering an air-filled passage, these solutions lose their excess carbon dioxide and precipitate their accumulated load of carbonate material. Thrailkill (1965b) found that the carbon-dioxide content of incoming drip water in Carlsbad Cavern is over 20 times that of the cave air.

The above carbon-dioxide scheme is the exclusive mechanism of carbonate deposition in many or most caves, but

TABLE 30—Number of occurrences of minerals in speleothems, Carlsbad Cavern. After Thrailkill (1971).

	Calcite	Aragonite	Hydro-magnesite	Huntite	Dolomite	Calcite + Aragonite	Calcite + Dolomite	Aragonite + Hydro-magnesite	Aragonite + Dolomite	Hydro-magnesite + Dolomite	Calcite + Aragonite + Dolomite
Coatings (wall)											
Outer layers	1	0	0	0	0	2	2	0	0	0	2
Inner layers	3	0	0	0	0	0	1	0	0	0	0
Coralloids (popcorn)											
Outer layers	6	12	13	0	0	2	0	8	0	0	0
Inner layers	2	6	2	0	1	7	0	0	1	0	1
Flowstone	6	2	0	0	0	2	0	0	0	0	0
Moonmilk	0	7	5	1	0	0	0	0	0	1	0

TABLE 31—Major and trace elements in aragonite flowstone, Carlsbad Cavern. After Tankersley et al. (1983).

Major elements (%)	
Al_2O_3	0.01
CaO	High
Fe_2O_3	0.02
K_2O	0.12
MgO	1.33 (moderate)
MnO	0.01
Na_2O	0.02
P_2O5	0.04
SiO_2	low
SrO	0.05
Trace elements (ppm)	
Ba	141
Cr	—
Cu	3
Ni	8
Pb	—
Th	1
V	8
Y	6
Zn	20

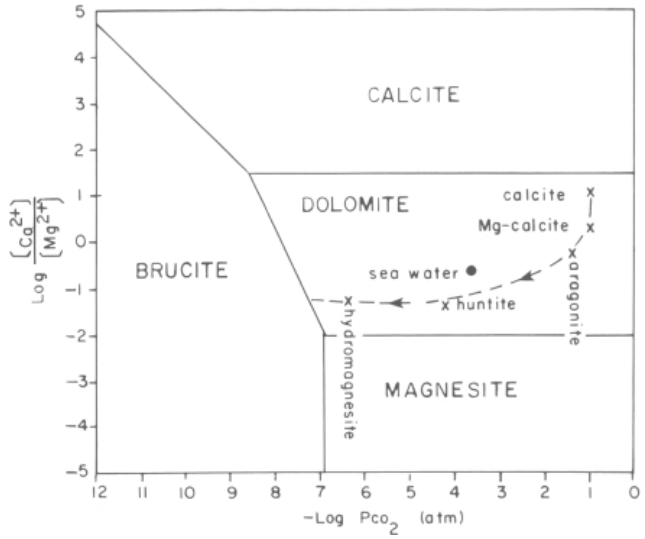

FIGURE 96—Evolution of cave water in Guadalupe caves. As water loses carbon dioxide and as evaporation increases, the water moves down and then toward the left of the graph along the dashed line, depositing calcite, Mg-calcite, aragonite, huntite, and hydromagnesite, in that order. After Lippmann (1973).

in Guadalupe caves another, perhaps even more important, mechanism is at work causing precipitation of calcium- and magnesium-carbonate minerals. Humidity in Guadalupe caves ranges from 34 to 100%, with a mean value of around 85–90% for air equilibrated with the cave environment (Table 4, Fig. 21); therefore, in most cave passages, evaporation of incoming cave water is also a major influence on precipitation. Thrailkill (1965b) calculated that in one area of Carlsbad Cavern as much as 40% of the carbonate deposition was caused by evaporation. Hill (1978b) determined that evaporation was a controlling factor in the deposition of carbonate minerals in Ogle Cave, with respect to both the kind of mineral expected and the speleothem morphology and type. Hill estimated that in a cave of 88% humidity, 10 times more evaporation will occur than in a cave of 99% humidity (as is common for caves in the eastern United States, such as Flint–Mammoth, Kentucky).

Stability

Evaporation is an important control on the type of carbonate mineral deposited because, during evaporation, water which remains saturated with respect to calcite will shift toward a relatively higher magnesium concentration. The concentration of magnesium ion in solution is the reason why the usually rare hydromagnesite, huntite, and dolomite are relatively common in Guadalupe caves. The process can be visualized by examining the phase diagram in Fig. 96. Following the dashed line in the dolomite stability field, note how the mineral species changes with a loss of carbon dioxide and an increase in evaporation. As ground water entering the cave degasses carbon dioxide, calcite is precipitated first and the magnesium ion increases relative to the calcium ion (a move down on the vertical axis of the diagram). High-magnesium calcite (Mg-calcite) deposits next, then aragonite, then huntite, and finally hydromagnesite. A Ca^{++}/Mg^{++} plot of vadose water in Carlsbad Cavern shows that most drip water and practically all pool water lie to the right of the Ca^{++}=Mg++ line (Fig. 97). This relationship suggests a late-stage evolution towards decreasing calcium content at approximately constant magnesium concentration, as would be expected to occur where calcite-saturated seepage is subject to evaporation.

The geochemical shift toward water high in magnesium is reflected in the mineral trends of Guadalupe speleothems on both a small and a large scale. Low to high magnesium-mineral trends (e.g. calcite–aragonite, dolomite–huntite, aragonite–hydromagnesite) within individual speleothems have been reported by several investigators (Thrailkill, 1965b; Hill, 1973c; Folk and Asserto, 1976). Small-scale changes in mineralogical composition are especially pronounced in cave popcorn, where the general sequence of popcorn deposition is rhombohedral calcite surrounded by nodular overgrowths of spicular aragonite capped by blebs of hydromagnesite moonmilk on the tips of the aragonite spicules (Fig. 107).

On a large scale, a transition from calcite dripstone to aragonite anthodites to hydromagnesite moonmilk can be followed in Carlsbad Cavern from the Big Room to the Lunch Room to Left Hand Tunnel, respectively. This trend may reflect changes in stratigraphy from reef to forereef (Fig. 18), or be a function of increased temperature and evaporation from the Big Room into Left Hand Tunnel (Fig. 19), or both. Another such transition in mineralogical composition can be seen in the Lake of the Clouds Passage where evaporation again seems to control mineralogy. Bushes of coralloidal calcite surround the Lake of the Clouds where

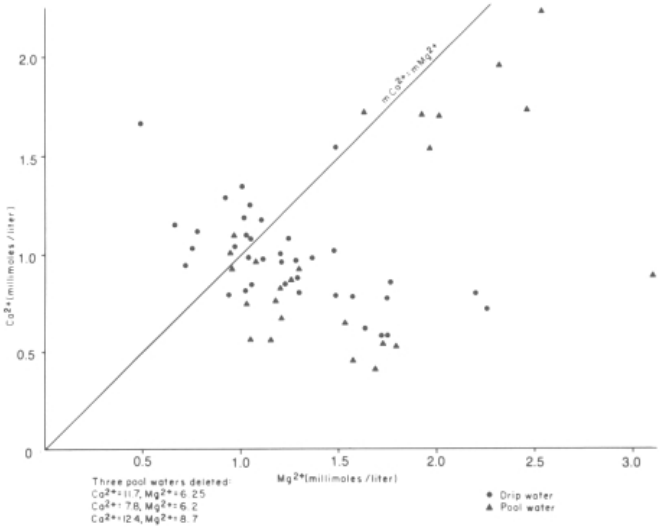

FIGURE 97—Ca/Mg ratio in vadose water, Carlsbad Cavern. Data taken from Boyer (1964).

the humidity is relatively high. Directly upslope from the Lake, the bushes grade into blunted aragonite spicules and then, higher upslope, delicate acicular-aragonite frostwork occurs (Fig. 93).

The effect of evaporation and carbon-dioxide loss on the various types of carbonate speleothems deposited can be understood by examining the carbon–oxygen-isotope values of speleothems (Fig. 98). (For an explanation of the carbon- and oxygen-isotope methods see Part I of this pa-per.) Most of the speleothems in Fig. 98 lie along Slope 1 which represents the deposition of speleothems due primarily to carbon-dioxide loss. Note that only popcorn and moonmilk lie on Slope 2, which represents the deposition of speleothems due primarily to evaporation. These findings agree with Thrailkill's (1971) mineral-occurrence chart (Table 30), where popcorn and moonmilk are composed of aragonite, hydromagnesite, huntite, and dolomite, minerals that are known to deposit by evaporation from solutions high in magnesium. Of some surprise is the occurrence of aragonite anthodites along Slope 1, which implies precipitation primarily by carbon-dioxide loss rather than by evaporation. Evidently, aragonite in Guadalupe caves can form with or without evaporation being directly responsible for its precipitation.

Speleothems

The number of carbonate minerals in Guadalupe caves is small, but the variety of mechanisms that control carbonate deposition causes a large number of speleothem types. Five basic hydrologic mechanisms, dripping water, flowing water, seeping water, pool water, and condensation water, influence the type of speleothem. Examples of primarily dripping-water speleothems are stalactites and stalagmites which are elongate in the vertical direction of dripping. Flowstone forms from thin films of water which uniformly flow over cave walls or floors and deposit thin layers of travertine. Helictites twist in every direction because they grow by water seeping through tiny, internal, capillary canals. Cave rafts are flat, planar speleothems because they form on the surfaces of cave pools, and rims are deposits which form where water is condensing on bedrock or speleothems. Compound speleothemic shapes result where two or more of these basic mechanisms are operating simultaneously. For example, a drapery speleothem is created when a drop of water flows down an inclined ceiling and then drips to the floor. Shelfstone is a morphological extension of a cave raft produced when water moves by capillary action onto the upper surface of the raft, thereby increasing the raft in

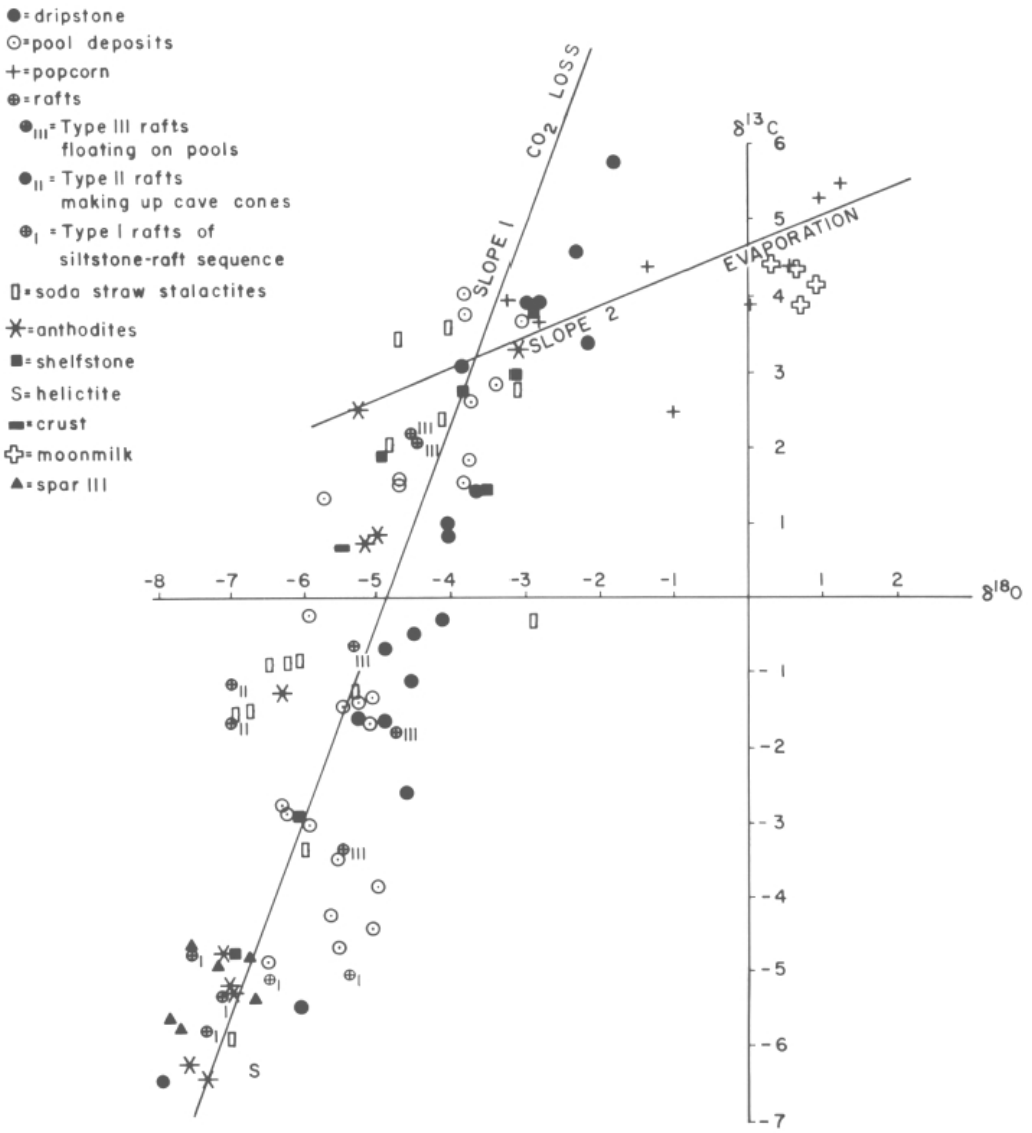

FIGURE 98—Carbon–oxygen-isotope compositions of different speleothem types, Carlsbad Cavern (L. Gonzalez's unpubl. data 1985, and this study).

thickness. Cave pearls form when water drips into a shallow pool. And so on.

Added to these five basic hydrologic mechanisms are other factors, such as bedding, limestone porosity, and evaporation, which influence speleothem type and shape. Bedding can influence speleothem deposition in a number of ways. In Fint–Mammoth Cave, Kentucky, an impermeable sandstone caps the caves so that speleothem-depositing water enters the system only where the sandstone is truncated by valley erosion. The silty Yates and Tansill Formations, on the other hand, are sufficiently fractured and bedded so that surface water easily moves downward along joints and dipping bedding planes. Vadose seepage thus enters the underground throughout the whole Guadalupe Mountain recharge area, the diffuse penetration accounting for the fact that in Guadalupe caves speleothems occur practically everywhere and in great profusion (Palmer, 1975).

Bedding and permeability factors can influence cave mineralogy in other ways. In Carlsbad Cavern the type of speleothem changes as one traverses from the bedded-backreef Tansill and Yates Formations at and near the cave entrance down into the unbedded Capitan Limestone (Hill, 1972). Speleothems found in the impermeable (0.01 millidarcies) Tansill Formation at the cave entrance are primarily travertine deposits—dripstone which drips from ceiling joints, or flowstone which issues forth along horizontal bedding planes and flows down along cave walls (Fig. 99). As one descends along the Main Corridor into the unbedded, more permeable (14 millidarcies) Capitan reef limestone (just beyond the Whale's Mouth), popcorn becomes increasingly abundant on cave walls. The pattern of vadose-water flow creating these different types of speleothems can be visualized as follows: water from the surface descends into Guadalupe caves mainly along vertical joints and deposits dripstone (rows of stalactites and stalagmites) wherever the joint intersects a cave passage; or, where water moves along a bedding plane, flowstone can form below where the bed-ding plane intersects the cave (Fig. 100). But, if solutions move down far enough to reach the massive Capitan Limestone, they no longer intersect bedding planes but instead diffuse through interconnected pores in the limestone and move toward the cave walls where they form popcorn-type speleothems.

Bedding and dip are factors which can control the position and quantity of travertine deposited. Along the joint passage connecting the Main Corridor with the New Mexico Room, a cascade of massive dripstone and flowstone covers the left (west) wall of the passage, whereas the right (east) wall is devoid of speleothems. This distribution of travertine is produced by the intersection of the passage with the eastward-dipping beds of the Bell Canyon(?) Formation. Water moving downdip along bedding planes intersects the west wall and deposits its load of calcium carbonate there. Along the east wall, where beds intersect the passage at an obtuse angle, the water supply is cut off from the wall by the passage void, resulting in absence of speleothems. A similar situation exists both along Left Hand Tunnel and the south end of the Big Room, where dipping forereef beds divert water away from the reef and produce an absence or an uneven distribution of travertine.

The types of carbonate speleothems in Guadalupe caves are discussed in alphabetical order. The classification scheme of Hill and Forti (1986) is used throughout for speleothem types and subtypes.

FIGURE 99—Flowstone issuing from a bedding plane, Tansill Formation, Carlsbad Cavern. Photo Alan Hill.

Anthodites

Anthodites *(anthos* = flower) are speleothems which consist of clusters of colorless to white, needle or quill-like, crystal sprays. "Frostwork" is the term used for the acicular, needle-like variety of aragonite anthodite that resembles cactus or thistle plants (Pl. 11B). Anthodites are found in

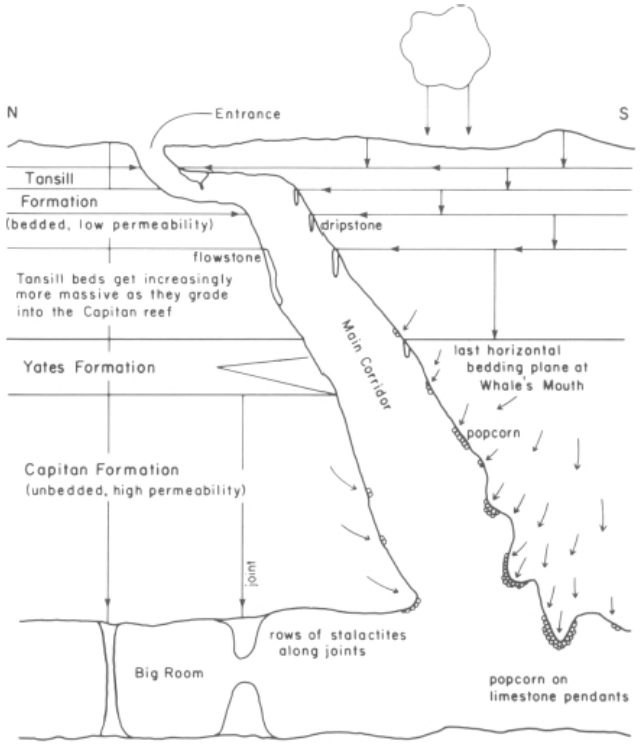

FIGURE 100—Influence of bedding and permeability on speleothem type, Carlsbad Cavern. After Hill (1972).

practically every Guadalupe cave, but form particularly exquisite arrays in the Medusa Room of Spider Cave and in the Christmas Tree and Bifrost Rooms of Carlsbad Cavern (Hill, 1979, 1982a). In the Medusa Room, a spray of aragonite frostwork almost 0.3 m long rests on top of a ledge. In the Christmas Tree and Bifrost Rooms, aragonite stalagmites up to 1.2 m high look like real Christmas trees, complete with spiny branches and needles. When flashed with a strobe light, the Bifrost Room frostwork displays a green phosphorescence, especially on recently formed growth tips.

Anthodites are believed to form where slowly moving, thin films of water seep between and over the surface of individual crystal needles, thus increasing the speleothem in breadth and height. Stalagmites often take on spiny, Christmas tree-like shapes because drops of water in overhead stalactites precipitate their load of calcite first and become increasingly enriched in magnesium; as the overhead drops fall to the floor and stalagmites are built up, this enrichment favors the deposition of aragonite over calcite.

Balloons, Cave

Cave balloons are roundish, thin-walled speleothems with gas inside of a mineralized, bag-like pouch. The best balloon specimens in Guadalupe caves occur in the Left Hand Tunnel of Carlsbad Cavern. These balloons are composed of hydromagnesite, are up to 2.5 cm in diameter with an approximate wall thickness of 0.1 mm, and are white with a satiny or pearly luster (Hill, 1973b, d; Fig. 101). One of the hydromagnesite balloons in Left Hand Tunnel hangs from the tip of an acicular aragonite needle on a small Christmas tree stalagmite, itself fed by drops from a calcite stalactite. Other, less perfect, deflated or desiccated balloons have been observed on the northeast wall of the New Mexico Room (C. M. Seanor, pers. comm. 1985), in an area about 1 m^2 in the Grinder Passage, Virgin Cave (H. DuChene, pers. comm. 1985), and in a number of places in Lechuguilla Cave (Hill, 1986).

Cave balloons are believed to be an extremely short-lived speleothem, transient in the time it takes for their initial growth and also in the time it takes for them to desiccate and disintegrate. Balloons may possibly grow when incoming solutions under pressure inflate carbonate moonmilk material. Moonmilk is usually a cryptocrystalline substance which exhibits a high plasticity when it contains just the right amount of water (Bernasconi, 1961). The plasticity of moonmilk increases when the aqueous phase comprises about 35% of the total mass, attaining a maximum at 37–40% and then decreasing rapidly up to 65%. If water under pressure reaches moonmilk blebs on the tips of popcorn, the plastic moonmilk can blow up in exactly the same manner as does a rubber balloon. In a relatively low-humidity cave like Carlsbad or Virgin, cave balloons can quickly dry, crack, deflate, and change in luster. Between 1973 and 1981, a small hole developed in one of the hydromagnesite balloons in Left Hand Tunnel and, during this time, the balloon also changed from a translucent to a more opaque luster (Hill, 1973d, 1981b).

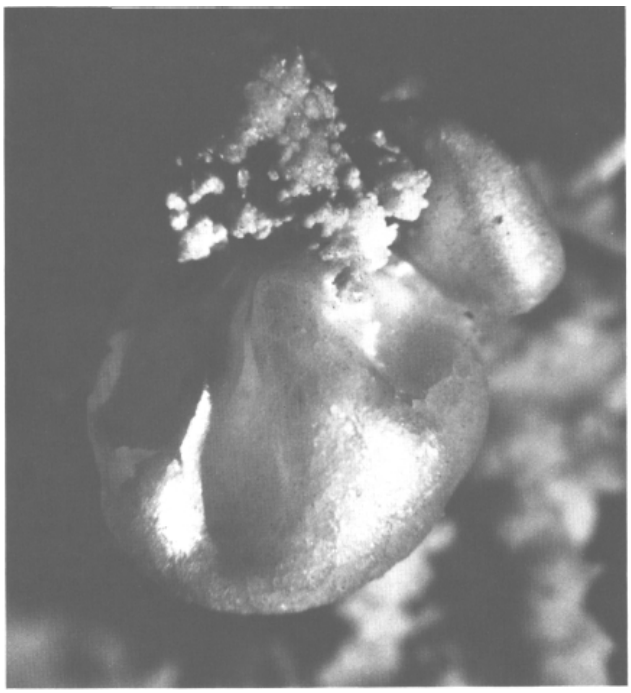

FIGURE 101—Hydromagnesite balloon 2.5 cm in diameter, Left Hand Tunnel, Carlsbad Cavern. Photo Pete Lindsley.

Boxwork

Boxwork is so named because of its resemblance to a maze of crisscrossing post-office boxes. Thin, compact blades of crystalline material stand out in relief as a network of intersecting fins or plates corresponding to fractures in bedrock. Boxwork is not a common speleothem type in the Guadalupe Mountains because of the general lack of bedrock fracturing in the caves, but one small exposure of boxwork fins a few millimeters in width has been found in Lower Devil's Den, Carlsbad Cavern, near the calcified siltstone–cave rafts. Also, a small amount of boxwork has been noted in Wind (Hicks) and Spider Caves, the latter occurrence with fins 3 cm long and 1 mm thick.

The association of the boxwork with calcified siltstone in Lower Devil's Den may not be a coincidence. The contact zone between the shelf facies and reef core has been an area of past weakness. The calcified siltstone–cave rafts are found along this contact, and breccia deposits are there as well (Figs. 30, 40). A zone of weakness is exactly where one would expect bedrock fractures to develop and boxwork fracture fillings to form.

Coatings and crusts

Perhaps the most non-descript of all speleothems are the light-colored carbonate coatings and crusts which line the walls, ceilings, floors, and pools of most Guadalupe caves. This type of speleothem is formed either subaerially or subaqueously.

Subaerial coatings and crusts—Subaerial coatings line cave walls and ceilings, acting as a backdrop for the more showy popcorn or helictite speleothems. Of mineralogical note are the dolomite coatings identified by Thrailkill (1968) in Carlsbad Cavern. The dolomite has acicular crystals of aragonite in the coating and, for this reason, Thrailkill speculated that the dolomite had formed from the aragonite in the presence of high-magnesium solutions.

Floor silt in Guadalupe caves is often covered with a crust of white carbonate material (Fig. 36). These crusts form when carbonate-bearing solutions seep up through the silt toward the dry cave passage and deposit their mineral load at the surface of the silt. The crusts covering the silt are a few centimeters to tens of centimeters thick. Perhaps the best display of this type of crust is in Lower Cave, Carlsbad Cavern, where it overlies some of the thick silt banks (Fig. 34).

Subaqueous coatings and crusts—In the underwater variety the carbonate material lines the sides and floors of cave pools. The most notable example of such pool linings are the "clouds" of the Lake of the Clouds Passage, Carlsbad Cavern (cover photo). The calcite of the cloud linings is fine-grained, having formed from numerous crystal nuclei under supersaturated conditions. Orange clouds also occur at the bottom of Lechuguilla Cave (D. Davis, pers comm. 1986).

Conulites

A conulite is a conical shell of carbonate material which visually resembles an ice-cream cone with its apex pointing down. Conulites are rare speleothems originating as drip tubes in soft sediment that becomes subsequently lined with calcite. When the sediment (usually mud or sand) is eroded away, the calcite lining is left exposed as a hollow, cone-shaped speleothem.

Two conulite localities are known in Carlsbad Cavern. The most unusual one is in Lower Cave, in the fissure passage leading from the bottom of Mabel's Room toward the Boneyard. This particular conulite is unique because it has formed in moonmilk rather than in sediment (Hill, 1984a). The conulite in moonmilk is shaped like a horn coral (Fig. 102); it is 5-12.5 cm high, 6-7.5 cm wide across its top, and has a wall thickness of less than 1 cm. A piece of light-green, waxy, endellite clay is attached to a lower, outside portion of the conulite.

More typical conulites occur in the Balcony of the New Mexico Room, in sandy floor just past the climb up into the first room. The largest of the four conulites is 25 cm deep and 15 cm across the top. Shifting of the overhead drip point has created vertical flutes on the insides of these conulites.

"Bird baths" are low-angle, bowl-shaped conulites which form in soft sediment. Tiny bird baths, 2 to 3 cm across and 2 cm high, have been found in floor silt at the bottom of the first pit in the Hall of the White Giant, New Section, Carlsbad Cavern.

Coralloids

"Coralloid" is a collective term used for a number of morphological varieties of nodular speleothems. This type of speleothem has been discussed above in Part I, where it was related to late-stage speleogenesis events. Coralloids also relate to other problems, such as air-flow direction (Fig. 24) and past climate. Like coatings and crusts, coralloid speleothems can be either subaerial or subaqueous in origin.

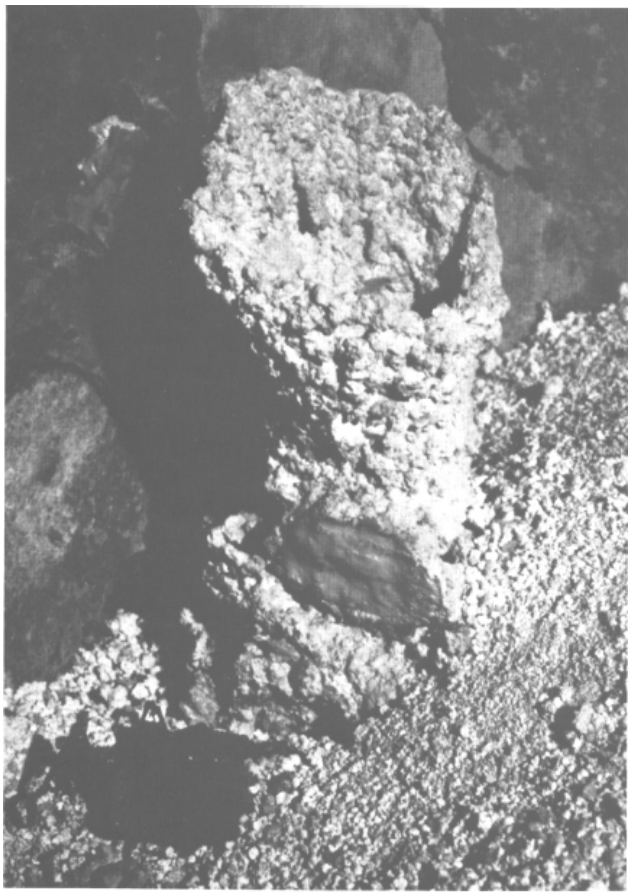

FIGURE 102—A conulite in moonmilk, Lower Cave, Carlsbad Cavern. Conulite is 12.5 cm high. A mummified bat is in lower left of figure. Photo Cyndi Mosch Seanor.

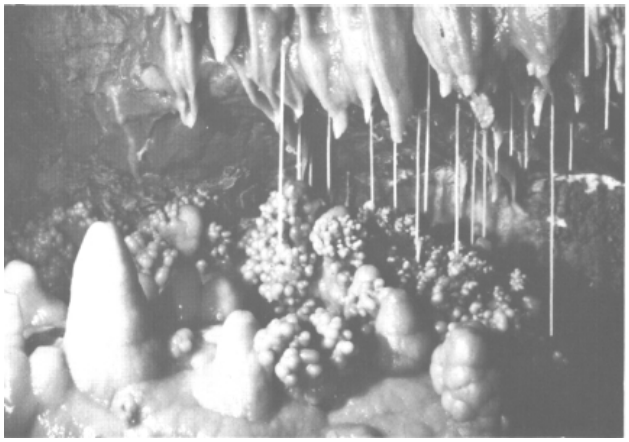

FIGURE 103—Soda-straw stalactites and grape coralloids. Photo Kenrick Day.

Subaerial coralloids—An estimated 95% of all coralloids in Guadalupe caves are subaerial. They assume a variety of unusual and fascinating shapes depending on their history of development. Most common are the grape-shaped (Fig. 103), coral-like (Fig. 104), or popcorn-shaped coralloids (Fig. 66, Pl. 11B). Four morphological variations of popcorn coralloids are button popcorn, flat-bottomed popcorn, palm-stem popcorn, and calcite blades.

"Button" popcorn is a type of knobby popcorn with concentrically plicate surfaces which sometimes appear to be twisted or folded (Thrailkill, 1953). Good examples of this type of popcorn occur in Manhole, Virgin, Three Fingers, Mad Russian, Lechuguilla, and Wind (Hicks) Caves (Hill, 1976c).

"Flat-bottomed" popcorn consists of clusters of popcorn which terminate in flat, horizontal tiers. The popcorn in the clusters grows on limestone ceiling and wall pendants, and

FIGURE 104—A growing coral frond, Ogle Cave. Photo Pete Lindsley.

the clusters get continually thicker down to their horizontal terminations. Flat-bottomed popcorn can be observed in many places along Left Hand Tunnel, the Big Room, Lower Cave, and Secondary Stream Passage of Carlsbad Cavern. This form is best developed where a main passage meets a side passage (e.g. at the entrance to Billing Dove Tunnel, Big Room).

"Palm-stem" popcorn is similar to flat-bottomed popcorn except that the flat surfaces are tilted from the horizontal so as to resemble tiers of cut palm-stems. Palm-stem popcorn often extends out from the sides of walls or stalagmites at angles of approximately 60°. Two of the best places to observe this kind of popcorn are in the Big Room along the trail by the Lion's Tail and along the south wall of Jim White's Tunnel where the passage starts to descend at a steep angle. In the latter occurrence, the popcorn masses are tilted both in the horizontal and vertical direction.

"Calcite blades" are a type of monocrystalline popcorn composed of calcite rhombohedrons oriented at slightly different angles on the blade (Hill et al., 1972; Hill, 1978c; Fig. 106). In Guadalupe caves, "normal" nodular popcorn usually begins its growth as a monocrystalline rhomb (Fig. 105); then, as the shape evolves and becomes increasingly rounder, the popcorn assumes the rosette form of a calcite blade (Fig. 106), and finally the form evolves into a smooth, nodular shape. This gradual transition of form is beautifully displayed in Musk Ox Cave (Hill, 1976b) and in the Lunch Room of Carlsbad Cavern. In the Lunch Room there is, in addition to the first three transitions, an added sequence of aragonite needles overlying normal popcorn and blebs of hydromagnesite moonmilk on the tips of the aragonite needles (Fig. 107).

In Guadalupe caves, subaerial popcorn forms by (1) water seeping through wallrock or speleothems, (2) thin films of condensation water, (3) splash from overhead dripping, and (4) splash from a pool. All four mechanisms have one thing in common: they all involve thin films of water as the critical criterion for popcorn deposition. When thin films of water move over surface irregularities in the limestone, more carbon-dioxide loss and evaporation take place at the apex of the irregularity than at the base, and deposition thus occurs preferentially at the apex and a nodular shape eventually results (Thrailkill, 1965a).

Seeping water (mechanism 1) explains popcorn which has pushed gypsum rinds out from cave walls (Fig. 66). It is probably the most universal mechanism by which popcorn has formed in Guadalupe caves, although this mechanism may have been operative primarily in the past, during or just after the time when the water table descended out of

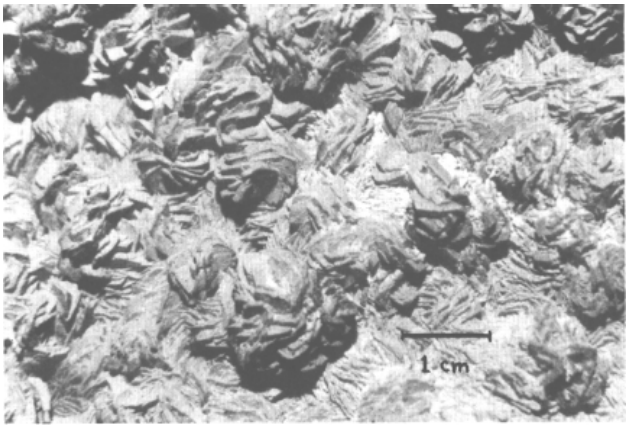

FIGURE 106—Facets of rosette-shaped rhombohedral calcite called "calcite blades," Appetite Hill, Carlsbad Cavern. Photo David Jagnow.

a passage and the limestone was losing its interstitial water. This mechanism, and also especially mechanism (2), is probably responsible for much of the popcorn associated with the condensation–corrosion "popcorn line" of Hell Below Cave and the Left Hand Tunnel–Big Room of Carlsbad Cavern (see Part I of this paper for a discussion of the condensation–corrosion process). Acidic condensation water corrodes the limestone and speleothems on or near the ceilings where CO_2 levels are high (Table 5), and the water runs down the side of the wall to form popcorn below the area of corrosion. A good place to view actively forming condensation popcorn is in the Left Hand Tunnel near the second bridge, where water droplets are condensating on the eastward side of a limestone pendant, while flat-bottomed popcorn is growing on the bottom and westward side of the pendant.

Thrailkill (1965b) thought that most of the popcorn in Carlsbad Cavern had formed by mechanisms (3) or (4). It would have been more correct to say that most of the pop-corn forming today grows by splash, primarily by mechanism (3), because mechanisms (1) and (2) are probably no longer operative on a large scale. Most actively growing popcorn occurs on the tops and sides of stalagmites where water is dripping from the roof and splashing onto stalagmites. Type (3) popcorn can be seen in the New Year's Eve Gallery of Hell Below Cave and in many places along the trail in Left Hand Tunnel of Carlsbad Cavern. It may also be seen in the Main Corridor by the Whale's Mouth, on the

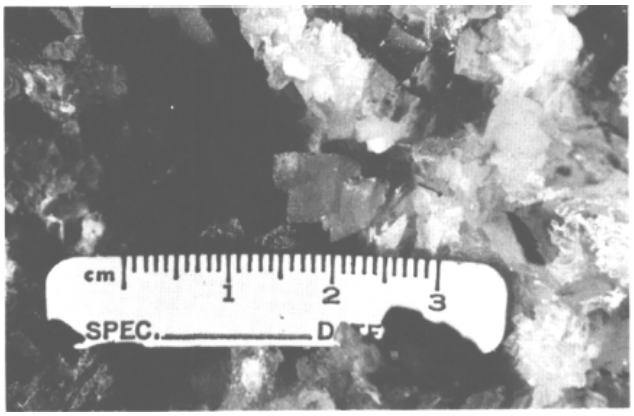

FIGURE 105—Monocrystalline rhombohedral popcorn, Appetite Hill, Carlsbad Cavern. Popcorn in the caves of the Guadalupe Mountains often begins its growth cycle as rhombohedral spar. Photo David Jagnow.

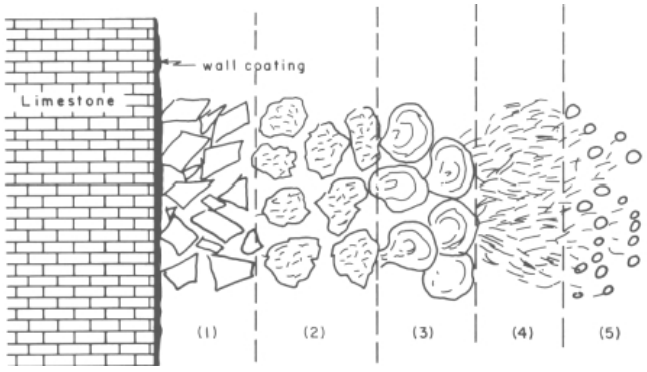

FIGURE 107—Diagrammatic presentation of five stages of popcorn growth in Guadalupe caves: (1) monocrystalline rhombohedrons of calcite; (2) calcite blades with rhombohedral crystal faces discernible; (3) "normal" rounded nodules of popcorn with microcrystalline, radial structure; (4) spicules of aragonite; (5) berry-like terminations of hydromagnesite moonmilk.

north wall, where dripping water has splashed on the apex of the stalagmite and has created a ring of popcorn on the wall concentric around the stalagmite's apex. Type (4) coralloids are the least common. They can be seen around and just above the edge of the pool at Devil's Spring in the Main Corridor and also in Lower Cave, in the "coral" alcove just below and beyond the Jumping Off Place.

Subaqueous coralloids—This type displays cauliflower- or grapefruit-like surfaces and shapes. Good examples are at Devil's Spring and about midway along Left Hand Tunnel, Carlsbad Cavern, and in Virgin Cave (Pl. 13B).

Tower coral is a variety of subaqueous coralloid which sticks straight up like so many toy towers (Fig. 108), except in places where constant dripping has caused coralloid growth to incline away from the vertical. Cross sections of tower coral exhibit a radial, layered structure characteristic of all coralloids, but the layers are elongate in the vertical direction rather than symmetrical as in most coralloids. Black (1956) referred to the tower coral in the Chinese Wall section of New Cave as "free, gravel-like accretions with rough granular surfaces." Hill (1978b) reported tower coral in Ogle Cave and also in the Black Forest section of New Cave (Sheet 7), and related both occurrences to high evaporation rates in these caves. According to Hill's interpretation, tower coral forms in shallow pools where the top part of the pool is supersaturated with calcite compared to the less saturated, lower part of the pool; precipitation is greatest along the top of the growing coralloid and a vertical shape is favored.

Popcorn growth and air flow—Oriented popcorn is popcorn which has grown on walls or speleothems in a direction which either points away from, or towards, the cave entrance or the direction of air flow in a passage. Hill (1978b) related entrance-oriented popcorn in Ogle Cave to differences in evaporation relative to the two cave entrances. Sides of speleothems facing the Ogle entrance and an inflow of dry, outside air have experienced greater evaporation, which in turn has favored slow-moving films of water and popcorn growth. Speleothem sides facing away from the Ogle entrance have experienced less evaporation loss and hence are covered with flowstone deposited from faster-flowing, thicker films of water. Queen (1981) likewise attributed oriented popcorn to air flow and, based on the direction of popcorn growth in Carlsbad Cavern, constructed a map of atmospheric circulation in the cave (Fig. 24).

Flat-bottomed popcorn and palm-stem popcorn are varieties which are probably also related to air flow. The palm-stem popcorn in Jim White's Tunnel is located where air is ascending from a lower passage; the popcorn, in both its horizontal and vertical components, is oriented in the direction of ascending air. Air flow may move fine films of water to the far end of a growing popcorn nodule, thereby influencing its orientation commensurate with the direction of that flow. Flat-bottomed popcorn seems to be the most pronounced in areas of high air flow and evaporation, or at least in areas transitional between high and low air flow (such as the entrance to Billing Dove Tunnel). Martini (1986) attributed the growth of flat-bottomed popcorn ("trays" he called them) to evaporation and undersaturated solutions where growth is possible only upward and laterally along a rock pendant. In Carlsbad Cavern the undersaturated solutions are probably condensation water.

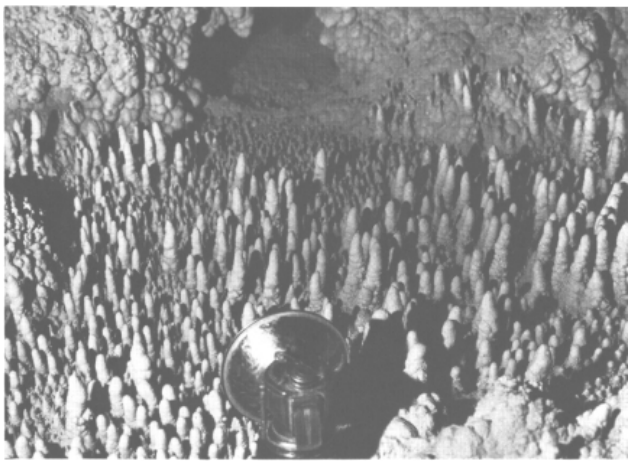

FIGURE 108—A "forest" of tower coral, Ogle Cave. Photo Pete Lindsley.

Popcorn growth and climate—Queen (1981) also noted the evolution of popcorn where rhombohedral calcite is overlain by nodular popcorn, acicular aragonite, and berry-like terminations of moonmilk (Fig. 107), and related these growth stages to past climatic events, the rhombohedrons corresponding to wet and humid conditions and the moon-milk blebs to relatively dry cave conditions. Monocrystalline rhombohedral crystals typically form in humid caves, and this first stage of popcorn growth may correspond to an earlier, wetter, climatic episode in the Pleistocene.

While Queen's hypothesis is probably valid, it needs to be tempered by other factors. The stage of evolution of a cave may influence the type of popcorn. In Fiume Vento Cave, Italy, where sulfuric-acid dissolution and condensation–corrosion are going on today, rhombohedral-popcorn growth is the norm, while the other, later types of popcorn have not yet developed (P. Forti, pers. comm. 1985). Also, there is, in real time, a change from high-calcium to high-magnesium concentration in the normal evolution of cave waters. Evaporation will cause chemistry changes in a drop of water so that it shifts from a calcium-precipitating solution to a magnesium-precipitating solution within a short time, producing first calcite and last hydromagnesite.

Coral pipes

Coral pipes are speleothems that outwardly resemble tower coral but differ from them in internal structure, occurrence, and origin. Coral pipes are thin, pipe-like structures which have a soft interior (usually mud) surrounded by a thin shell of calcite. They are essentially calcified pillars that develop where mud has been drilled by dripping water and where the outside calcitic shell has been deposited concurrently with erosion.

The only Guadalupe cave where coral pipes are known to occur is Carlsbad Cavern: in the Rim Room and New Mexico Room (C. M. Seanor, pers. comm. 1985), in the Big Room by the Bottomless Pit, and also in the Mystery Room near the Mabel's Room Overlook. The Mystery Room coral pipes are unusual in that they have formed in bat guano instead of sand or mud. These are 2–4 cm in diameter, about 20 cm tall, and possess a 3–4 mm thick shell of calcite surrounding a reddish interior of bat guano (Fig. 109).

Draperies

A drapery is a vertically folded, curtain-like speleothem that hangs from an inclined cave ceiling or wall (Fig. 110). When draperies are thin, translucent, and stained in bands, they take on the appearance of bacon; such "bacon" is especially beautiful when lighted from behind so that its translucency and color-banding are accentuated. Most draperies are composed of calcite, but one drapery in Pink Dragon Cave is reportedly composed of calcite and dolomite (B. Rogers, pers. comm. 1979). Draperies are essentially a composite dripstone–flowstone speleothem. When water flows down an inclined surface, it builds up ribbons of flowstone material along its sloping path of descent before it drips to

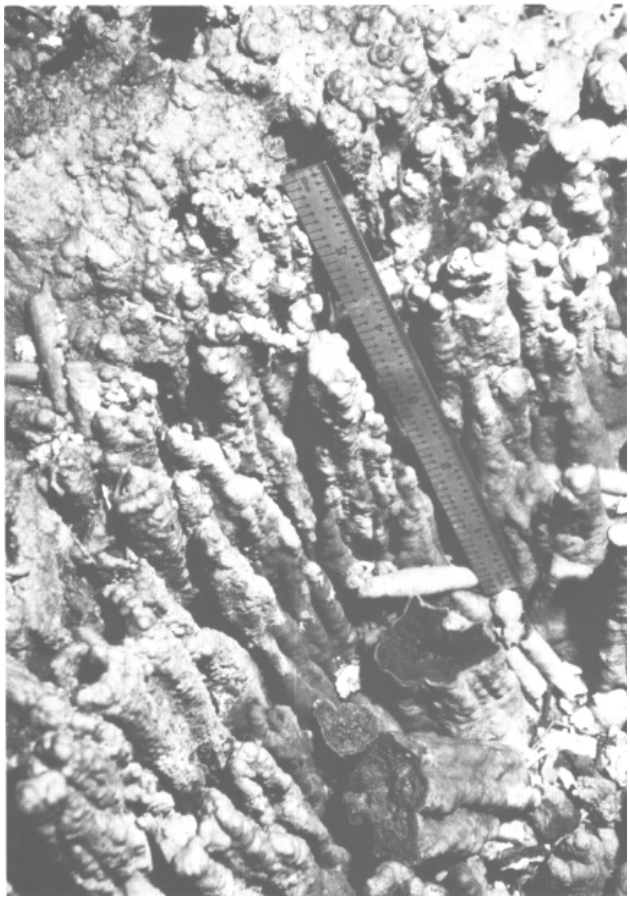

FIGURE 109—Coral pipes in the Mystery Room, Carlsbad Cavern. Material in the center of the largest coral pipe (lower right) is bat guano. Photo Alan Hill.

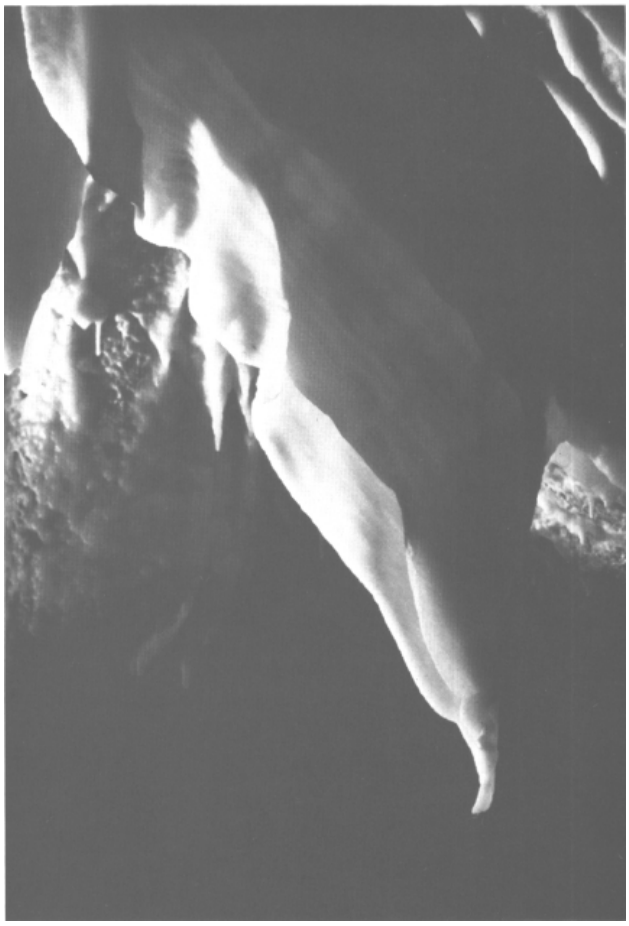

FIGURE 110—A drapery formed along an inclined ceiling, Carlsbad Cavern. Photo Kenrick Day.

the floor. Severely furled draperies form on steeply sloping walls, whereas fringed draperies form under gentler slopes where slow-moving droplets of water are held between individual serrations along the drapery's bottom edge. A good example of a fringed drapery occurs in the side passage off the Boulder Room in Ogle Cave.

Practically every cave in the Guadalupe Mountains has drapery speleothems, the most notable specimens occurring at the Whale's Mouth and in the Dome and Mystery Rooms of Carlsbad Cavern, and also in Three Fingers, Hell Below, and Virgin Caves. In the Lake Room of Virgin Cave is a composite-drapery–column called the "Peppermint Tree." About a dozen draperies, stained in various shades of brown and tan, adorn the Peppermint Tree, looking like sticks of peppermint candy ready for the picking (Pl. 12). An exquisite lace-like drapery occurs in the very bottom of the Mystery Room, the lace effect having been created by alternating strips of crystalline calcite and moonmilk. When the moonmilk layers dried out and flaked to the floor, the strips of crystalline calcite were left, giving the speleothem the appearance of being edged with lace.

Flowstone

Flowstone is one of the most common speleothem types, covering the floors, embankments, and walls of numerous Guadalupe caves (Fig. 111). Flowstone is usually composed of calcite or aragonite (Table 30), but rarely it can be composed of the magnesium carbonate minerals huntite and dolomite. In caves such as the Flint-Mammoth Cave, Kentucky, or Blanchard Springs Cavern, Arkansas, massive flowstone deposits form "frozen waterfalls"—cascades of travertine deposited from solutions which issue out along bedding planes and flow over bedrock ledges. In Guadalupe caves, waterfall-type flowstone is uncommon because the reef and near-reef limestones are usually unbedded or only crudely bedded. One notable exception to this rule is the Chocolate Drop in the New Mexico Room of Carlsbad Cavern, a 7 m high and wide flowstone cascade chocolate-mocha ice cream in color. Other exceptions are the 4–5 m high frozen waterfall of Lake Cave in Slaughter Canyon, the colorful 6 m high Temple of the Fire God in Three Fingers Cave (Pl. 16A), and the 15 m high flowstone cascade in Lechuguilla Cave (Hill, 1986).

Flowstone, as is more typically seen in Guadalupe caves, occurs as a sheet-like deposit associated with stalagmitic travertine, either covering the sides of stalagmites as protruding bulges or extending away from the base of stalagmites along the floor. In some cases, flowstone covers clastic silt or bat guano; when this material is eroded away from beneath the flowstone, a canopy may be left as a projecting travertine sheet. One example of this type of clastic-related canopy flowstone occurs in New Cave where protruding travertine has been undermined of bat guano. A canopy deposit that is not related to clastic material is the "baldacchino canopy," which forms when flowstone reaches the surface of a pool. Baldacchino canopies can be seen along the lower edge of the Crystal Springs Dome stalagmite, next to the trail in the Big Room, and also in Billing Dove Tunnel, Big Room, Carlsbad Cavern.

A prevailing type of canopy-flowstone deposit in Guadalupe caves is the "bell canopy," good examples of which are in New, Ogle, Three Fingers, Pink Panther, Christmas Tree, and Virgin Caves. Bell canopies are essentially flowstone modifications of dripstone stalagmites and columns

FIGURE 111—A cascade of flowstone, Hell Below Cave. Photo Alan Hill.

FIGURE 112—A bell canopy, Three Fingers Cave. Photo Kenrick Day.

which assume an odd assortment of shapes, the most common being a bell-like figure (Fig. 112). Bretz (1949, p. 456) was the first to recognize the peculiar bell-canopy form: "differential solution has largely spared the top while eating away the sides, so that the form produced suggests a gigantic canopy umbrella or toadstool, the underside of the cap and irregular stem showing the concentric growth structure." Bretz thought that bell canopies formed when the host stalagmite or column was partly or completely submerged under water, but Black (1954, p. 140) proposed another, non-flood origin for this type of travertine: "a formation alternately spreading and contracting showing beautifully the effect of the increase and diminuation of water falling on them." Black's hypothesis of origin of this type of flowstone speleothem is essentially correct. Hill (1973a) named the form and elaborated on Black's hypothesis, invoking flow rates which equal or just barely exceed preceding flow rates so that new travertine layers deposit directly over previously precipitated layers but not beyond them. In this manner, carbonate material builds up to form laterally protruding ledges or projections of travertine. Hill went on to explain the prevalence of bell canopies in Guadalupe caves as being due to the relatively low humidity and high rate of evaporation.

Infrequently, huntite and dolomite also form as flowstone. The fine-grained, moonmilk-like consistency of these minerals causes the flowstone material to swell and buckle, and then to dry and crack, the whole mass finally resembling a pile of corn flakes or Chinese fortune cookies (Fig. 113). Such buckled-flowstone deposits are called "crinkle blisters" and are best displayed in Wind (Hicks) Cave, in side passages off of Left Hand Tunnel, and in the New Mexico Room and Bifrost Rooms of Carlsbad Cavern (Hill, 1973c, 1976c).

Oddly shaped or textured flowstone may be produced by other factors. In some places, such as near the Chinese Wall of New Cave, flowstone surfaces are covered with microgours—tiny rimstone dams which crenulate the surface of the flowstone. Microgoured flowstone may result from pulsating or irregular patterns of incoming water flow rather than from continuous flow that produces smooth

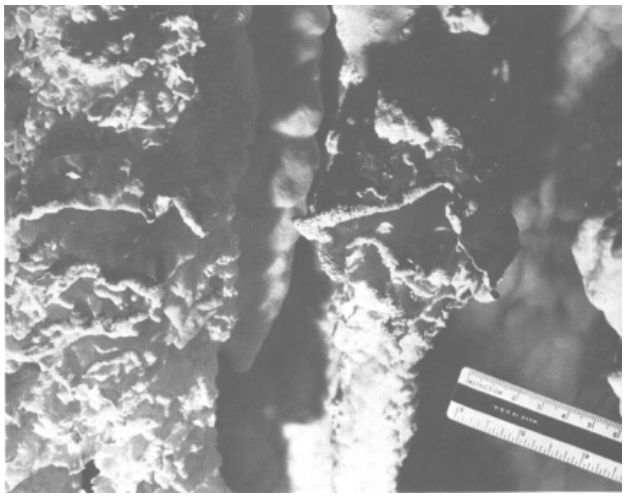

FIGURE 113—"Crinkle blisters," crinkled flowstone composed of huntite and dolomite, in a side passage off Left Hand Tunnel, Carlsbad Cavern. Photo Pete Lindsley.

flowstone surfaces. A high proportion of silt in the calcite making up flowstone can produce sharply pointed edges somewhat like the teeth of a saw blade (Fig. 114). Examples of this type of silt-laden flowstone exist in the New Mexico Room at the point of descent into the East Annex, and also in Lechuguilla Cave on ledges along the 50 m drop (Hill, 1986).

Folia

Folia are speleothems which resemble inverted rimstone dams or interlocking wavy ribs. Named for their resemblance to the rumpled leaves of a book, folia project down-ward and outward from ceilings and overhanging walls at an angle averaging (with much variation) about 20° from the horizontal. The bottom edges of folia may be horizontal or inclined several degrees.

The origin of folia is uncertain, but is believed to be due to a fluctuating water level. In all known instances, folia coexist with clouds and/or cave rafts. At first, cave rafts form as a thin, scum-like layer on the surface of a body of water. If the water level fluctuates upward so that it reaches a wall overhang or cave ceiling, the "scum" attaches to the ceiling along surface irregularities. As the water level in the pool slowly subsides, the precipitate is continually supplied to the lower edge of the forming folia, creating its usually horizontal bottom ridge, and additional material is pulled up onto the growing ridges by surface tension. Water flowing from above may accentuate the lateral rib shape and can also produce a non-horizontal bottom edge.

Folia are best developed in the Christmas Tree Room of Carlsbad Cavern; less well-developed folia occur nearby, off of the Lake of the Clouds Passage (Davis, 1970). The folia of the Christmas Tree Room have ribs averaging 5.0–7.5 cm in length. They are associated with cave rafts stranded on wall ledges.

Helictites

A helictite is a speleothem that can twist in any direction. Unlike stalactites, helictites are formed by seeping rather than dripping water. In the center of each helictite is a tiny capillary tube through which water moves under hydrostatic pressure to the outer growth tip. The growth is therefore not controlled by gravity and can proceed in any direction.

Helictites can be divided into four groups based on size and shape: (1) a filiform variety consists of tiny hair-like filaments; (2) a beaded variety is shaped like a string of rosary beads; (3) a vermiform variety is worm-like in appearance; and (4) a twig- or antler-like variety is thick and

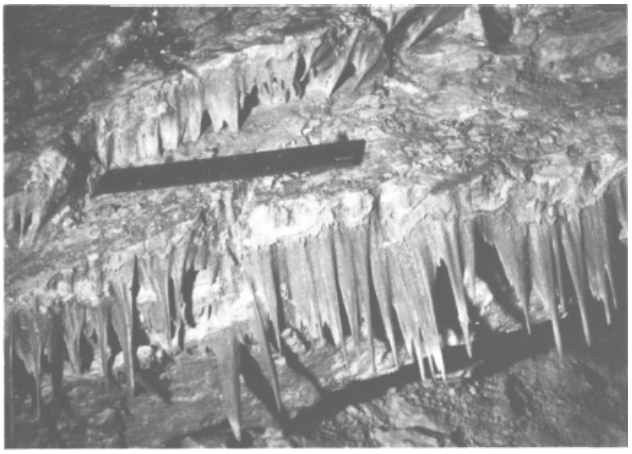

FIGURE 114—Sawtooth-like flowstone containing a high proportion of silt, New Mexico Room, Carlsbad Cavern. Photo Cyndi Mosch Seanor.

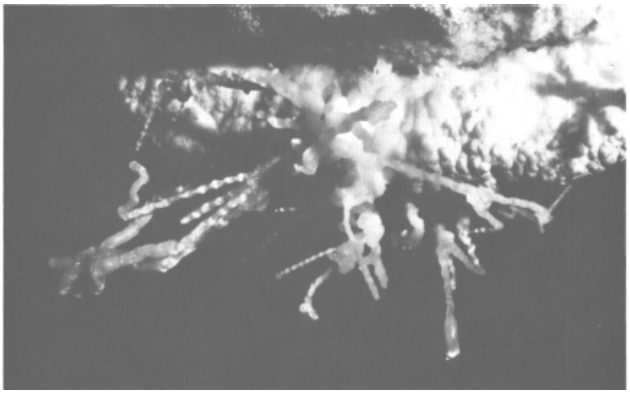

FIGURE 115—Beaded helictites in a side passage off the New Mexico Room, Carlsbad Cavern. Photo Alan Hill.

has straight stems and bifurcating branches. Guadalupe caves have all four varieties. Aragonite alternating with calcite is responsible for the "beaded" or "seaweed" filamental forms; aragonite makes up the radiating, beaded part of the helictite and calcite makes up the straight-stemmed part. Good examples of beaded helictites occur in Musk Ox Cave (Hill, 1976b), in the New Mexico Room of Carlsbad Cavern (Fig. 115), and in the Southern Splendor Passage of the New Section, Carlsbad Cavern, near the Hall of the White Giant.

Vermiform helictites are found in many Guadalupe caves, the "snake dancers" of Hell Below and Virgin Caves being two of the finest examples of this kind of helictite (Pl. 13A, Fig. 116). Other exceptional displays of vermiform helictites are in the Queens Chamber of Carlsbad Cavern, where

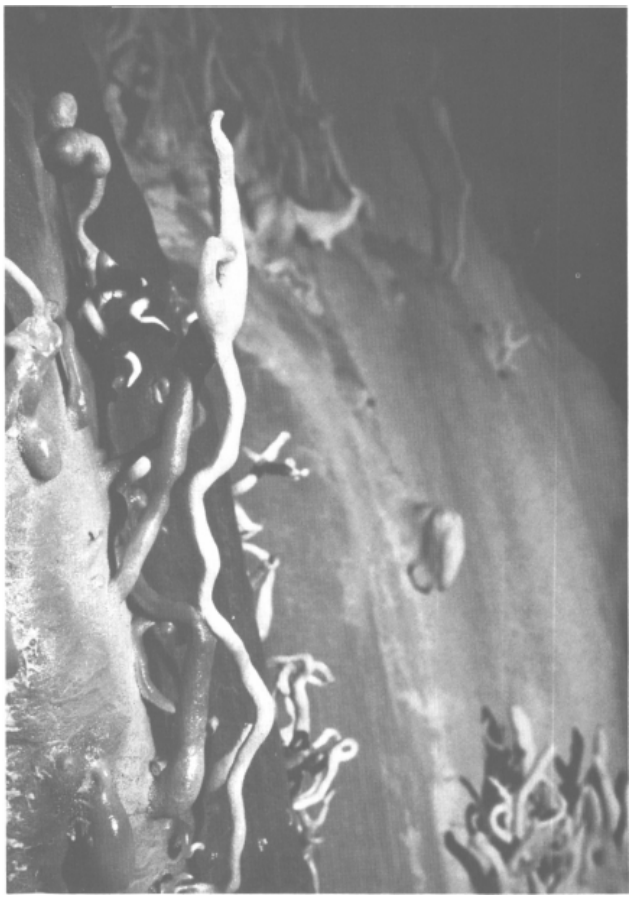

FIGURE 116—The "snake dancer" helictites of Virgin Cave. Photo Alan Hill.

thousands of helictites interweave on the ceiling above the trail, and at the Wall of Medusa, Spider Cave, where a tangled web of helictites adorns a 12 m long wall (Hill, 1979). Near the Wall of Medusa is the "Plumber's Nightmare," an aggregate of soda straws and helictites so interconnected as to resemble the pipeline under one's kitchen sink.

Antler helictites have bifurcating branches up to 15 cm thick that resemble deer antlers. More often than not, the branches take off in an almost horizontal or vertical direction. The Scenic Rooms, Left Hand Tunnel, and Vegetable Room of the Lake of the Clouds area, Carlsbad Cavern, contain the best displays of this kind of helictite. Antler helictites seem to have a distribution similar to that of moonmilk and of deflected stalactites. The cause of this apparent connection is not clear. While some antler helictites (and deflected stalactites) contain moonmilk layers between crystalline layers, still others seem to be devoid of moonmilk. One cross-sectioned antler helictite was found to contain microscopic channels ("canalicules") radiating away from its central canal and towards the outer surface of the helictite, suggesting that perhaps capillary water seeps from the central canal through the canalicules to the outside of the helictite, thereby thickening it.

Moonmilk

This term describes aggregates of microcrystalline carbonate minerals of varying composition. Moonmilk is soft, plastic, and pasty when wet but crumbly and powdery when dry. Wet moonmilk looks and feels like white cream cheese when rubbed between the fingers, while dry moon-milk resembles talc. Texture, not composition, is implied by the term moonmilk. Nine mineral varieties of moonmilk have been described (Hill and Forti, 1986), but only aragonite, hydromagnesite, dolomite, and huntite have been identified in Guadalupe caves (Table 30; Hill, 1979).

Guadalupe caves possess an abundance of moonmilk. One walks through it, crawls through it, and finds it as tufts on the tips of popcorn or anthodites, as creamy-white flowstone, and even as cave pearls. Chalk-white flowstone "rivers" of moonmilk adorn the cave walls in Pink Dragon Cave. In Left Hand Tunnel of Carlsbad Cavern and in Hell Below Cave, moonmilk is so abundant in certain areas that one's boots inadvertently stick to it along the trail.

In Guadalupe caves, moonmilk seems to be most abundant in areas where the Capitan reef is interbedded with the more dolomitic backreef or forereef facies. A perfect example of this is Spider Cave, formed in dolomitic units of the Yates Formation. There piles of dolomite moonmilk are up to 2 m deep and stalactites are sometimes layered with moonmilk between and over layers of more crystalline calcite (Hill, 1979). Left Hand Tunnel, a passage which is developed along the reef-forereef-facies contact (Fig. 18), has such an abundance of moonmilk in reef sections that the trail was constructed with moonmilk in these areas.

Many investigators feel that moonmilk is the product of bacterial action. Gerundo and Schwartz (1949) found denitrifying bacteria in Carlsbad Cavern but did not relate these bacteria to moonmilk generation. G. Moore (pers. comm. 1970) identified possible organic filaments in hydromagnesite moonmilk collected in Left Hand Tunnel, Carlsbad Cavern. While some moonmilk production in Guadalupe caves may be aided by microorganisms, most of it is probably the result of direct chemical precipitation of the high-magnesium carbonate minerals such as hydromagnesite, huntite, and dolomite. It is the finely crystalline nature of these minerals that gives the moonmilk its pasty and plastic-like qualities.

Pearls, Cave

A cave pearl is a banded, pearl-like concretion that forms in shallow cave pools or floor depressions where water is dripping from above. Cave pearls can be spherical, cylindrical, or irregularly shaped, depending on the shape of their nucleus. They are usually polished to a high glow and their appearance is nearly identical to that of real pearls (Fig. 117). Cave pearls form around any nucleus, be it a grain of sand, a bat bone, or another speleothem (Hess, 1929; Baker, 1963). Black (1951a, 1952) speculated that spherical cave pearls require constant turning to maintain their roundness, dripping water being the most efficient turning mechanism. If a pearl cannot turn, then the lower side will grow flat while the upper side will become top-heavy with more precipitate matter. Pearls that are free to turn develop calcite "cups" or "nests" below them (Fig. 117).

Carlsbad Cavern is the classic locality for cave pearls. The Rookery of Lower Cave was lined with hundreds of cave pearl "nests" before the guides in the 1920's and 1930's handed most of the pearls out to visitors as souvenirs. Although the cave pearls in the Rookery are now but a meager remnant of what once used to be there, other occurrences remain undamaged, the most notable being the golf-ball-sized pearls in the Cave Pearl Room. Boyer (1964, p. 18) described these pearls as: "found at the foot of a large flowstone mass, up to 4 cm in diameter, remarkably spherical, and of a bluish-white color, the upper portion of each pearl generally being stained darker. Each one is free, but occupies its own facet, or 'nest,' amongst the others."

Other Guadalupe caves also contain cave pearls, but not in the same profusion as in Carlsbad Cavern. The Cave of the Madonna has its nests of cave pearls (Fig. 117), and so does Hell Below Cave. In Hell Below hundreds of marble-sized cave pearls used to adorn cave floors; the largest pearl was supposedly "as big as a billiard ball" (Nymeyer, 1938, p. 38). Cave pearls composed of aragonite moonmilk have been found in Able Goat Cave (Hill et al., 1972a), and white and dark gray cave pearls have been discovered in Lechuguilla Cave (Hill, 1986).

Rafts, Cave

Cave rafts are thin, planar deposits of crystalline calcite or aragonite that float on the surfaces of cave pools (Pl. 13B). Raft growth is oriented with the c-axes of calcite or aragonite crystals parallel to the water surface. Rafts grow on the surface of quiet cave pools until some force such as dripping water sinks them to the bottom of the pool. Repeated sinking of cave rafts at a drip point results in the rafts piling up on the pool bottom in conical masses called "cave cones."

Cave rafts occur in many Guadalupe caves, either as Type I rafts in the cave walls, Type II rafts usually found in cave cones, or Type III rafts floating on the surfaces of small cave pools. The three types have different carbon-oxygen corn-

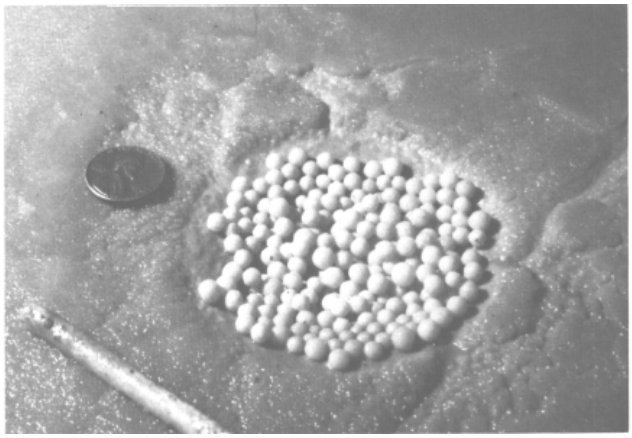

FIGURE 117—A "nest" of cave pearls, Cave of the Madonna. Photo Kenrick Day.

positions (Fig. 98). Based on their carbon–oxygen signatures, Type I rafts are believed to have formed at the water-table surface during an early stage of speleogenesis (see Part I of this paper for the origin of the calcified siltstone-cave raft sequence). Type II rafts have the same oxygen composition as Type I, but have a higher $\delta^{13}C$ value which suggests that when they formed the cave was experiencing more air flow and CO_2 loss. Type III rafts are different from Types I and II in both oxygen and carbon composition. Type III formed in pools of meteoric water (rather than at the water table) under conditions of increased air flow and pas-sage dryness.

The best occurrence of Type III rafts is in the Left Hand Tunnel of Carlsbad Cavern. At the end of the Right Hand Fork, a large pool of water is almost completely covered with a sheet of calcite, looking much like a winter pond about to freeze over. Black (1953) reported another small pool with floating rafts of aragonite in Left Hand Tunnel.

Cones up to 4 m high and composed of Type II rafts are present on the Balcony overlooking the Lake of the Clouds, Carlsbad Cavern (Fig. 93). Cones up to 1.2 m high also occur in the East Annex of the New Mexico Room, and cones with exposed sides up to 0.5 m high occur in the Bell Cord Room. In all three instances, the cones are associated with corrosion features and are believed to have precipitated during the time when condensation–corrosion processes were active in these passages. In the Balcony of the Lake of the Clouds, aragonite anthodites are perched on the apices of some of the cones, having formed subaerially from the same drip points that formerly sank the cave rafts (Hill, 1981a). Volcano-like cones are present in the Bell Cord Room, at one locality as a cluster of about 35 separate cones and at another locality in a cluster of about 20 cones (Fig. 93). The cones in the Bell Cord Room are pastel yellow, peach, and brown, with individual rafts oriented at about a 45° angle to the vertical axes of the cones and with layers of dark-gray manganese alternating between calcite raft layers. These cones have drip tubes drilled down their apices. One hole in a 45 cm high volcano cone was plumbed at depth of 1.5 m, showing that the cave cone extends much lower than its visible base. Very large cave cones are known only from Carlsbad Cavern. One 12.5 cm high cone has been observed in a small pool in Three Fingers Cave (C. M. Seanor, pers. comm. 1985), and even smaller cave cones are known to occur in other Guadalupe cave pools.

Rims

A rim is a shell of material that lines bedrock or other speleothems and is scoured on the inside and rough and coralline on the outside. Rims may be vent-shaped, rimming aperatures where holes or small passages emerge into a larger passage or room (Fig. 118), or they may be projections of material rimming corroded speleothems (Fig. 63). Carbonate rims are known from a number of Guadalupe caves. The largest rim is about 1 m high and 6 cm thick at the base, and is located where the smallest of three ascending routes meets with the Cavernacle in Virgin Cave (D. Davis, pers. comm. 1985). In Carlsbad Cavern almost all of the carbonate rims are associated with corrosion features, an example of which is the rim on the stalagmite known as the Creeping Ear in the Lake of the Clouds Pas-sage (Fig. 63). The rim lining the Creeping Ear stalagmite is 15 cm wide and 0.5 cm thick, and has faint growth layers parallel to its outer edge which appear to be composed of acicular aragonite. The stalagmite is corroded on the side facing the Lake of the Clouds and the rim projects outward from the corroded part, its smooth inner side being an ex-tension of the corrosion. Several vent-shaped rims 3–4 cm high and 6 cm across occur high on the wall along the trail between Appetite Hill and the Boneyard (Fig. 118).

Davis (1982b) proposed that rims deposit from conden-

FIGURE 118—Vent-shaped rims on the wall, Appetite Hill, Carlsbad Cavern. Photo Cyndi Mosch Seanor.

sation water where warm, moist air meets with cooler, drier air. Hill (1984b) discussed the factors of temperature, pressure, carbon-dioxide equilibrium, evaporation, and air flow as they relate to the origin of rims, and proposed a model of rim formation for the Lake of the Clouds area where rims line the flanks of corroded stalagmites such as the Creeping Ear. As warm, moist air moved up from the Lake of the Clouds, it collided with the Creeping Ear stalagmite, reached its dew point, and condensed on the surface of the stalagmite. This condensation water had a high dissolved content of CO_2 (Table 5) and, due to its acidic nature, corroded the part of the stalagmite facing the Lake of the Clouds. Air flow then moved this condensation water, now saturated with calcium carbonate, to the flanks of the stalagmite where the calcium carbonate precipitated as rim material.

Rimstone dams

Rimstone dams are barriers of calcite or aragonite that impound cave streams or shallow pools. Carbonate material builds up at the point where water overflows the dam and where turbulence and carbon-dioxide loss are the greatest. As dams grow upward, water always seeks the lowest out-let; hence dams build up evenly, with deposition alternating between shallow points on the dam.

Black (1951b) described the rimstone dams at Mirror Lake, Longfellow's Bathtub, and Devil's Spring, Carlsbad Cavern, and Hill (197Th, 1980a) described the 40 cm high rimstone dams in Damn Cave and the 1.8 m high dams in Hidden Cave (Fig. 119). The most impressive rimstone dam in any Guadalupe cave is the Chinese Wall of New Cave. The Chinese Wall is only about 10 cm tall, but it is unique in that it is severely convoluted and furled, some of the individual furls having curved all the way back on themselves

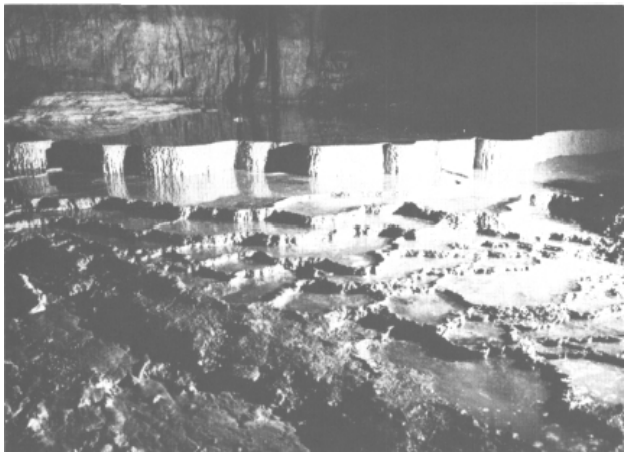

FIGURE 119—Rimstone dams in Hidden Cave. The height of the tallest dam is approximately 1.8 m. Photo Jeep Hardinge.

so as to form vertical tubes (Fig. 120). If the furls in the Chinese Wall were stretched out straight, it is estimated that they would total about 10 m in length.

The height and convolution of rimstone dams is related to the gradient of slope: the greater the slope, the higher the rimstone dams; the shallower the slope, the lower and more convoluted the dams. Steep dams curve gently lengthwise, corresponding to topographic contours, and they are convex at spill-over points. Shallow dams curve around and back on themselves much like the meanders of a low-gradient river. Where dams are subject to slightly aggressive water, individual furls may become isolated from the rest of the dam in a manner resembling an oxbow cutoff of a meandering river.

Shelf stone

Shelfstone is a flat carbonate deposit that is attached as a ledge or eave-like projection along the edge of a cave pool or other speleothems submerged in a cave pool. When shelf-stone lines columns, candlestick-like forms result (Fig. 121); when it forms over the top of stalagmites, lily pad or coke table forms result. Shelfstone begins its growth when cave rafts or other material attach to the sides of a pool. These can build in thickness and width until they partially or completely cover the surface of the pool. Shelfstone ledges always denote a present or past pool level.

Most small pools in Guadalupe caves contain at least some shelfstone. Good displays of shelfstone are in Sand Cave, in the bottom of the Cave of the Madonna, and in the Lake Passage of Cottonwood Cave. One coke table in the Lake Passage used to have a candle-shaped stalagmite in its center, but the stalagmite was vandalized; this was called the "Wine Table" (Hill, 1977a). Alternation of dark-gray manganese with white calcite layers in shelfstone in the Lake of the Clouds Passage, Carlsbad Cavern, shows that shelfstone growth starts evenly on both the bottom and top sides of the shelfstone, but as the deposit thickens, preferential growth occurs along the top side of the shelf-stone.

A peculiar, crescent-shaped variety of shelfstone can be seen along the trail by Mirror Lake, Big Room, Carlsbad Cavern, and also in Cottonwood Cave. This type of shelf-stone forms in areas where water drips into a shallow pool. The convex parts of the crescent shelfstone point consistently toward the location of the drip, and the crescent shapes are produced by "waves" or ripples of water radiating from the drip point and deflecting off the shelfstone.

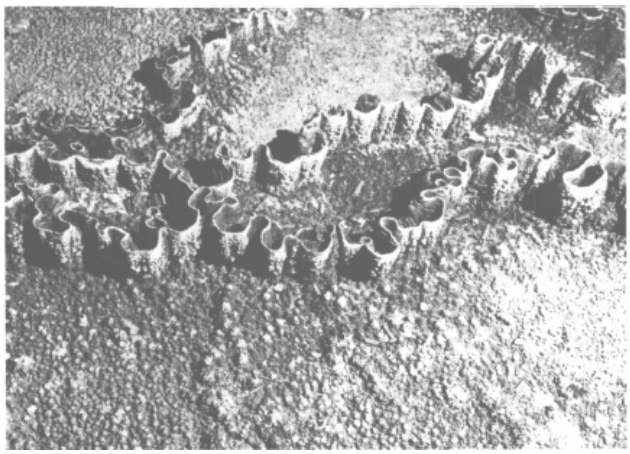

FIGURE 120—The "Chinese Wall" of New Cave. The dam is about 10 cm in height. Photo Jeep Hardinge.

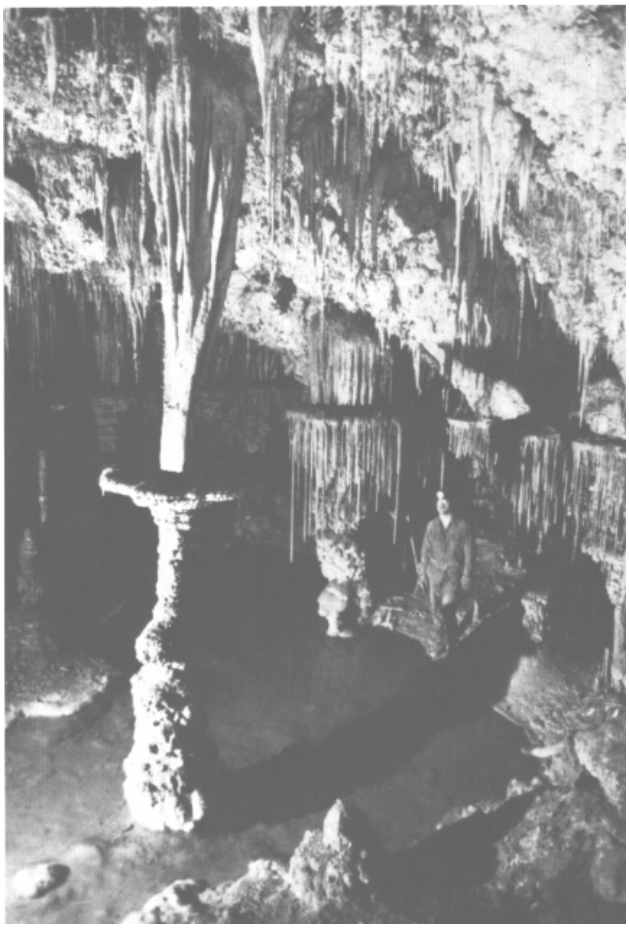

FIGURE 121—The "Candlestick," Cave of the Madonna. The shelf-stone of the candlestick and the shelfstone along the wall mark a former pool level. Photo Kenrick Day.

Shields, Cave

Shields (sometimes called "palettes") are speleothems consisting of two parallel, spherical plates separated by a medial, planar crack. Viewed from above, a shield resembles a shield of armor; from below, it looks like a column without a top (Fig. 122). Massive flowstone usually hangs from the lower hemisphere of a shield, and if this travertine gets heavy enough, the shield will separate along its medial crack and its bottom part will crash to the floor.

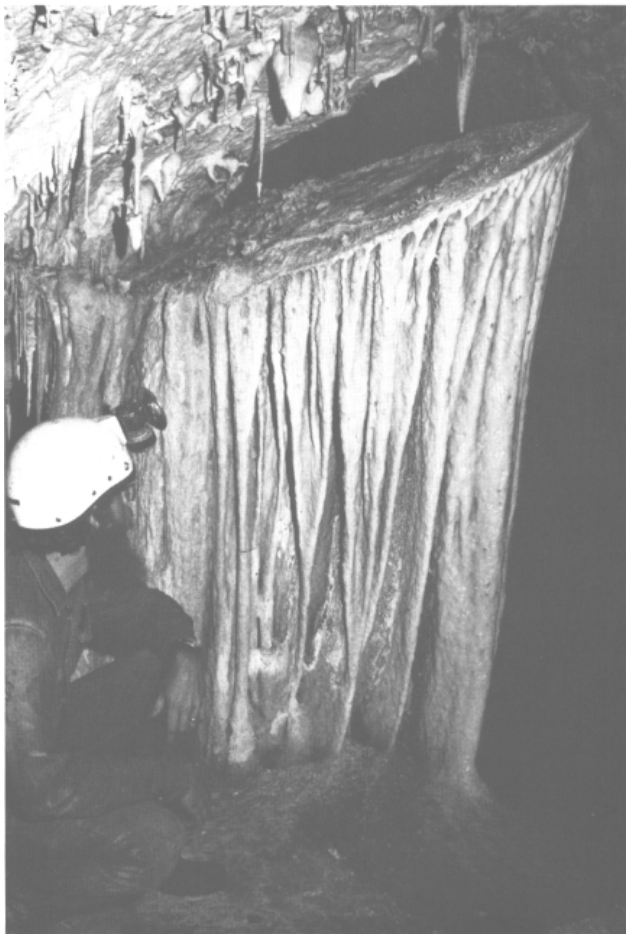

FIGURE 122—A shield developed along a wall joint, Ogle Cave. Photo Jon Vinson.

Like helictites, shields grow by water moving under hydrostatic pressure through the speleothem's interior to its outer, growth surface. Unlike in helictites, the water does not move through a capillary tube, but instead seeps through a planar crack and so creates the shield-like shape of the speleothem. It used to be thought that shields were a very rare speleothem, but exploration in the Guadalupe Mountains over the last 20 years has substantiated that shields are common. Pink Palette (the cave derives its name from the shields present), Pink Dragon, New, Madonna, Ogle, Deep, Corkscrew, and Carlsbad are among a number of Guadalupe caves known to contain shields. In Deep Cave, two shields have formed along the cracks in a large stalagmite rather than along cracks in the wall; the shields, 2 and 0.3 m in diameter, are oriented perpendicular to each other (Hill, 1978a). In Pink Dragon Cave, five nearly vertical shields occur at the ceiling, four of which are aligned parallel to the passage direction (along a major joint trend) and one aligned perpendicular to this direction (Hill, 197Th). The Pink Dragon shields are spectacular in that they seem to "hang in thin air."

A "welt" is a nubin-like shield which forms along cracks in a column or a cave wall. Welts have been noted in Hidden Cave (Hill, 1980a), Ogle Cave (Hill, 1978b), and in the Guadalupe Room of Carlsbad Cavern. Welts and shields often grow next to each other, the welts being incipient shields formed along the same crack as the shields and by the same solutions under pressure. Usually the upper sides of welts and shields are covered with helictites.

Spar

As discussed in Part I of this paper, spar crystals occur in many Guadalupe caves, either as dogtooth-shaped crystals (Fig. 60) or as nailhead-spar linings. Good localities of dogtooth spar are in Carlsbad Cavern, Cottonwood Cave, Geode Cave, Three Fingers Cave, Crystal Cave, Idono Crystal Cave, Virgin Cave, Frank's Cave, and Pink Fink Owlcove. In Crystal Cave, the walls, floors, and ceilings are covered with dogtooth spar up to 55 cm long, the crystals "bristling in every direction like a million spikes" (Nymeyer, 1938, p. 40). Dogtooth spar crystals up to 35 cm long (some of them twinned) have been reported lining cavities of Idono Crystal Cave (DuChene, 1967). In Geode Cave, spar crystals up to 23 cm long adorn the walls (J. Burke, pers. comm. 1982).

Nailhead-spar linings are best developed in the Nailhead Spar Lining Room, at the very bottom of the Mystery Room, Carlsbad Cavern. Columnar nailhead spar with blunted facets forms as 7.5-10 cm thick linings on the ceiling of this room. In places this lining is still intact, but in other places sections of it have fallen to the floor, leaving a linoleum-like pattern on the ceiling.

Most of the spar crystals and crystal linings in Guadalupe caves are phreatic spar; that is, they formed in the phreatic zone under saturated conditions. Other spar, called "chenille spar" forms in cave pools, usually directly underneath shelfstone. Chenille spar does not have well-developed, external crystal faces, but rather looks somewhat like a subaqueous coralloid. However, these are not layered structures like coralloids, but single crystals of calcite. Chenille spar can be seen in Carlsbad Cavern in the New Mexico Room by the Chocolate Drop, and in the Big Room along the trail in the Polar Regions and near the Top of the Cross. The Park guides call the chenille spar at the Top of the Cross "hula skirts" because of its palisade-like appearance (D. and A. Cordera, pers. comm. 1985).

Small dogtooth spar crystals also exist as surface features on speleothems, causing them to sparkle with a velvety luster. "Velvet" spar crystals are approximately 1 mm from base to tip and grow perpendicular to the surfaces of speleothems. One of the best occurrences of cave velvet in Guadalupe caves is in the Texas Pit Passage of Lower Cave, Carlsbad Cavern.

Stalactites

Stalactites are the most familiar of all speleothem types, readily remembered for their icicle-like pendant shape and the fact that they hang "tite" to the ceiling. Stalactites in Guadalupe caves differ from those in other caves in that they often assume war-club-like shapes where the bottom part of the stalactite is thicker than the top part, or in that they are often deflected from the vertical so as to appear curved at their tips.

All stalactites begin their growth as soda straws, thin-walled tubular stalactites with hollow centers (Fig. 123). Water droplets saturated with calcium carbonate collect on cave ceilings and then as carbon dioxide is lost, a thin film of carbonate material precipitates over the surfaces of the water drops. As more water accumulates in each drop, the drop becomes heavier and begins to oscillate. This causes the calcite film to spin up toward the ceiling and to adhere there by surface tension. When the drop falls to the floor, the carbonate film is left on the ceiling as a round rim of material—the initial ring of a soda straw. Subsequent precipitation extends the straw's length and water continues to move through the hollow tube and to the tip of the growing straw. If the center of the tubular stalactite is blocked, solutions flow down on the outside of the straw and create the carrot shape of a "normal" stalactite (Pl. 11A).

When a stalactite becomes submerged, a war-club shape

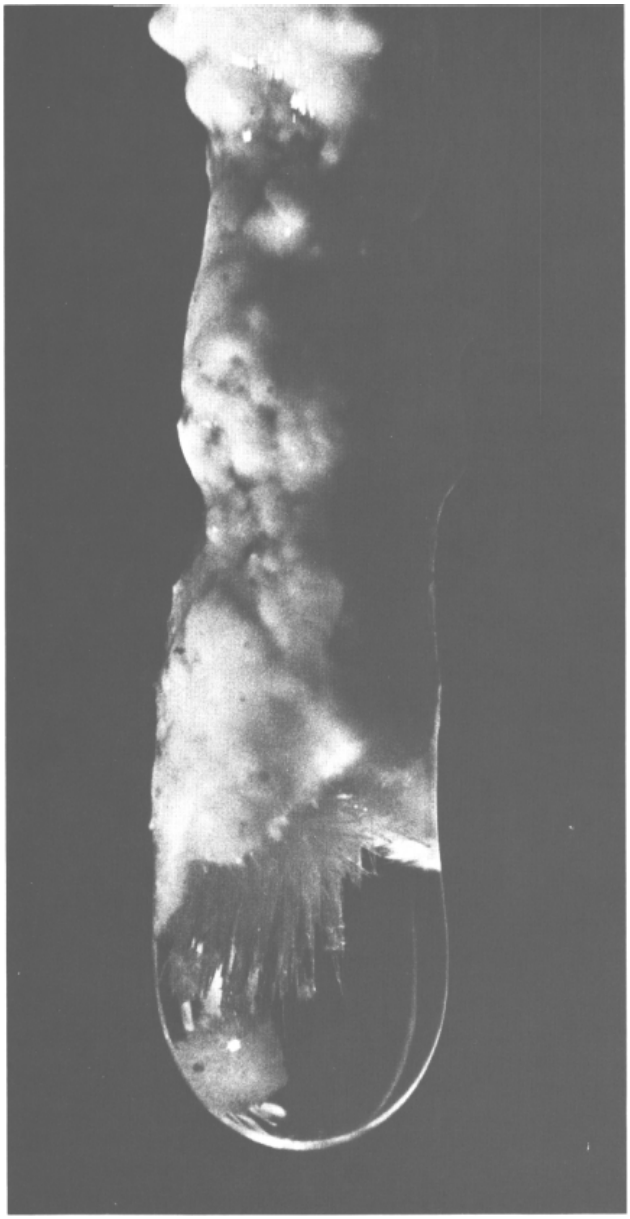

FIGURE 123—Crystals growing on the tip of a soda-straw stalactite, Carlsbad Cavern. Photo Pete Lindsley.

FIGURE 124—A deflected stalactite in Lower Cave, Carlsbad Cavern. Photo David Jagnow.

can result. The "war clubs" in the War Club Rooms of End-less Cave, Hidden Cave, Pink Dragon Cave, and Carlsbad Cavern are related to a back-up of pool water where subaqueous coralloids coat the surfaces of the submerged stalactites. "Spanish moss," a variation of war-club stalactite, is known only from Cottonwood Cave (Hill, 1977a). These moss-like speleothems are milk-chocolate brown, porous, and very fragile; internally, they are composed of an inner stalactitic core overlain by a porous war-club-like covering, itself overgrown by the "Spanish moss" (Pl. 14A).

Deflected stalactites can be seen in many parts of Carlsbad Cavern (the Scenic Rooms, Left Hand Tunnel, Lower Cave; Fig. 124) and also in other caves such as New Cave and Christmas Tree Cave. They start out as curved soda straws and continue growing in this curved mode. The precise cause of deflected-stalactite growth is not known. Queen (1981) suggested that deflected stalactites are related to air flow, but, as Sanchez (1964) pointed out, curvature and orientation may be uniform in a single stalactite, but may differ in adjoining stalactites (within tens of centimeters). If deflection is connected to air flow as Queen suggested, then this connection is very subtle and must be related to extremely localized air-flow patterns. A deflected stalactite thickens by water flowing through the stalactite rather than over its surface, otherwise the deflected bottom would have a drapery build-up of material on its lower end. Perhaps solutions which thicken the deflected stalactite move through the stalactite via tiny channels ("canalicules"), like they probably do in antler helictites.

Stalagmites

Stalagmites are convex floor deposits which form when water drips from a stalactite or the cave ceiling. When drops of water impact the floor, carbon dioxide is expelled and calcium carbonate is precipitated. Stalagmites assume a variety of shapes depending on their particular history of development: broomsticks, totem poles, fried eggs, toad-stools, and Christmas trees are some forms that occur frequently enough to have earned their own special label. The shape of a stalagmite depends on the drip rate and also on the crystallizing mineral making up the stalagmite. Aragonite forms spiny "Christmas tree" anthodite stalagmites, whereas calcite forms typically smooth-sided stalagmites. Totem-pole or broomstick stalagmites have small or non-existent counterpart stalactites; these stalagmites build up where water drips rapidly into a cave. Good examples of the tall, skinny, totem-pole variety of stalagmite are in Three

Fingers Cave, Carlsbad Cavern, and Deep Cave (Fig. 125). Fried-egg stalagmites topped on their apex with a yellow "yolk" surrounded by "white" crystalline calcite can be seen in Pink Dragon Cave, New Cave, and in the New Mexico Room of Carlsbad Cavern. Hollow stalagmites are those composed primarily of aragonite or popcorn. This type is found in areas of pronounced corrosion of bedrock and speleothems, and is believed to be the result of acidic solutions dripping from the ceiling onto the stalagmites.

Stalagmites in Guadalupe caves are often massive. The Monarch in New Cave, according to the Guiness Book of Records, is supposedly the tallest stalagmite in the world, being almost 36 m high. Bell-canopy flowstone can modify the basically convex shape of stalagmites into bizarre and interesting forms. The Christmas Trees of New Cave and Christmas Tree Cave, Snoopy of Ogle Cave (Fig. 126), and the Clansman of New Cave (Fig. 127) are examples of composite stalagmites and bell-canopy flowstone. Burnet (1938, p. 382) made the Clansman famous by describing his first impression of it in these words:

> ... the sight would strike terror into one with a faint heart. The white mantle shrouded an older formation of dark yellow and brown, the whole effect being that of a huge, cruel face beneath the white robe. Small stalactites hung from the bestial upper lip, giving the appearance of monstrous fangs. The jutting chin hangs slack, and stains at the side of the mouth make the figure appear to drool. There could be no doubt that this figure should be called the Clansman, for the white robe and whole general effect was a perfect caricature of that fanatic nightrider of the past.

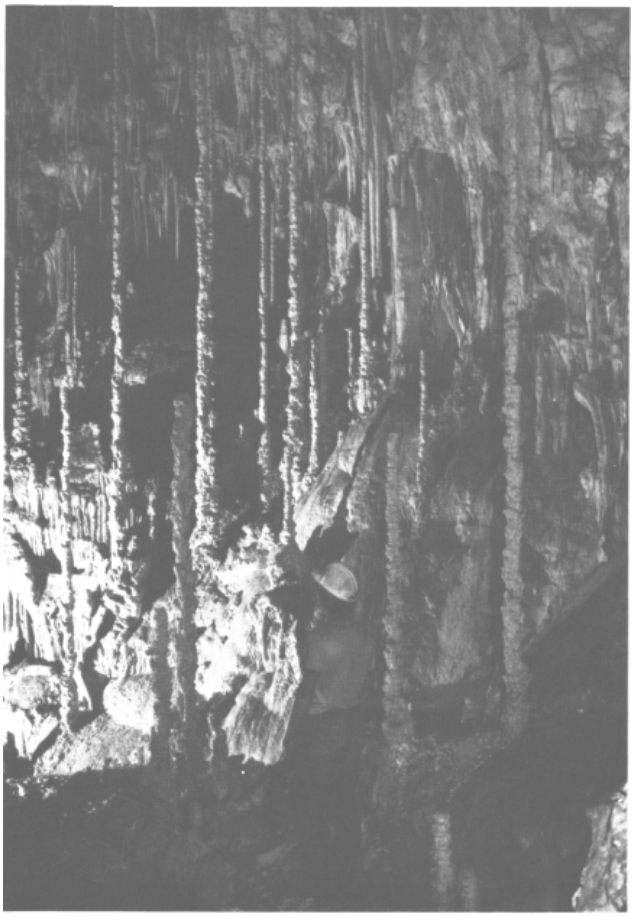

FIGURE 125—"Broomstick" stalagmites, Deep Cave. Photo Kenrick Day.

A stalactite joined with its counterpart stalagmite is called a column (Pl. 14B). Columns in Guadalupe caves assume incredibly large dimensions—sometimes over 20 m in height and 7.5 m in diameter (Fig. 128). The largest columns are typically aligned along ceiling joints where the greatest amount of water drips into the cave. Hill (1978b) correlated the location of the most massive columns and stalagmites in the Sequoia Room of Ogle Cave with a valley depression on the surface overlying the cave (Sheet 6). The depression has been responsible for directing water in along a ceiling joint and the columns have formed along this same joint.

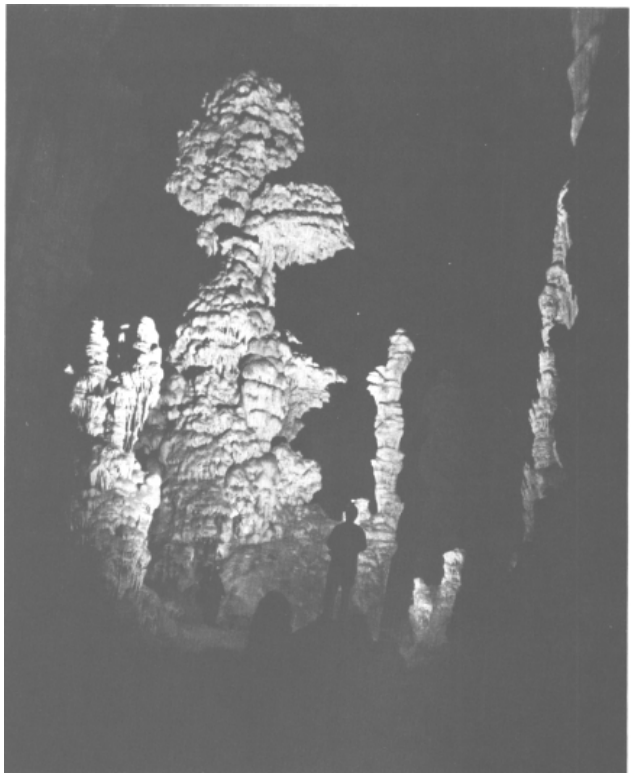

FIGURE 126—The stalagmite known as "Snoopy," Ogle Cave. Photo Pete Lindsley.

FIGURE 127—The famous "Clansman" stalagmite of New Cave. Photo Jeep Hardinge.

Sulfates

Compared to carbonate minerals, sulfate minerals are rare in Guadalupe caves. Cottonwood Cave is the only cave that contains abundant sulfate speleothems. Secondary sulfate minerals identified in Guadalupe caves are gypsum ($CaSO_4•2H_2O$), epsomite ($MgSO_4•7H_2O$), mirabilite ($Na_2SO_4•10H_2O$), and celestite ($SrSO_4$). All four occur in Carlsbad Cavern; gypsum and epsomite occur in Cottonwood Cave, and gypsum in Hell Below Cave, Wind (Hicks) Cave, and Spider Cave.

Deposition

The origin of sulfate minerals is not as well understood as that of carbonate minerals. Vadose seepage is the mechanism by which the sulfate ion enters the caves and evaporation is the cause of precipitation, but the ultimate source of the sulfate ion is still a matter of speculation. Three possible sources are: (1) the massive gypsum blocks and rinds in the caves, (2) evaporite beds of the Ochoan Series which might have once existed above the caves, and (3) pyrite in the overburden. Before sulfur-isotope data had been obtained on some of the sulfate speleothems, the first source was considered to be the most likely because of the spatial correlation of some of the secondary-gypsum mineralization relative to some of the gypsum blocks. Most of the gypsum and epsomite speleothems in the lower Gypsum Passage of Cottonwood Cave occur below a number of partially dissolved gypsum blocks residing in the upper Gypsum Passage. Gypsum stalagmites in Lower Cave, Carlsbad Cavern, are located below a number of gypsum blocks encountered on the climb up toward Mabel's Room and the Talcum Passage. In the New Mexico Room of Carlsbad Cavern, gypsum flowers and crust in the East Annex occur below gypsum blocks in the Balcony.

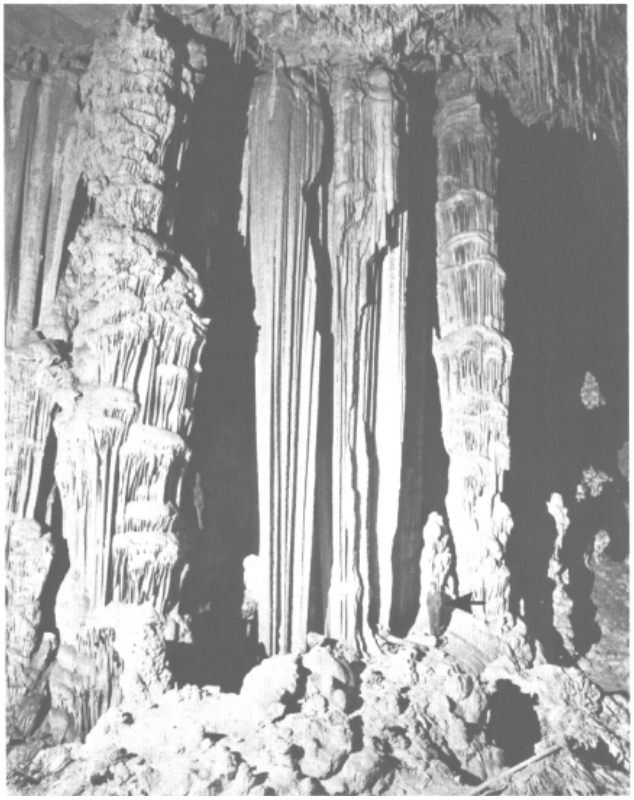

FIGURE 128—The massive columns of Ogle Cave. A caver (arrow) serves as a scale. Photo Pete Lindsley.

The isotope data do not support a genetic connection between the massive gypsum and the sulfate speleothems. The sulfate flowers and crusts in the East Annex of the New Mexico Room have 8^34S values of +9.2 and +8.7, respectively, while the gypsum blocks in the Balcony overlying the East Annex have a $\delta^{34}S$ value of -25.6 (Table 22). Similarly, the gypsum stalagmites in Lower Cave have a $\delta^{34}S$ value of + 7.3, while the gypsum blocks on the climb up to Mabel's Room have a value of -17.8. This difference in isotopic composition shows that the two types of deposits are genetically unrelated.

The second possibility is that the sulfate mineralization in Guadalupe caves has derived from evaporite deposits that may have once existed in the overburden (i.e. the Salado and Rustler Formations; Fig. 4). Smith (1978b, fig. 3) showed the Salado Formation overlying the Yates and Tansill Formations in the vicinity of the McKittrick Hill caves; however, it is not known if the Salado and Rustler Formations ever extended over the Tansill Formation in the vicinity of Carlsbad Cavern. The Castile Formation in the basin has an average $\delta^{34}S$ value of +10.3 (Table 23), and sulfate beds within the overlying Salado and Rustler Formations may have similar isotopic compositions. This value correlates closely with the $\delta^{34}S$ values for the sulfate speleothems in Carlsbad Cavern, but not with the Cottonwood Cave sulfate speleothem ($\delta^{34}S$=–0.8) (Table 22).

The most likely source of the sulfate ion for sulfate speleothems in Guadalupe caves is pyrite disseminated in backreef (mainly Yates Formation) beds. When pyrite weathers to limonite, it produces the SO_4^{2-} ion in solution which, when combined with calcium and magnesium derived from limestone and dolomite, forms gypsum and epsomite, respectively. Sulfate mineralization is most pronounced in the northwest parts of Carlsbad Cavern (i.e. along the north wall of the New Mexico Room, the northwest part of the Mystery Room, and near the Cable Slot in Lower Cave; Fig. 95), a relationship which suggests that the sulfate may have derived from Northwest Shelf beds. Cottonwood Cave contains more secondary gypsum and epsomite mineralization than any other Guadalupe cave, a fact that may relate to its stratigraphic position directly underlying the pyritic and dolomitic Yates Formation. The one isotope measurement done on a piece of secondary gypsum crust collected in Cottonwood Cave was -0.8; this compares with a $\delta^{34}S$ value of -2.5 for a piece of pyrite collected on Guadalupe Ridge near Cottonwood Cave (Table 22).

Stability

Sulfate minerals have a high solubility and for this reason are usually found in dry cave passages. Gypsum is stable when exposed to the air at ordinary cave temperatures and humidities, but the more soluble magnesium and sodium sulfates, epsomite and mirabilite, are unstable. Above a certain humidity, these two minerals absorb moisture from the air and dissolve. Even breathing on these minerals or bringing one's carbide lamp too close to them causes epsomite and mirabilite to melt. When the humidity of a cave rises in the summer months, as it does in Carlsbad Cavern (Fig. 21), epsomite and mirabilite will absorb moisture from the air, dissolve in that moisture, and remain dissolved within bedrock and silt. When the humidity lowers in the winter months, epsomite and mirabilite "sprout up" as efflorescences out of the silt, or deposit as dripstone. Due to their very soluble and deliquescent nature, epsomite and mirabilite also experience a very rapid growth and decline, disappearing or appearing in only a few weeks.

The growth of epsomite with respect to humidity was monitored from March 1985 to June 1985 in Lower Cave, Carlsbad Cavern, near the epsomite cotton (Fig. 95). Hydrothermograph measurements showed that the epsomite was in the crystallized state in March when the humidity and temperature were 87–88% and 12.2°C, respectively, but was in the deliquescent (dissolved) state in June when the humidity and temperature were 88–89% and 12.2°C, respectively. Apparently, 88% is the critical humidity at which the partial pressure of the water vapor in the air exceeds the vapor pressure of a saturated solution of epsomite at this temperature.

No similar hydrothermograph measurements were obtained for the mirabilite cotton in the Lunch Room of Carlsbad Cavern, but in April 1984 the mirabilite was observed to be in the process of disappearing, which may approximately correlate with the April 1969 humidity measurement of 87% made in the Lunch Room by McLean (1971) (Fig. 21).

Speleothems

Sulfate speleothems in Guadalupe caves vary in type de-pending on whether they have deposited from dripping water or seeping water, and whether they have formed on bedrock or sediment. Various types of sulfate speleothems observed in Guadalupe caves are: stalactites, stalagmites, helictites, popcorn, crusts, cotton, flowers, rope, hair, and selenite needles. The stalactites and stalagmites have deposited from dripping water, whereas the other types have deposited from seeping water. Sulfate solutions may seep out of cave walls to form crusts, flowers, or rope, or may seep up through cave sediment to form cotton or selenite needles. Sulfate speleothems are discussed in alphabetical order. As in the discussion of carbonate minerals, the classification system of Hill and Forti (1986) is followed.

Coralloids

In Lower Cave, Carlsbad Cavern, small (1 cm or less) nodules of white gypsum popcorn directly overlie more opaque knobs of carbonate popcorn. The gypsum covers the very tips of carbonate fronds and is more translucent than the calcite it overlies.

Gypsum popcorn is believed to deposit by evaporation from slowly moving films of water (instead of by carbon-dioxide loss). Carbonate popcorn is known to form partially by evaporation in Carlsbad Cavern, as can be seen by its position on the evaporation slope of Fig. 98, and this fact may also relate to gypsum-popcorn growth in the cave. If incoming solutions contain both carbonate and sulfate ions, then, upon evaporation, the sequence of deposition will be carbonate popcorn and sulfate popcorn as solutions evaporate to dryness.

Coral pipes

Gypsum coral pipes form in the same manner as calcite ones, except that soft gypsum takes the place of soft silt or guano in their genesis. Dripping water drills drip tubes into soft massive gypsum, and an outer, harder layer of more crystalline gypsum coats the sides of the tubes, protecting them from further erosion.

Good examples of gypsum coral pipes in Guadalupe caves are those near the Top of the Cross in the Big Room of Carlsbad Cavern. These are up to 1 m deep and centimeters in width, and consist of tabular gypsum crystals overlying a softer core of massive alabaster gypsum.

Crusts

Gypsum crusts line portions of wall in the lower Gypsum Passage, Cottonwood Cave (White, 1960), or they may occur as thin coatings over carbonate speleothems in parts of that passage (Hill, 1977a). The gypsum crust is massive granular and in some cases tabular, the tablets being up to 5 cm long in the area of the large gypsum stalactite known as the Chandelier. Gypsum crust can also be found with small gypsum flowers in Spider Cave; with selenite needles in the climb up to Mabel's Room and on the north wall of the Main Corridor, Carlsbad Cavern; and with gypsum stalactites in Dry Cave (Lindsley and Lindsley, 1978). A thin crust of gypsum also coats the surface of the large stalagmite known as the Christmas Tree in New Cave.

Celestite crusts have been found associated with gypsum crusts in Pickle Alley, off Left Hand Tunnel near the Lunch Room, Carlsbad Cavern. The crusts occur on the ceiling in two separate patches, one about 2 m^2 and the other about 0.5 m^2. The celestite crystals are tabular, grayish-blue, trans-parent, and up to 5 mm long.

Sulfate crusts deposit from solutions which seep uniformly out of bedrock or preferentially out along joints and seams in the bedrock. Uneven growth results in buckled or blistered crusts. "Tabular gypsum" refers to crusts where tabular crystals have grown to a macroscopic size.

Fibrous sulfates

Sulfate minerals often assume a fibrous habit that resembles cotton, hair, or rope. Fibrous sulfates grow as efflorescences on cave silt or bedrock. As solutions evaporate, crystals precipitate out as fibers which correspond to pore spaces within the silt or bedrock. Continued precipitation causes new growth to push old growth outward from the silt or away from the wall.

Hair—Cave hair is composed of thin, single-fiber strands of sulfate material. Gypsum hair has been observed in the Nailhead Spar Lining Room, Carlsbad Cavern, where it occurs as 5 cm long strands on ceilings and walls.

Cotton—Cave cotton consists of crystal fibers 1 cm or so long, which are intergrown and matted together. The cotton effloresces from cave dirt. As sulfate solutions evaporate at the surface of the dirt, crystals precipitate out as a fuzzy growth mat. Tufted cotton, composed of both gypsum and epsomite, can be seen in Cottonwood Cave (White, 1960; Hill, 1977a). The epsomite cotton fills wall recesses in the winter months, but the masses disappear in the summer months. A. Komensky (pers. comm. 1971) observed fibrous crystals of epsomite on the floor of the lower Gypsum Passage, Cottonwood Cave, which "blossomed" into a full growth of 25–35 cm in about a week's time. In Carlsbad Cavern "filamental hairy stuff" has been reported growing along the trail in the Amphitheatre region, the "stuff" being epsomite (report to the park from Edwin C. Alberts, Park Naturalist, 1945). Bitter-tasting epsomite also appears as cottony fibers on the floor of the Big Room and Lower Cave during the winter, most conspicuously in Lower Cave near the climb up to Mabel's Room (Hill, 1973b; Pl. 15A) and in the little crawlway at the top of the ladder going down into Lower Cave (N. Bullington, pers. comm. 1971). Salty-tasting, clear-white, fluffy mirabilite cotton up to 15 cm high forms during the winter months in the Lunch Room on the right side of the trail just before reaching the elevators (Hill et al., 1972, 1972b).

Rope—Cave rope is composed of bundles of parallel mineral fibers which hang down from ceilings or overhanging ledges and have the appearances of unspun rope flax. One gypsum rope 3–4 m long and 2.5 cm in diameter used to spiral down from a limestone ledge in the lower Gypsum Passage of Cottonwood Cave (J. Trout, pers. comm. 1982; Fig. 129a). This extremely rare speleothem was vandalized soon after the lower Gypsum Passage was discovered in 1960 (Fig. 129b), and since that time there has been no new growth.

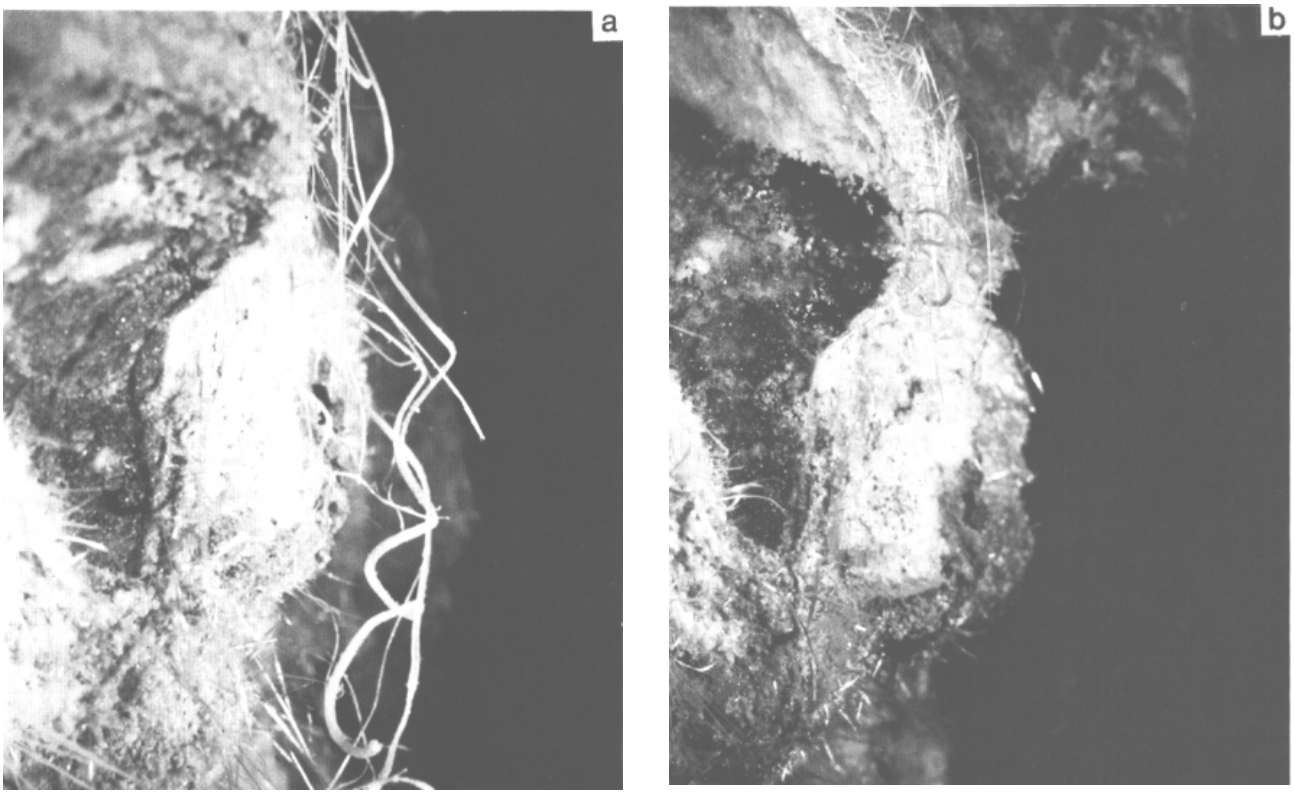

FIGURE 129—Before (a) and after (b) pictures of gypsum rope and needles, lower Gypsum Passage, Cottonwood Cave. In (a) the gypsum rope is 3-4 m long and the selenite needles are up to 1.8 m long. Photo of the same location (b) after the rope and most of the needles were vandalized. Photos Jerry Trout.

Flowers, Cave

Cave flowers are a type of speleothem which have "petals" that radiate away from a common center, the petals being composed of branching and curving bundles of acicular crystals loosely bound together in a polycrystalline matrix. Cave flowers grow from the base, often transporting rock away from the wall with them as they grow. As sulfate solutions seep out from the wall, they crystallize at the air-wall boundary; subsequent crystallization pushes older flower growth out from the wall. If growth is somewhat more rapid on one side of the flower than on the other, a well-proportioned curve is the result.

When the Gypsum Passage of Cottonwood Cave was discovered in 1960, gypsum flowers were present all along the right wall of the passage. Since that time almost all of these flowers have been vandalized, with the exception of a few exquisite flowers up to 10 cm long remaining in a small room beneath floor breakdown (Hill, 1977a). A few epsomite flowers exist in the lower Gypsum Passage, just past the large gypsum stalactite known as the Chandelier, and also along the right-hand wall.

Carlsbad Cavern has gypsum flowers, the best of which occur in the Sand Pit area of the New Mexico Room (R. Kerbo, pers. comm. 1985). Also, a few small gypsum flowers occur in Lower Cave near the climb up to Mabel's Room, along the sides of the Bottomless Pit, Big Room, in the lower part of the Mystery Room, and in the Remarkable Crack, New Section. In Spider Cave the longest gypsum flower observed reaches 6 cm in length, and in the Gyp Joint, Hell Below Cave, gypsum flowers up to 15 cm long directly overlie gypsum rinds (Hill, 1983).

Helictites

One epsomite helictite 1.5 cm long and 0.5 cm in diameter has been observed on an epsomite soda straw in the Epsomite Room, lower Gypsum Passage, Cottonwood Cave. This is the only known occurrence of this speleothem type in a Guadalupe cave (Hill, 1976a, 1977a). Sulfate helictites are believed to form similarly to carbonate helictites, i.e. by hydrostatic pressure which forces solutions through a tiny capillary tube in the center of the helictite to its growth tip.

Needles, Selenite

Selenite needles are swallow-tail twins of gypsum which grow upward from cave silt, or, more rarely, outward from cave walls. Selenite needles grow from the base. Sulfate solutions move up through the silt to the base of the needle and new crystal growth pushes old growth up and out of the silt.

Stubby subhedral needles of selenite up to 2 cm long have been observed in the silt of Wind (Hicks) Cave (Hill, 1976c), and euhedral selenite needles up to 25 cm long occur in the area under the second bridge, Left Hand Tunnel, Carlsbad Cavern. The best selenite needles known to occur in any Guadalupe cave are in Cottonwood Cave (Fig. 129a). When the lower Gypsum Passage of Cottonwood Cave was discovered in 1960, wall needles up to 1.8 m long were found; free-hanging, they bent toward the floor, and upon touching the floor carved zig-zag paths in the silt (J. Trout, pers. comm. 1982). Since that time most of these needles have been vandalized (Fig. 1296).

Rims

A gypsum rim is analogous to a carbonate rim. It is a shell or projection of material smooth and scoured on the inside and rough on the outside, which surrounds an aperature in the cave wall or floor. Gypsum rims surround commode holes, a dissolution feature in massive gypsum, and these forms have been found in Carlsbad Cavern, Endless Cave, Cottonwood Cave, Hell Below Cave, and Spider Cave.

The best developed gypsum rim occurs in Endless Cave; this is "the Commode," a rim 1 m high and 6 cm thick at the base which surrounds a hole over 2 m deep in the floor (Fig. 58). Other well developed rims are the "lace" rims in Lechuguilla Cave. These are thin rims partially dissolved so as to display a lacy texture (Hill, 1986).

The origin of gypsum rims and carbonate rims is similar except that evaporation alone is responsible for precipitation of the gypsum. Moist air moving up through a commode hole in a gypsum block condenses out on the massive gypsum, partly dissolving and scouring the inside of the hole. Where this condensation water containing dissolved calcium sulfate meets with the dry air of a large room, evaporation causes the precipitation of a sulfate rim around the lip of the hole.

Stalactites

Gypsum stalactites can be observed in Cottonwood Cave, Carlsbad Cavern, and Dry Cave. These speleothems are faceted on their lower ends, the facets or blades extending downward and outward like claws. The largest gypsum stalactite known to occur in any Guadalupe cave is the Chandelier in Cottonwood Cave. When discovered in 1960, the Chandelier was 4–5 m long and extended all the way down to the passage floor, but since that time vandals have chipped away at the stalactite so that it is now only about 2–3 m long. Smaller gypsum stalactites occur in the Big Room of Carlsbad Cavern (along the trail near the Salt Flats) and in the Balcony of the New Mexico Room going toward the Rim Room. In the New Mexico Room, they have well-developed bladed ends, like the Chandelier. Small stalactitic gypsum adorns the bottom parts of gypsum blocks at the Jumping Off Place, Big Room, and Upper Devil's Den, Carlsbad Cavern.

Epsomite stalactites up to 0.8 m long and 20 cm in diameter occur in the Epsomite Room of the lower Gypsum Passage, Cottonwood Cave (Pl. 15B). These are smooth, colorless, and transparent, very similar in appearance to icicles (White, 1960; Russell, 1961; Frost, 1971). Epsomite stalactites, like their gypsum and carbonate counterparts, begin their growth as soda straws. Epsomite stalactites are very clear and transparent when first deposited, but they get more opaque when solutions cease to moisten their sides.

Stalagmites

The Chandelier stalactite with its many "claw" arms has its counterpart gypsum stalagmites, but these are comparatively small (only a few centimeters high) and have been partially covered over by silt kicked on them from the nearby path. Other, warty-looking gypsum stalagmites occur along the path just beyond the Chandelier, but these seem to be without counterpart stalactites (Hill, 1977a). The largest sulfate stalagmite in the lower Gypsum Passage is an epsomite one, 2.1 m tall and 0.9 m wide at its base. It is in part transparent and in part opaque, the transparent growth presumably having formed later than the opaque growth.

In Lower Cave, Carlsbad Cavern, near the climb up to Mabel's Room, is a cluster of four gypsum stalagmites 0.3–0.7 m tall that have drip tubes down their centers. The stalagmites have no counterpart stalactites, but directly above the stalagmites are gypsum crystals overlying carbonate popcorn on the ceiling. Gypsum stalagmites up to 1.3 m tall have also been observed in the Lower Guadalupe Room of Carlsbad Cavern (C. M. Seanor, pers. comm. 1984).

Other minerals

Phosphate and silicate minerals also occur in the caves of the Guadalupe Mountains, but these are rare compared to carbonate and sulfate minerals in the caves.

Phosphates

Where phosphate minerals do occur in Guadalupe caves, they are derived from bat guano. Fleischer (1951) reported "collophanite" (a collective name for a hydrous calcium phosphate) as a brown coating on a stalactite in Carlsbad Cavern, which he believed had formed by the reaction of calcium carbonate with bat guano. Hill et al. (1972a) reported fluorapatite, $Ca_5(PO_4)_3F$, as a blue-green layer in bat guano in a mined section of New Cave. On the basis of an optical analysis, Hill et al. (1972a) reported brushite, $CaHPO_4 \cdot 2H_2O$, in Ogle Cave, but a later analysis of this material by x-ray diffraction showed it to be gypsum, the isomorph of brushite.

Silicates

Silicate minerals in Guadalupe caves are discussed in the speleogenesis section of this paper and will not be repeated here. They include: endellite (Pl. 6B), montmorillonite (Pl. 6A), and palygorskite (attapulgite). The endellite is believed to have derived from montmorillonite in the presence of low-pH, sulfuric-acid solutions. The attapulgite may have derived from montmorillonite when the clay was exposed to air.

Color of speleothems

Compared to speleothems in many other caves, carbonate speleothems in Guadalupe caves are usually not brightly colored, but rather are delicately shaded in the pastel colors of cream, pink, and orange. There are exceptions to this rule, the most notable being the Temple of the Fire God in Three Fingers Cave (Pl. 16A). Sulfate speleothems are usually white or transparent, but selenite needles can be tinged a light tan due to included impurities.

The cause of coloration in speleothems is very complex and includes such factors as crystallinity, trace amounts of metal ions, complex organic chelates, surface contaminants, and even bacteria (Hill and Forti, 1986). Most of the orangered–yellow–brown coloration of carbonate speleothems in Guadalupe caves is believed to be caused by iron oxide, but may also be caused by differences in crystallinity or incorporation of impurities into the travertine. Hill (1984c) speculated that the tan-to-brown travertine coloration seen everywhere in Virgin Cave (Pl. 12) may be caused by mud staining. Coloration of "fried egg" stalagmites in such caves as Pink Dragon is probably due to crystallinity factors.

Some coloration of Guadalupe speleothems may relate to impurities in the bedrock. In the Bell Cord–Bifrost Rooms, Carlsbad Cavern, speleothems such as cave cones and stalactites are peach to lemon yellow (Pl. 11A), a coloration that may be derived from the high silt content of the forereef limestone at this locality. Bright-red to purple stains on the

limestone of the Secondary Stream Passage (near its junction with the Lunch Room) have been analyzed as iron oxide (memorandum to the park from Edwin C. Albert, Park Naturalist, 1945). Caldwell and Caldwell (1980) identified the filamentous iron bacteria *Leptothrix* from small pools in Left Hand Tunnel, Carlsbad Cavern; such bacteria may implement coloration by changing speleothem-depositing solutions from a ferrous-oxidation state to a ferric-oxidation state.

Gray, dark-brown, and black coloration of speleothems may result from manganese-oxide minerals, dirt, guano, or soot. A positive test for manganese has been obtained for black layers in the clouds and shelfstone of the Lake of the Clouds Passage, Carlsbad Cavern (Fig. 64). Black material in the shelfstone has been analyzed as 1.4% Mn and 6.4% Fe, and x-ray diffraction of the black material indicates the possible presence of kutnohorite, $Ca(Mn,Mg,Fe^{2+})(CO_3)_2$ (J. Husler, pers. comm. 1986).

Black Cave was named for the blackened nature of its speleothems and for the dark material which rests on the floor of the cave. Hill (1982b) proposed that the black of Black Cave is carbonaceous material originating from a surface fire and brought into the cave during a time of flooding. Davis (1982a) disagreed with Hill and proposed that the cause of the black material was airborne soot from a surface fire.

Suspended material settling out of the air has also been proposed as the cause of blackened speleothems in other Guadalupe caves. A dark coating on the massive stalagmites and columns at the cave entrance of Cottonwood Cave supposedly resulted from a goat-manure fire (Corcoran and Willis, 1964). The fire smoked for two weeks at the cave entrance and speleothems which were glistening white turned a dull gray from the airborne soot. In a side gallery known as the Black Dust Room off the Sand Passage, Carlsbad Cavern, speleothems and rocks are blackened on their upward-facing surfaces but not on their undersides; this black material has been attributed to guano dust which settled out of the air (Hill, 1982b). Other blackened areas in the side galleries of Sand Passage such as the black flowstone in Black River and Black Bat Bone Hollow may also be attributable to airborne guano dust or, alternatively, to black material which has been leached from bat guano in overlying Bat Cave (Pl. 16B). The blackened speleothems on the ceiling of the Lunch Room area are due to the smoke of kerosene lamps used by the early explorers and visitors to the cave.

The blackened speleothems in the front chambers of New Cave have alternately been explained as being due to manganese, bat guano, or soot from guano fires, but it now appears that the black may be guano dust that settled out of the air during the period of guano-mining activity in the 1920's-1940's. Many lines of evidence lead to this conclusion. The black material is not manganese as determined by chemical tests (less than 0.005% manganese), and x-ray-diffraction analyses show a carbon line. The black material cannot be soot from guano fires because the limestone ceiling is not blackened adjacent to blackened speleothems as would be expected from rising smoke. It is not bat guano staining as proposed by Baker (1960) because the black material occurs as a fine, dust-like layer only on the upper surfaces of speleothems, and not as pellets, streaks, or a slippery coating of dark material such as is found where bat guano covers speleothems. It is not black material leached from bat guano in above-lying chambers because gypsum blocks on the floor are blackened on their upfacing surfaces. The black material occurs only in guano-lined passages in the front part of the cave, whereas speleothems in the back of the cave (such as the Christmas Tree) are a pristine white. The blackening event was fairly recent as evidenced by non-black travertine that has grown over the blackened part of some speleothems. In one area in the front part of the cave, where the limestone wall has been gouged by a guano-mining cable, a white, fringed drapery 20 cm long and 1 cm wide partly covers the gouge, showing that non-blackened travertine has grown since the guano-mining era. It may be that a combination of guano dust, oil dust, and diesel fuel dust became suspended in the air during guano mining, and that this dust settled out on wet speleothem surfaces in the front part of the cave.

Age and growth rate of speleothems

Growth rates of Guadalupe speleothems have been measured, but these rates must be used very cautiously when estimating a speleothem's age. Water-seepage patterns change continually so that a speleothem which is actively growing for 10 years may be dormant for the next 100 or 1,000 years. Black (1954) arrived at a growth rate of 4.5 cm^3/yr for Crystal Spring Dome, the largest active travertine formation in Carlsbad Cavern. Hill (1978b) reported 2 cm of cave-coral growth and 1 mm of flowstone growth on a metal drain pipe in Ogle Cave, placed there by guano miners some 40–60 years ago (Fig. 130).

Periods of activity and inactivity can be determined from an inspection of travertine material, and these can be important indicators of past climate. Columns in Ogle Cave record three periods of growth: they have an inner crystalline core indicating a wet period of uninterrupted growth, a continuous dark- and light-ringed shell around the core indicating a period of alternating wet and dry episodes, and a discontinuous light-colored outer rind indicating prolonged interrupted growth during a final dry period (Hill, 1978b; Fig. 131). This three-fold sequence of growth has also been noted in travertine deposits in Virgin Cave, Deep Cave, and Pink Panther Cave. Periodic growth of travertine may also be indicated by inclusion-defined growth surfaces. Kendall and Broughton (1977) noted that stalactites with inclusion-defined growth surfaces have been subjected to numerous interruptions in their deposition.

FIGURE 130—Cave coral on a drain pipe, Ogle Cave, showing the amount of growth since the 1930's. Photo Pete Lindsley.

FIGURE 131—Three generations of travertine growth displayed by a naturally cross-sectioned column, Ogle Cave. The macrocrystalline core (a) represents an initial, continuous, wet period of growth; the banded zone (b) represents alternating wet and dry periods of growth, while the outer light-colored shell (c) represents a final dry period of growth. Photo Ron Miller.

The only sure way of knowing the absolute age of a speleothem is to date it (Table 24). A number of dates have been obtained on Guadalupe speleothems by carbon-14, uranium-series, and Electron Spin Resonance (ESR) methods (see Part I of this paper for a discussion of these dating methods). Spar crystals have been dated at >350,000 years by the U-series method and 879,000 ± 124,000 years by the ESR method for spar collected at the Big Room level of Carlsbad Cavern. Type I cave rafts exposed in the wall have been dated from about 213,800 yrs to >350,000 yrs, but Type II rafts piled up into cones on the floor of the Balcony of the Lake of the Clouds have a U-series date of only 50,000 ybp. Various pieces of flowstone and dripstone material, from both Carlsbad Cavern and Ogle Cave, have absolute ages ranging from 20,000 to 600,000 ± 200,000 ybp. Popcorn has been dated from 33,000 to >350,000 ybp, and one moon-milk sample has a date of 18,000 ybp (Dunham, 1972).

Summary

(1) Guadalupe speleothems are large because: (a) a sulfuric-acid mode of dissolution created huge chambers in which speleothems could grow large; (b) the caves are very old and, therefore, there has been sufficient time for speleothems to grow large; and (c) wet climatic episodes earlier in the Pleistocene provided the moisture necessary for the growth of large speleothems.

(2) The profuseness of speleothems in Guadalupe Mountain caves is related to the fact that ground water easily descends everywhere into underground chambers through the jointed and bedded Tansill and Yates Formations and the porous reef.

(3) A variety of speleothem types occur in Guadalupe caves because a variety of factors have influenced the diversity of speleothem form: permeability, bedding, and jointing differences in the various limestone facies; dolomitic as well as calcitic rock; and evaporation as well as carbon-dioxide loss. Dolomitic rock supplies magnesium to the high-magnesium carbonate minerals hydromagnesite, huntite, and dolomite; evaporation causes these minerals to precipitate and also affects the morphology of speleothems such as bell canopies, popcorn, and tower coral. Jointing and bedding favor dripstone and flowstone speleothems, whereas high porosity and permeability of bedrock favor popcorn growth.

(4) The dominance of popcorn-type speleothems in Guadalupe caves relates to the porous and massive nature of the Capitan reef core facies, to condensation-corrosion processes, and to the lower humidity and high rate of evaporation in the caves. Water seeping through porous limestone results in thin films of water necessary for popcorn growth. High rate of evaporation turns flowstone-depositing or condensation water into slowly moving films of popcorn-depositing water.

(5) Most of the speleothems in Guadalupe caves are composed of carbonate rather than sulfate minerals. Sulfur-isotope data suggest that the sulfate minerals derived from pyrite in the overburden; the general lack of sulfate speleothems in these caves is due to the relative scarcity of pyrite in the Guadalupe Mountains. The exception to this rule is Cottonwood Cave which lies directly below a pyrite-rich section of the Yates Formation, and consequently has abundant gypsum and epsomite speleothems in its Gypsum Passage.

(6) Speleothems in Guadalupe caves are, for the most part, dry and inactive because the present climate in the Guadalupe Mountains is semiarid. Most travertine in the caves formed earlier in the Pleistocene when the climate was more humid and moist than it is today.

References

Achauer, C. W., 1969, Origin of Capitan Formation, Guadalupe Mountains, New Mexico: American Association of Petroleum Geologists, Bulletin, v. 53, no. 11, pp. 2314-2323.

Adams, J. E., 1944, Upper Permian Ochoa Series of Delaware Basin, West Texas and southeastern New Mexico: American Association of Petroleum Geologists, Bulletin, v. 28, pp. 1596-1625.

Adams, J. E., and Frenzel, H. N., 1950, Capitan barrier reef, Texas and New Mexico: Journal of Geology, v. 58, pp. 289-312.

Allen, J. R., 1982, Sedimentary structures, their character and physical basis: Elsevier, Amsterdam, Developments in sedimentology, 30A, v. I, 593 pp., 30B, v. II, 663 pp.

Allison, V. C., 1937, Evening bat flight from Carlsbad Caverns: Journal of Mammalogy, v. 18, pp. 80-82.

Anderson, G. M., and Macqueen, R. W., 1982, Ore deposit models—Mississippi Valley-type lead-zinc deposits: Geoscience Canada, v. 9, no. 2, pp. 108-117.

Anderson, R. Y., 1981, Deep-seated salt dissolution in the Delaware Basin, Texas and New Mexico: New Mexico Geological Society, Special Publication 10, pp. 133-145.

Anderson, R. Y., Dean, W. E., Kirkland, D. W., and Snider, H. I., 1972, Permian Castile varved evaporite sequence, West Texas and New Mexico: Geological Society of America, Bulletin, v. 83, pp. 59-85.

Anderson, R. Y., and Kirkland, D. W., 1966, Intrabasin varve correlation: Geological Society of America, Bulletin, v. 77, pp. 241-256.

Arnold, E. C., Hill, J. M., and Donaldson, D. A., 1980, Oil and Gas; *in* Arnold, E. C., and Hill, J. M. (compilers), New Mexico energy resources: New Mexico Bureau of Mines and Mineral Resources, Circular 172, pp. 9-27.

Ash, D. W., and Wilson, W. L., 1985a, A model of cavern development by ascending hydrogen sulfide gas for the Guadalupe Mountains, New Mexico (abstract): Geological Society of America, South-Central Section, Abstracts with Program, Fayetteville, Arkansas, p. 149.

Ash, D. W., and Wilson, W. L., 1985b, The development of secondary porosity by ascending hydrogen sulfide gas in the Guadalupe Mountains, New Mexico: National Speleological Society, Bulletin, v. 47, no. 1, p. 63.

Atkinson, T. C., Smart, P. S., and Wigley, T. M., 1983, Climate and natural radon levels in Castleguard Cave, Columbia Icefields, Alberta, Canada: Arctic and Alpine Research, v. 15, no. 4, pp. 487-502.

Ayer, M. Y., 1937, The archaeological and faunal material from Williams Cave, Guadalupe Mountains, Texas: Academy of Natural Sciences of Philadelphia, Proceedings, v. 88, pp. 599-618.

Bachman, G. O., 1974, Geologic processes and Cenozoic history related to salt dissolution in southeastern New Mexico: U.S. Geological Survey, Open File Report 74-194, 81 pp.

Bachman, G. O., 1976, Cenozoic deposits of southeastern New Mexico and an outline of the history of evaporite dissolution: U.S. Geological Survey, Journal of Research, v. 4, no. 2, pp. 135-149.

Bachman, G. O. 1980, Regional geology and Cenozoic history of Pecos region, southeastern New Mexico: U.S. Geological Survey, Open File Report 80-1099, 116 pp.

Bachman, G. O., 1984, Regional geology of Ochoan evaporites, northern part of Delaware Basin: New Mexico Bureau of Mines and Mineral Resources, Circular 184, 22 pp.

Bachman, G. O., and Johnson, R. B., 1973, Stability of salt in the Permian salt basin of Kansas, Oklahoma, Texas, and New Mexico: U.S. Geological Survey, Open File Report 4339-4, 66 pp.

Baker, J. K., 1963, Fossilization of bat skeletons in the Carlsbad Caverns: National Speleological Society, Bulletin, v. 25, pt. 1, pp. 37-44.

Baker, K., 1960, Fabulous New Cave: National Speleological Society News, v. 18, no. 4, pp. 36-37.

Bates, T. F., Hildebrand, F. A., and Swineford, A., 1950, Morphology and structure of endellite and halloysite: American Mineralogist, v. 35, nos. 7 & 8, pp. 463-484.

Beckman, R. T., and Rapp, D. D., 1976, Radiation survey of Carlsbad Caverns National Park: U.S. Department of the Interior Mining Enforcement and Safety Administration, Report D1118-R69, 13 pp.

Beckman, R. T., Rapp, D. D., and Rathbun, L. A., 1975, Radiation survey of Carlsbad Caverns National Park: U.S. Department of the Interior, Mining Enforcement and Safety Administration, Report D853-R53, 8 pp.

Berg, R. R., 1979, Reservoir sandstones of the Delaware Mountain Group, southeast New Mexico; in Guadalupian Delaware Mountain Group of west Texas and southeast New Mexico: Society of Economic Paleontologists and Mineralogists, Permian Basin Section, Publication 79-18, pp. 75-95.

Bernasconi, R., 1961, L'evolution physico-chimique du mondmilch: Rassegna Speleologica Italiana, Memoir 5, pp. 75-100.

Berner, R. A., 1971, Principles of chemical sedimentology: McGraw-Hill, New York, 240 pp.

Bethke, C. M., 1985, A numerical model of compaction-driven groundwater flow and heat transfer and its application to the paleohydrology of intracratonic sedimentary basins: Journal of Geophysical Research, v. 90, pp. 6817-6828.

Bjorklund, L. J., and Motts, W. S., 1959, Geology and water resources of the Carlsbad area, Eddy County, New Mexico: U.S. Geological Survey, Open File Report 59-9, 322 pp.

Black, D. M., 1951a, Loose carbonate accretions from Carlsbad Caverns, New Mexico: Science, v. 114, pp. 126-127.

Black, D. M., 1951b, Origin and development of "positive" water catchment basins, Carlsbad Caverns, New Mexico: National Speleological Society, Bulletin, v. 13, pp. 27-29.

Black, D. M., 1952, Cave pearls in Carlsbad Caverns: Scientific Monthly, v. 74, no. 4, pp. 206-210.

Black, D. M., 1953, Aragonite rafts in Carlsbad Caverns, New Mexico: Science, v. 117, no. 3030, pp. 84-85.

Black, D. M., 1956, Chinese walls of New Cave, Carlsbad Caverns National Park: Science, v. 123, no. 3024, pp. 937-938.

Black, T. H., 1954, The origin and development of the Carlsbad Caverns: New Mexico Geological Society, Guidebook 5, pp. 136-142.

Blatt, H., Middleton, G., and Murray, R., 1972, Origin of sedimentary rocks: Prentice-Hall, Englewood, New Jersey, 634 pp.

Bogli, A., 1980, Karst hydrology and physical speleology: Springer-Verlag, Berlin, 284 pp.

Boyer, P. S., 1964, Analysis of cave waters from Carlsbad Caverns, New Mexico: Unpublished report on file at Carlsbad Caverns National Park, 58 pp.

Bretz, J. H., 1949, Carlsbad Caverns and other caves of the Guadalupe block, New Mexico: Journal of Geology, v. 57, no. 5, pp. 447-463.

Bretz, J. H., and Horberg, L., 1949a, Caliche in southeastern New Mexico: Journal of Geology, v. 57, no. 5, pp. 491-511.

Bretz, J. H., and Horberg, L., 1949b, The Ogallala Formation west of the Llano Estacado: Journal of Geology, v. 57, no. 5, pp. 477-490.

Brindley, G. W., and Comer, J. J., 1956, The structure and morphology of a kaolin clay from Les Eyzies (France); Swineford, A. (ed.), Proceedings of National [U.S.] Conference of Clays and Clay Mineralogy: National [U.S.] Academy of Science-National Research Council Publication, v. 456, pp. 61-66.

Brook, G. A., Ellwood, B. B., Cowart, J. B., Eubanks, J. K., Wenner, D. B., Ford, D. C., and Schwarcz, H. P. (manuscript), Paleoenvironmental data from speleothems in Carlsbad Caverns, New Mexico, 180,000 yrs B.P. to the present.

Bullington, N. R., 1968, Geology of the Carlsbad Caverns; *in* Delaware Basin exploration: West Texas Geological Society, Guide-book 68-55, pp. 20-23.

Burnet, R. M., 1938, Exploring a new cave—remains of animals and pottery 1000 years old are found amid unearthly splendors of a recently discovered cavern in the Guadalupe Mountains of New Mexico: Natural History, v. 41, no. 5, pp. 374-383.

Caldwell, D. E., and Caldwell, S. J., 1980, Fine structure of in situ microbial iron deposits: Geomicrobiology Journal, v. 2, no. 1, pp. 39-53.

Callaghan, E., 1948, Endellite deposits in Gardner Mine Ridge, Lawrence County, Indiana: Indiana Department of Conservation, Bulletin 1, pp. 1-47.

Candelaria,.M. P., 1982, Sedimentology and depositional environment of upper Yates Formation siliciclastics (Permian, Guadalupian), Guadalupe Mountains, southeast New Mexico: Unpublished M.S. thesis, University of Wisconsin, 267 pp.

Chambers, L. A., and Trudinger, P. A., 1979, Microbiological fractionation of stable sulfur isotopes: a review and a critique: Geomicrobiology Journal, v. 1, no. 3, pp. 249-293.

Clark, S. P., 1966, Handbook of physical constants: Geological Society of America, Memoir 97, 587 pp.

Corcoran, J., and Willis, B., 1964, Assault on Guadalupe ridge; *in* Anderson, S. (ed.), Special issue on the Guadalupes: Southwestern Caver, v. 3, no. 8, pp. 60-61.

Cox, E. T., 1875, Sixth annual report of the Geological Society of Indiana made during the year 1874: Geological Society of Indiana, v. 6, pp. 13-23.

Crisman, B. L., 1960, Other caves in the vicinity; *in* Moore, G. W. (ed.), A guidebook to Carlsbad Caverns National Park: National Speleological Society, Guidebook Series, no. 1, pp. 31-35.

Cronoble, J. M., 1974, Biotic constituents and origin of facies in Capitan reef, New Mexico and Texas: Mountain Geologist, v. 11, no. 3, pp. 95-108.

Curl, R. L., 1974, Deducing flow velocity in cave conduits from scallops: National Speleological Society, Bulletin, v. 26, no. 2, p. 74.

Davies, W. E., 1964a, Attapulgite from Carlsbad Caverns, New Mexico (abstract): National Speleological Society, Bulletin, v. 26, no. 2, p. 74.

Davies, W. E., 1964b, Attapulgite from Carlsbad Caverns, New Mexico: U.S. Geological Survey, Professional Paper 501-C, pp. C82-C83.

Davies, W. E., and Moore, G. W., 1957, Endellite and hydromagnesite from Carlsbad Caverns: National Speleological Society, Bulletin, v. 19, pp. 24-25.

Davis, D. G., 1970, Folia in Carlsbad Cavern: Unpublished report to Carlsbad Caverns National Park, 2 pp.

Davis, D. G., 1973, Sulfur in Cottonwood Cave, Eddy County, New Mexico: National Speleological Society, Bulletin, v. 35, no. 3, pp. 89-95.

Davis, D. G., 1979a, Cave development in the Guadalupe Mountains, New Mexico, Texas: Caving International Magazine, v. 3, p. 43.

Davis, D. G., 1979b, Geology and speleogenesis of Ogle Cave: discussion: National Speleological Society, Bulletin, v. 41, no. 1, pp. 21-22.

Davis, D. G., 1980, Cavern development in the Guadalupe Mountains: a critical review of recent hypotheses: National Speleological Society, Bulletin, v. 42, pp. 42-48.

Davis, D. G., 1982a, Origin of black deposits in caves: discussion: National Speleological Society, Bulletin, v. 42, p. 42.

Davis, D. G., 1982b, Rims, rills, and rafts: shaping of cave features by water condensation from air: Cave Research Foundation, Annual Report 24, p. 29.

Davis, J. B., and Kirkland, D. W., 1970, Native sulfur deposition in the Castile Formation, Culberson County, Texas: Economic Geology, v. 65, pp. 107-121.

Davis, W. M., 1930, Origin of limestone caverns: Geological Society of America, Bulletin, v. 41, pp. 475-628.

Dean, W. E., 1967, Petrologic and geochemical variations in the Permian Castile varved anhydrite, Delaware Basin, Texas and New Mexico: Unpublished Ph.D. dissertation, University of New Mexico, 326 pp.

Dean, W. E., and Anderson, R. Y., 1978, Salinity cycles: evidence for subaqueous deposition of Castile Formation and lower part of Salado Formation, Delaware Basin, Texas and New Mexico; *in* Austin, G. S. (compiler), Geology and mineral deposits of Ochoan rocks in Delaware Basin and adjacent areas: New Mexico Bureau of Mines and Mineral Resources, Circular 159, pp. 15-20.

DeKimpe, C., Gastuche, M. C., and Brindley, G. W., 1964, Low-temperature synthesis of kaolin minerals: American Mineralogist, v. 49, pp. 1-16.

Diamond, S., and Bloor, J. W., 1970, Globular cluster microstructure of endellite (hydrated halloysite) from Bedford, Indiana: Clays and Clay Minerals, v. 18, pp. 309-312.

DuChene, H. R., 1966, A preliminary report on the geology of the Rainbogle Cave System, Carlsbad Caverns National Park: Unpublished report to Carlsbad Caverns National Park, 14 pp.

DuChene, H. R., 1967, Idono Crystal Cave, Eddy County: Southwestern Caver, v. 6, no. 4, p. 62.

DuChene, H. R., 1971, Discussion to accompany tectonic map of the Guadalupe Mountains and vicinity, Texas and New Mexico: Unpublished report to Carlsbad Caverns National Park, 17 pp.

DuChene, H. R., 1972, A survey of cave sediment studies with special emphasis on the sediments in the Lower Cave portion of Carlsbad Caverns: Unpublished report on file at Carlsbad Caverns National Park, 21 pp.

DuChene, H. R., 1978, Geologic history of the Guadalupe Mountains region: National Speleological Society, Bulletin, v. 40, pp. 3-6.

DuChene, H. R., 1986, Observations on previous hypotheses and some new ideas on cavern formation in the Guadalupe Mountains; *in* Jagnow, D. H. (ed.), Geology Field Trip Guidebook: 1986 National Speleological Society Convention, Tularosa, New Mexico, pp. 96-100.

Dunham, R. J., 1972, Capitan reef, New Mexico and Texas: facts and questions to aid interpretation and group discussion: Society of Economic Paleontologists and Mineralogists, Permian Basin section, Publication 72-14, pp. II-71-II-81.

Egemeier, S. J., 1971, A comparison of two types of solution caves: Unpublished report to Carlsbad Caverns National Park, 7 pp.

Egemeier, S. J., 1973, Cavern development by thermal waters with a possible bearing on ore deposition: Unpublished Ph.D. dissertation, Stanford University, 88 pp.

Egemeier, S. J., 1981, Cavern development by thermal waters: National Speleological Society, Bulletin, v. 43, no. 2, pp. 31-51.

Ewing, R. I., 1982, Environmental gamma ray spectra from selected sites in southeastern New Mexico: Sandia National Laboratory, Report SAND 82-0738, 41 pp.

Ferdon, E. N., 1946, An excavation of Hermit's Cave, New Mexico: School of American Research, Monographs, v. 10, pp. 1-29.

Fiedler, A. G., and Nye, S. S., 1933, Geology and ground water resources of the Roswell artesian basin: New Mexico Geological Society, Water Supply Paper 639, 378 pp.

Findley, J. S., 1965, Shrews from Hermit Cave, Guadalupe Mountains, New Mexico: Journal of Mammalogy, v. 46, no. 2, pp. 206-210.

Fleischer, M., 1951, Report on the identification of 14 samples of crystalline materials—mostly carbonate—from Carlsbad Caverns, New Mexico: Unpublished report to Carlsbad Caverns National Park, 4 pp.

Fleischer, M., 1983, Glossary of mineral species: Mineralogical Record, Tucson, 202 pp.

Folk, R. L., 1968, Petrology of sedimentary rocks: University of Texas Press, Austin, 170 pp.

Folk, R. L., and Assereto, R., 1976, Comparative fabrics of length-slow and length-fast calcite and calcitized aragonite in a Holocene speleothem, Carlsbad Caverns, New Mexico: Journal of Sedimentary Petrology, v. 46, no. 3, pp. 486-496.

Ford, D. C., and Ewers, R. O., 1978, The development of limestone cave systems in the dimensions of length and depth: Canadian Journal of Earth Sciences, v. 15, no. 11, pp. 1783-1798.

Forti, P., and Utili, F., 1984, Le concrezioni della Grotta Guisti: Speleo, v. 7, no. 2, pp. 17-25.

Friedman, G. M., and Sanders, J. E., 1978, Principles of sedimentology: Wiley & Sons, New York, 792 pp.

Friesen, W. B., 1967, Clays of Carlsbad Caverns: Unpublished report to Carlsbad Caverns National Park, 10 pp.

Frost, R., 1971, A new cave mineral: Xanadu Quarterly, v. 2, no. 1, p. 1.

Gale, B. T., 1957, Geologic development of the Carlsbad Caverns; *in* Hayes, P. T., Geology of the Carlsbad Caverns east quadrangle, New Mexico: U.S. Geological Survey, Geologic Quadrangle Map 98, scale 1:62,500.

Gardner, J. H., 1935, Origin and development of limestone caverns: Geological Society of America, Bulletin, v. 46, no. 8, pp. 1255-1274.

Gascoyne, M., Latham, A. G., Harmon, R. S., and Ford, D. C., 1983, The antiquity of Castleguard Cave, Columbia Icefields, Alberta, Canada: Arctic and Alpine Research, v. 15, no. 4, pp. 463-470.

Gehlbach, F. R., and Holman, J. A., 1974, Paleoecology of amphibians and reptiles from Pratt Cave, Guadalupe Mountains National Park, Texas: Southwestern Naturalist, v. 19, no. 2, pp. 191-198.

Gerundo, M., and Schwartz, G. L., 1949, The role of denitrifying bacteria in the genesis of formations found in the Carlsbad Caverns: Texas Journal of Science, v. 4, pp. 58-61.

Given, R. K., and Lohmann, K. C., 1986, Isotopic evidence for the early meteoric diagenesis of the reef facies, Permian reef complex of west Texas and New Mexico: Journal of Sedimentary Petrology, v. 56, no. 2, pp. 183-193.

Good, J. M., 1957, Non-carbonate deposits of Carlsbad Caverns: National Speleological Society, Bulletin, v. 19, pp. 11-23. Goodwin, A. M., Monster, J., and Thode, H. G., 1976, Carbon and sulfur isotope abundances in Archean iron-formations and early

Precambrian life: Economic Geology, v. 71, pp. 870-891.
Gloppen, T. G., and Steel, R. J., 1981, The deposits, internal structure and geometry in six alluvial fan-fan-delta bodies (Devonian-Norway)—a study in the significance of bedding sequence in conglomerates: Society of Economic Paleontologists and Mineralogists, Special Publication 31, pp. 49-69.
Grauten, W. F., 1965, Fluid relationships in Delaware Mountain sandstone; *in* Young, A., and Gallery, J. E. (eds.), Fluids in subsurface environments: American Association of Petroleum Geologists, Memoir 4, pp. 294-307.
Gutierrez, A. A., 1981, Geomorphology and hydrology of the Carlsbad Gypsum Plain, Eddy County, New Mexico: Proceedings of Eighth International Congress of Speleology, Bowling Green, Kentucky, pp. 45-47.
Harmon, R. S., and Curl, R. L., 1978, Preliminary results on growth rate and paleoclimate studies of a stalagmite from Ogle Cave, New Mexico: National Speleological Society, Bulletin, v. 40, no. 1, pp. 25-26.
Harris, A. H., 1970, The Dry Cave mammalian fauna and late pluvial conditions in southeastern New Mexico: Texas Journal of Science, v. 22, no. 1, pp. 3-27.
Harris, A. H., 1978, Paleontology; *in* Kunath, C. E. (ed.), The caves of McKittrick Hill: Texas Speleological Society, pp. 69-83.
Harris, A. H., 1980, The speleoecology of Dry Cave, New Mexico: National Geographic Society, Research Reports, v. 12, pp. 331-338.
Harris, A. H., 1985, Late Pleistocene vertebrate paleoecology of the West: University of Texas Press, Austin, 293 pp.
Harris, A. H., and Mundel, P., 1974, Size reduction in Bighorn sheep *(Ovis canadensis)* at the close of the Pleistocene: Journal of Mammalogy, v. 55, no. 3, pp. 678-680.
Harris, A. H., and Porter, L. S., 1980, Late Pleistocene horses of Dry Cave, Eddy County, New Mexico: Journal of Mammalogy, v. 54, pp. 512-513.
Hart, W. G., 1969, Microfacies analysis of the Permian reef complex (Guadalupian), Carlsbad Caverns, New Mexico: Unpublished M.S. thesis, Texas Tech University, 68 pp.
Hayes, P. T., 1957, Geologic map of Carlsbad Caverns east quadrangle, New Mexico: U.S. Geological Survey, Geologic Quadrangle Map 98, scale 1:62,500.
Hayes, P. T., 1964, Geology of the Guadalupe Mountains, New Mexico: U.S. Geological Survey, Professional Paper 446, 69 pp.
Hayes, P. T., and Bachman, G. O., 1979, Examination and reevaluation of evidence for the Barrera Fault, Guadalupe Mountains, New Mexico: U.S. Geological Survey, Open File Report 79-1520, pp. 1-9.
Hayes, P. T., and Koogle, R. L., 1958, Geology of the Carlsbad Caverns west quadrangle, New Mexico-Texas: U.S. Geological Survey, Geologic Quadrangle Map 112, scale 1:62,500.
Hennig, G. J., and Griin, R., 1983, ESR dating in Quaternary geology: Quaternary Science Reviews, v. 2, pp. 157-238.
Hess, F. L., 1929, Oolites or cave pearls in Carlsbad Caverns: U.S. National Museum, Proceedings, v. 76, art. 16, p. 1.
Hester, J. J., 1960, Late Pleistocene extinction and radiocarbon dating: American Antiquity, v. 26, pp. 58-77.
Hill, C. A., 1972, Lithographic controls on speleothem development in Carlsbad Caverns: Guadalupe Cave Survey Report to Carlsbad Caverns National Park, 17 pp.
Hill, C. A., 1973a, Bell canopies: National Speleological Society News, v. 31, no. 5, p. 58.
Hill, C. A., 1973b, Guadalupe Cave Survey mineralogical report for field trip of May 27, 1973: Guadalupe Cave Survey report to Carlsbad Caverns National Park, 5 pp.
Hill, C. A., 1973c, Huntite flowstone in Carlsbad Caverns: Science, v. 181, no. 4095, pp. 158-159.
Hill, C. A., 1973d, Hydromagnesite balloons in Carlsbad Caverns: National Speleological Society News, v. 31, no. 10, p. 16.
Hill, C. A., 1973e, Mineralogy of Carlsbad Caverns and caves of the Guadalupe Mountains: Cave Research Foundation, Annual Report 15, pp. 29-30.
Hill, C. A., 1976a, Cave minerals: National Speleological Society, Huntsville, Alabama, 137 pp.
Hill, C. A., 1976b, Mineralogy of Musk Ox Cave, Carlsbad Caverns National Park: Cave Research Foundation, Annual Report 18, p. 30.
Hill, C. A., 1976c, Mineralogy of Wind Cave, Eddy County, New Mexico: Cave Research Foundation, Annual Report 18, pp. 29-30.
Hill, C. A., 1977a, Mineralogy of Second Parallel Passage, Cottonwood Cave, Guadalupe Mountains, New Mexico: Cave Research Foundation, Annual Report 19, pp. 14-15.
Hill, C. A., 197Th, Mineralogy of the Pink Caves, Guadalupe Mountains, New Mexico: Cave Research Foundation, Annual Report 19, p. 15.
Hill, C. A., 1978a, Mineralogy of Deep Cave, Carlsbad Caverns National Park: Cave Research Foundation, Annual Report 20, p. 18.
Hill, C. A., 1978b, Mineralogy of Ogle Cave: National Speleological Society, Bulletin, v. 40, no. 1, pp. 19-24.
Hill, C. A., 1978c, Mineralogy of Three Fingers Cave, Lincoln National Forest, New Mexico: Cave Research Foundation, Annual Report 20, p. 18.
Hill, C. A., 1979, Mineralogy of Spider Cave: Cave Research Foundation, Annual Report 22, pp. 13-14.
Hill, C. A., 1980a, Mineralogy of Hidden Cave: Cave Research Foundation, Annual Report 22, p. 10.
Hill, C. A., 1980b, Speleogenesis of Carlsbad Caverns and other caves of the Guadalupe Moutnains: Unpublished report to the National Park Service, Forest Service, and Bureau of Land Management, 201 pp.
Hill, C. A., 1981a, Giant "cones" found on the balcony of the Lake of the Clouds, Carlsbad Caverns: Cave Research Foundation, Annual Report 23, p. 9.
Hill, C. A., 1981b, Hydromagnesite balloons deflating in Carlsbad Caverns: Cave Research Foundation, Annual Report 23, p. 9.
Hill, C. A., 1981c, Origin of cave saltpeter: National Speleological Society, Bulletin, v. 43, pp. 110-126.
Hill, C. A., 1981d, Speleogenesis of Carlsbad Caverns and other caves of the Guadalupe Mountains: Eighth International Congress of Speleology, Bowling Green, Kentucky, Proceedings, pp. 143-144.
Hill, C. A., 1982a, Mineralogy of the newly discovered Bifrost Room, Carlsbad Caverns: Cave Research Foundation, Annual Report 24, pp. 19-20.
Hill, C. A., 1982b, Origin of black cave deposits: National Speleological Society, Bulletin, v. 44, pp. 15-19.
Hill, C. A., 1983, Mineralogy of Hell Below Cave, Lincoln National Forest, Guadalupe Mountains: Cave Research Foundation, Annual Report 25, p. 8.
Hill, C. A., 1984a, A conulite formed in moonmilk, Carlsbad Cavern: Cave Research Foundation, Annual Report 26, pp. 11-12.
Hill, C. A., 1984b, The origin of rims: Cave Research Foundation, Annual Report 26, pp. 9-11.
Hill, C. A., 1984c, Virgin Cave, Guadalupe Mountains, New Mexico: a preliminary report on its geology and mineralogy: Cave Research Foundation Annual Report 26, p. 13.
Hill, C. A., 1986, Geology of Lechuguilla Cave—preliminary observations: Unpublished report to Carlsbad Caverns National Park, 10 pp.
Hill, C. A. (in press), Fiume Vento Cave, Italy—a "baby" Carlsbad Cavern: Cave Research Foundation, Annual Report 28.
Hill, C. A., and Forti, P., 1986, Cave minerals of the world: National Speleological Society, Huntsville, Alabama, 238 pp.
Hill, C. A., and Gillette, D. D., 1985, Bones of the Pleistocene ground sloth *Nothrotheriops* in Carlsbad Cavern, New Mexico: Cave Research Foundation, Annual Report 27, pp. 23-24.
Hill, C. A., and Gillette, D. D., 1987, A uranium-series date for the Shasta ground sloth, *Nothrotheriops shastensis,* from Carlsbad Cavern, New Mexico: Journal of Mammalogy, v. 68, no. 3, pp. 718-719.
Hill, C. A., DuChene, H. R., and Jagnow, D. H., 1972a, Mineralogy of Carlsbad Caverns: Cave Research Foundation, Annual Report 14, pp. 24-25.
Hill, C. A., DuChene, H. R., and Jagnow, D. H., 1972b, Preliminary geological and mineralogical investigations of the Lower Cave and Left Hand Tunnel portions of Carlsbad Caverns: Guadalupe Cave Survey Report of Carlsbad Caverns National Park, 18 pp.
Hill, C. A., Jagnow, D. H., and Deal, D. E., 1972, Guadalupe Cave Survey Mineralogical report for geology field trip of 12 February 1972: Guadalupe Cave Survey Report to Carlsbad Caverns National Park, 7 pp.
Hinds, J. S., and Cunningham, R. R., 1970, Elemental sulfur in Eddy County, New Mexico: U.S. Geological Survey, Circular 628, pp. 1-12.
Hiss, W. L., 1974, Capitan aquifer observation—well network, Carlsbad to Jai, New Mexico: New Mexico Engineer, Technical Report 38, 19 pp.
Hiss, W. L., 1975, Stratigraphy and ground-water hydrology of the

Capitan aquifer, southeastern New Mexico and western Texas: Unpublished Ph.D. dissertation, University of Colorado, 396 pp.
Hiss, W. L., 1980, Movement of ground water in Permian Guadalupian aquifer systems, southeastern New Mexico and western Texas; *in* Dickerson, P. W., and Hoffer, J. M. (eds.), Trans-Pecos region, southeastern New Mexico and west Texas: New Mexico Geological Society 31st Field Conference, Guidebook, pp. 289-290.
Holser, W. T., and Kaplan, I. R., 1966, Isotope geochemistry of sedimentary sulfates: Chemical Geology, v. 1, pp. 93–135.
Horberg, L., 1949, Geomorphic history of the Carlsbad Caverns area, New Mexico: Journal of Geology, v. 57, no. 5, pp. 464–476.
Houghton, F. E., 1967, Carlsbad Caverns, New Mexico; in Climatic summaries of resort areas: U.S. Department of Commerce, Climatography of the United States 21-29-2, 4 pp.
Howard, E. B., 1932, Caves along the slopes of the Guadalupe Mountains: Texas Archaeological and Paleontological Society, Bulletin, v. 4, pp. 7-20.
Howard, H., 1971, Quaternary avian remains from Dark Canyon Cave, New Mexico: Condor, v. 73, pp. 237-240.
Hutchinson, G. E., 1950, The biochemistry of vertebrate excretion: American Museum of Natural History, Bulletin, v. 96, 554 pp.
Ikeya, M., 1975, Dating a stalactite by electron paramagnetic resonance: Nature, v. 255, pp. 48–50.
Ikeya, M., 1978, Electron spin resonance as a method of dating: Archaeometry, v. 20, no. 2, pp. 147-158.
Jagnow, D. H., 1977, Geologic factors influencing speleogenesis in the Capitan Reef complex, New Mexico and Texas: Unpublished M.S. thesis, University of New Mexico, 197 pp.
Jagnow, D. H., 1978, Geology and speleogenesis of Ogle Cave: National Speleological Society, Bulletin, v. 40, pp. 7–18.
Jagnow, D. H., 1979, Cavern development in the Guadalupe Mountains: Cave Research Foundation, Columbus, Ohio, 55 pp.
Kaplan, I. R., and Rittenberg, S. C., 1964, Microbiological fractionation of sulphur isotopes: Journal of General Microbiology, v. 34, pp. 195–212.
Keller, W. D., McGrain, P., Reesman, A. L., and Saum, N. M., 1966, Observations on the origin of endellite in Kentucky and their extension to "indianaite": Clay and Clay Minerals, v. 13, pp. 107-120.
Kelley, V. C., 1971, Geology of Pecos County, southeastern New Mexico: New Mexico Bureau of Mines and Mineral Resources, Memoir 24, 77 pp.
Kelley, V. C., 1972, Geometry and correlations along Permian Capitan escarpment, New Mexico and Texas: American Association of Petroleum Geologists, Bulletin, v. 56, no. 11, pp. 2192–2211.
Kemp, A. L., and Thode, H. G., 1968, The mechanism of the bacterial reduction of sulphate and of sulphite from isotope fractionation studies: Geochimica et Cosmochimica Acta, v. 32, pp. 71–91.
Kendall, A. C., and Broughton, P. L., 1977, Discussion of "Calcite and aragonite fabrics, Carlsbad Caverns" by R. L. Folk and Riccardo Assereto: Journal of Sedimentary Petrology, v. 46, pp. 486-496.
Kendall, A. C., and Broughton, P. L., 1978, Origin of fabrics in speleothems composed of columnar calcite crystals: Journal of Sedimentary Petrology, v. 48, no. 2, pp. 519–538.
King, P. B., 1942, Permian of West Texas and southeastern New Mexico: American Association of Petroleum Geologists, Bulletin, v. 26, no. 4, pp. 535–763.
King, P. B., 1948, Geology of the southern Guadalupe Mountains, Texas: U.S. Geological Survey, Professional Paper 215, 183 pp.
Kirkland, D. W., 1982, Origin of gypsum deposits in Carlsbad Caverns, New Mexico: New Mexico Geology, v. 4, pp. 20–21.
Kirkland, D. W., and Anderson, R. Y., 1970, Microfolding in the Castile and Todilto evaporites, Texas and New Mexico: Geological Society of America, Bulletin, v. 81, pp. 3259–3282.
Kirkland, D. W., and Evans, R., 1976, Origin of limestone buttes, Gypsum Plain, Culberson County, Texas: American Association of Petroleum Geologists, Bulletin, v. 60, no. 11, pp. 2005–2018.
Krauskopf, K. B., 1967, Introduction to geochemistry: McGraw–Hill, New York, 721 pp.
Krumbein, W. C., and Sloss, L. L., 1963, Stratigraphy and sedimentation: Freeman, San Francisco, 660 pp.
Kunath, C. E., 1978, Endless Cave; *in* Kunath, C. E. (ed.), The caves of McKittrick Hill, Eddy County, New Mexico: Texas Speleological Survey, pp. 21–31.
Kurtén, B., 1975, A new Pleistocene genus of American mountain deer: Journal of Mammalogy, v. 56, no. 2, pp. 507–508.
Lambert, S. J., 1978, Geochemistry of Delaware Basin ground waters; *in* Austin, G. S. (compiler), Geology and mineral deposits of Ochoan rocks in Delaware Basin and adjacent areas: New Mexico Bureau of Mines and Mineral Resources, Circular 159, pp. 33–38.
Lee, W. T., 1924a, A visit to Carlsbad Cavern: National Geographic Magazine, v. 45, no. 1, pp. 1–40.
Lee, W. T., 1924b, Erosion by solution and fill: U.S. Geological Survey, Bulletin, v. 760, pp. 1–12.
Lee, W. T., 1925a, Carlsbad Cavern: Scientific Monthly, v. 21, pp. 186–190.
Lee, W. T., 1925b, New discoveries in Carlsbad Cavern: National Geographic Magazine, v. 48, no. 3, pp. 301-319.
Libby, W. F., 1954, Radiocarbon dates: Science, v. 120, pp. 733–742.
Light, T. D., Domenico, J. A., and Smith, S. M., 1985, Geochemical map of the Guadalupe escarpment wilderness study area, Eddy County, New Mexico: U.S. Geological Survey Field Study Map MF-1560B, scale 1:24,000.
Lindsley, P., and Lindsley, K., 1978, Dry Cave; in Kunath, C. E. (ed.), The caves of McKittrick Hill, Eddy County, New Mexico: Texas Speleological Survey, pp. 36–46.
Lippmann, F., 1973, Sedimentary carbonate minerals: Springer-Verlag, New York, 228 pp.
Lloyd, E. R., 1929, Capitan Limestone and associated formations of New Mexico and Texas: American Association of Petroleum Geologists, Bulletin, v. 13, pp. 645–658.
Logan, L. E., 1975, The quaternary vertebrate fauna of Upper Sloth Cave, Guadalupe Mountains National Park, Texas (abstract): Geological Society of America, Abstracts with Programs, p. 210.
Logan, L. E., 1977, The paleoclimatic implications of the avian and mammalian faunas of Lower Sloth Cave, Guadalupe Mountains, Texas: Unpublished M.S. thesis, Texas Tech University, 72 pp.
Logan, L. E., 1981, The mammalian fossils of Musk Ox Cave, Eddy County, New Mexico: Proceedings of Eighth International Congress of Speleology, Bowling Green, Kentucky, pp. 159–160.
Logan, L. E., 1983, Paleoecological implications of the mammalian fauna of Lower Sloth Cave, Guadalupe Mountains, Texas: National Speleological Society, Bulletin, v. 45, pp. 3–11.
Logan, L. E., and Black, C. C., 1979, The quaternary vertebrate fauna of Upper Sloth Cave, Guadalupe Mountains National Park, Texas; *in* Genoways, H. H., and Baker, R. J. (eds.), Biological investigation in the Guadalupe Mountains National Park, Texas: National Park Service, Washington D.C., Proceedings and Trans-actions, ser. 4, pp. 141–158.
Lundelius, E. L., 1979, Mammalian remains from Pratt Cave, Culberson County, Texas; *in* Genoways, H. H., and Baker, R. J. (eds.), Biological investigations in the Guadalupe Mountains National Park, Texas: National Park Service, Washington D.C., Proceedings and Transactions, ser. 4, pp. 239–258.
Martini, J., 1986, The trays; an excellent example of evaporation-controlled speleothems: South African Speleological Association, Bulletin, v. 27, no. 1, pp. 46–51.
Maslyn, R. M., 1979, Cavern development via H_2S dissolved in hot spring and natural gas field waters (abstract): National Speleological Society, Bulletin, v. 41, no. 4, p. 115.
Mazzullo, S. J., 1986, Mississippi Valley-type sulfides in Lower Permian dolomites, Delaware Basin, Texas: implications for basin evolution: American Association of Petroleum Geologists, Bulletin, v. 70, no. 8, pp. 943–952.
McAnulty, N., 1980, Barite deposits at Seven Heart Gap, Apache Mountains, Culberson County, Texas; in Dickerson, P. W., and Hoffer, J. M. (eds.), Trans-Pecos region, southeastern New Mexico and west Texas: New Mexico Geological Society, 31st Field Conference, Guidebook, pp. 259–261.
McAuliffe, C. D., 1979, Oil and gas migration—chemical and physical constraints: American Association of Petroleum Geologists, Bulletin, v. 63, no. 5, pp. 761–781.
McLean, J. S., 1970, Cave climate study, Carlsbad Caverns, New Mexico—a progress report: Unpublished report to Carlsbad Caverns National Park, 23 pp.
McLean, J. S, 1971, The microclimate in Carlsbad Caverns, New Mexico: U.S. Geological Survey, Open File Report 71-198, 67 pp.
McLean, J. S., 1976, Factors altering the microclimate in Carlsbad Caverns, New Mexico: U.S. Geological Survey, Open File Report 76-171, 55 pp.
Mercer, J. W., 1983, Geohydrology of the proposed waste isolation Pilot Plant site, Los Medaños area, southeastern New Mexico: U.S. Geological Survey, Water Resources Investigations Report 83-4016, 113 pp.

Moore, G. W., 1960a, Geology of Carlsbad Caverns, New Mexico: National Speleological Society, Guidebook, ser. 1, pp. 10–17.
Moore, G. W., 1960b, Origin and chemical composition of evaporite deposits: Unpublished Ph.D. dissertation, Yale University, 174 pp.
Moore, P. C., 1984, Gamma exposure measurements at selected sites in the Carlsbad Caverns: Unpublished report on file at Carlsbad Caverns National Park, 9 pp.
Moran, W. R., 1955, Sandstone in the New Mexico Room of Carlsbad Caverns, New Mexico: American Association of Petroleum Geologists, Bulletin, v. 39, no. 2, pp. 256–259.
Morehouse, D. F., 1968, Cave development via the sulfuric acid reaction: National Speleological Society, Bulletin, v. 30, no. 1, pp. 1–10.
Motts, W. S., 1957, Geology and ground-water resources of the Carlsbad area, New Mexico: Unpublished Ph.D. dissertation, University of Illinois, 120 pp.
Motts, W. S., 1959, Age of the Carlsbad Caverns and related caves in rocks of Guadalupe age west of the Pecos River in southeastern New Mexico (abstract): Geological Society of America, Bulletin, v. 70, no. 12, pt. 2, p. 1737.
Newell, N. D., Rigby, J. K., Fischer, A. G., Whiteman, A. J., Hickox, J. E., and Bradley, J. S., 1953, The Permian reef complex of the Guadalupe Mountains region, Texas and New Mexico—a study in paleoecology: Freeman, San Francisco, 236 pp.
Nymeyer, R. B., 1938, Wonders below: New Mexico Magazine, v. 16, no. 12, pp. 9–11, 38–40.
Olive, W. W., 1957, Solution–subsidence troughs, Castile Formation of Gypsum Plain, Texas and New Mexico: Geological Society of America, Bulletin, v. 68, pp. 351–358.
Palmer, A. N., 1975, The origin of maze caves: National Speleological Society, Bulletin, v. 37, no. 3, pp. 57-76.
Palmer, A. N., and Palmer, M. V., 1975, Geologic reconnaissance, Wind Cave, New Mexico: Cave Research Foundation, Annual Report 17, pp. 31–33.
Pecos River Joint Investigations, New Mexico and Texas, 1942, Reports of participating agencies: National Resources Planning Board, pt. 10, p. 61.
Pettijohn, F. J., 1957, Sedimentary rocks: Harper & Row, New York, 628 pp.
Powers, D. W., Lambert, S. J., Shaffer, S. E., Hill, L. R., and Weart, W. D. (eds.), 1978, Geological characterization report, Waste Isolation Pilot Plant (WIPP) Site, southeastern New Mexico: Sandia Laboratory, Report SAND 78-1596, v. 1 & 2.
Queen, J. M., 1973, Large scale replacement of carbonate by gypsum in some New Mexico caves (abstract): National Speleological Society Convention, Bloomington, Indiana, Abstracts with Programs, p. 12.
Queen, J. M., 1981, A discussion and field guide to the geology of Carlsbad Caverns: Unpublished report to Carlsbad Caverns National Park, 64 pp.
Queen, J. M., Palmer, A. N., and Palmer, M. V. 1977a, Speleogenesis in the Guadalupe Mountains, New Mexico: gypsum replacement of carbonate by brine mixing: Proceedings of Seventh International Congress of Speleology, Sheffield, U.K., pp. 333–336.
Queen, J. M., Palmer, A. N., and Palmer, M. V., 197Th, Speleogenesis of the Guadalupe Mountains, New Mexico: gypsum replacement of carbonates by brine mixing: Cave Research Foundation, Annual Report 19, pp. 22–23.
Reilinger, L. E., Brown, L. D., Oliver, J. E., and York, J. E., 1979, Recent vertical crustal movements from leveling observations in the vicinity of the Rio Grande Rift; *in* Riecker, R. E. (ed.), Rio Grande rift: tectonics and magmatism: American Geophysical Union, Washington D.C., 438 pp.
Richardson, W. A., 1919, The origin of Cretaceous flint: Geological Magazine, v. 58, pp. 535-547.
Romer, A. S., 1966, Vertebrate paleontology (3rd edition): University of Chicago Press, Chicago, 468 pp.
Ross, C. S., and Kerr, P. F., 1934, Halloysite and allophane: U.S. Geological Survey, Professional Paper 185, pp. 135–148.
Russell, B., 1961, Cottonwood Cave, the big cavern in the Guadalupe pines: Texas Caver, v. 6, pp. 4–5.
Sanchez, P. G., 1964, Geology of the Capitan reef complex of the Guadalupe Mountains, Culberson County, Texas and Eddy County, New Mexico: Roswell Geological Society, Field Trip Guidebook for May 6–9, 1964, 65 pp.
Sares, S. W., 1984, Hydrologic and geomorphic development of a low relief evaporite karst drainage basin, southeastern New Mexico: Unpublished M.S. thesis, University of New Mexico, 123 pp.
Schmidt, V. A., 1982, Magnetostratigraphy of sediments in Mammoth Cave, Kentucky: Science, v. 212, pp. 827–829.
Schultz, C. B., and Howard, E. B., 1935, The fauna of Burnet Cave, Guadalupe Mountains, New Mexico: Academy of Natural Science of Philadelphia, Proceedings, v. 87, pp. 273–298.
Schultz, C. B., Martin, L. D., and Tanner, L. G., 1970, Mammalian distribution in the great Plains and adjacent areas from 14,000 to 9,000 years ago (abstract): American Quaternary Association, Abstracts, 1970, pp. 119–120.
Schwarcz, H. P., and Harmon, R. S., 1976, Stable isotope studies of fluid inclusions in speleothems and their paleoclimatic significance: Geochimica et Cosmochimica Acta, v. 40, pp. 657-665.
Smith, A. R., 1978a, Sulfur deposits in Ochoan rocks of southeast New Mexico and West Texas; *in* Austin, G. S. (compiler), Geology and mineral deposits of Ochoan rocks in Delaware Basin and adjacent areas: New Mexico Bureau of Mines and Mineral Resources, Circular 159, pp. 71–77.
Smith, A. R., 1978b, The caves of McKittrick Hill: geology; *in* Kunath, C. E. (ed.), The caves of McKittrick Hill, Eddy County, New Mexico: Texas Speleological Survey, pp. 56–68.
Smith, A. R., 1981, Evaporite karst, Gypsum Plain, Culberson County, Texas: Eighth International Congress of Speleology, Bowling Green, Kentucky, Proceedings, p. 482.
Spaulding, W. G., and Martin, L. O., 1979, Ground sloth dung of the Guadalupe Mountains; *in* Genoways, H. H., and Baker, R. J. (eds.), Biological investigations in the Guadalupe Mountains National Park, Texas: National Park Service, Proceedings and Transactions, ser. 4, pp. 259-269.
Stanier, R. Y., Doudoroff, M., and Adelberg, E. A., 1957, Microbial world: Prentice–Hall, Englewood Cliffs, New Jersey, 682 pp.
Sweeting, M. M., 1973, Karst landforms: Columbia University Press, New York, 362 pp.
Swenson, F. A., 1974, Rates of salt solution in the Permian Basin: U.S. Geological Survey, Journal of Research, v. 2, no. 2, pp. 253-257.
Tankersley, K. B., Munson, P. J., and Munson, C. A., 1983, Physical and chemical properties of Wyandotte Cave aragonite and their implications: Geo^2 (National Speleological Society, Section of Cave Geology and Geography), v. 71, no. 1, pp. 2–5.
Thomas, R. G., 1971, The geomorphic evolution of the Pecos River system: Unpublished M.S. thesis, Baylor University, 31 pp.
Thrailkill, J. V., 1953, Manhole Cave: Colorado Grotto News and Notes, v. 2, no. 1, pp. 13–16.
Thrailkill, J. V., 1963, Mineralogy and water composition in the Crystal Spring Dome area: Unpublished report to Carlsbad Caverns National Park, 3 pp.
Thrailkill, J. V., 1964, Some preliminary results of a study of Carlsbad Caverns (abstract): National Speleological Society, Bulletin, v. 26, no. 2, p. 77.
Thrailkill, J. V., 1965a, Origin of cave popcorn (abstract): National Speleological Society, Bulletin, v. 27, no. 2, p. 59.
Thrailkill, J. V., 1965b, Studies in the excavation of limestone caves and the deposition of speleothems: Unpublished Ph.D. dissertation, Princeton University, 193 pp.
Thrailkill, J. V., 1968, Dolomite cave deposits from Carlsbad Caverns: Journal of Sedimentary Petrology, v. 38, no. 1, pp. 141–145.
Thrailkill, J. V., 1971, Carbonate deposition in Carlsbad Caverns: Journal of Geology, v. 79, no. 6, pp. 683-695.
Tyrrell, W. W., 1964, Petrology and stratigraphy of near-reef Tansill–Lamar strata, Guadalupe Mountains, Texas and New Mexico; *in* Roswell Geological Society Guidebook, Geology of the Capitan Reef Complex of the Guadalupe Mountains, pp. 66–82.
United States Department of Energy, 1983, Brine reservoirs in the Castile Formation: Waste Isolation Pilot Plant (WIPP) Project, southeastern New Mexico, THE 3153, p. C-31.
Van Devender, T. R., Spaulding, W. G., and Phillips, A. M., 1977, Late Pleistocene plant communities in the Guadalupe Mountains, Culberson County, Texas; *in* Genoways, H. H., and Baker, R. J. (eds.), Biological investigations in the Guadalupe Mountains National Park, Texas: National Park Service, Proceedings and Transactions, ser. 4, pp. 13–30.
Vear, A., and Curtis, C., 1981, A quantitative evaluation of pyrite weathering: Earth Science Processes and Landforms, v. 6, pp. 191–198.
Ward, R. F., Kendall, C. G., and Harris, P. M., 1986, Upper Permian (Guadalupian) facies and their association with hydrocarbons—Permian Basin, west Texas and New Mexico: American Associ-

ation of Petroleum Geologists, Bulletin, v. 70, no. 3, pp. 239-262.
Watson, W. G., 1979, Inhomogeneities of the Ramsey Member of the Permian Bell Canyon Formation, Geraldine Ford Field, Culberson and Reeves Counties, Texas; *in* Sullivan, N. M. (ed.), Guadalupian Delaware Mountain Group of west Texas and southeast New Mexico, Symposium and Field Conference Guide-book: Society of Economic Paleontologists and Mineralogists, Permian Basin section, Publication 79-18, pp. 2-38.
Weberneck, N. E., 1952, Gypsum karst, Culberson County, Texas: Unpublished M. S. thesis, University of Texas at Austin, 53 pp.
White, E. L., and White, W. B., 1968, Dynamics of sediment transport in limestone caves: National Speleological Society, Bulletin, v. 30, no. 4, pp. 115-129.
White, W. B., 1960, Cottonwood Cave, Eddy County, New Mexico: Nittany Grotto Newsletter, v. 3, pp. 5-12.
Wilkening, M. H., and Watkins, D. E., 1976, Air exchange and Rn^{222} concentrations in the Carlsbad Caverns: Health Physics, v. 31, pp. 139-145.
Williams, P. W., 1983, The role of the subcutaneous zone in karst hydrology: Journal of Hydrology, v. 61, pp. 45-67.
Williamson, C. R., 1979, Deep-sea sedimentation and stratigraphic traps, Bell Canyon Formation (Permian), Delaware Basin; *in* Sullivan, N. M. (ed.), Guadalupian Delaware Mountain Group of west Texas and southeast New Mexico, Symposium and Field Conference Guidebook: Society of Economic Paleontologists and Mineralogists, Permian Basin section, Publication 79-18, pp. 39-74.
Wilson, W. L., and Ash, D. W., 1984a, Stratigraphy of the New Mexico and Guadalupe rooms in Carlsbad Caverns, New Mexico: Cave Research Foundation, Annual Report 26, pp. 13-15.
Wilson, W. L., and Ash, D. W., 1984b, The New Mexico Room as a model of cavern development in the Guadalupe Mountains: Cave Research Foundation, Annual Report 26, pp. 15-17.
Young, G. J., 1915, A cave deposit: Economic Geology, v. 10, pp. 186-190.

Index

(Page numbers in Roman refer to the text, page numbers in bold refer to heads of sections, and page numbers in italics refer to tables, figures, and table/figure captions.)

Selected conversion factors*

TO CONVERT	MULTIPLY BY	TO OBTAIN
Length		
inches, in	2.540	centimeters, cm
feet, ft	3.048×10^{-1}	meters, m
yards, yds	9.144×10^{-1}	m
statute miles, mi	1.609	kilometers, km
fathoms	1.829	m
angstroms, Å	1.0×10^{-8}	cm
Å	1.0×10^{-4}	micrometers, μm
Area		
in^2	6.452	cm^2
ft^2	9.29×10^{-2}	m^2
yds^2	8.361×10^{-1}	m^2
mi^2	2.590	km^2
acres	4.047×10^{3}	m^2
acres	4.047×10^{-1}	hectares, ha
Volume (wet and dry)		
in^3	1.639×10^{1}	cm^3
ft^3	2.832×10^{-2}	m^3
yds^3	7.646×10^{-1}	m^3
fluid ounces	2.957×10^{-2}	liters, l *or* L
quarts	9.463×10^{-1}	l
U.S. gallons, gal	3.785	l
U.S. gal	3.785×10^{-3}	m^3
acre-ft	1.234×10^{3}	m^3
barrels (oil), bbl	1.589×10^{-1}	m^3
Weight, mass		
ounces avoirdupois, avdp	2.8349×10^{1}	grams, gr
troy ounces, oz	3.1103×10^{1}	gr
pounds, lb	4.536×10^{-1}	kilograms, kg
long tons	1.016	metric tons, mt
short tons	9.078×10^{-1}	mt
oz mt^{-1}	3.43×10^{1}	parts per million, ppm
Velocity		
ft sec^{-1} (= ft/sec)	3.048×10^{-1}	m sec^{-1} (= m/sec)
mi hr^{-1}	1.6093	km hr^{-1}
mi hr^{-1}	4.470×10^{-1}	m sec^{-1}

TO CONVERT	MULTIPLY BY	TO OBTAIN
Pressure, stress		
lb in^{-2} (= lb/in^2), psi	7.03×10^{-2}	kg cm^{-2} (= kg/cm^2)
lb in^{-2}	6.804×10^{-2}	atmospheres, atm
lb in^{-2}	6.895×10^{3}	newtons (N)/m^2, N m^{-2}
atm	1.0333	kg cm^{-2}
atm	7.6×10^{2}	mm of Hg (at 0° C)
inches of Hg (at 0° C)	3.453×10^{-2}	kg cm^{-2}
bars, b	1.020	kg cm^{-2}
b	1.0×10^{6}	dynes cm^{-2}
b	9.869×10^{-1}	atm
b	1.0×10^{-1}	megapascals, MPa
Density		
lb in^{-3} (= lb/in^3)	2.768×10^{1}	gr cm^{-3} (= gr/cm^3)
Viscosity		
poises	1.0	gr cm^{-1} sec^{-1} *or* dynes cm^{-2}
Discharge		
U.S. gal min^{-1}, gpm	6.308×10^{-2}	l sec^{-1}
gpm	6.308×10^{-5}	m^3 sec^{-1}
ft^3 sec^{-1}	2.832×10^{-2}	m^3 sec^{-1}
Hydraulic conductivity		
U.S. gal day^{-1} ft^{-2}	4.720×10^{-7}	m sec^{-1}
Permeability		
darcies	9.870×10^{-13}	m^2
Transmissivity		
U.S. gal day^{-1} ft^{-1}	1.438×10^{-7}	m^2 sec^{-1}
U.S. gal min^{-1} ft^{-1}	2.072×10^{-1}	l sec^{-1} m^{-1}
Magnetic field intensity		
gausses	1.0×10^{5}	gammas
Energy, heat		
British thermal units, BTU	2.52×10^{-1}	calories, cal
BTU	1.0758×10^{2}	kilogram-meters, kgm
BTU lb^{-1}	5.56×10^{-1}	cal kg^{-1}
Temperature		
°C + 273	1.0	°K (Kelvin)
°C + 17.78	1.8	°F (Fahrenheit)
°F − 32	5/9	°C (Celsius)

**Divide by* the factor number to reverse conversions.
Exponents: for example 4.047×10^{3} (see acres) = 4,047; 9.29×10^{-2} (see ft^2) = 0.0929.

Editor: Jiri Zidek
Drafters: Irean Rae
Charles Ferguson
Michael Wooldridge

Typeface: Palatino

Presswork: Miehle Single Color Offset
Harris Single Color Offset

Binding: Perfect bound with softbound cover

Paper: Cover on 17-pt. Kivar Text on
70-lb White Matte Color
section on 70-lb Enamel

Ink: Cover—4 color and PMS 320
Text—4 color

Quantity: 2,000

Pocket Contents

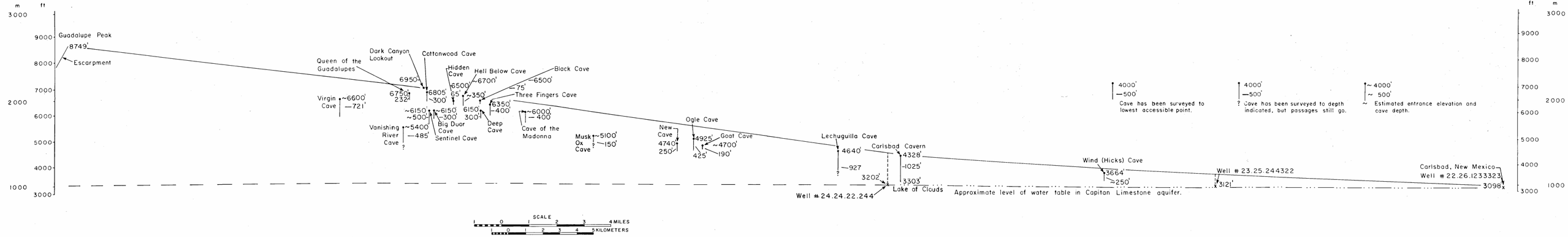
m
ft
3000
9000
8000
2000
7000
6000
5000
4000
1000
Guadalupe Peak
8749'
Escarpment
Queen of the Guadalupes
Dark Canyon Lookout
Cottonwood Cave
Hidden Cave
Hell Below Cave
Black Cave
6950'
6500'
6700'
6500'
65'
350'
75'
Three Fingers Cave
6750'
232'
6805'
300'
Virgin Cave
~6600'
721'
~6150'
~500'
6150
300'
6150'
300'
6350'
400'
~6000'
400
Vanishing River Cave
~5400'
485'
?
Big Door Cave
Sentinel Cave
Deep Cave
Cave of the Madonna
Musk Ox Cave
~5100'
150'
?
New Cave
4740'
250'
Ogle Cave
4925'
Goat Cave
~4700'
190'
425'
Lechuguilla Cave
4640'
927'
?
Carlsbad Cavern
4328'
1025'
3202'
3303'
Well # 24.24.22.244
Lake of Clouds
Approximate level of water table in Capitan Limestone aquifer.
Wind (Hicks) Cave
3664'
≈250'
Well # 23.25.244322
3121'
Carlsbad, New Mexico
Well # 22.26.1233323
3098'
4000'
500'
Cave has been surveyed to lowest accessible point.
4000'
500'
? Cave has been surveyed to depth indicated, but passages still go.
~ 4000'
~ 500'
~ Estimated entrance elevation and cave depth.
SCALE
1 0 1 2 3 4 MILES
0 1 2 3 4 5 KILOMETERS

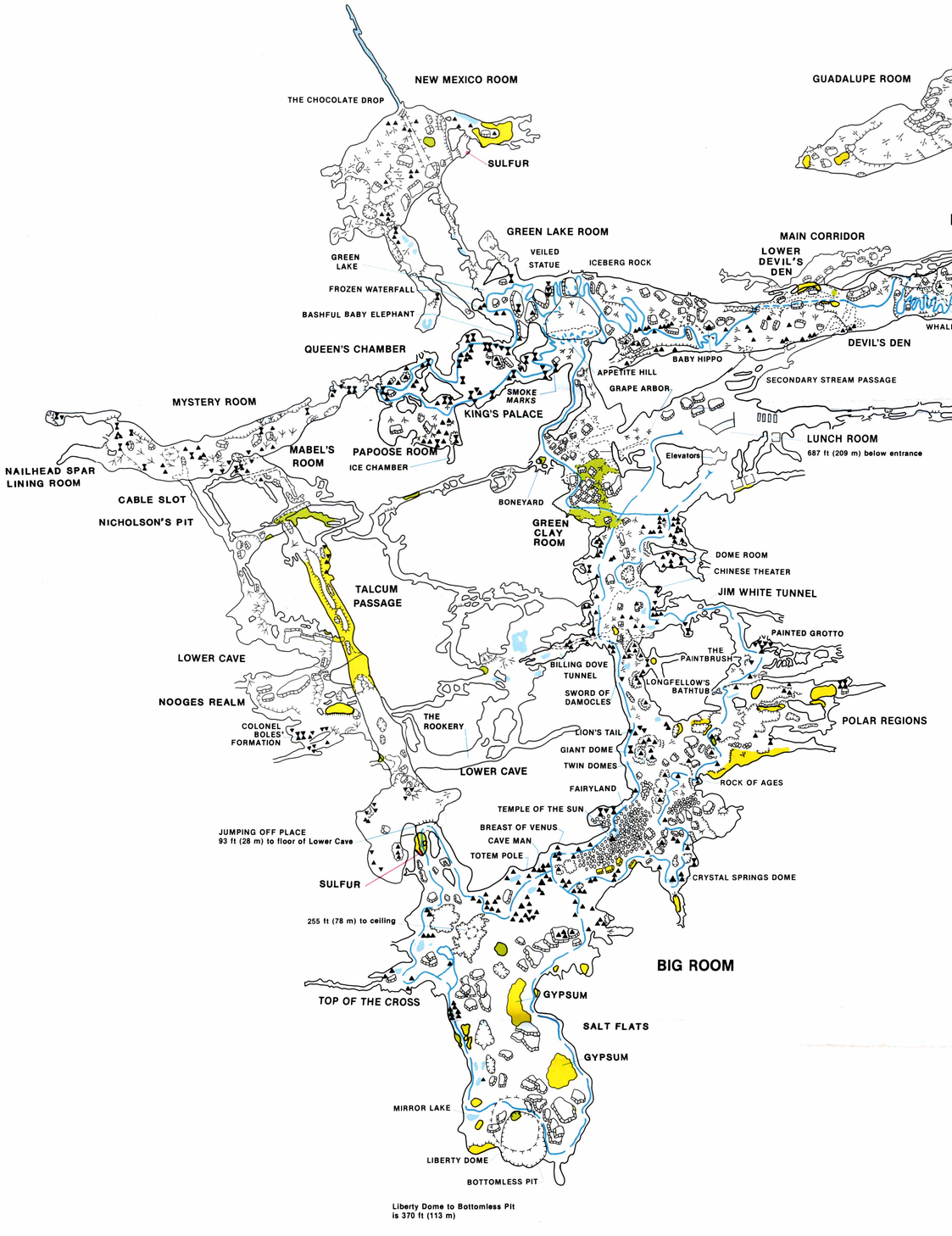

EXPLANATION

- Stalactite
- Stalagmite
- Column
- Many Small Stalagmites
- Large Block on Floor
- Small Blocks on Floor
- Bat Guano
- Pool
- Flowstone
- Gypsum
- Endellite – montmorillonite clay
- Sulfur
- Trail (solid line is Walk-in tour, dashed line is Big Room tour)
- Passage (lower passage is dashed)
- Passage Not Surveyed
- Slope (lines diverge downhill)
- Sharp Drop in Floor (hatchures on downhill side)
- Sharp Drop in Ceiling

N

0 100 200 400 FEET

0 50 100 METERS

CARLSBAD CAVERN

CARLSBAD CAVERNS NATIONAL PARK, NEW MEXICO

Copyright © 1979 by Cave Research Foundation

CARLSBAD CAVERN PROFILE

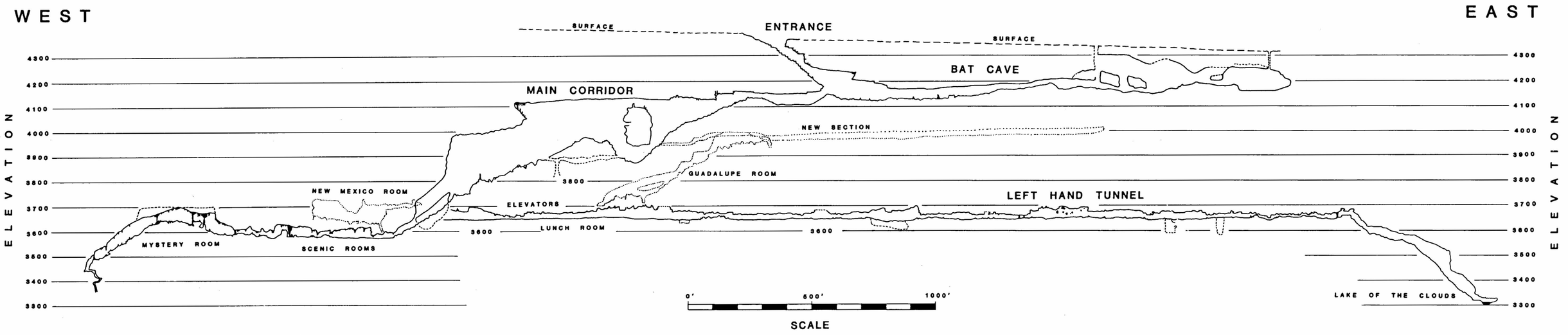

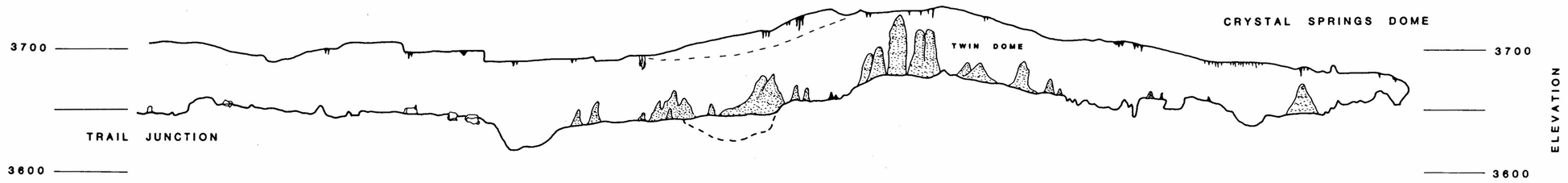

PROFILE - TRAIL JUNCTION TO CRYSTAL SPRINGS DOME

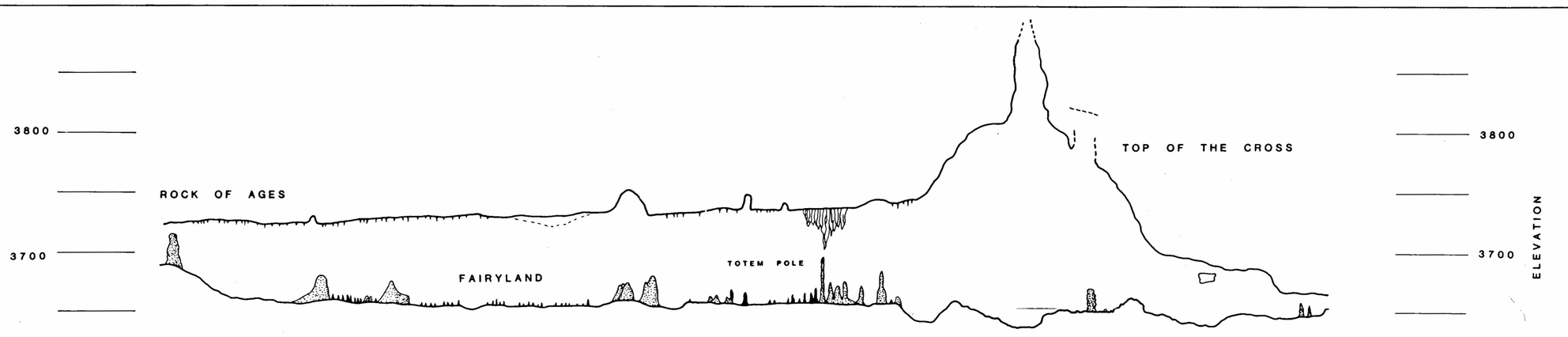

PROFILE - TOP OF THE CROSS TO ROCK OF AGES

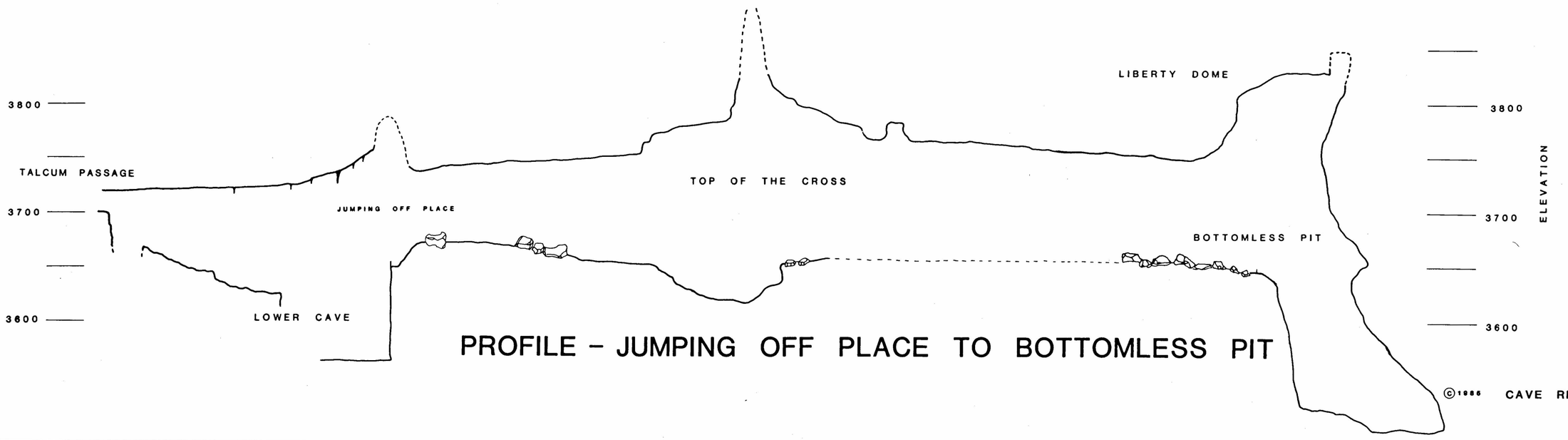

PROFILE - JUMPING OFF PLACE TO BOTTOMLESS PIT

BIG ROOM PROFILES CARLSBAD CAVERN

©1986 CAVE RESEARCH FOUNDATION

SCALE 1" = 50'

Walnut Canyon

4200

4400

Oak Spring

4200

7

Spider Cave

Cavern Entrance

Visitor Center

36

Carlsbad Cavern

31

4400

4200

Chimney Cave

4000

© CAVE RESEARCH FOUNDATION

CARLSBAD CAVERN SURFACE TOPOGRAPHY

CARLSBAD CAVERNS NATIONAL PARK, NEW MEXICO

1"= 400'

40' Contour intervals

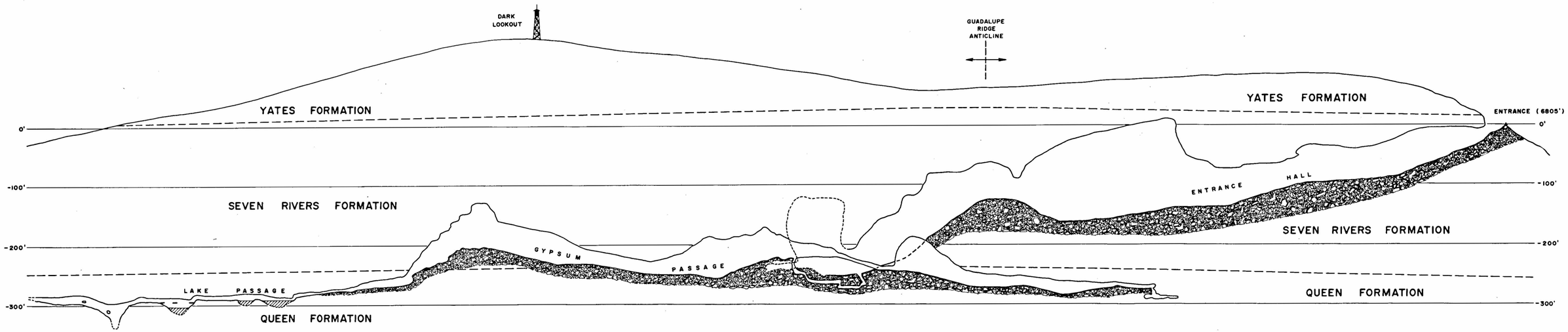

LEGEND

- PASSAGE OUTLINE
- UNSURVEYED OR LOWER LEVEL PASSAGE
- GEOLOGIC CONTACT
- SHARP DROP IN CEILING
- SHARP DROP IN FLOOR
- PIT
- DOME
- SLOPE (DIVERGE DOWNSLOPE)
- LINE OF CROSS SECTION
- CEILING HEIGHT IN FEET
- SURVEY STATION
- BREAKDOWN FLOOR (MAP VIEW)
- BREAKDOWN (CROSS SECTION)
- FLOWSTONE ON FLOOR
- RIMSTONE DAMS
- SILT AND CLAY
- MUD
- STANDING WATER
- INDIVIDUAL BREAKDOWN BLOCK
- STALACTITE AND STALAGMITE
- COLUMN AND COKE TABLE
- MASSIVE GYPSUM BLOCK
- SULFUR DEPOSITS

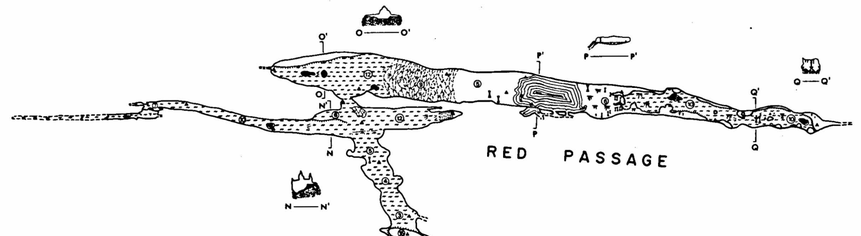

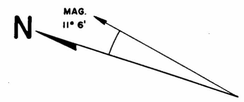

COTTONWOOD CAVE

EDDY COUNTY, NEW MEXICO

BRUNTON AND TAPE SURVEY BY GUADALUPE CAVE SURVEY, JANUARY 2, 1966.

SKETCH REVISION, CROSS SECTIONS, GEOLOGIC INTERPRETATION, AND DRAFTING BY DAVID JAGNOW, 1973 - 1974

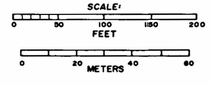

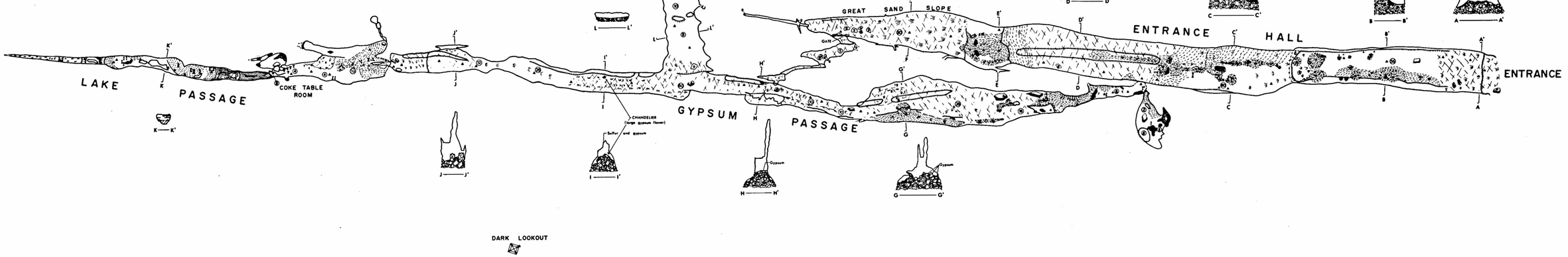

DARK LOOKOUT

N-S PROFILE

ELEVATION
METERS | FEET

1550 5100
5000
1500 4900
4800
1450 4700
1400 4600

CAPITAN LIMESTONE
(MASSIVE MEMBER)

SANDSTONE DIKE
IN N.E. WALL

CAPITAN LIMESTONE
(BRECCIA MEMBER)

CONTACT

OGLE ENTRANCE

SEQUOIA ROOM

INSIDE TUNNEL

BOULDER ROOM

EAST CHAMBERS

GUANO HOPPERS

SPOOL

LION

SIFTERS

RAINBOW MAZE

BLOOD FISSURE

RAINBOW ENTRANCE

RAINBOW VESTIBULE

MINE TUNNEL

HELEN'S CAVE

ENTRANCE

SECTION CORNER
T25S, R23E

3,497.87' to CT-1

2,743.70' to CT-1

N_T 11°30' N_{Mag}

Survey and map by Cave Research Foundation in cooperation with the National Park Service

BREAKDOWN BLOCK	SOIL SAMPLE	RIDGE	STALAGMITE	POOL	CEILING FEATURE
MASSIVE FORMATION	TRAP	SLOPE	STALACTITE	FLOWSTONE	COLUMN
SURVEY POINT	CONTROL POINT	DROP	BAT GUANO	RUBBLE	FALLEN COLUMN

C-08 1:250,000 relative to CT-1 survey by N.P.S.
CT-2 1:250,000
— CONTROL SURVEY —
Brunton traverse C-08 to CT-2 1:150 horiz.
1:70 vertical

OGLE CAVE

CARLSBAD CAVERNS NATIONAL PARK
EDDY COUNTY, NEW MEXICO
Cave Research Foundation © 1975

0 100 200 FEET
0 25 50 METERS

MAP COMPILED BY
J. CORCORAN III
J. HARDY

NEW CAVE

CARLSBAD CAVERNS NATIONAL PARK

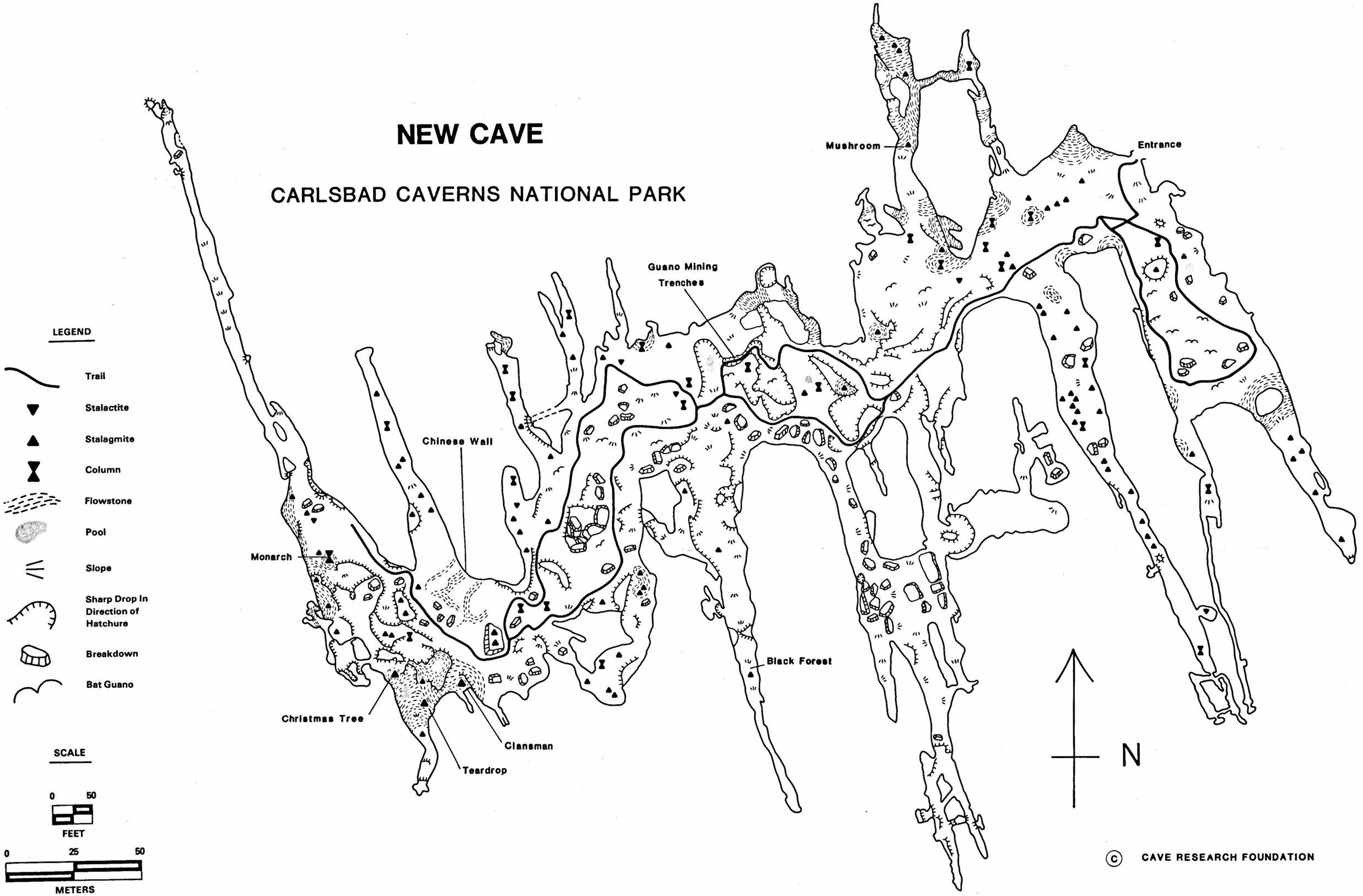

© CAVE RESEARCH FOUNDATION

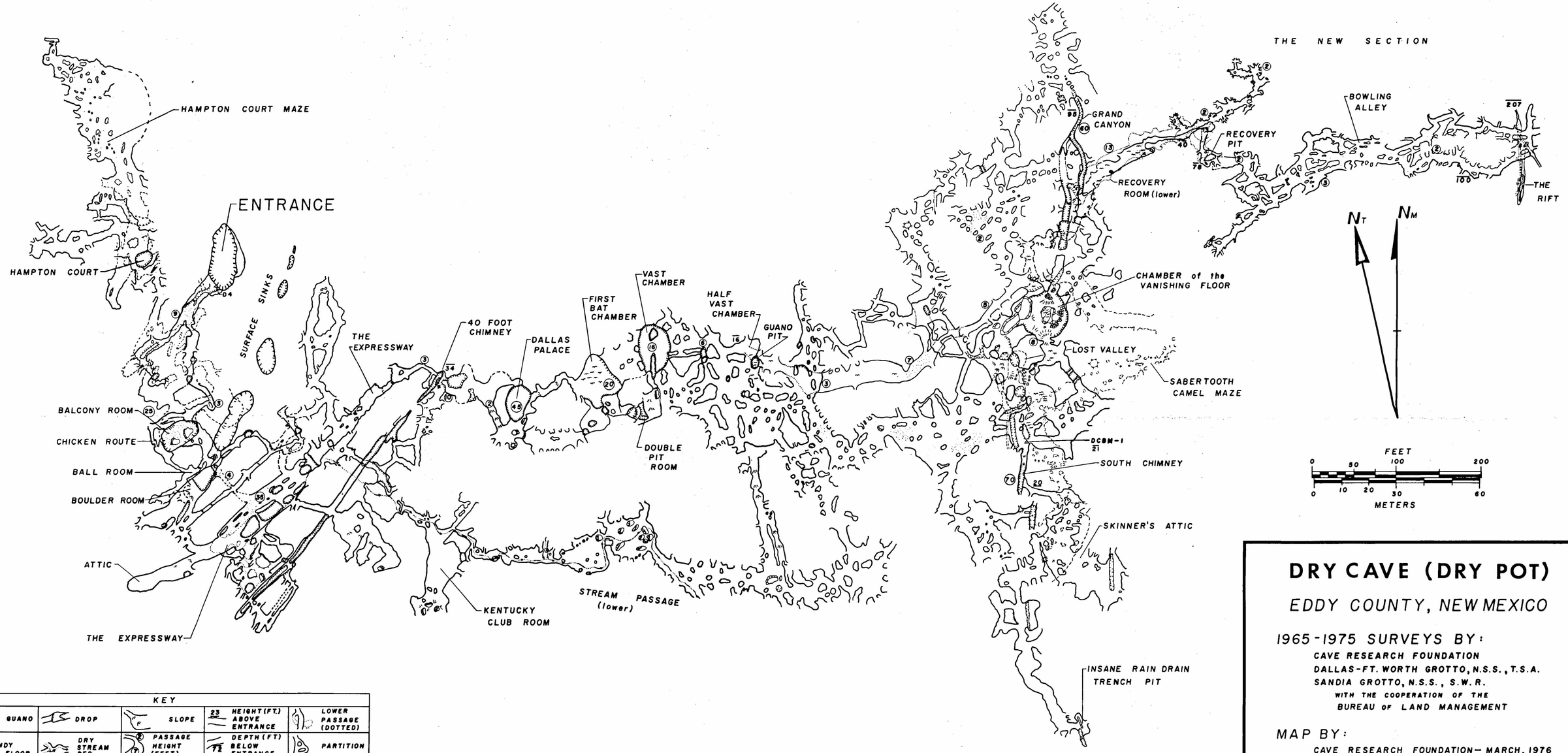

KEY				
BAT GUANO	DROP	SLOPE	HEIGHT (FT.) ABOVE ENTRANCE	LOWER PASSAGE (DOTTED)
SANDY FLOOR	DRY STREAM BED	PASSAGE HEIGHT (FEET)	DEPTH (FT) BELOW ENTRANCE	PARTITION
BREAKDOWN	SURVEY STATION	UNSURVEYED PASSAGE	UNSURVEYED LEADS	PIT

DRY CAVE (DRY POT)

EDDY COUNTY, NEW MEXICO

1965-1975 SURVEYS BY:

CAVE RESEARCH FOUNDATION
DALLAS-FT. WORTH GROTTO, N.S.S., T.S.A.
SANDIA GROTTO, N.S.S., S.W.R.
WITH THE COOPERATION OF THE BUREAU OF LAND MANAGEMENT

MAP BY:

CAVE RESEARCH FOUNDATION— MARCH, 1976

©1976 BY CAVE RESEARCH FOUNDATION

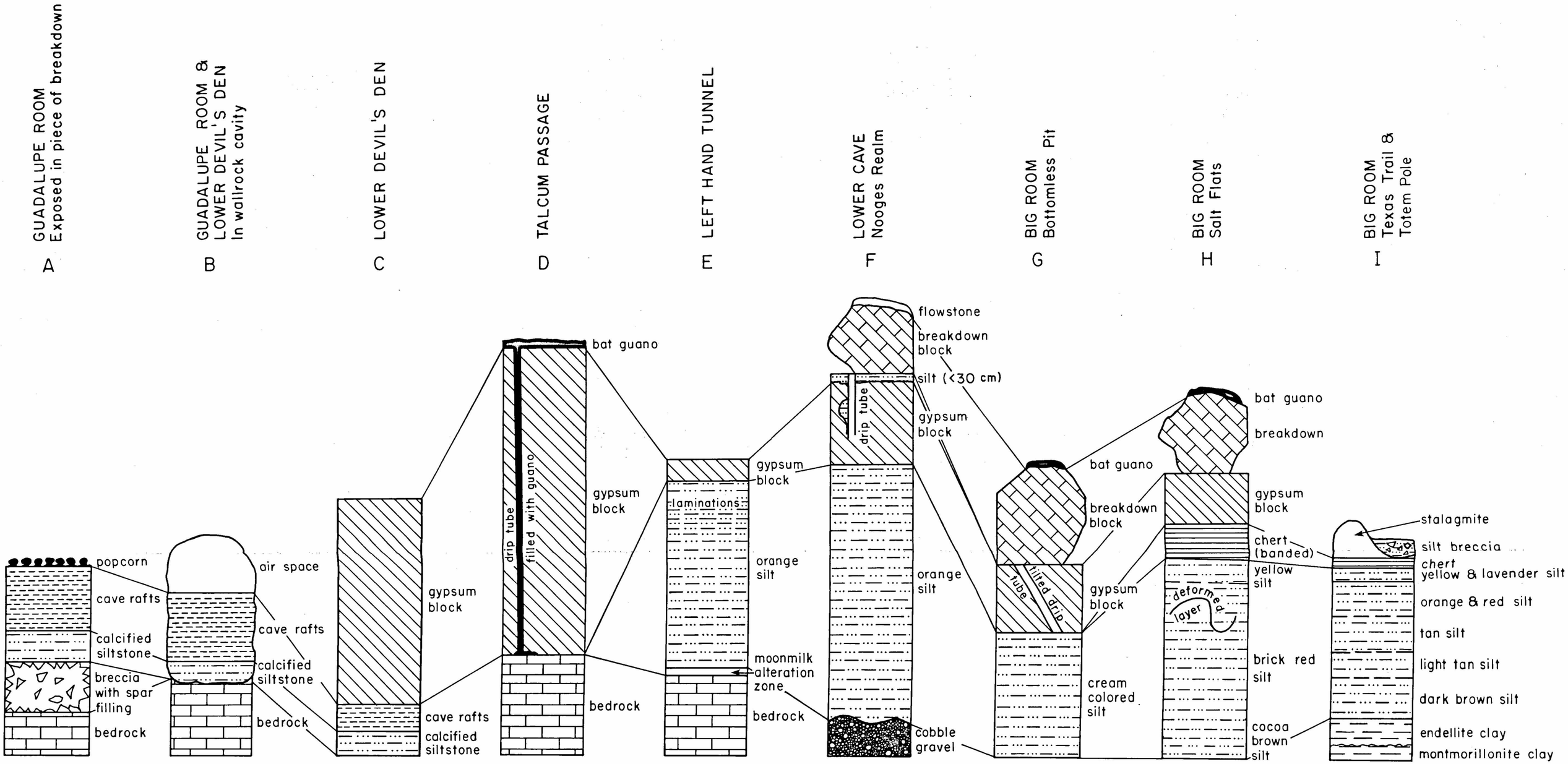
A
GUADALUPE ROOM
Exposed in piece of breakdown
popcorn
cave rafts
calcified siltstone
breccia with spar filling
bedrock
B
GUADALUPE ROOM & LOWER DEVIL'S DEN
In wallrock cavity
air space
cave rafts
calcified siltstone
bedrock
C
LOWER DEVIL'S DEN
gypsum block
cave rafts
calcified siltstone
D
TALCUM PASSAGE
bat guano
drip tube
filled with guano
gypsum block
bedrock
E
LEFT HAND TUNNEL
gypsum block
laminations
orange silt
moonmilk alteration zone
bedrock
F
LOWER CAVE
Nooges Realm
flowstone
breakdown block
silt (<30 cm)
drip tube
gypsum block
orange silt
cobble gravel
G
BIG ROOM
Bottomless Pit
bat guano
breakdown block
tilted drip tube
gypsum block
cream colored silt
H
BIG ROOM
Salt Flats
bat guano
breakdown
gypsum block
chert (banded)
yellow silt
deformed layer
brick red silt
cocoa brown silt
I
BIG ROOM
Texas Trail & Totem Pole
stalagmite
silt breccia
chert
yellow & lavender silt
orange & red silt
tan silt
light tan silt
dark brown silt
endellite clay
montmorillonite clay